THE BRACE POSITION FOR PASSENGER AIRCRAFT
A BIOMECHANICAL EVALUATION

PETER BROWNSON

Submitted for the Degree of Doctor of Medicine

Department of Orthopaedic and Accident Surgery
University Hospital
Nottingham

Nottingham May 1993

CONTENTS

LIST OF TABLES

LIST OF FIGURES

ACKNOWLEDGEMENTS

This work would not have been possible without the help and advice of the following individuals.

I must begin by expressing my gratitude to Professor W. Angus Wallace and Wing Commander David J. Anton who acted as my supervisors during the writing of this thesis. Their efforts to facilitate my forward progress as well as their infectious enthusiasm for this research did not go unnoticed.

I am indebted to Mr Raf Haider (Hawtal Whiting Structures, Royal Leamington Spa) who performed the mathematical modelling.

I am grateful to Mr Nigel Stallard and Mr Andrew Belyavin (Statistics Department, IAM Farnborough) who performed the statistical analysis of the impact test results.

Special thanks must go to the Institute of Aviation Medicine, Farnborough, who allowed me the use of their impact test facility. In particular, I am indebted to Mr L. Neil and Mr G. Hall for their practical assistance and to Surgeon Commander P Waugh for his help with the data acquisition and processing systems.

This research was a natural progression from the research carried out by Mr JM Rowles into the M1 Kegworth accident. I am indebted to John for his support.

I am grateful to Mrs Marina Skinner who as my secretary was responsible for the typing of this thesis.

The research was funded by a grant from the Special Trustees of the Nottingham University Hospitals and by the Civil Aviation Authority.

Finally, I must thank my wife, Georgina, for her uncomplaining support over a period of sixteen months.

DECLARATION

I declare that I am responsible for the planning and conduct of the work contained in this manuscript with the exception of the following:

The mathematical modelling was carried out by Mr Raf Haidar (Hawtal Whiting Structures, Royal Leamington Spa).

Mr Nigel Stallard (Statistics Department, IAM Farnborough) carried out the statistical analysis of the impact test results.

All the work was carried out during my appointment as Clinical Research Fellow in the Department of Orthopaedic and Accident Surgery, University Hospital, Nottingham.

SYNOPSIS

Hypothesis

A modified brace position would help to prevent injury to some aircraft passengers in the event of an impact accident.

Aim of Experiments

To evaluate a modified crash brace position.

Materials and Methods

1. Impact Testing

Impact testing was performed at the RAF Institute of Aviation Medicine, Farnborough. Aircraft seats, mounted on a sled, were propelled down a track at an acceleration of 16G. A 50% Hybrid III dummy was used as the experimental model. Four dummy positions were investigated: upper torso either braced forwards or sitting upright and lower legs placed either forwards or rearwards. The impact pulses used were based upon guidelines defined in Aerospace Standard AS8049 which relates to the dynamic testing of aircraft seats. Transducers located in the head, lumbar spine and lower limbs of the dummy recorded the forces to which each body segment was exposed during the impact. These forces were compared for each brace position.

2. Computer Simulation

A mathematical model was developed to simulate occupants kinematics during an impact aircraft accident. This was based upon MADYMO - a crash victim simulation computer programme for biomechanical research and optimization of designs for impact injury prevention.

Results

Impact testing revealed that the risk of a head injury as defined by the Head

Injury Criterion was greater in the upright position than in the braced forwards position ($p < 0.001$).

The risk of injury to the lower limbs was dependant in part to their flailing behaviour. Flailing did not occur when the dummy was placed in a braced legs back position.

Computer simulation revealed that lower limb injury may result from the feet becoming entrapped under the luggage retaining spar of the seat ahead.

Conclusion

A modified brace position would involve passengers sitting with their upper torso inclined forwards so that their head rested against the structure in front if possible. Legs would be positioned with the feet resting on the floor in a position slightly behind the knee.

This position differs from those previously recommended in that the feet are positioned behind the knee.

This study suggests that such a position would reduce the potential for head and lower limb injury in some passengers given that only a single seat type and single size of occupant have been evaluated.

Standardisation to such a position would improve passenger understanding and uptake.

Such a recommendation should not obscure the fact that an occupant seated in a forward facing aircraft seat, restrained only by a lap belt is exposed to considerable forces during an impact accident. Such forces are capable of producing injuries in the femur, pelvis and lumbar spine.

ABBREVIATIONS

Text

ATD	Anthropomorphic Test Device
ACIR	Automobile Crash Injury Research
AvCIR	Aviation Crash Injury Research
CAA	Civil Aviation Authority
CAMI	Civil Aeromedical Institute
cm	centimetre
DASH16	DASH 16 Acquisition Board
DL	Datalab
FAA	Federal Aviation Authority
FSD	Full Service Deflection
Fx	Force in x-axis
Fy	Force in y-axis
Fz	Force in z-axis
G	Gravity
Gx	Acceleration in horizontal plane
Gy	Acceleration in a lateral plane
Gz	Acceleration in a vertical plane
HIC	Head Injury Criterion
IAM	Institute of Aviation Medicine
lb	pound
kg	kilogram
kN	kilonewton
MADYMO	Mathematical Dynamics Modelling Programme
Mx	Moment about x-axis
My	Moment about y-axis
Mz	Moment about z-axis
m	metre
mm	millimetre
N	Newton

NASA	National Aeronautics and Space Administration
NLDB	Nottingham, Leicester, Derby, Belfast Study Group
Nm	Newton metre
PORTAX	DT 2821 Acquisition Board
RAF	Royal Air Force
"	inch
%	percentage

Statistical Analysis

B/LB	Braced legs back
U/LB	Unbraced legs back
B/LF	Braced legs forward
U/LF	Unbraced legs forward
p	Significance value (*$p<0.05$, **$p<0.01$, ***$p<0.001$)
ns	Not significant ($p>0.05$)
B	Brace position
S	Seat pitch
O	Order effect
DF	Degrees of freedom
F	Ratio

INTRODUCTION

Aircraft passengers are advised to adopt a "brace for impact position" prior to a crash landing with the aim of reducing occupant injuries from secondary impacts. Whilst the aim is simple, the many conditions that can exist in commercial aviation have resulted in a number of different crash brace positions being advocated. This has led to a lack of understanding and uncertainty amongst air passengers about which position to adopt (6).

On 8th January 1989 a Boeing 737-400 aircraft crashed on the M1 motorway near Kegworth, England. Subsequent research revealed that the passengers had suffered a large number of injuries. In particular injuries to the head and the lower limbs were prevalent. If there had been a post-crash fire this combination of injuries would have severely limited the ability of the occupants to escape from the aircraft fuselage.

Following the M1 Kegworth accident it was suggested that the brace for impact position might be modified in order to reduce the incidence of head and lower limb injuries. It was suggested that an occupant adopting a braced forward position with the feet placed firmly on the floor but in a position slightly rearwards of the knee might suffer a reduced incidence of head and lower limb injury. The aim of this research was to evaluate biomechanically this modified brace for impact position.

This research was carried out over a period of 18 months between January 1992 and July 1993. An approximate timetable of the events which occurred during that 18 months is given below.

January 1992 - Mr. Peter Brownson appointed as clinical research fellow, Department of Orthopaedic and Accident Surgery, University Hospital, Queens Medical Centre, Nottingham.

May 1992 - start of impact testing and development of mathematical model.

September 1992 - completion of impact testing and initial phase of development of computer model.

October 1992 - presentation of research findings to the Air Operators Committee at Gatwick Airport, London. Decision to proceed with further research aimed at improving the understanding of the spinal loads to which the occupant is exposed during an impact accident.

May 1993 - report submitted to the CAA entitled 'Passenger Brace Position Study - Impact Testing'.

June 1993 - meeting at Hawtal Whiting Structures, Royal Leamington Spa. Discussion of the results of the impact testing study and the mathematical modelling study into the brace for impact position.

August 1993 - thesis entitled 'The Brace Position Study - A Biomechanical Evaluation' submitted to the University of Nottingham by Mr. Peter Brownson.

With the knowledge that, in the future, this thesis may be read by individuals about to undertake a similar project, I feel that it would be appropriate to give a short account of the 18 months over which this research was carried out, outlining some of the difficulties with which one can be presented when entering the field of passenger safety research.

On the 13th January, 1992, I was appointed as the Clinical Research Fellow in the Department of Orthopaedic and Accident Surgery in Nottingham. I had just completed my basic surgical training and had recently become a Fellow of the Royal College of Surgeons of Edinburgh.

It seemed appropriate that I should be involved in research relating to the M1 Kegworth accident, as I had been a junior member of the orthopaedic team in

Nottingham at the time of the accident. Unfortunately, my knowledge of passenger safety research and, in particular, impact testing was all but non-existent as I embarked upon this project.

The first difficulty which I encountered was in attempting to review the literature on aircraft passenger safety. In this specialized field, research is presented at certain international meetings and the results published in the proceedings of those meetings. Unfortunately, if one is not intimately involved in this field, one is presented with two problems. Firstly, it is not easy to identify research which is related to one's own planned field of investigation and, secondly, if such research can be identified, it is not always easy to access the relevant documents, although, in this respect, the Society of Automotive Engineers in the United States can be particularly helpful.

In May 1993, impact testing commenced at the RAF Institute of Aviation Medicine in Farnborough. This facility had been selected by the Civil Aviation Authority primarily because of its involvement in the initial phase of the research following the Kegworth accident. Unfortunately, the design of the impact test facility is somewhat limited and, in particular, the following points should be noted.

1. The facility is a deceleration-type impact facility which necessitates the dummies being placed in position prior to acceleration down a track before an impact with an arrestor block. This makes positioning of the dummy somewhat inaccurate as inevitably there will be some movement between the time of the initial firing and the time of impact.
2. Only a single Hybrid III anthropomorphic test dummy was available. Previously the Hybrid II anthropomorphic test dummy has been recommended for impact testing relating to the aircraft passenger.

3. The test vehicle is propelled by stretched bungee cords. This makes fine control of the impact pulse somewhat difficult. This problem being further compounded by the fact that leads running from the vehicle to the transducer monitors, introduce a drag coefficient which further retards the vehicle velocity during any impact test. The effect of this combination of factors was that one had to accept a slightly reduced impact velocity when compared to the impact velocity recommended in Aerospace Standard 8049 relating to dynamic performance testing of aircraft seats.
4. Whilst an instrumented Hybrid III dummy was available not all of the instrumentation was present. Particularly, it was not possible to include a cervical spine load cell nor any instrumentation relating to thoracic injury potential.
5. Due to financial considerations it proved necessary to use ten sets of triple row seats from the Kegworth accident as new seats were not available. Initial discussions between Mr. Peter Brownson and Mr. Raf Haidar highlighted the desirability of new aircraft seats for testing particularly for the correlation of the mathematical model.

In September 1992, the impact testing had been completed at Farnborough. In addition, a mathematical model had been developed and an attempt made to correlate this model to impact tests.

In October 1992 the initial results of the research were presented to the Air Operators Committee at Gatwick Airport, London. At this dicussion it was pointed out that the loads recorded in the lumbar spine during both the impact testing and computer simulation studies were causing concern. It was suggested that further information might be obtained by either cadaver testing or incorporating a more advanced mathematical model representation of the spine into the already developed mathematical model. Over the next two months the possibility of performing a limited number of cadaver tests was explored. This proved impossible as the legislation to allow for such testing does not exist in the United Kingdom. Fortunately, a mathematical model representation of the human spine was acquired from Wayne State University, and this was incorporated by Mr. Raf Haidar into the Hybrid III data set of the MADYMO model which had been correlated to earlier impact test study.

In May 1993, a report was submitted to the Civil Aviation Authority entitled 'Report No.1 Passenger Brace Position Study - Impact Testing' by Mr. Peter Brownson.

In June 1993 a meeting was held at Hawtal Whiting Structures Limited, Royal Leamington Spa. At this meeting a discussion was held between the Civil Aviation Authority, Hawtal Whiting Structures Limited and the Department of Orthopaedic and Accident Surgery in Nottingham. The results of the impact testing studies and computer simulation studies were discussed and recommendations were made relating to the "brace for impact position".

In August 1993 this thesis was submitted to the University of Nottingham.

REVIEW OF THE LITERATURE

1. AIRCRAFT ACCIDENT STATISTICS

As a form of transport, commercial scheduled aviation must be regarded as extremely safe.

In 1979, Wilson (42) analyzed for a variety of activities, the risks estimated to increase the chance of death in any year by 0.000001 (1 part in one million):

Activity	**Cause of death**
Travelling 10 miles by bicycle	Accident
Travelling 150 miles by car	Accident
Travelling 1000 miles by jet	Accident
Living 150 years within 20 miles of a nuclear power plant.	Cancer caused by radiation

However as Anton (2) has stated the perception of safety bears little relation to real risk and flying is regarded with apprehension by many. This appears to be because of the lack of personal control over the risk and because when accidents occur, large numbers of people may be killed at one time.

Flight International in an editorial in January 1990 (21) stated that for decade upon decade the chances of a (non-USSR) scheduled passenger being involved in a fatal accident have nearly halved. Today, the safe passenger distance in revenue passenger kilometres between fatal accidents, is two and a half times what it was in the 1970's. On charter airlines the safe passenger distance trebled.

Today's average scheduled passenger would have to make 571,000 flights before boarding one which had a fatal accident. Even on that flight, the passenger's chance of survival would be 65%, for in the average fatal airline accident, only 35% of passengers and 40% of crew die (21).

This improvement in safety has been achieved largely by improvements in primary safety or airworthiness and hence a reduction in the accident rate.

However, despite the obvious improvement in air safety in the early 1980's compared with the 1970's the trend has not been sustained over the last decade. The annual average number of fatal accidents during the second half of the decade was 21.4, where in the first half it was 20; the annual average number of deaths for the second five years was 752 where in the first five it was 588 (21).

Human error is now the major contributory factor in most aircraft accidents (22). Whilst attention has been directed towards this area, the difficulty in predicting how an individual will react to a given situation precludes a simple solution.

Consequently, attention has been directed towards improving air safety by improvements in secondary safety or crashworthiness.

Improvements in crashworthiness involve development in many areas including aircraft design, seat design and perhaps most importantly, fire safety.

Fire is a significant factor in a large number of deaths following aircraft accidents.

The National Aeronautics and Space Administration (NASA) (41) sponsored a study of transport aircraft crashworthiness for the period 1959 - 1979. Worldwide transport aircraft data were reviewed. The Boeing Commercial Aircraft Company, which took part in the study, selected 153 impact survivable accidents out of a worldwide total of 583. Of 3791 fatalities in the 153 impact survivable accidents, Boeing reported that 1356 were known to be related to fire (although the occupant may have sustained serious crash trauma in addition), 476 to trauma, 218 to other, unspecified, causes and 1741 for unknown reasons. Fire clearly presents a considerable hazard.

The scope for reducing trauma related casualties might appear low. The FAA estimate that it is likely that only a small percentage of passengers will be helped by the new seat standards; the estimate being a 3-15% reduction in fatalities and a 2-9% reduction in serious injuries. However the FAA estimates that as a result of overall improvements in fire safety, in air traffic control systems, in training of crew members and in aircraft design, the prospective casualty rate can be reduced by 50% from that in the study period (1970-1978) (2).

Improved air safety remains a worthwhile and achievable goal and this is especially so in view of the plans to increase the carrying capacity of passenger aircraft.

At present a billion passengers per year are carried by air but that figure is expected to double by 2005 and the world's busiest airports and air traffic control system are already stretched close to their limit. The only practical way to cope, without creating further congestion in the sky, is to build much bigger aircraft.

Boeing's 747 is currently the world's largest airliner, capable of carrying 400 passengers 13,000 kilometres (or half way round the world) nonstop. Boeing has already increased the carrying capacity of a short range 747 to carry 500 passengers for Japan Airline's packed domestic routes. However airlines in the Far East are demanding an 800 seater plane before the end of the century.

Boeing has already designed a 612 seater mega-jet which has a new three deck fuselage.

The European consortium Airbus has the most radical ideas about mega-jet design. One Airbus design is a giant flying wing whilst another design incorporates a "double bubble" design to the fuselage with two tubes side-by-side or a "clover leaf" design with a wide lower deck and a smaller upper deck. Both of these planes could carry 800 passengers or possibly 1,000 if the fuselage was elongated (24).

2. CRASH INJURY RESEARCH AND AIRCRAFT SAFETY

2.1 THE PRE-WAR ERA

The first documented powered aviation accident was in 1908 when Lieutenant Thomas Selfridge of the US Army Evaluation Board was killed whilst flying with Orville Wright in 'Wright Flyer' (3). Selfridge died of skull fractures, his autopsy being, apparently, the first recorded aviation pathology case. Little appears to have been learnt from Selfridge's accident and the high toll in death and injury continued to be exacted in the early years of aviation.

The concept of personal protection was almost completely ignored in the quest for improved aircraft control and structural reliability. The emerging requirement to restrain the pilot to the airframe arose more from examples of unrestrained individuals fouling controls or falling from the aircraft during flight manoeuvres, than from consideration of crash impact injury prevention.

The importance of adequate restraint was, in part, overlooked because of the lack of crash worthiness in early types of aircraft.

2.2 THE FIRST WORLD WAR

The First World War did little to advance impact protection. Parachutes were developed to save airman's lives from crashes, although few aircrew carried them routinely. Restraint systems were adopted but with the principal objective of securing the pilot against flight loads. However, some studies were, directed towards crash injury protection; Chandler (7) refers to observations made in 1919 that, in one type of aircraft, cutting 20.3 cm (8 inches) away from the cowl, to allow clearance for the pilots head, practically eliminated head injuries.

2.3 THE SECOND WORLD WAR

In 1924, in America, civil pilots experienced a fatal accident every 13,500 miles flown. Little real progress was made until the Second World War which brought fresh problems due to the advent of metal monocoque airframes and aeroengines of greater power. These advances allowed the speed of aircraft to increase substantially and pilots could no longer abandon a stricken aircraft manually because of the increase in aerodynamic load and the risk of striking the tail fin of the aeroplane. Although a patent for an aircraft escape system had been filed in the United States in the 1920's it was research in Germany and Sweden that led to the development of the first practical ejection seats.

Questions raised regarding the tolerance of the pilot to the loads imposed by the ejection seat led to what was possibly the first research study into what could be termed the biomechanics of impact.

Arno Geertz of the Heinkel Aircraft Company, submitted a doctoral thesis in 1944 describing his work investigating human tolerance to ejection stress. He made the important observation that an acceleration can be of any magnitude from the point of view of skeletal strength, if its duration is correspondingly brief.

2.4 THE POST-WAR ERA

In North America, De Haven, who had been seriously injured in an aircraft crash in the First World War, founded the Crash Injury Research Project at Cornell University Medical College and in 1945 he reported the results of the first systematic analysis of injuries in aircraft accidents (10).
He concluded that:

1. In accidents where the cabin's structure was distorted but remained substantially intact, the majority of serious and fatal injuries were

caused by dangerous cabin installations.

2. Crash force, sufficient to cause partial collapse of the cabin structure, was often survived without serious injury.

3. The head was the first, and often the only, vital part of the body exposed to injury.

4. The fundamental causes of head injury were set up by heavy instruments, solid instrument panels, seat backs and unsafe design of control wheels.

5. The probability of severe injuries of the head, extremities and chest was increased by failure of safety belt assemblies or anchorages.

6. Failure of the 454 kg (1000 lb) (breaking strain) safety belt occurred in 94 cases among 260 survivors of the crashes. Only 7 survivors showed evidence of injury to the abdominal viscera; 2 of these injuries were classified as serious.

7. The tolerance of crash forces by the human body has been grossly underestimated.

8. If spin stall dangers were lessened and safer cabin installations were used, fatal or serious injuries should be rare in the types of aircraft studied in extreme accidents.

De Haven's study was a forerunner of the systematic combined engineering and medical/pathological investigation which now characterises investigations in a number of countries.

Stapp explored the field of human tolerance to short duration accelerations.

He showed that the primary forces acting in the majority of car collisions were survivable if the packaging of the human frame was satisfactory (37). In the 1950's Mathewson and Severy were developing the technique of experimental crash testing with instrumented dummies and high speed film analysis.

In 1959, Eiband summarised the literature on human tolerance to impact (12). He indicated adequate torso and extremity restraint was the principal variable in establishing tolerance limits. Survival of impact forces increased with increased distribution of force to the entire skeleton for all impacts, from all directions.

In 1967 the first issue of the "Aircraft Crash Survival Design Guide" was produced; an organised compendium of the research conducted on both human tolerance of impact and crashworthiness. At this time, the majority of crash injury research was centred in America. It was here that two movements took place which were to greatly influence the direction of efforts in the field of crash injury reduction.

Firstly, the principles resulting from the Crash Injury Research Project had been found to apply to the automobile industry and the project was divided into Aviation Crash Injury Research (AvCIR) and Automobile Crash Injury Research (ACIR). The ACIR studies encouraged large amounts of research funded by the automobile industry and the insurance companies. From this time, automobile crash injury research has maintained a higher priority than that of aviation (8).

The second event which took place was the development of the legal concept of strict liability. As Chandler has stated (8): "For our purposes, strict liability means that a manufacturer can be held liable for injuries sustained in an accident involving his product even though the accident was not the fault of the manufacturer. This concept meant that adhering strictly to the practises of accident prevention would no longer be an effective argument for protecting the manufacturer from law suits involving crash injuries."

In North America the manufactures of small airplanes were seriously affected by this new legal development. The accident prevention efforts had not had the same level of success for small private airplanes as had been achieved for large transport airplanes. Litigation under the strict liability concept was continuing to increase and was resulting in greatly increased insurance premiums. Because of these problems, and many others, the production of private airplanes had almost stopped by the early 1980's.

In 1982 the FAA instigated the formation of the General Aviation Safety Panel. This group contained members from all areas of the aircraft industry. It presented specific recommendations in February, 1983. The recommendations suggested included improved crashworthiness for small airplanes.

The group went on to provide specific recommendations for a dynamic test procedure for small aeroplane seats, restraints and interior fittings with defined performance standards for the structure and for crash injury protection. A Final Rule adopting the recommendations was issued in August, 1988.

Once these recommendations had been made it was apparent that similar action would be necessary for other categories of airplanes.

3. THE DEVELOPMENT OF THE 16G AIRCRAFT PASSENGER SEAT

In 1983 the FAA published a review of crash injury protection in survivable US civil air transport accidents between 1970-1978 (14). The purpose of the review was to:

a) compile a data base on passenger seat and restraint system performance in survivable accidents;

b) determine if a correlation existed between occupant, seat and restraint system performance, airframe and floor deformation, and passenger injuries and fatalities.

The report indicated that: "although injuries and fatalities seem to be decreasing in the more recent survivable crashes, seat performance continues to be a factor in these crashes. Failures ranging from seat pan collapse to complete break-away of the seat assembly from the floor are reported. Floor or cabin deformation is frequently a cause of seat failure. Flailing injuries, due either to bending over the restraint system or secondary impact with the aircraft interior appear to be common".

The study listed 327 fatalities and 294 serious injuries to passengers involved in accidents with US carriers where seats could have been a contributing factor.

Four areas were indicated which required attention in order to improve occupant protection:

a) Definition of the survivable crash environment.

b) Development of an understanding of structural component and whole aircraft response to the crash environment.

c) Development of validated analytical modelling and test engineering methods.

d) Definition of human factors and injury mechanisms for occupants of transport aircraft.

In 1984, after the announcement of the General Aviation Safety Panel recommendations, the Aerospace Industries Association and the Air Transport Association joined with the Civil Aeromedical Institute (CAMI) in a special project.

A programme was developed to investigate the effects of impact pulse shape, impact deceleration level and impact velocity on the seat structure and floor deformation. Test configurations and methodology developed in the earlier General Aviation Safety Panel project were adapted for passenger seats.

From this study the FAA announced its intention to introduce new seat and restraint standards for new type certificate passenger aircraft. The existing requirements provided that seats and safety belts should sustain the following load factors assuming a minimum seat occupant weight of 77.18 kg (170 lbs) (2).

Forward	$-9.0\ G_x$
Sidewards	$+/-1.5\ G_y$
Downwards	$+4.5\ G_z$
Upwards	$-2.0\ G_z$

Seat manufacturers were allowed to demonstrate compliance with the load and safety factors by static testing.

The new FAA standards, which took effect in June 1988, provided for static load factors of:

Forwards	-9.0 G_x
Rearwards	+ 1.5 G_x (no previous requirement)
Sidewards	+/-3.0 G_y airframe, 4G seats and attachments
Downwards	+ 6.0 G_z
Upwards	-3.0 G_z

Additionally two dynamic tests were defined, using instrumented 50% 49 CFR Part 572 anthropomorphic test dummies to simulate seat occupants:

Test 1 approximates to a near vertical impact, with some forward speed, applying a minimum of 14G deceleration from a minimum velocity of 10.67 $m.sec^{-1}$, canted aft 30° from the vertical axis of the seat.

Test 2 approximates a horizontal impact with some yaw, applying a minimum 16G deceleration from a minimum of 13.41 $m.sec^{-1}$, the seat yawed 10° from the direction of deceleration. To simulate the effects of cabin floor deformation, the parallel floor rails or fittings in test 2 are misaligned by at least 10° in pitch, and 10° in roll before the dynamic test. The tests require that the seat remains attached although, it may yield to a limited extent.

The tests also include a requirement limiting the pelvic load to 6.7kN (1500lbs), head deceleration to a HIC = 1000 (Head Injury Criterion) and axial femoral load to 10.0kN (22501b).

Of these two tests, Test 2 is considered the more stringent. The peak deceleration (16G) and the velocity change (13.41 $m.sec^{-1}$) were chosen as the result of a study of crash dynamics and the levels were also considered to be compatible with existing floor strengths in the current fleet of transport aircraft.

Subsequent to the promulgation of these rules the FAA issued a Notice of Proposed Rule Making to cover the installation of the upgraded seats in new aircraft of current type and within the existing fleet; all transport category aircraft would be required to have seats installed, meeting the new criteria, by June 1995.

4. PASSENGER SEAT ORIENTATION

The question of passenger seat orientation has been a matter of debate for many years. Eiband suggested that a rearward facing passenger seat would offer the best protection in an impact (12). He cautioned that such a seat should include a lap and chest strap, a winged back with full head rest, load bearing arm rests with recessed hand holds and provision to prevent arm and leg flail. For forward facing seats Eiband recommended full body restraint and a full height seat back with integral head support.

Pinkel analysed the theoretical performance of forward and rearward facing seats in transport aircraft (32). He assumed that passenger restraint forces were applied through the seat back attachment points on the forward facing seats, and through the seat back, for the rearward facing seats. Using these assumptions he calculated that rearward facing seats would have half of the design strength of forward facing seats, if the increase in weight due to the need for a stronger seat back was ignored. In summarising Pinkel's findings, Chandler (7) discussed the relative merits of forward and rearward facing seats in the following terms:

> "In crashes involving fire or ditching, it is important that the passengers survive the actual crash with only minor injuries, so that they can evacuate the aeroplane. Rearward facing seats should provide better protection from injury, and appear to have an advantage under these conditions".
>
> "In crashes which do not involve fire or ditching, rapid and unassisted evacuation of the aeroplane is not so critical, and a higher level of injury might be acceptable. The forward facing seat should have greater strength than a rear facing seat of equivalent weight, and thus restrain the passenger in more severe crashes. Since a passenger who is held in place by his seat generally fares better than one who breaks free, a forward facing seat appears to have an advantage under these conditions".

Mason reviewed practical experience with rearward facing seats (26). He quoted one series of investigations in which 19% of forward facing passengers died compared with 5% of rearward facing occupants. In another study 11% of passengers in forward facing seats were killed and 84% were uninjured with comparable figures for rearward facing seats of 1% killed and 98% uninjured.

Notwithstanding the obvious biomechanical advantages of a rearward facing seat the overwhelming number of passengers in commercial aircraft travel facing forwards, restrained only by a lap belt. There are several reasons for this:

Firstly, as Pinkel's work indicates, on a material for material basis, rearward facing seats are heavier than forward facing ones if the same impact performance is required. Increased floor strength, and hence mass, is also required if the increased loads on impact, with a rearward facing seat, are to be resisted by the structure, without failure. The cost implications of mass increase were addressed by the FAA, which calculated that each 0.454kg (1lb) weight increase in an aircraft can cause 56.8 litres (15 United States gallons) of additional fuel burn per annum (2).

Secondly, there is a considerable reluctance on the part of the airlines to fit rearward facing seats. It is claimed that passengers do not like them. This is borne out by apparent passenger preference for forward facing seats in those aircraft where both seat types are fitted. Regrettably, many rearward facing seats have not been correctly designed and are uncomfortable. Experience in those aircraft fitted only with correctly designed rearward facing seats shows that passengers are frequently unaware of seat orientation (2).

Thirdly, there is evidence to suggest that passengers in rearward facing seats are at risk from being struck in the face by objects falling from overhead bins during impacts. The risk of head and facial injury is believed to be less when seats face forwards.

5. THE BIOMECHANICS OF RESTRAINT

Most passengers in commercial aircraft travel facing forwards, restrained only by a lap belt. A lap belt refers to a single belt which sits across the anterior aspect of the pelvis.

5.1 THE DEVELOPMENT OF THE SAFETY BELT

In 1910 a safety belt was used in US Army airplane No. 1. A luggage strap was modified in such a way as to prevent the pilot from falling out of the aircraft (5).

During the First World War many fighter aircraft were equipped with cruciform types of upper torso restraint systems, usually without lap belts or other lower torso restraints. However, most of these early devices were developed primarily to keep the occupant coupled to the aircraft during normal operation.

In the Second World War investigations into human tolerance to ejection stress led to the realization that safety belts were more than a means of coupling the pilot to the aircraft.

In the post war era attention turned towards the use of safety belts in automobiles. Safety belts were first offered in the United States in 1955 by Ford and Chrysler (35).

The early restraint devices used in automobiles were of a lap belt design. Lap belts were subsequently replaced by seat belts, the term seat belt referring to any combination of lap and torso restraint.

5.2 THE LAP BELT

The majority of research studies into lap belt restraint originated in the automobile industry. The lap belt restraint system used in commercial aircraft is broadly similar to that used in the automobile however, differences do exist. In particular, the seat anchorage points in an automobile are different to those in an aircraft. This affects the angle at which the belt sits over the pelvis and results in an increased potential for the belt to ride up over the lower abdomen and allow "submarining" of the automobile occupant. This is associated with an increased potential for injury.

In 1962 Garrett, referring to automobiles, reported that lap belts could save at least 5,000 lives per year and reduce injuries by one third. He also stated that the reduction in the frequency of major injuries amongst belt users was related largely to the performance of lap belts in preventing the occupant from being ejected from the vehicle under crash conditions. This was confirmed by Campbell and Kihlberg in 1963 (52). Their Automobile Crash Injury Research study reported on a matched pair study of 232 lap belted occupants half wearing belts and half not. They concluded that whilst lap belts could save thousands of lives, no substantial benefits were shown beyond ejection control. They went on to state that substantial further increases in protection would probably require the use of upper body restraint in addition to pelvic restraint.

In a review of lap belt restraint systems in automobiles, Biss et al concluded that lap belts were associated with a 15-20% reduction in overall mortality but that this effectiveness was reduced to between -10% and +10% in frontal impacts, ie lap belts are partial restraint systems only and their limitations show up most markedly in the most frequent type of accident, the frontal impact (4).

Lap belts have been associated with a number of different injury mechanisms. Initially it was thought that lap belts might reduce head injury potential by directing the head at a specific target area which could be treated with energy absorbing material. However, subsequent research showed this to be a tenuous assumption at best with the head target area being difficult to predict in an oblique impact (4). Moreover the head velocity may be increased in an impact as a result of adding the vertical force vector to the horizontal force vector as the occupant jack-knives around the lap belt (i.e. a release of potential energy).

Garrett and Braunstein analyzed reports of 944 injured occupants wearing lap belts (15). There were 150 serious lower torso injuries, of which 26 might have been attributable to the wearing of the lap belt. The injuries which they related directly to the wearing of a lap belt included: intra-abdominal injuries, pelvic injuries, lumbar spine injuries and soft tissue bruising.

In 1948, Chance (49) reported 3 unusual fractures of the lumbar spine where horizontal splitting of the spinous process and neural arch occurred. The patho-mechanics of the injury were clarified by Smith and Kaufer who reviewed fractures of the lumbar spine associated with the wearing of lap belts, including 5 "Chance fractures" (34). They deduced that distraction was an important component of the disruptive force and that injury took place when the subject "submarined" under the lap belt at impact, with hyperflexion of the lumbar spine over the fulcrum of the high riding lap belt. Such injuries remain rare and in their review of 1982, Gumley et al reported that in a search of the literature only 36 Chance fractures had been identified (17).

The automobile industry realising the limitations of lap belt restraint moved to the three point belt system with its advantages in terms of upper torso restraint.

In the aircraft industry the move to a three point belt system has been resisted as such a measure would not be cost effective due to the relatively infrequent nature of aircraft accidents.

5.2.1 Human Tolerance to Lap Belt Forces in an Impact

Lewis and Stapp investigated human tolerance to lap belt forces in an impact (23).

In 1958 they reported on a series of human volunteer experiments in which the volunteers were exposed to horizontal impacts restrained by a lap belt only (3 inches width). They reported that subjective reactions to 15-20G impacts included complaints of abdominal pain. It was concluded that decelerative forces up to 10G at 300G per second rate of onset, for 0.002 second duration would result in minimal contusion over the hip region due to lap belt impingement. At 13G with the same time duration and rate of onset, in addition to contusions, strain of abdominal muscles could be expected with accompanying discomfort.

In these volunteer experiments, belt forces from 1,518 to 3,588 pounds were recorded. No serious injuries were sustained.

On one run, reported to be at 26G, the highest human voluntary impact of that series, the subject complained of severe epigastric pain persisting for 30 seconds with pain in the area of the thoracic vertebrae continuing for 48 hours. Seat belt forces in this case were 4,290 pounds.

After the M1 Kegworth accident, pelvic injuries were attributed to the wearing of a lap belt. Subsequent impact tests revealed that the occupants had experienced loads of 9kN (33).

6. THE BRACE FOR IMPACT POSITION

6.1 GENERAL PRINCIPLES

In 1988 Chandler discussed the brace for impact position (6). His comments are summarised below.

Chandler stated that the purpose of the brace for impact position was to pre-position the occupant's body against whatever it was most likely to hit during a crash and hence avoid secondary impacts.

Whilst the aim is simple, the many conditions that can exist in aircraft operations have resulted in variations in the brace position advised and this in turn has led to a lack of understanding and uncertainty amongst air passengers.

Secondary impacts take place because there is a space between the body segment and whatever it might hit during the crash. Secondary impact is a potential problem because the deceleration experienced can be much higher than the deceleration of the crashing aircraft.

Chandler points out that the effects of secondary impacts can be minimised in one of several ways:

1. The use of a restraint system either a lap belt or combination lap belt and shoulder belt system which will retard forward motion.

2. The interior of the aircraft may be designed using energy absorbing materials.

3. The body can be placed in contact with the aircraft interior thus avoiding a secondary impact.

It is this third principle which led to the recommendation of a brace for impact position.

Reviewing the evolution of the brace for impact position Chandler states that:

"In 1966 Swearingen evaluated eight different passenger seat designs by impacting a dummy head against various locations on the seat back (38). He estimated that of 34 test impacts of the head, with an impact velocity of 30 feet per second, 30% would have been fatal, 97% would have rendered the passengers unconscious, and 80% would have resulted in facial fractures. Only 3% would have produced no injury or unconsciousness. Whilst his conclusions focused on the design characteristics of seats, he also indicated the importance of a proper brace for impact position so that passengers could avoid these potentially fatal secondary impacts.

"The first study into the optimum crash brace position was performed at the Civil Aeromedical Institute (CAMI) in December 1967 by JD Garner. The test was done at the CAMI sled facility, and used two rows of passenger seats spaced at a 35" seat pitch. Passengers were represented by 95th percentile anthropomorphic dummies, which were instrumented with accelerometers in their heads. The dummies were restrained with conventional lap belts. The test indicated that the greatest head impact, as high as 80G, was recorded when dummies were initially seated in the upright position. The lowest head impacts, 8 to 32G, were recorded when the dummies were seated so that their heads were resting against crossed arms which were placed against the seat back in front of the dummies.

"The test results also indicated that bending all the way forward so that the torso rested on the thighs would put the head directly against the lower seat back in front of the dummy and compress the neck and the head between the torso and the seat, generating concern about cervical spine injury."

This study provided the basis for an early Air Carrier Operations Bulletin pertaining to the brace position (Air Carrier Operations Bulletin No.69-16/) (46).

As Chandler states:

"One of the limitations recognised by Garner in his study was that the anthropomorphic dummies then available were poor representations of the human passenger seated in the brace for impact position. The current standard 50th percentile dummy is considerably improved in both biofidelity and repeatability over the dummies available in the 1960s. These new dummies were used in a broad study of transport aircraft passenger seats conducted at CAMI in 1981. Tests to evaluate the brace for impact position were included in this series of tests.

"The tests evaluated passenger injury through the use of the Head Injury Criterion. Seven tests using three different seat designs were conducted in this series. Sled impact velocity was varied between 48.3 and 51.2 feet per second, and sled deceleration was varied between 6 and 9G. Seat pitch was varied between 30" and 34". 5th percentile female, 50th percentile male and 95th percentile male dummies were used as passengers seated behind the seats.

"The highest HIC measured in these tests was 863, well below the 1,000 level considered as life threatening. This was measured on a 95th percentile dummy which was initially seated in the upright position. Dummies placed in a brace for impact position as described by Garner in the early studies at CAMI experienced HIC values which were only about half of those measured when the dummies were seated upright."

The results of these tests were reflected in a new Air Carrier Operations Bulletin (Air Carrier Operations Bulletin No.1-76-23) (47).

Chandler stated that the best brace for impact position for each occupant of an aircraft will depend on many factors, such as the environment of the crash (magnitude, direction and sequence of crash forces), the layout of the interior configuration of the aircraft within the strike envelope of the occupant, the design and use of the seats/restraint system provided to the occupant, and the size and physical characteristics of the occupant. Obviously with so many factors involved it is impossible to describe a single simple brace for impact position which would be best in every situation. However, Chandler goes on to say, that fortunately, it is possible to identify a few general principles which will allow an appropriate brace for impact position to be selected. Such principles will involve limiting the effect of secondary impacts and reducing flailing behaviour.

1. The seat belt should always be located low on the torso just above the legs.

2. The seat belt should be adjusted after the occupant has pushed back in the seat so that the lower torso is firmly placed against the seat back.

3. The more tightly the seat belt is adjusted, the better the restraint it will provide.

4. The occupant's feet, unless the occupant is a crew member who must use the feet for aircraft control, should be placed firmly on the floor, slightly in front of the edge of the seat.

5. Passengers should not attempt to put their feet on the seat in front of them and brace with their legs, because this could double the loads acting on the seat in front. The seat is not designed to accept these additional loads and may fail. Likewise, the feet should not be wedged under the seat in front because the legs may act as levers trying to prize the seat off the floor breaking the seat legs.

6.2 FORWARD FACING PASSENGERS

Chandler states that for an occupant in a forward facing seat restrained with a lap belt, the following position should be used: *"the occupant should bend forward over the snug lap belt. If this moves the occupant's head so that it would contact the seat back or other parts of the aircraft interior, the hands and arms should be placed so that they are between the head and the contact surface, to provide secure support for the head. In the case of an occupant resting against the seat back with a "break over feature", it should be possible to get better support with the seat folded over until it rests gently on the occupant in front.*

"If the seat is located so that the head will not contact any portion of the aircraft interior as the occupant bends forward over the lap belt, the occupant should continue to bend forward and rest the upper torso against the upper leg. The head should be tucked down, and not twisted to one side. Twisting the head will twist the neck and this will reduce the ability of the neck to withstand loading during impact. Flailing of the arms may be reduced in lower energy impacts if the occupants grasp their ankles or legs."

It is pointed out that there may be installations where the forward seat is too far away to provide a secure support for the head and upper body, but will still be close enough to contact the head during the crash. It has been shown that the head strike envelope for a 95th percentile male will extend 40 to 42" in front of the intersection between the seat cushion and the seat back. If the seat interior is, for example 38" away, it will be too far away to provide support when bracing for impact, but will still be a potential source of secondary impact for the occupant. No completely satisfactory brace for impact position can be given for such installation. Perhaps the only suggestion is to take the brace position described previously and keep the head well tucked in.

6.3 REARWARD FACING PASSENGERS

Chandler advises that for the occupant in a rearward facing seat, with a seat belt restraint, passengers should be advised to push themselves back into the seat and tighten the seat belts. They should sit upright with their heads firmly against the head rest. The lower arms should be placed on the arm rest which may help to reduce loads in the spinal column. If arm rests are not available, the arms can be positioned with the hands on the thighs or clasped in front of the waist. The feet should rest flat on the floor. Clasping the hands behind the head is not recommended because this may increase the stresses on the neck due to the mass of the arms and the hands acting on the head.

IMPACT BIOMECHANICS

Viano *et al* (39), in 1939, published a review of injury biomechanics research. Much of the following section is based upon that review.

1. THE PRINCIPLES OF IMPACT BIOMECHANICS

Viano stated that:

"In an impact, injuries to the human body are caused by deformation of biological tissues beyond their recoverable limit, resulting in damaged anatomical structures or alteration in normal functions.

"The science of impact biomechanics uses the principles of mechanics to investigate and explain the physical and physiological responses to impact that result in injury.

"The aim of impact biomechanics research is to develop an understanding of an injury process so that methods may be developed to reduce or eliminate the structural and functional damage that can occur in an impact environment. To achieve this aim researchers must identify and define a mechanism of impact injury, quantify the responses of body and tissues in defined impact conditions and determine the level of response at which the tissues or systems will fail to recover. This will allow the development of protective materials and structures that reduce the level of impact energy delivered to the body."

1.1 INJURY MECHANISMS

Viano stated that:

"A mechanism of injury is a description of the mechanical and physiological changes that result in anatomical and functional damage.

"Deformation of tissues beyond their recoverable limit is the general injury mechanism associated with blunt impact trauma. This mechanism is measured in terms of strain, defined as the change in a dimension divided by the original dimension. The primary types of strain that damage tissues are tensile strain and shear strain. A third type is compressive strain which produces crushing injuries."

Biological tissues are viscoelastic and therefore the rate of loading and the strain rate are also important factors in the production of injury. In a viscoelastic structure, the faster the load is applied, the stiffer the material behaves. In addition, strain energy stored elastically in the tissue will vary with strain rate (at higher rates of deformation strain energy becomes greater for any specific amount of strain, but smaller for any specific amount of load). When loaded to failure, total energy absorption increases dramatically with increased rates of loading.

1.2 MECHANICAL RESPONSES

Viano states that:

"Once a mechanism is described or hypothesized, the biomechanical response during impact deformation must be quantified."

Ideally such response measurements would be obtained from living human subjects under various impact conditions, but this is largely not practical. People involved in accidental impacts are not instrumented with electronic measuring devices and the experimental impact of human volunteers can only be done up to the pain threshold.

Therefore, although measures of response to non injurious impact can be obtained from volunteer experiments, the primary data on impact response and injury tolerance levels must be obtained using human surrogates.

1.3 TOLERANCE LEVELS

At some measurable level of deformation magnitude and rate, the tissue will not be able to recover and damage or injury will occur. This level of response is the injury threshold and indicates the tolerance of the body organ or tissue to impact.

Although any injury is of concern, it is common in impact biomechanics to try to identify a response threshold beyond which there is unacceptable damage to tissues or structures, such as gross anatomical injury or injuries that result in a permanent alteration of normal functions. Thus, the definition of an acceptable injury is not fixed but is a function of a variety of parameters, including the body region, the type of tissue, and for experimental purposes, the type of test subject used.

The current state of knowledge concerning human impact tolerance is very incomplete, and experimental impact data are practically non-existent for adult females and for children (39).

2. EXPERIMENTAL MODELS IN IMPACT BIOMECHANICS RESEARCH

In impact biomechanics, the definition of injury mechanisms, biomechanical responses and tolerance levels, requires an exploratory approach using experimental models.

The following experimental models may be used. Each model is associated with particular advantages and disadvantages.

2.1 BIOLOGICAL MODELS

2.1.1 The Accident Victim

Although the accident victim is not an experimental model, it is an important source of data. However, careful analysis of injuries in accident victims cannot replace the experimental situation because the lack of knowledge of crash parameters means that only rarely are reliable kinematic and dynamic data available to determine relevant tolerance levels.

2.1.2 The Volunteer

The volunteer is an excellent model since he is human and living. However, when using a volunteer, the results obtained are limited and sometimes may be misleading. This is due to several reasons:

1. A volunteer can only be subjected to levels of impact up to the pain threshold.

2. The volunteer is not representative of the population at risk. Usually he is a young adult, enjoying good health.

3. In the experimental situation the volunteer can prepare himself for the impact.

In spite of these limitations, volunteer experiments can give useful information on kinematics at low impact levels. However, these data cannot be extrapolated easily to higher levels.

2.1.3 The Animal

The animal is a living model but in contrast to the volunteer, it can be subjected to high impact levels likely to produce severe injury.

However, the animal is anatomically quite different from the human. Therefore the results from animal experiments cannot be applied directly to the human situation, especially as concerns their quantitative aspects.

2.1.4 The Human Cadaver

This model contrasts strongly with the preceding models (especially the animal) because, whilst it is perfect from a morphological point of view, it is an inert model.

The main problems encountered in cadaver experiments can be summarised as follows:

1. The lack of muscle tone with, in its place, cadaveric rigidity, significantly changes the kinematic behaviour with respect to the living model.

2. The lack of blood circulation means that all organs normally turgid become flaccid. This results in lower inertia forces and decreased sensitivity to loads.

3. Experimental cadavers have very heterogeneous individual characteristics. This implies that corrective factors need to be determined and applied to the results in order to make them more homogeneous before establishing relationships between mechanical variables and body injury.

In conclusion the cadaver is a useful model especially with regard to bone tolerance but as in all the other cases, has its limitations as an experimental model.

2.2 MECHANICAL MODELS

Mertz has reviewed the roles of mechanical models (30). His comments are summarised below:

Anthropomorphic dummies are mechanical surrogates of the human body or body parts which are used to assess the potential for human injury in a prescribed impact and/or acceleration environment.

The dummies are designed to mimic pertinent human physical characteristics (size, shape, mass, stiffness, articulation, energy dissipation).

Dummy responses (head acceleration, lumbar spine and leg loads) are measured with transducers. Analyses of the timed histories of these measurements are used to estimate the potential for various types of injury to the human.

Anthropomorphic models are classified according to their physical size, for example, the height and weight of a 50th percentile adult male dummy approximates the median height and weight of the adult male population of the United States. Other adult dummy sizes are the 5th percentile adult female dummy and the 95th percentile adult male dummy. Child dummies are classified according to the age of the child they aim to represent.

The efficacy of an anthropomorphic model for injury prediction is dependant on 3 factors (30):

1. The degree to which pertinent human physical characteristics are simulated (commonly referred to as biofidelity).

2. The ability to measure appropriate mechanical responses.

3. The ability to predict injury, its type and severity based on analyses of the measured responses.

A deficiency in any one of these factors will reduce the effectiveness of the anthropomorphic model as an injury predictive surrogate.

If pertinent physical characteristics are not mimicked by the model, its responses to a prescribed acceleration or impact environment will not be representative of a human's response to the same environment and the credibility of any injury prediction based on the model's responses will be questionable.

If the model is not instrumented to measure a given mechanical response or if the relationship between a measured response and associated human injury is not known, injury prediction is made impossible.

Most anthropomorphic models mimic the total weight and size of their human counterparts accurately because these human characteristics are easy to determine and incorporate into the model design. In contrast, mass distribution is more difficult to represent as metals are usually used for the structural aspects of the model in order to provide adequate durability for testing in the severe impact environment.

Appropriate mechanical responses can be measured but the ability to predict injury from an analysis of these measured responses in the dummy, is impaired by the relative paucity of data available regarding injury tolerance in the human.

2.3 MATHEMATICAL MODELS

2.3.1 Types of Mathematical Model

Mathematical models of humans can be divided into three groups:

a) Lumped Parameter Models

These models use common engineering analogs, such as springs and dampers, to represent the tissue, fluid and bones. If the primary purpose is to represent the anatomic kinematics, lumped parameter models are excellent. They are commonly used for whole body simulations and articulated regions, such as the neck. However, these models cannot calculate stresses in the tissues or trace distribution of force in the various internal body structures. Thus, they do not predict tissue failure. Only with extensive injury test correlation can the kinematics be related to trauma.

b) Distributed Parameter Models

Models in this category are most often of the finite element type. Structures to be analyzed are divided into small elements -blocks, tetrahedrons, plates, membranes - each having the continual material properties of the host structures. The mass is concentrated at points in the corners or along the sides of the elements. These points are referred to as "element nodes". Equations for nodes are developed and then combined to form a differential equation for the entire system. Using this technique unusual shapes and combined materials can be analyzed. This procedure requires many equations. The volume of data and the number of calculations requires powerful data handling techniques. Unfortunately, the cost of the solutions increases exponentially with the increase in the number of equations. Because of the size of the matrices, non linearities are not easy to handle; they increase cost and influence computational accuracy. Non linearities produced by large rotations and displacements are especially difficult to accommodate and require special numerical analysis techniques, which few finite element codes possess. For these reasons a finite element model of the entire body does not exist.

Moreover the use of distributed parameter models for human tissue studies is rendered even more difficult as the suitable tissue properties are largely unknown.

The value of finite element idealisations lie in their ability to calculate internal stresses and subtle internal motions and displacement. This information cannot be obtained by any other means. Using these idealisations, the researcher can obtain facts that could not have been anticipated. Since failures of tissue and bone can be predicted, these models are excellent for the study of trauma, provided that the body part can be modelled.

c) Lumped and Distributed Parameter Models

To reduce the complexity of the finite element representation, regions of the body that are remote from the area of interest are approximated with lumped parameter idealisations. Although they are more difficult to solve, these hybrid models avoid some of the disadvantages of lumped parameter models and make the finite element representation of a complex biologic structure feasible.

2.3.2 Limitations of Mathematical Models

Mathematical models are valuable tools in the study of trauma. They can be used to predict responses to injury producing conditions which cannot be simulated experimentally.

However, there are limitations in mathematical modelling and these include (40):

1. Over-sophistication - This remains a problem for it is often easier to make a model overly complex than to make limiting assumptions.

2. Lack of validation - Validation is essential and correlation with experimental test data remains the most important requirement for any biodynamic model. Unfortunately experimental tests are costly in all respects and the number of experiments used to provide validation have to be limited. It is assumed that if a model's predicted response comes close to the measured result then it is validated, but this assumption is not necessarily correct and a mathematical idealisation must be tested in many situations before it can be considered validated.

3. Lack of good physical properties data.

2.3.3. Occupant Simulation as an Aspect of Flight Safety Research With Particular Application to MADYMO

Nieboer in 1992 published a review of occupant simulation as an aspect of flight safety research. Much of the following discussion is based upon that review (54).

In recent years there has been an increasing trend towards using mathematical models in crash simulation studies.

As Nieboer states *"examples of computer simulation programmes for aircraft crash safety analyses are KRASH, SOMLA/SOMTA (Seat Occupant Model - Light Aircraft/Seat Occupant Model - Transport Aircraft) and ATB (Articulated Total Body). The programme KRASH uses masses interconnected by massless beams and springs to model the crash behaviour of aircraft structures, while seats and passengers can be represented by mass-spring systems in order to obtain a rough indication of the injuries sustained (55, 56)."*

"The programmes SOMLA and SOMTA combine a three-dimensional multi-body model of aircraft occupants with a finite element model of seat structure (57, 58). SOMLA models a single occupant, whereas SOMTA has the capability to model up to three passengers. Only a fixed number of segments can be specified for representation of the occupant in SOMLA/SOMTA."

"The ATB programme is based on the CAL 3D Multi-Body Model for crash victim simulation in the automotive field."

"Due to modifications in the federal aviation regulations, in view of an increased on board passive safety level and the growing awareness that a high percentage of aircraft crashes are survivable nowadays, the aeronautics industry started to use advance simulation tools which have become commonplace in the automotive industry. Among such tools are several explicit finite element codes, especially useful in determining the crash behaviour of aircraft structures, as well as the integrated multi-body/finite element programme for crash analyses - MADYMO."

"Recently, the two-dimensional version of this programme has been successfully applied to reconstruction of seat and passenger behaviour during the M1 Kegworth accident (59)."

2.3.4. MADYMO

MADYMO is a worldwide accepted engineering analysis programme developed by the TNO Crash Safety Research Centre for the simulation of systems undergoing large displacement. The programme has been designed especially for the study of the complex dynamic response of the human body and its environment under extreme loading conditions as occurs in crash situations (54).

MADYMO combines in one simulation programme, in an optimal way, the capabilities offered by the multi-body approach (for the simulation of the gross motion of systems of bodies connected by complicated kinematical joints) and the finite element method (for the simulation of structural behaviour) (54).

MADYMO as an injury biomechanics programme offers, in addition to standard output quantities, like displacements and accelerations, which can be visualized through advanced animation and time history programmes, the possibility to calculate injury criteria like femur and tibia load, internal joint loads and HIC values. A number of standard databases are available including the 50th Percentile Hybrid III Dummy. The MADYMO model has been used in the computer simulation of the Kegworth aircrash (59).

The use of MADYMO in aircraft simulation has undoubtedly proved of benefit. Such benefits will continue as the model becomes more refined. However, like all mathematical models the output data is limited by the paucity of data relating to injury tolerance in the human subject, and is also dependent upon accurate correlation to an impact test.

3. HUMAN INJURY TOLERANCE

In this discussion of human injury tolerance I have concentrated upon those areas which I considered most relevant to this research, i.e. head, lumbar spine and lower limb. A discussion of human tolerance to lap belt forces is included in Section 5.2.1.

3.1 HEAD

A variety of head injury mechanisms have been postulated but, all are related to head acceleration. The most severe accelerations are usually the result of direct impact to the skull or face.

The actual mechanisms of injury may include the following:

1. Direct brain contusion from skull deformation at the point of contact.

2. Brain contusion from movements of the brain against rough and irregular skull surfaces (including the contre coup injury).

3. Brain and spinal cord deformation in response to pressure gradients and motions relative to the skull.

4. Subdural haematoma from movement of the brain relative to its dural envelope resulting in tears of connecting blood vessels.

The Wayne State Tolerance Curve is said to provide a dividing line that represents the onset of concussion. The curve is based on the hypothesis that the dominant head injury mechanism is linear acceleration. It was derived from experiments on embalmed cadavers striking rigid surfaces on the forehead in the antero-posterior direction for a duration of 1 to 6 milliseconds. The results were correlated with concussive effect generated in animals and were later supplemented by additional experiments on primates (16). The procedures for deriving the curve exhibited certain deficiencies and within a few years a determined effort had been made to represent the Wayne State Tolerance Curve in analytic forms. Ultimately this gave rise to the Head Injury Criterion which is now defined according to the equation

$$\mathrm{HIC} = \left[(t_2 - t_1) \quad [(1/(t_2 - t_1)) \int_{t_1}^{t_2} a(t)dt]^{2.5} \quad \mathrm{MAX.} \right]$$

Where: t_1, t_2 = any two points in time during the head impact, in seconds

$a(t)$ = the resultant head acceleration during the head impact, in multiples of g's

The Head Injury Criterion is based upon the relationship between tolerable acceleration level and the associated duration as described by the Wayne State tolerance curve, but allows the analysis of a complex acceleration-time wave form.

Statistical analysis of direct head impact cadaver test data has been used to define a relationship between HIC values and the probability of sustaining a particular level of injury, thus providing a continuous ability to interpret HIC values (16). A HIC value of 1,000 was found to produce an expected 16% incidence of life threatening brain injury in the adult population (16).

Criticisms of the Head Injury Criterion include:

1. There is no correlation between the HIC and the head injury severity.

2. Matching of the criterion to the Wayne State Tolerance Curve is erroneous.

3. The criterion considers only linear motion.

4. Its use in conjunction with dummy tests is limited by the accuracy of the specifications for such dummies and the correlation of their performance with that of the living human.

Despite these deficiencies, the Head Injury Criterion remains the most widely accepted method of assessing head injury potential and a value of 1,000 is the accepted injury threshold (13).

3.2 LUMBAR SPINE

Injuries to the spinal column may cause permanent and serious disability due to associated spinal cord injury and therefore an understanding of spinal injury mechanisms is essential.

Injuries to the lumbar spine can be grouped as follows (18):

1. **Anterior wedge fracture** - this is the most common type of traumatic lumbar spinal injury seen in automotive and aircraft crash victims. It results from spinal flexion with associated axial compression. The most common site for anterior wedge fractures is between T10 and L2.

2. **Burst fracture** - this injury is associated with higher levels of impact energy which results in the vertebral body breaking up into two or more segments. The integrity of the spinal cord is threatened in this situation. The mechanism of injury appears to be extreme flexion associated with axial compression.

3. **Dislocation and fracture dislocation** - the essential difference between a simple wedge fracture and a fracture dislocation is that in the latter case, rupture of the posterior inter-spinal ligament occurs. A high probability of neurological damage exists and the injury is considered to be unstable. Dislocations in isolation occur when a shearing force is applied to the vertebral column in a posterior to anterior direction.

4. **Chance fracture** - in this type of fracture, the vertebra is split in the transverse plane beginning with the spinous process or the posterior ligaments. The injury was first described by Chance who did suggest an injury mechanism for his observation. Subsequent studies (4) attributed the injury to the improper wearing of a lap belt restraint while involved in a frontal (-Gx) impact. The belt rides over the iliac crests and acts as a fulcrum over which the lumbar spine flexes causing separation of the posterior elements without wedging.

5. **Rotational injury** - if the spine is twisted about its longitudinal axis and is subjected to axial and/or shearing loads, one can expect lateral wedge fractures and fractures of the articular facets and laminae.

6. **Hyperextension injury** - this type of injury is usually associated with the three point harness. The mechanism is hyperextension.

Injury tolerance limits in the human spine are not well defined (18).

Human tolerance to caudo-cephalad (+Gz) acceleration has been analyzed as a result of research into ejection seats. However, such research assumed that the torso was fully restrained and hence the results cannot be extrapolated to an aircraft crash even if the major force component of the impact is in a +Gz direction.

Studies undertaken by Yamada have defined the tensile breaking load of the lumbar vertebrae to be on average 409 kg in the adult with an average compressive breaking load of 505 kg (44).

Melvin et al extrapolated injury loads in the lumbar spine of the Hybrid III dummy to the human (29). The calculations were based on injury tolerance levels determined in the cervical spine and the characteristics of lumbar and cervical vertebrae as described by Yamada. Essentially the lumbar vertebrae are larger than the cervical vertebrae but the compressive failure stress of the lumbar vertebrae is only one half of the cervical vertebrae.

The injury thresholds determined by Melvin et al were as follow:

Tension	12.7 kN
Shear	10.7 kN
Compression	7 kN

3.3 LOWER LIMB

In 1985 Melvin and Evans (28) published an extensive review of injury tolerance in the human lower limb. The subsequent section based upon static testing is based largely on data published in this review.

3.3.1 Static Testing

The earliest research into the static failure of bones was conducted by Weber in 1856 and was reported by Melvin and Evans (28). Weber determined the loads required to fracture the entire bone by three point bending transverse to the long axis of the bone. The extremity bones were mounted in a test fixture whilst still articulating with the entire body. The load measurement indicated the applied force in 245N increments with a support distance of 183 mm. The test included 509 bones from four men and five women. The maximum load to fracture for the femur and tibia is given in the table below.

Table 1 - Fracture Loads due to Bending (Weber)

	Femur	Tibia
Male, Nm	233	165
Female, Nm	180	125

The most comprehensive, and one of the earliest studies of the failure characteristics of whole bones of the extremities was conducted by Messerer in 1880 and is again reported by Melvin and Evans (28). Messerer's experiments on the bending and compression of long bones were conducted with an hydraulic testing machine that today would be considered a quasi-static universal testing machine. Load measurement was performed by an accurate beam balance system with a resolution of load differences in the order of 10 to 15N. The torsional strength of long bones was determined with a specially developed torsion testing machine.

The results of lateral bending tests with centre loading and a support span of two thirds of the length of each bone are given in Table 2. The average load and a range are given for each bone type for male and female test subjects. Bones were obtained from 6 males with ages ranging from 24 to 78 years and 6 females with ages ranging from 20 to 82 years.

Table 2 - Fracture Loads due to Bending (Messerer)

	Femur	Tibia
Male, kN	3.92	3.36
Average maximum moment,Nm	310	207
Female, kN	2.58	2.24
Average maximum moment,Nm	180	124

The torsion tests conducted by Messerer were the first of their kind. He tested the same types of bones as for his bending tests. Bones from 4 males (ages 27-56 years) and 7 females (ages 19-81 years) were tested. The table below gives the average bone fracture torques and associated ranges for males and females.

Table 3 - Failure Torques due to Torsion about the Bone Axis (Messerer)

	Femur	Tibia
Male, Nm	175 (141-222)	89 (63-110)
Female, Nm	136 (78-207)	56 (47-63)

Messerer conducted a number of different types of compression tests on long bones. These included loading whole bones in axial compression. The ends of the bones were covered with felt to prevent local failure of the bone ends. A table of failure loads for compression along the bone axis is given below.

Table 4 - Failure Loads for Compression along the Bone Axis (Messerer)

	Femur (Shaft Failures)	Tibia	Fibula
Male, kN	7.72 (6.85-8.56)	10.36 (7.05-16.39)	0.60 (0.24-0.88)
Female, kN	7.11 (5.63-8.56)	7.49 (4.89-10.37)	0.48 (0.20-0.83)

A more recent study of the static strength of long bones was conducted by Motoshima and has been summarised by Yamada (44). Motoshima determined the bending properties of the major long bones of 35 individuals. The bones were tested wet in lateral bending with a central load applied in the antero-posterior direction. The average breaking loads for five age groups are given in the table below.

Table 5 - Fracture Loads due to Bending (kN) (Yamada)

Age Groups	Femur kN	Tibia kN
20-39 Yrs	2.72±0.11	2.90±0.11
40-49 Yrs	2.47±0.05	2.52±0.11
50-59 Yrs	2.35±0.09	2.43±0.05
60-69 Yrs	2.33±0.06	2.39±0.09
70-89 Yrs	2.14±0.11	2.29±0.09
Adult Average	2.45	2.60

Motoshima found that the tibia, rather than the femur, had the highest load to fracture of any bone, in contrast to the findings of Weber and Messerer.

3.3.2 Dynamic Testing

The studies of Weber and Messerer involved, of necessity, the static measurement of failure loads. Virtually all forms of skeletal trauma, involve rapid or dynamic loading of the bones. It is only in the last 30 years that methods able to produce dynamic loads experimentally have been developed and accurate measurements taken. Interest in this area has been generated largely by the automotive safety problem of protecting vehicle occupants in crashes.

Bone, like many biological materials, exhibits viscoelastic or rate-sensitive behaviour. Thus, it is expected that, under dynamic loading, a particular bone would require a greater load and a smaller deflection to produce a fracture when compared to the static loading situation.

Mather (27) demonstrated this effect using 32 pairs of human femurs. One member of each of the paired sets was tested statically in a materials testing machine, and the other matching member was tested in a drop-weight testing apparatus with an impact velocity of 9.75 m/sec. The impact load was not measured directly, but the test apparatus was capable of indicating the impact energy absorbed by the bone. These data were compared to the static energies absorbed by the companion bones as calculated from the areas under the load-deflection curves for the static tests. The mean value of the ratio of dynamic energy to static energy was 1.66, and wide variations among the ratios were evident (standard deviation 0.77). The mean static energy to failure was 28.7 joules, while the mean impact energy to failure was 42.5 joules. This represents a 48% increase due to impact loading.

Torsional loading of the long bones with the lower extremities has become of particular interest in relation to skiing injuries. Martens et al reported on a study involving femoral and tibial bone samples obtained from 65 autopsy subjects ranging from 27 to 92 years of age (25). The ends of the bones were embedded in blocks of plastic and loaded in torsion by an impact torsional loading machine. The time of loading to failure was less than 100 ms. The femoral test produced a mean torque load to failure for males of 204Nm (range 122-291). For the tibia the mean torque load to failure was 111Nm (range 70-179) for males and 71.4Nm (range 61-159) for females. Comparisons of these values with those values of Messerer (see table) shows that for the male data, the mean dynamic failure torque are greater than the comparable static values. The female data for the tibia are in agreement with the male data with a 27% increase. The female femur dynamic value however is actually lower than the static value. This is most likely due to bone dimensional defects with Messerer's smaller sample (7 versus 13 tests) being influenced by two large bone subjects. The average energy to failure for dynamic torsional loading was, for the femur, 37.5 joules (male) and 29.8 joules (female) and, for the tibia, 27.3 joules (male) and 18.4 joules (female).

These values are comparable in magnitude to the bending failure energy of Mather.

Recent research into the response of the human leg to dynamic loading has been undertaken by St-Laurent et al (36). The research involved the development of a motorcyclist anthropometric test device and the following values were selected for the dynamic properties of the surrogate bones:

Femur:	
Axial compressive load (dynamic)	10.5 kN
Bending load (dynamic)	328 Nm
Tibia:	
Axial compressive load (static)	10 kN
Bending load (static)	294 Nm

The bone of the lower extremities can be subjected to a variety of dynamic loads in impact accidents. This is true for both restrained and unrestrained occupants. The first research into the impact tolerance of the lower extremities with respect to the automobile occupant was by Patrick et al (31). Ten unrestrained, seated and embalmed cadavers were impacted into the instrumented chest, head and knee targets designed to simulate a vehicle interior. Fractures of the femur were produced at loads as low as 6.67kN while loads as high as 17.13kN were sustained with no fracture of the femur but with fractures of the patella and pelvis. A majority of the femoral fractures were found to occur at the distal end of the bones. The authors concluded that failure of the femur occurred at slightly lower load levels than in either the patella or pelvis. They suggested a conservative overall injury threshold level of 6.23kN which was later increased to 8.68 kN (31).

3.3.3 Variation in Skeletal Strength

In the above discussion the mean load to failure for different loads applied to different bones have been given. The strength of an individual's bones will depend upon many factors.

Bone strength is diminished in the elderly as a result of bone loss (20). Such effects are more marked in females who experience a period of accelerated bone loss in the immediate post menopausal period.

THE M1 KEGWORTH ACCIDENT

On 8th January 1989, a Boeing 737-400 aircraft (G-OBME) crashed on the M1 motorway near Kegworth, England. The aircraft was relatively new and had only 512 hours of flying time before it crashed whilst on its final approach to East Midlands Airport.

The crash sequence consisted of two impacts. On final approach and under reduced engine power, the aircraft, in a nose-up attitude, struck the top of the eastern motorway embankment after which the aircraft, rotating to a nose-down trajectory, made its final impact at the base of the western embankment. This impact generated high horizontal and vertical loads and resulted in severe fuselage damage.

The accident was unusual in several respects. Firstly, the loads generated were high and approached the survivable limit. Secondly, there was no post-crash fire. Hence a large number of seriously injured patients survived the accident.

Subsequently, the NLDB study group was formed under the direction of Professor W. A. Wallace and Mr C. L. Colton. The study group was so named as it included surgeons from the four main hospitals involved in the treatment of the survivors, ie Nottingham, Derby, Leicester and Belfast.

Uniquely, this study group brought together in one accident investigation clinicians, pathologists and accident investigators from the Air Accident Investigation Branch of the Department of Transport. A large amount of information was accumulated on the accident and a number of reports were published which included recommendations relating to aircraft safety (33).

There were 118 passengers on board the aeroplane including one baby, and eight crew members. 87 passengers survived the initial impact although there were 4 subsequent deaths within a short time of arrival at hospital and 4 deaths at a later date from complications.

A large number of injuries were recorded, affecting all body regions (Fig. 1). There was a preponderance of injuries to the head and the lower limbs. If there had been a fire these injuries would have severely hindered the ability of the occupants to escape. It has been shown that in an aircraft accident, where fire supervenes, up to 40% of the deaths will be attributable to the fire.

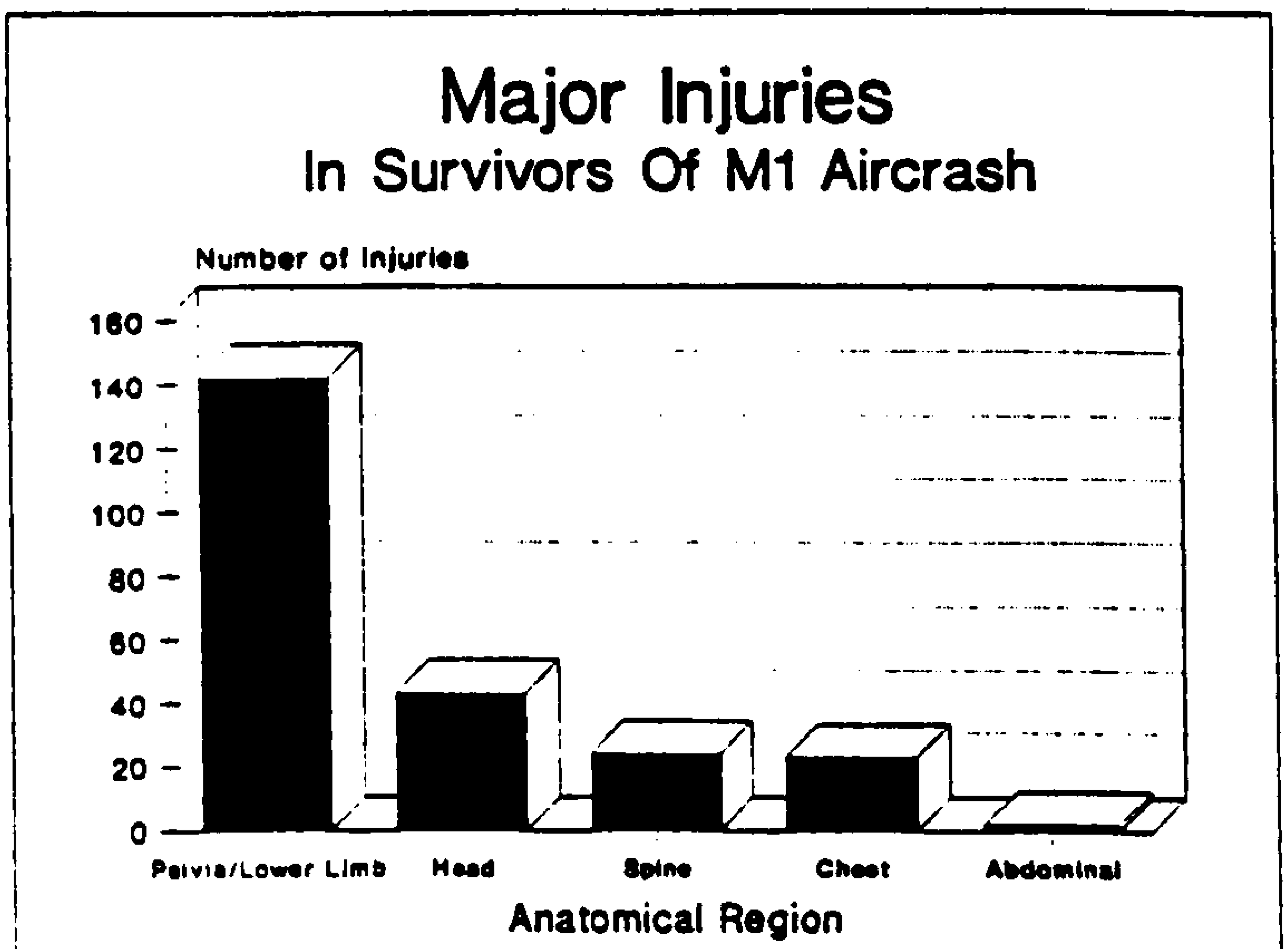

Fig. 1

There were 35 head injuries and 7 required neuro-surgical intervention. A large proportion of these injuries affected the posterior aspect of the skull. It was a conclusion of the NLDB study group that such injuries were related to objects falling down from the overhead luggage bins onto the passengers during the impact. It is a fact that at the end of the impact only one of the overhead luggage bins remained attached to the fuselage. (1)

Injuries to the lower limbs and to the pelvis were prevalent also. The injury mechanisms involved were investigated by reviewing the clinical records of the passengers involved in the accident and by impact testing using anthropomorphic test dummies. In addition, mathematical modelling was undertaken to define the occupant kinematics during the crash. This research has been described elsewhere by JM Rowles (33).

Mechanisms of pelvic and lower limb injuries in impact accidents have been related to axial loading of the femur and flailing of the lower limbs. Such a mechanism has found wide acceptance in the automobile industry. This mechanism involves the passenger being thrown forwards on impact so that the knees strike the bottom of the seat ahead causing trauma to the knee, upper tibia and lower femur. The impact forces are subsequently transmitted up the femur driving it backwards into the pelvis. This leads to femoral shaft fractures, hip dislocations, acetabular fractures and pelvic shear fractures.

As a result of the research performed under the auspices of the NLDB Study Group, the validity of such a mechanism was questioned in the seated occupants of an aircraft accident subjected to a similar crash pulse (33).

Clinical review revealed that a variety of fracture types were seen (including transverse) in the survivors suggesting one simple mechanism of injury could not explain all femoral fractures. In addition, no associations were found between soft tissue witness marks around the knee (indicating impact with the seat ahead) and femoral fractures (33).

Impact testing revealed no evidence of knee contact with the back of the seat ahead in the test configurations used. In addition the femur appeared to be loaded in a bending type configuration (33).

These findings were subsequently confirmed by mathematical modelling undertaken by HW Structures Ltd.

Subsequently, a modified brace for impact position was suggested which it was hoped, might minimise the potential for lower limb injury.

STUDY OBJECTIVES

1. To evaluate the effects which changes in body posture and seat pitch have upon the loads generated in the head, lumbar spine, pelvis and lower limbs of a 50th percentile occupant seated in a Weber type aircraft seat when exposed to horizontal and vertical impact pulses.

2. To correlate a three dimensional mathematical model against such impact tests.

3. To use the correlated mathematical model to explore further the effects which changes in specified parameters have upon the loads generated in the head, spine, pelvis and lower limbs of a passenger in a simulated impact.

IMPACT TESTING

The experimental method was based upon the Aerospace Standard AS8049 issued in 1990 which defined the performance standard for seats in civil rotorcraft and transport aeroplanes (13).

1. THE IMPACT TEST FACILITY

Impact testing was performed at the RAF Institute of Aviation Medicine, Farnborough. The impact test facility consists of a linear decelerator track as described by Dutton (11) (Fig. 2).

The decelerator track is 46 metres long. A test vehicle rides on the track and acts as a moving platform on which a variety of structures may be carried.

Vehicle propulsion is provided by stretched bungee cords.

To prime the system, the vehicles are pulled to the release position by a winch located at the release end of the track.

After release, the test vehicle and pusher accelerate together for a distance of 26 metres. The pusher is then arrested and the test vehicle coasts for a further 13 metres before it hits the main arrestor gear and is decelerated.

The main arrestor gear consists of 5 steel cables, stretched across the track. The cables pass around grooved bollards on either side of the track and each end is connected to the piston of an hydraulic cylinder. Hydraulic pressures of up to 17.25 MN/m^2 are built up within the hydraulic cylinders during operation by throttling the escape of the fluid into adjacent reservoirs. This causes a deceleration to be applied to the vehicle as it impacts and displaces the cables. The magnitude of the deceleration can be altered by varying the size of the orifices through which the hydraulic fluid is forced.

IMPACT TEST FACILITY

Fig. 2 Linear decelerator track, RAF IAM, Farnborough

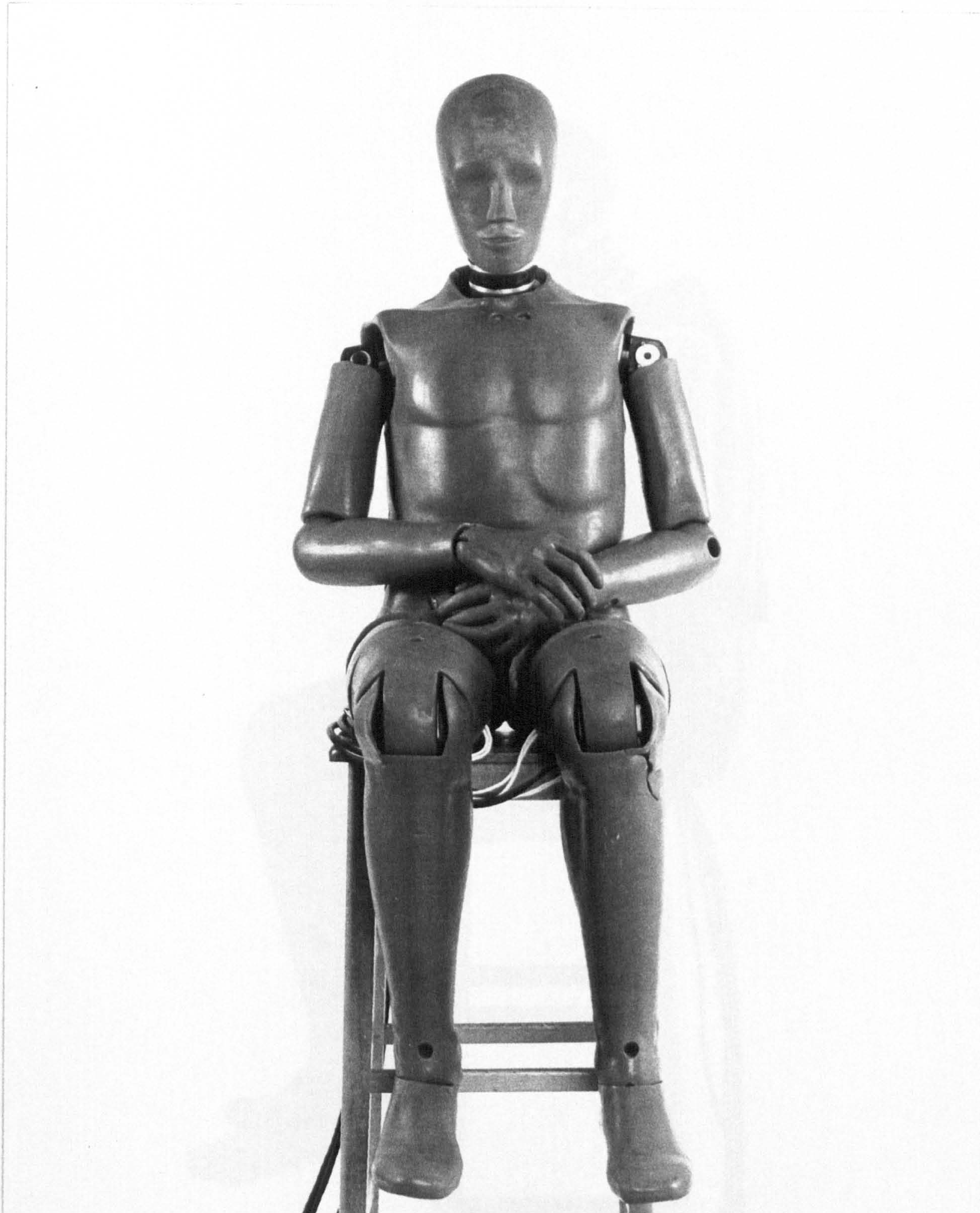

Fig. 3a Hybrid III Anthropomorphic Test Dummy (Front View)

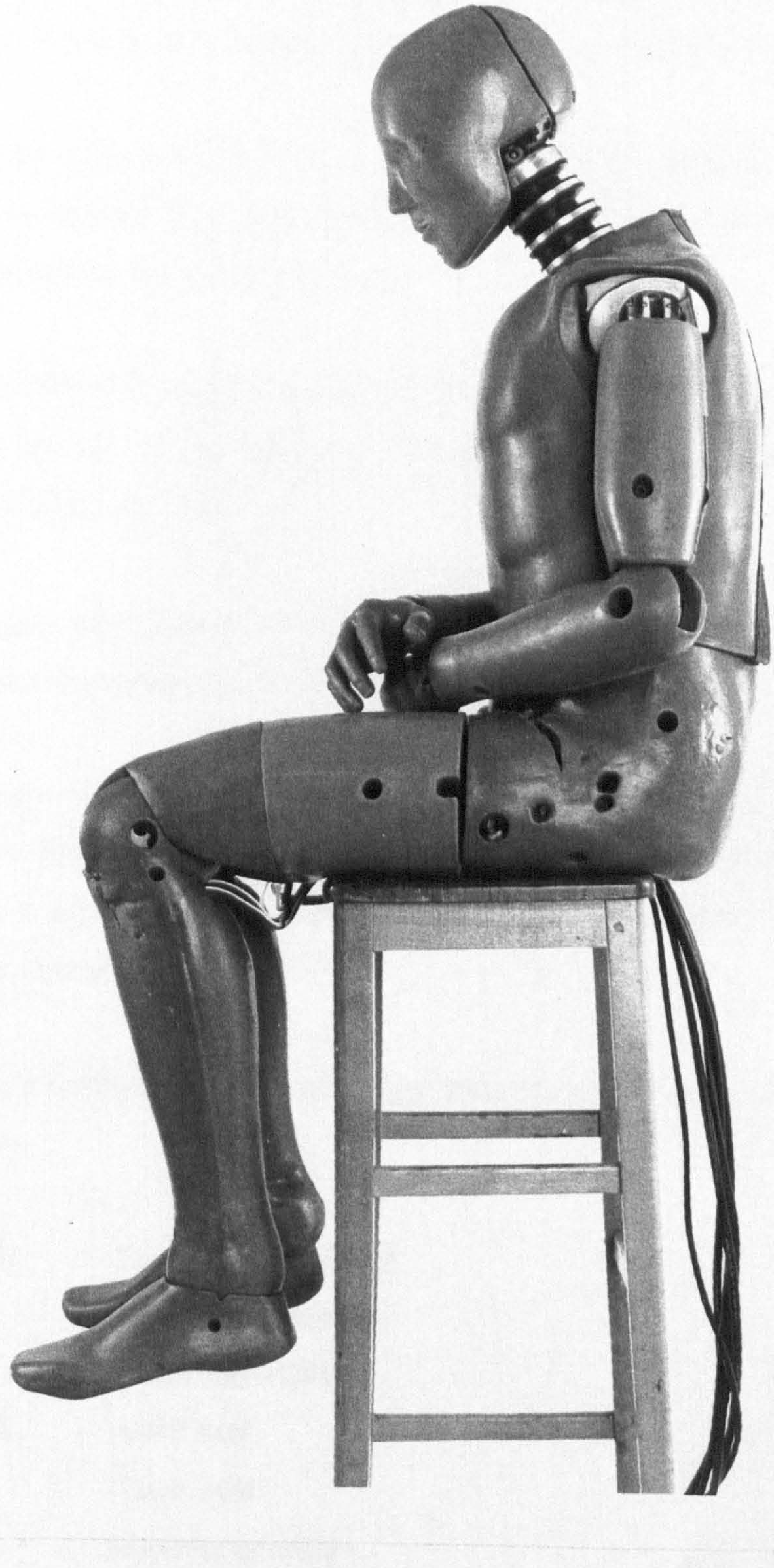

Fig. 3b Hybrid III Anthropomorphic Test Dummy (Side View)

2. THE EXPERIMENTAL MODEL

Aerospace Standard 8089 specifies that a Part 572B anthropomorphic dummy (ATD) representing a 50th percentile male be used as the experimental model.

This Part 572B anthropomorphic dummy has now been superseded by the Part 572E or Hybrid III anthropomorphic dummy in the automobile industry but not, as yet, in the aviation industry.

As the Hybrid III anthropomorphic dummy is the more advanced dummy, and in the absence of any alternative, this dummy was used as the experimental model (Figs. 3a, 3b).

The fully instrumented Hybrid III provides 44 response measurements for assessing occupancy protection potential.

The only biofidelity improvements made to the Hybrid III since 1977 have been to the knee and ankle joints. The current knee joint design allows the leg to translate relative to the thigh in a human-like fashion. The ankle joint allows lateral flexion.

The measurement capacity of a fully instrumented Hybrid III dummy is as follows:

HEAD	Tri-axial acceleration
	Angular acceleration
	Facial Laceration
NECK	Axial load
	Shear load
	Bending moment
CHEST	Tri-axial acceleration
	Sternum acceleration
	Deflection

PELVIS Tri-axial acceleration

Anterior/superior iliac spine load

UPPER EXTREMITIES

Lower arm bending moment

LOWER EXTREMITIES

Femur load

Femur/tibial translation

Tibia bending moment

Tibia axial load

Medial/lateral tibia plateau load

Lateral or fore/aft ankle bending moment

Shear load

Knee acceleration

The ATD may be modified to include a lumbar load cell to measure the axial compressive load between the pelvis and lumbar column.

3. VEHICLE AND DUMMY INSTRUMENTATION

The vehicle and dummy transducers used in the experiment operated by way of a bridge circuit. Signal conditioning equipment provided the power, then detected and amplified the bridge output.

The load cells used in the dummies were supplied by Robert A Denton Inc. of Michigan. USA and were issued with calibration certificates. Other transducers used included a vehicle accelerometer manufactured by Philips and Endevco Triaxial accelerometers manufactured by Endevco UK Ltd, Melbourn, Royston, Herts. The lap belt force link was manufactured by Kistler Instruments Ltd, Whiteoaks, The Grove, Hartley Wintny, Hants, England.

The instrumentation used complied with Aerospace Standard 8049.

Vehicle acceleration was measured in accordance with the requirements of Channel Class 60.

Restraint system loads were measured in accordance with the requirements of Channel Class 60.

ATD head accelerations used for calculating the head injury criterion (HIC) were measured in accordance with the requirements of Channel Class 1000.

ATD femur forces were measured in accordance with Channel Class 600.

ATD pelvic/lumbar column force were measured in accordance with the requirements of Channel Class 60.

Table 6 below gives an outline of the transducers:

CH	LOCATION	MODEL	SER NO	EXC V	GAIN	FSD SI	UNIT	SENS mV/V
1	R Tibia L Clev	1587	392	10	500	8900	N	1.233
2	R Tibia R Clev	1587	392	10	500	8900	N	1.247
3	Upr R Tib My	1583	423	10	500	395.5	Nm	2.96
4	Lwr R Tib My	1584-A	411	10	500	395.5	Nm	2.902
5	Lwr R Tib Fz	1584-A	411	10	500	11125	N	0.969
6	L Tibia L Clev	1587	391	10	500	8900	N	1.21
7	L Tibia R Clev	1587	391	10	500	8900	N	1.255
8	Upr L Tib My	1583	415	10	500	395.5	Nm	2.889
9	Lwr L Tib My	1584-A	410	10	500	395.5	Nm	2.958
10	Lwr L Tib Fz	1584-A	410	10	500	11125	N	0.97
11	R Femur Fx	1914A	220	10	500	13350	N	1.906
12	R Femur My	1914A	220	10	500	339	Nm	1.502
13	R Femur Fz	1914A	220	10	500	22250	N	1.174
14	L Femur Fx	1914A	219	10	500	13350	N	1.917
15	L Femur My	1914A	219	10	500	339	Nm	1.501
16	L Femur Fz	1914A	219	10	500	22250	N	1.185
17	R Femur Fy	1914A	220	10	500	13350	N	1.909
18	R Femur Mx	1914A	220	10	500	339	Nm	1.499
19	R Femur Mz	1914A	220	10	500	339	Nm	2.653
20	L Femur Fy	1914A	219	10	500	13350	N	1.922
21	L Femur Mx	1914A	219	10	500	339	Nm	1.516
22	L Femur Mz	1914A	219	10	500	339	Nm	2.674
23	Lumbar Fx	1842	99	10	500	13350	N	0.934
24	Lumbar My	1842	99	10	500	565	Nm	1.719
25	Lumbar Fz	1842	99	10	500	13350	N	0.945
26	Vehicle Acc	PR9367	L0701	4	1200	50	G	0.514
27	Head Gx	7267A	BB61	10	500	1500	G	19.17
29	Head Gz	7267A	BB61	10	500	1500	G	20.655
31	Lapbelt	300796		-	-	-	N	4 Pc/N
32	Head Gy	7267A	BB61	10	500	1500	G	22.065

The vehicle was fitted with an accelerometer to record the acceleration of the test fixture.

An accelerometer was placed in the head to record head acceleration in the horizontal (Gx and Gy) planes and in the vertical (Gz) plane. This permitted calculation of the Head Injury Criterion.

Lumbar loads were recorded using a pre-calibrated load cell which measured axial (Gz) forces, shear (Fx) forces and bending moments (My).

The lapbelt loads were measured using a pre-calibrated force link attached in series to the belt (but without cutting of the webbing) which had the effect of decreasing the amount of webbing in the belt by 14cm and this causing a minor alteration to the lap belt extensibility.

Femoral loads were recorded using pre-calibrated 6 axis load cells located at the mid-point of each femur. Forces were recorded in the vertical (Fx) and lateral (Fy) axis. Axial (Fz) forces and bending moments about the y, x and z axis.

Tibial loads were measured using pre-calibrated 3 axis load cells located in the upper and lower tibia of each leg. The forces measured by the upper load cell included forces around the knee (left and right) clevis and the bending moment about the Y axis. The lower load cell was used to record axial (Fz) forces and bending moments about the Y axis.

4. DATA ACQUISITION

4.1 DATA TRANSMISSION

Data was transmitted from the vehicle through a system of flying leads. The cable used was Filotex Multicore containing 25 wires per cable. Each channel required four wires, allowing six channels per cable. It is advisable to use the minimum number of cables in each test due to the friction which results from the cables dragging as they are drawn down the track. This friction has the overall effect of reducing the vehicle speed by 0.5 metres per second.

The flying leads were linked to the transducers via a patch panel mounted on the vehicle. This box consisted of 30 sockets so that channels may be easily interchanged.

At the other end of the leads was a similar panel mounted on the wall of the control room to which the signal conditioning equipment was connected.

4.2 SIGNAL CONDITIONING EQUIPMENT

With the exception of the lap belt load cells which used charge amplifiers, all the transducers required signal conditioning equipment to supply power to the bridge and to apply a gain to the output of the unbalanced bridge. The instrumentation used at the IAM were 2100 Series Strain Gauge Conditioning Amplifiers supplied by Vishay Measurements Group of North Carolina, USA. These amplifiers can provide bridge excitation of up to 12 volts and a gain of up to 2100.

The control panel provides for simple balancing of both amplifiers and bridge circuits.

4.3 DATA COLLECTION

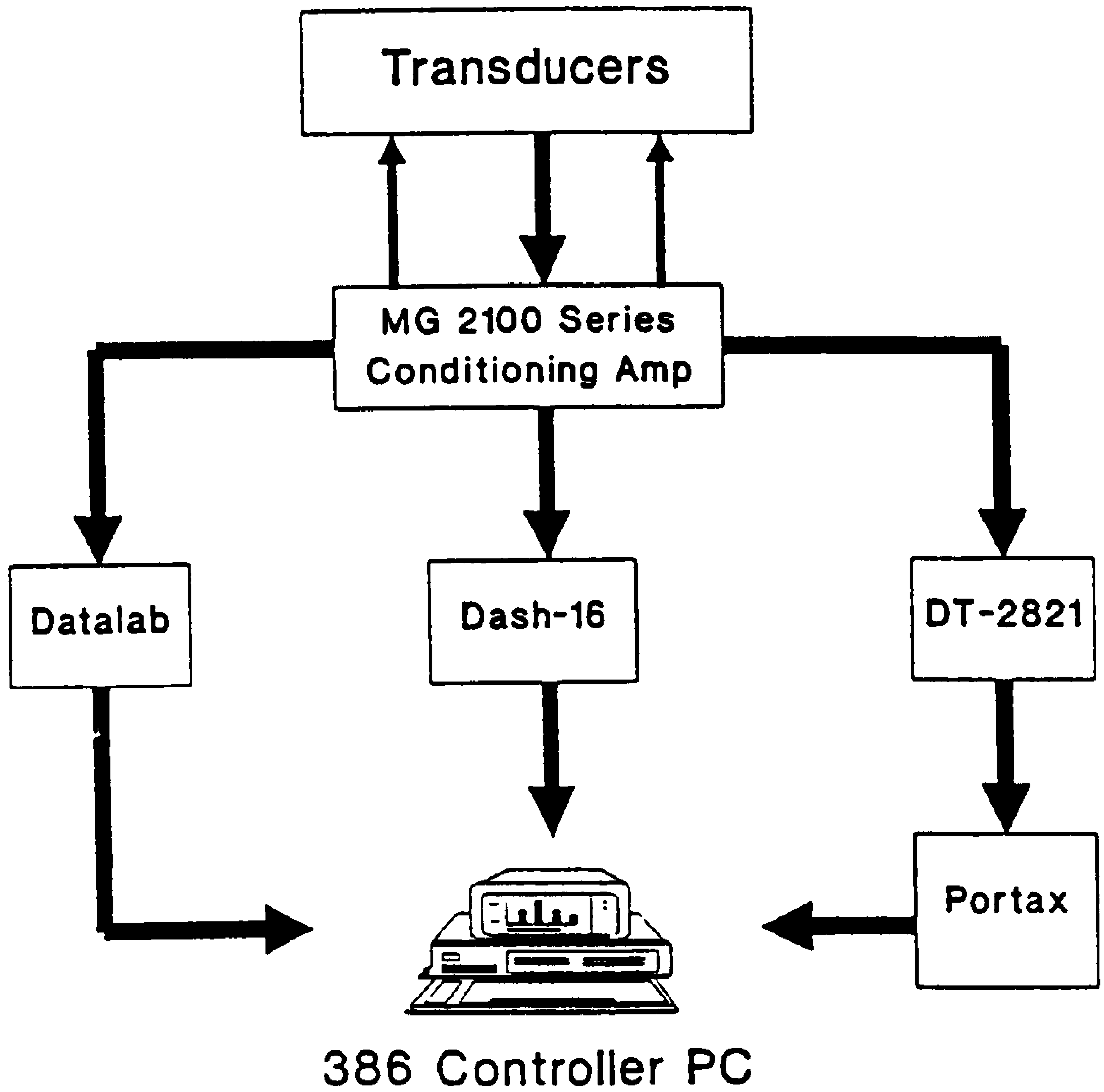

Fig. 4 Decelerator Track Data Acquisition System

The conditioned data was collected in three ways:

1) Dash 16 Acquisition Board

2) The Datalab Transient Recorder

3) The DT-2821 Acquisition Board (Portax)

Dash 16 Acquisition Board

This was the central method of data acquisition and was mounted inside the track computer. The Dash 16 is a high speed programmable analogue/digital expansion board for IBM compatible personal computers. The Dash 16 board has 12 bit resolution and is capable of a total of 100,000 conversions per second. The Dash 16 contains an additional port which takes an input from the velocity meter. This acts as the triggering mechanism.

Datalab Transient Recorder

The Datalab Transient Recorder is fundamentally different from the Dash 16 in operation. It contains 19 individual memory modules linked together by a master timebase and controller. Each memory module is capable of storing 4096 words, each of 10 bit resolution.

When sampling is complete the impact data is stored in the memory module. The information is then down-loaded into the track computer.

<u>DT-2821 Acquisition Board (Portax)</u>

This is a 16 channel data acquisition card which is mounted in a reinforced PC supplied by Kayser UK. The board is similar in operation to the Dash 16 and is also controlled and armed from the keyboard.

In summary, signals derived from the load cell transducers are transmitted via the flying leads to the conditioning amplifiers. From the conditioning amplifier the amplified analogue signals are then collected via either the Datalab Transient Recorder, the Dash 16 Acquisition Board or the DT-2821 Acquisition Board (Portax) with a common timebase. All information is then further downloaded into the track computer.

<u>Track computer</u>

The track computer is an IBM compatible PC.

Type 386 PC

Memory 640K (4096K with expanded memory)

Hard Disc Drive 120 Megabytes

The computer uses software designed by Surgeon Commander P J Waugh, RAF Institute of Aviation Medicine, Farnborough. The language used is Asyst, a scientific programming language produced by Keighley Instruments of Great Britain.

<u>Asyst Scientific Software</u>

Asyst is a PC based scientific programming language. It is designed for the acquisition, analysis and presentation of data.

Illustration shows a forward-facing seat Inertial load shown by arrow	TEST 1	TEST 2
	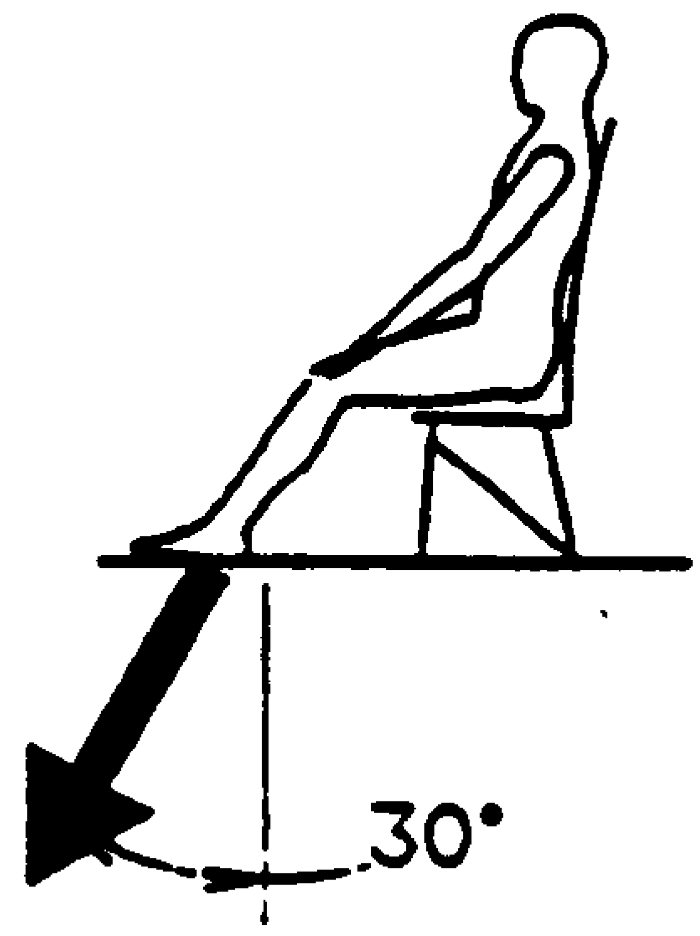 	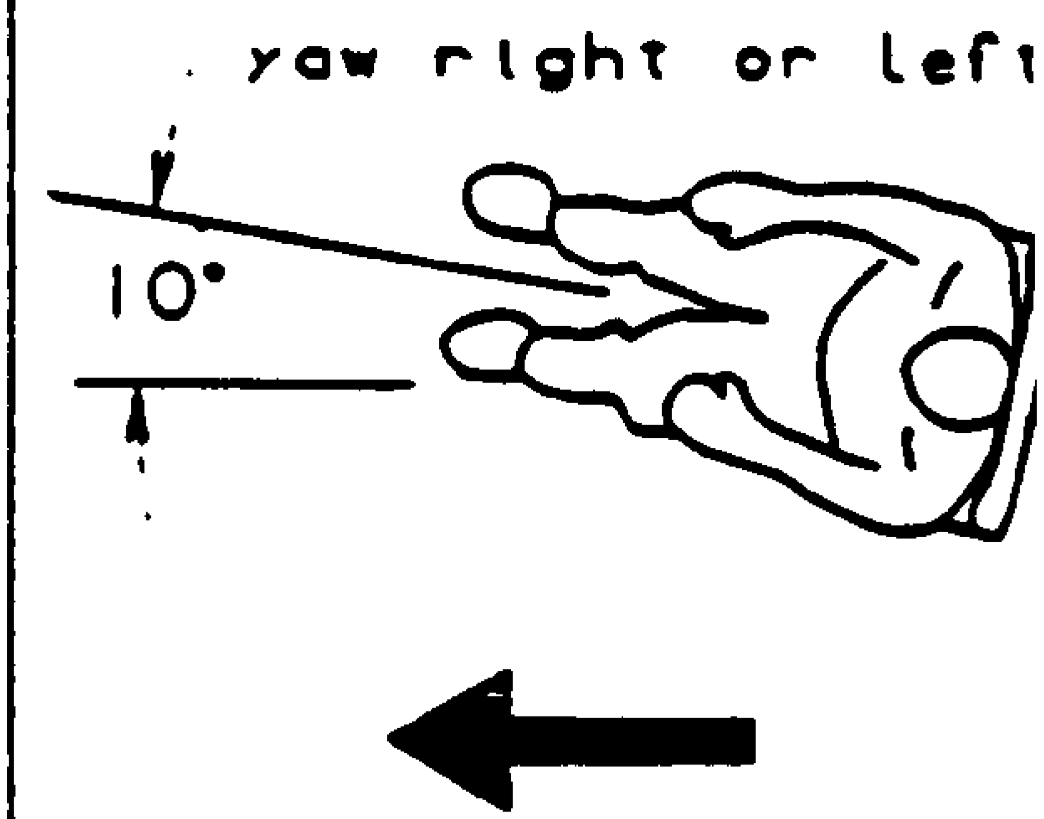
Min V_I m/s (ft/s)	10.67 (35)	13.41 (44)
Max t_r s	0.08	0.09
Min G.	14	16
Deform floor:		
Degrees roll	0	10
Degrees pitch	0	10

Test Pulse Simulating Aircraft Floor Deceleration-Time History:

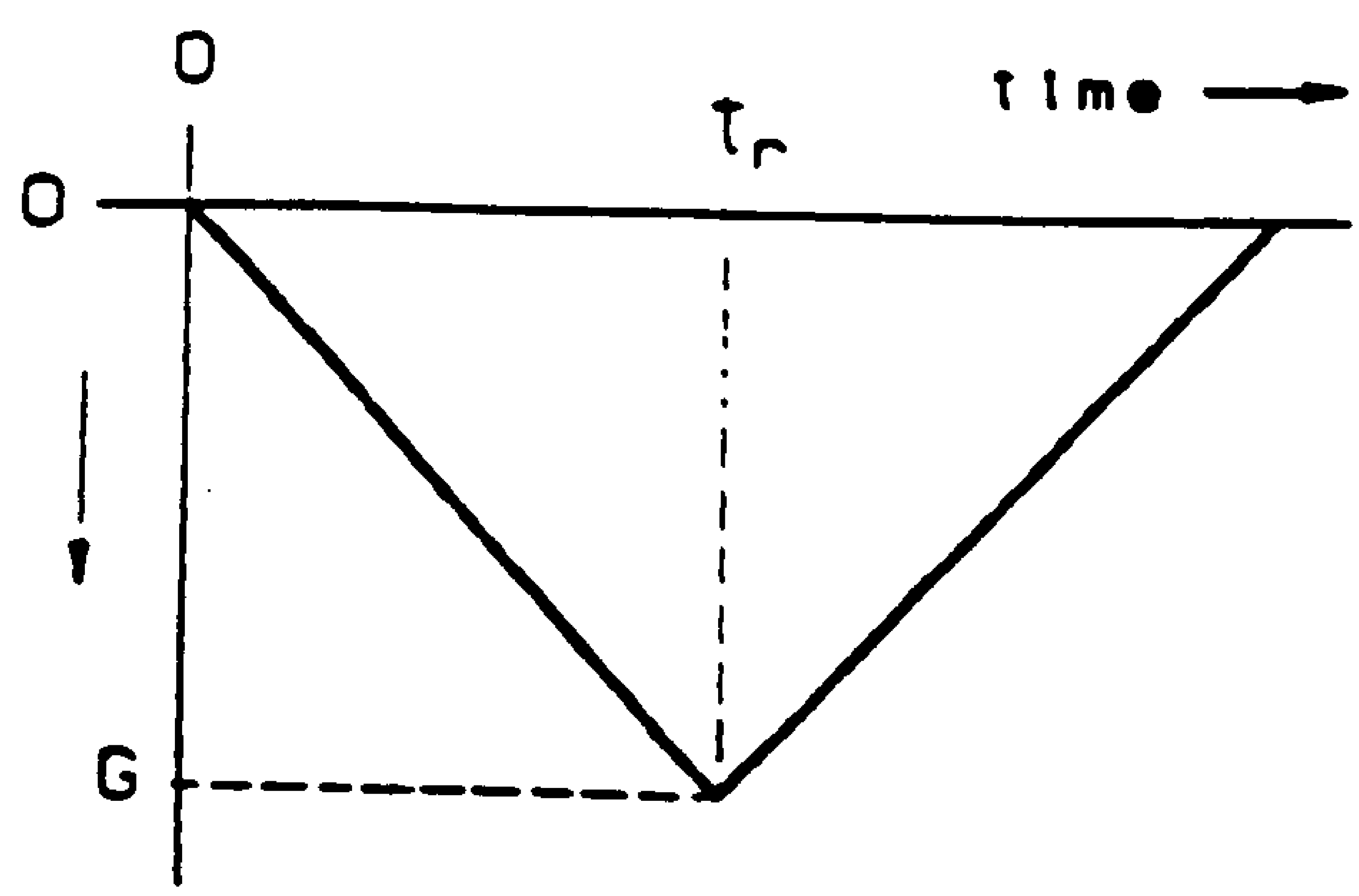

t_r = rise time

V_I = Impact Velocity

Fig. 5 Seat Dynamic Tests (Aerospace Standard 8049)

5. CALIBRATION

The load cells and the lapbelt force link were pre-calibrated at manufacture. A calibration signal was injected into the system and allowed conversion to SI units.

The accelerometers were calibrated on a centrifuge of known radius. Revolutions per minute were recorded on a calibrated tachometer. Calibration signals were therefore obtained by connecting the accelerometer to the datalab whilst centrifuging at a known rate. Calibration was carried out at the beginning of the experiments and at the end to confirm the integrity of the system.

6. IMPACT PULSES

Aerospace Standard 8049 specifies two tests for the dynamic evaluation of aircraft passenger seat performance. The impact pulses described were defined after review of previous aircraft accidents (14) and were thought to be of a magnitude which was compatible with current standards in terms of design strength of the aircraft fuselage and passenger compartment floor.

Two tests were described, one which represents predominantly vertical impact and a second which represents a predominantly horizontal impact (see Fig. 5).

Test 1:
This test, determines the performance of the system in a test condition where the predominant force component is along the spinal column of the occupant in combination with a forward impact force component as a result of the 30° pitch angle. This test evaluates the structural adequacy of the seat, critical pelvic/lumbar column forces and permanent deformation of the structure under downward and forward combined impact loading.

Test 2:

This test, determines the performance of a system where the predominant impact force component is along the aircraft longitudinal axis and is combined with a lateral impact force component as a result of the 10° yaw orientation. This test evaluates the structural adequacy of the seat and pelvic restraint behaviour and loads.

For seats placed in sequential rows an additional test condition using two seats in tandem placed at representative fore and aft distances between the seats (seat pitch), similar to Test 2, with or without the floor deformation, directly evaluates head and femur injury criteria. These injury criteria are dependant on seat pitch, seat occupancy and the effect of hard structures within the path of the head excursions in the -10 to +10° yaw attitude range of the Test 2 conditions.

Aerospace Standard 8049 was issued to provide performance standards for seats in civil rotorcraft and transport airplanes.

As the purpose of this experiment was to define the optimum crash brace position in an impact aircraft accident, the tests were modified and the impact pulses incorporated into two separate experiments.

Figure 6 shows the convention of signs for linear acceleration.

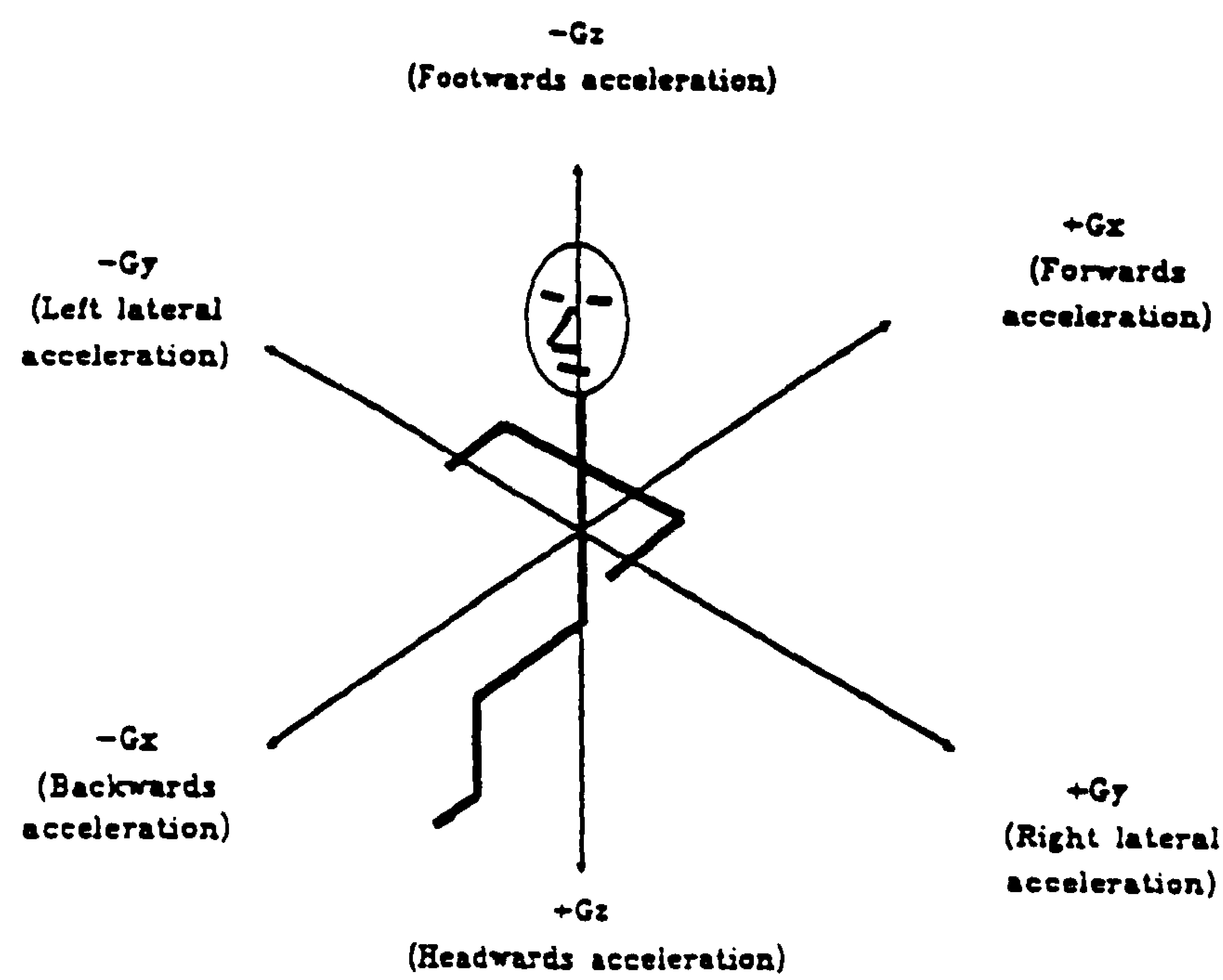

Fig. 6 Convention of Signs for Linear Acceleration

Fig. 6 Convention of Signs for Linear Acceleration

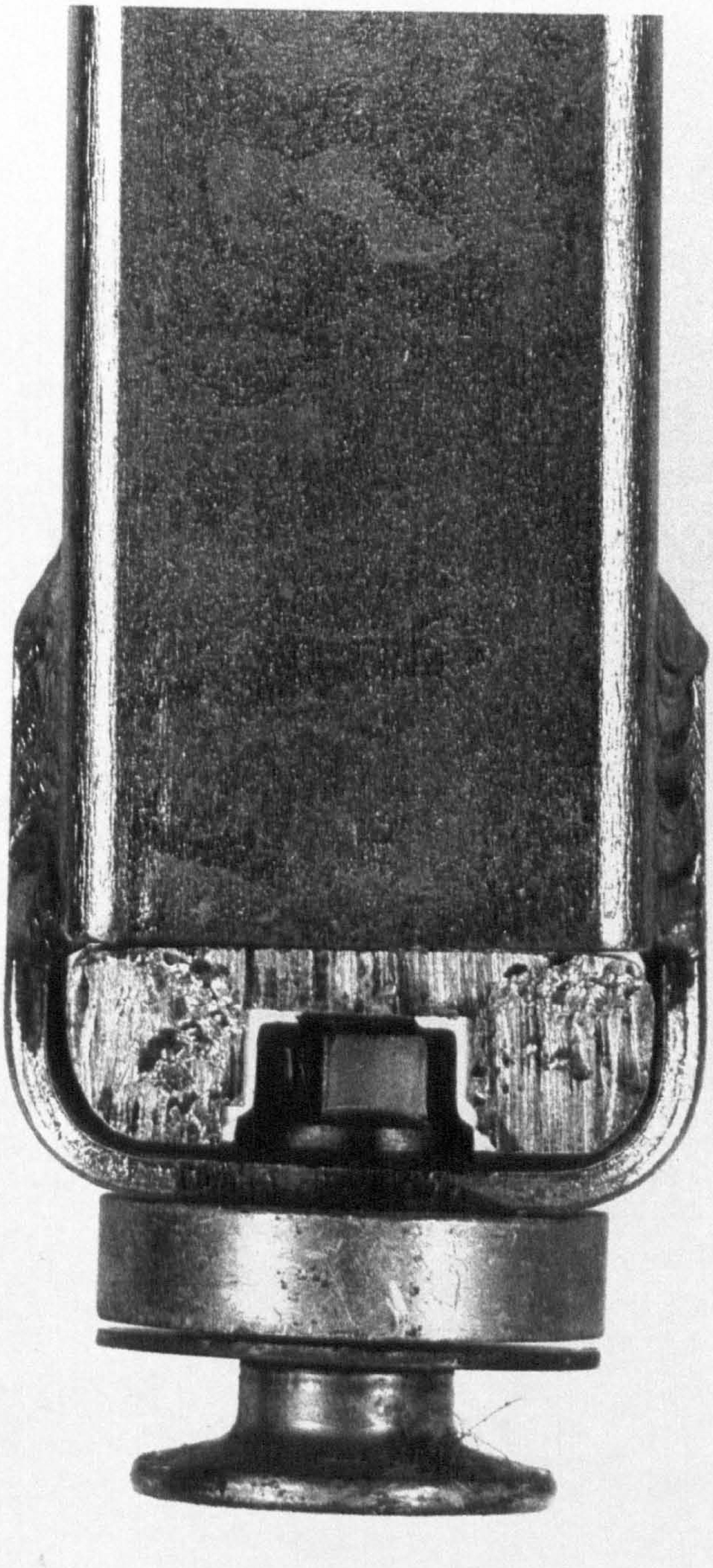

Fig. 7 Seat Leg Showing Reinforcement

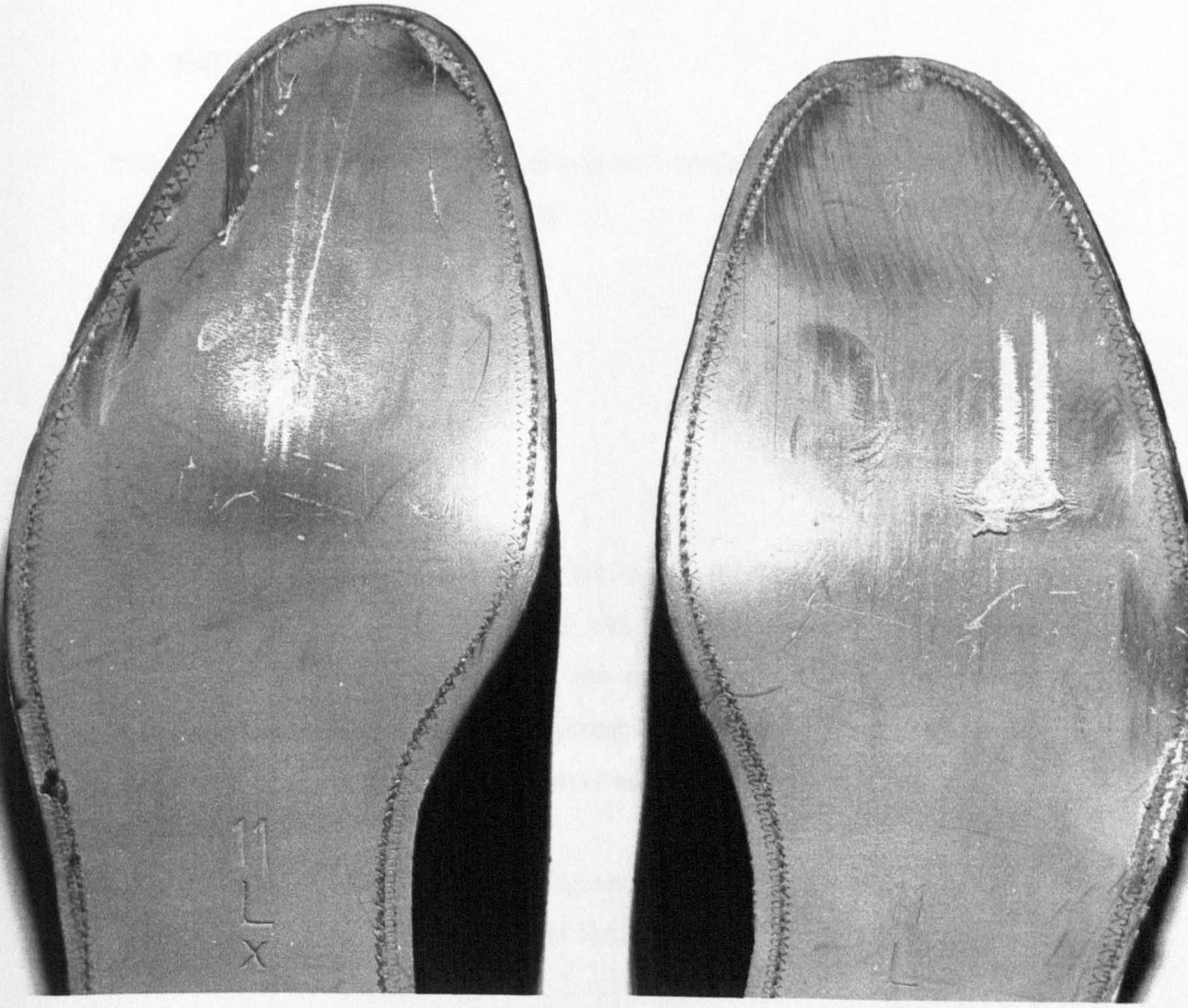

Fig. 8 Shoes used in testing showing smooth leather sole

7. EXPERIMENT 1 - Horizontal (-Gx IMPACT)

7.1 OBJECTIVE

To compare the values obtained from the transducers fitted to the dummy, for four dummy positions at two seat pitches during a horizontal (-Gx) impact.

7.2 IMPACT PULSE

The impact pulse measured on the vehicle was similar to the FAA -16G pulse specified in Aerospace Standard 8089.

Min G. = 16

Min Vt (m/s) = 13.41 (44 ft/s)

Max tr (s) = 0.09

Vt = Impact velocity

tr = rise time

However, no floor deformation was introduced prior to the test. (The seat structure itself was not being tested and the purpose of providing floor deformation is to demonstrate that the seat/restraint system will remain attached to the airframe and perform properly, even though the aircraft and/or seat are severely deformed by the forces associated with a crash.)

The seat was not aligned with 10 degrees of yaw in order to facilitate data interpretation by removing the lateral force component.

7.3 TEST FIXTURE

7.3.1 Seat

A multiple row test fixture (two rows of three seats in each row) was used to best evaluate head and knee impact conditions (Fig. 9a).

Undamaged or minimally damaged seat rows were taken from the Kegworth accident (G-OBME).

The seats were subjected to non destructive testing by the RAF (including magnetic particle analysis) prior to the experiment.

The seats were Weber Aircraft Forward Facing Passenger Seats (Specification NAS 809 Type 1) (13).

Two rows of seats were mounted onto the test vehicle.

The joint at which the seats were attached to the floor rails was reinforced with a metal block (see Fig. 7) to minimise the risk of the seats becoming detached during testing.

Panelling was removed from the armrest of the outside seats to facilitate the recording of displacement data.

The seats were mounted at either a 32" or a 28" seat pitch.

A suitable floor was constructed and this was carpeted.

7.3.2 Dummy

A 50% Hybrid III anthropomorphic dummy was used as the experimental model. The dummy was clothed in form fitting cotton stretch garments with mid-thigh length pants and size 11 E shoes weighing 11.6N (2.6 lbs).

The shoes had a smooth leather sole and the coefficient of friction of the shoe on the carpeted floor was determined prior to the experiment (Fig. 8) and measured 0.5.

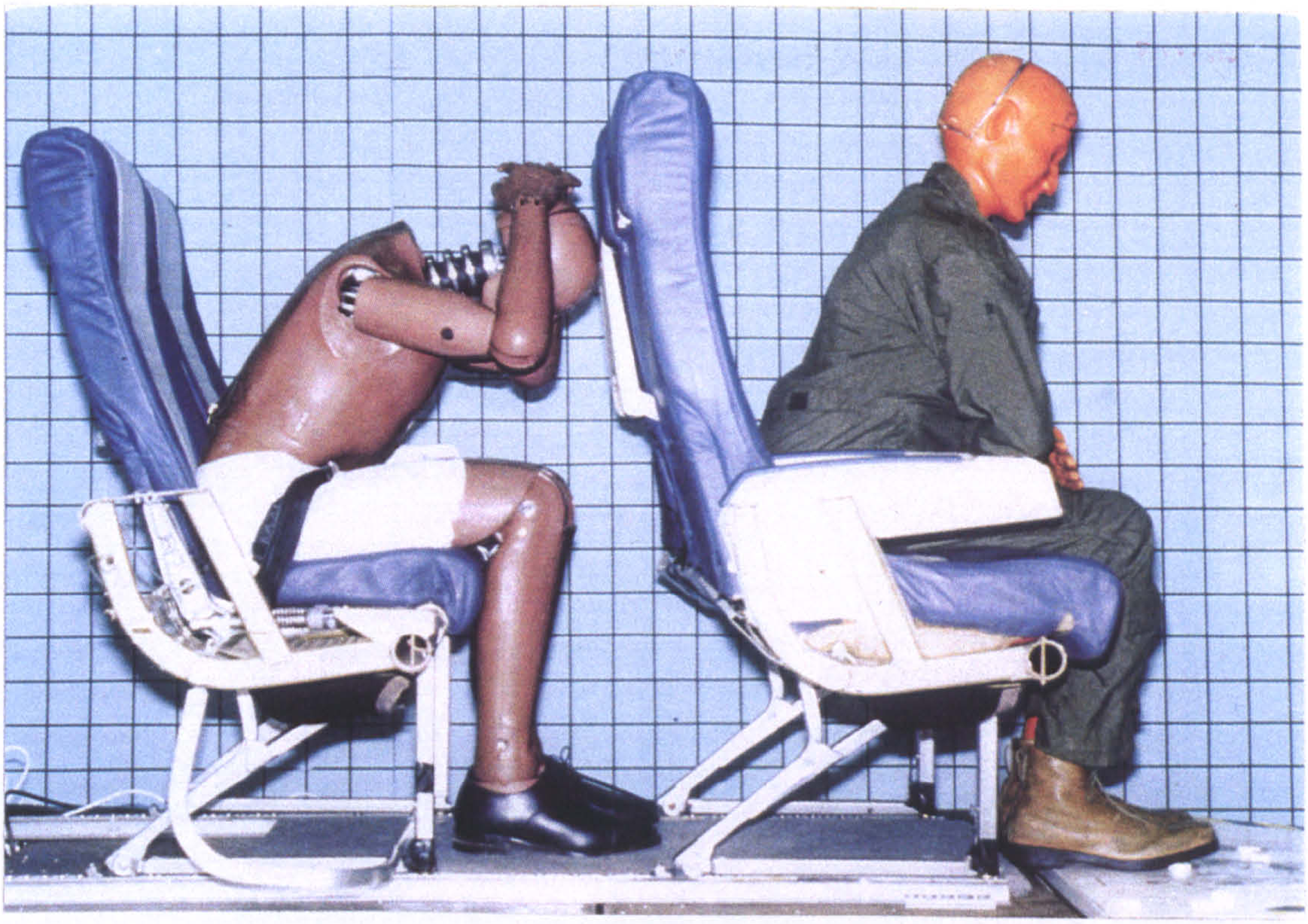

Fig. 9a Experiment 1
Braced/Legs Back Position, 32" Seat Pitch

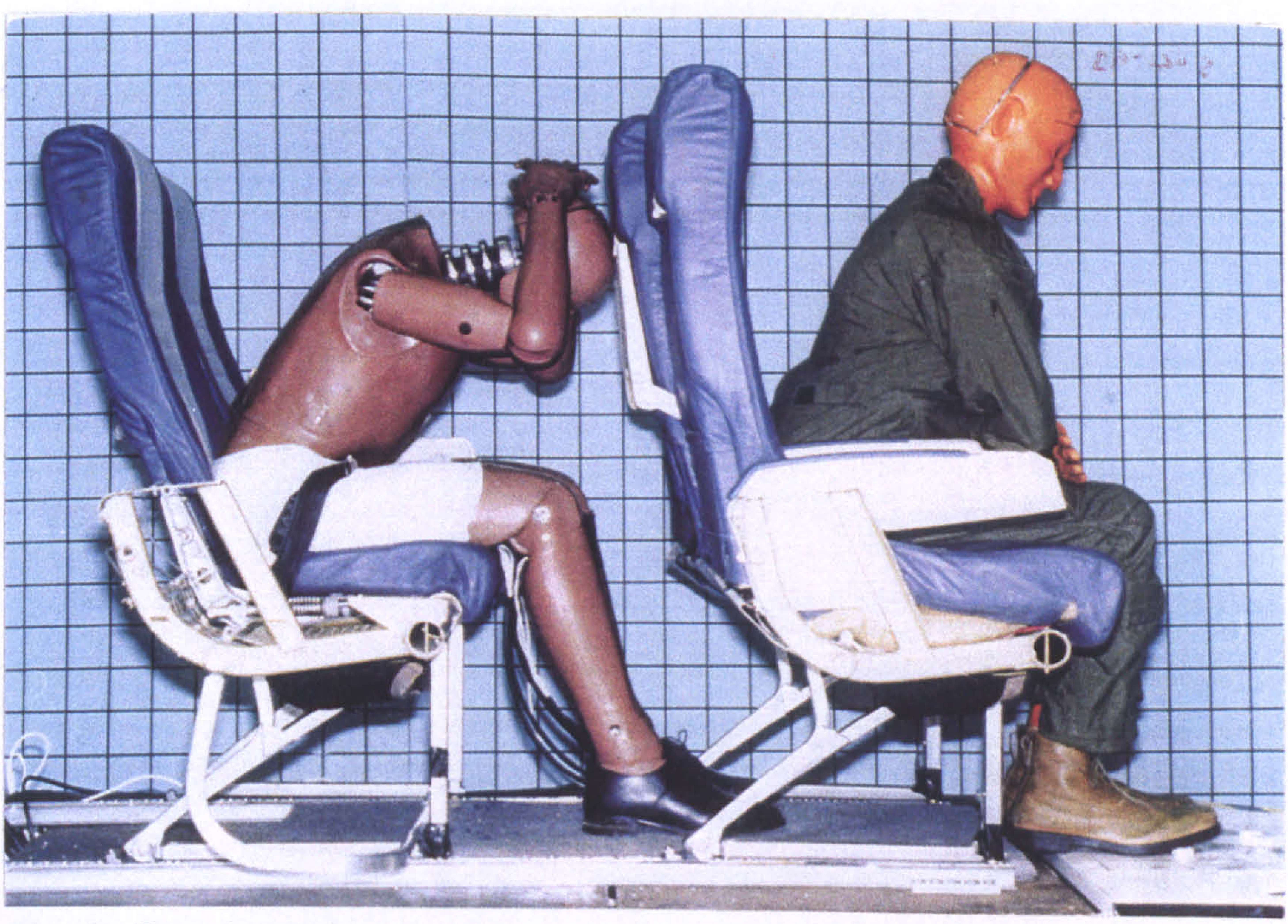

Fig. 9b Experiment 1
Braced/Legs Forward Position, 32" Seat Pitch

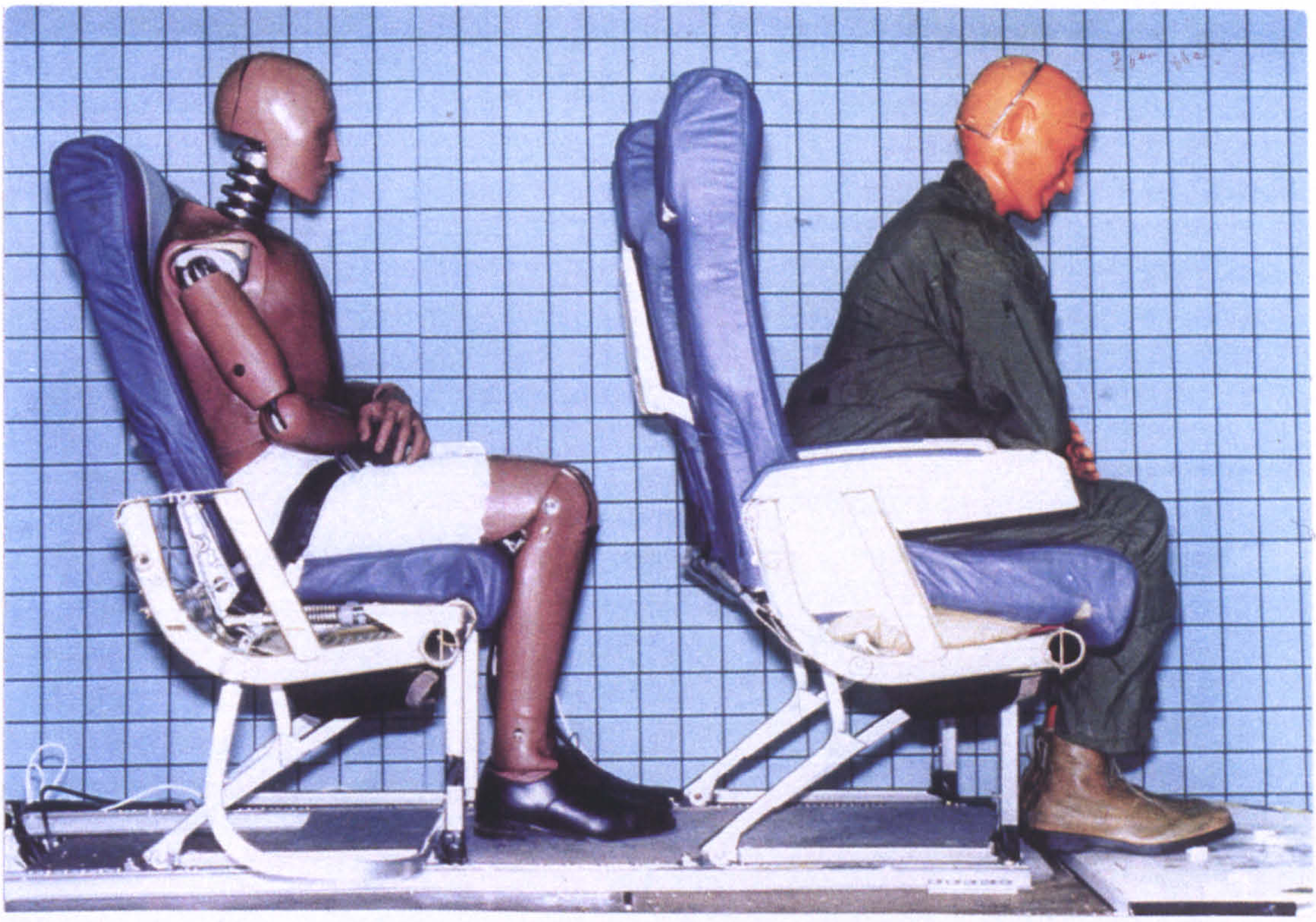

Fig. 9c Experiment 1
Unbraced/Legs Back Position, 32" Seat Pitch

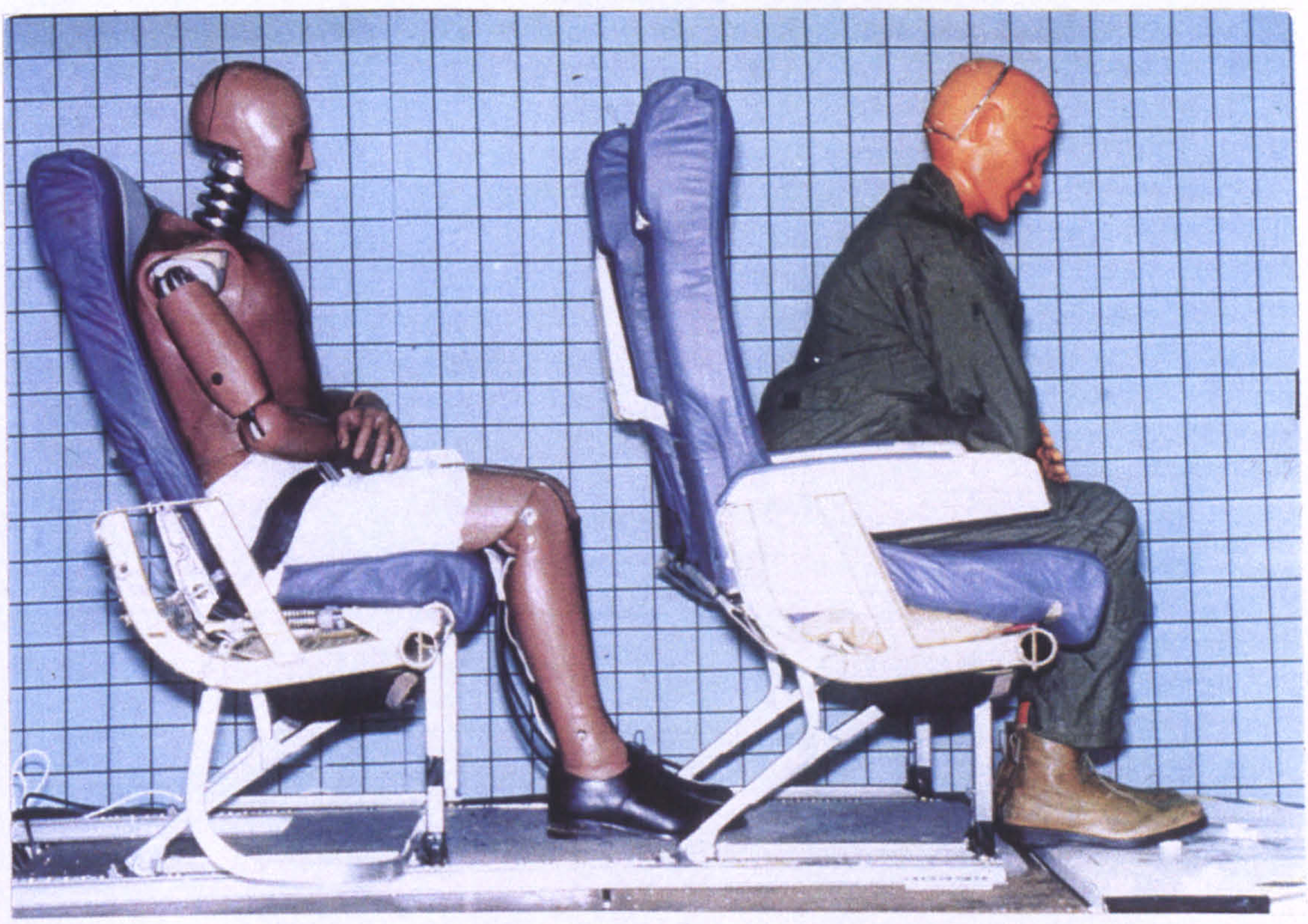

Fig. 9d Experiment 1
Unbraced/Legs Forward Position, 32" Seat Pitch

7.4 INSTRUMENTATION

The transducers were allocated channels in the following manner.

RECORDING CHANNELS

Channel	Transducer	Excitation	Gain	Recording
1	R Tibia L Clevis	10v	500	Datalab
2	R Tibia R Clevis	10v	500	Datalab
3	R Tibia U/My	10v	500	Datalab
4	R Tibia L/My	10v	500	Datalab
5	R Tibia L/Fz	10v	500	Datalab
6	L Tibia L Clevis	10v	500	Datalab
7	L Tibia R Clevis	10v	500	Datalab
8	L Tibia U/My	10v	500	Datalab
9	L Tibia L/My	10v	500	Datalab
10	L Tibia L/Fz	10v	500	Datalab
11	R Femur Fx	10v	500	Datalab
12	R Femur My	10v	500	Datalab
13	R Femur Fz	10v	500	Datalab
14	L Femur Fx	10v	500	Datalab
15	L Femur My	10v	500	Datalab
16	L Femur Fz	10v	500	Datalab
17	R Femur Fy	10v	500	Datalab
18	R Femur Mx	10v	500	Datalab
19	R Femur Mz	10v	500	Datalab
20	L Femur Fy	10v	500	Dash16
21	L Femur Mx	10v	500	Dash16
22	L Femur Mz	10v	500	Dash16
23	Lumbar Fx	10v	500	Dash16
24	Lumbar My	10v	500	Dash16
25	Lumbar Fz	10v	500	Dash16
26	Vehicle G	4v	1200	Dash16
27	Head Gx	10v	500	Dash16

Channel	Transducer	Excitation	Gain	Recording
28	Triaxial Head			.
29	Head Gz	10v	500	Portax
31	L Lapbelt	Piezo		Portax
32	Head Gy	10v	500	Portax
33	R Femur Result			
34	L Femur Result			

All impacts were recorded using a NAC 200 high speed video camera system operating at 200 fields per second.

7.5 EXPERIMENTAL VARIABLES

The experiment compared the values obtained from the transducers fitted to the dummy, for four dummy positions at two seat pitches.

The experimental variables were:

1) Brace position - braced
- unbraced

2) Lower leg position - forward
- backward

3) Seat pitch - 32"
- 28"

The four dummy positions used are illustrated in Figs. 9(a,b,c,d).
In the braced position the dummy was flexed forwards so that the head rested on the back of the seat ahead. The hands were placed on the head and were held in position by interlocking the fingers.

In the unbraced position the dummy was sat upright. The forward dummy was leaned forwards in all cases. This OGLG dummy did present support to the seat back. It was the only other dummy available for use during testing.

Two lower limb positions were identified.

In the first the lower legs were placed 20 degrees (±5%) forwards of a vertical line drawn through the knee (Figs. 9b, 9d). The angle was determined using 2 points - the centre of the knee joint and the centre of the ankle joint.

In the second the legs were placed 11.5 degrees (±5%) behind a vertical line drawn through the knee (Figs. 9a, 9c).

Both positions represented a reasonable seating position.

Seat pitch represents the distance from a given point on a seat to the same point on the seat ahead. Two seat pitches were used in this experiment.

The 32" seat pitch is a commonly used seat pitch and was the seat pitch most widely used in G-OBME.

A 28" seat pitch represented the shortest seat pitch used in G-OBME.

(Regulations introduced after the design of this experiment (Airworthiness Notice No. 64) by the CAA would prevent the use of a 28" seat pitch with Weber type seats as the distance between the seat backs is too short for emergency egress.)

7.6 TEST PROCEDURE

The 50th percentile instrumented Hybrid III dummy was located in the second row (from the front) in the centre of the three seat positions.

The dummy was placed in the seat in a uniform manner, with the back and buttocks against the seat back.

The friction of the limb joints was set so that the weight of the limb was barely restrained when extended horizontally.

The knees were separated by approximately 100mm (4").

The seat was placed in an "upright" position.

The dummy was placed in one of four different brace positions; braced/unbraced and legs forward/back and two seat pitches were used.

Another 50th percentile (OGLE) dummy was placed in the forward seat row ahead of the Hybrid III dummy in a braced position.

The lapbelt tension was set using a spring balance to a tension of 70N (15 lbs) which represents a firm but not uncomfortable tightness.

Before each test the vehicle was winched into position and the triggering device was armed.

The vehicle was released and the impact recorded.

After each test, all equipment was assessed for damage.

7.7 RANDOMIZATION

The tests were randomized to minimise linear order effects and each run was repeated 4 times.

The experiment was randomized according to the following schedule:

A - Legs forward }	Braced }	
B - Legs back }		Seat pitch 32"
C - Legs forward }	Unbraced }	
D - Legs back }		

E - Legs forward }	Braced }	
F - Legs back }		Seat pitch 28"
G - Legs forward }	Unbraced }	
H - Legs back }		

Run

1 F	17 C
2 E	18 D
3 D	19 A
4 C	20 B
5 H	21 E
6 G	22 F
7 B	23 G
8 A	24 H
9 B	25 G
10 A	26 H
11 H	27 E
12 G	28 F
13 D	29 A
14 C	30 B
15 F	31 C
16 E	32 D

7.8 ANALYSIS OF RESULTS

The raw data was entered into a computer. The data was manipulated using software developed at the Institute of Aviation Medicine, Farnborough, based upon the Asyst programme.

It was at this level that the calibration data for the load cells and accelerometers was added to allow the information to be expressed in SI units.

7.8.1 Zero-ing of Recordings

A zero level for each set of data was obtained by sampling the data between the trigger point and the point of impact.

When the data recording equipment is triggered the vehicle is in its coast phase. The impact point is 1 metre from the trigger point.

Therefore at a velocity of 12.7 m/s this represents 78ms.

With a sampling rate of 5000 samples per second this represents 400 counts between data recording trigger point and impact.

Therefore counts 10-110 were taken and the average obtained.

This value was then taken as the zero point.

This technique minimised the effects of the small movements which occur in dummy position during the acceleration phase of the impact test run - a recognised limitation in deceleration sled facilities.

7.8.2 Statistical Analysis

This study was designed to compare the effect of different passenger brace positions on injury arising from impact. Impact decelerations of -16Gx were conducted with the dummy placed in 4 positions; torso forward (=braced) or upright (=unbraced) with legs either forward or back. Each brace position was repeated 4 times for both a 32" and a 28" seat pitch, the experiment design being based on 2 latin squares so that the effects of brace position and seat pitch were orthogonal to linear changes over time. Measurements were made of tibial loads, femoral loads, lumbar loads, head injury criterion (HIC) and lap belt loads.

The maximum absolute value of each load measurement during the impact was subjected to analysis. The method of analysis of variance (ANOVA) was used with factors as given below.

Factor	Number of levels	Description
B	4	Brace position (torso & legs)
S	2	Seat pitch
O	4	Order of replications

The data were transformed as required to satisfy the assumptions of the analysis method.

Following the initial analysis of variance, significant effects of brace position, seat pitch or interactions between them were further investigated using t-tests. Further tests were also conducted when significant effects of order were indicated to determine if the effect of time could be described as a linear change with time. Where a non-linear block (order of replications) effect was indicated an attempt was made to correct the analysis for that effect by adjusting for linear and quadratic changes with run order.

7.9 RESULTS

The results of the impact tests performed in Experiment 1 are contained in the following tables. A key explaining the organisation of the tables is included below. Fig 9e shows the location of the load cells within the dummy.

7.9.1 Result Tables

Key to Results Tables

Run No.

The run no. is the unique number given to each impact test. The first run in Experiment 1 was 3674 and the last run was 3707. Run 3679 was repeated due to failure of the triggering mechanism and run 3699 was repeated due to failure of the data lab recording equipment.

Experiment 2 included runs from 3708 to 3725. Run 3721 was repeated due to failure of the triggering mechanism.

Cal. File

This is the number of the calibration file used to interpret the data from each test run.

Set Up

This refers to the configuration used during each test.

A - Braced/Legs forward	)	
B - Braced/Legs back	)	32" seat pitch
C - Unbraced/Leges forward	)	
D - Unbraced/Legs back	)	
E - Braced/Legs forward	)	
F - Braced/Legs back	)	28" seat pitch
G - Unbraced/Legs forward	)	
H - Unbraced/Legs	)	

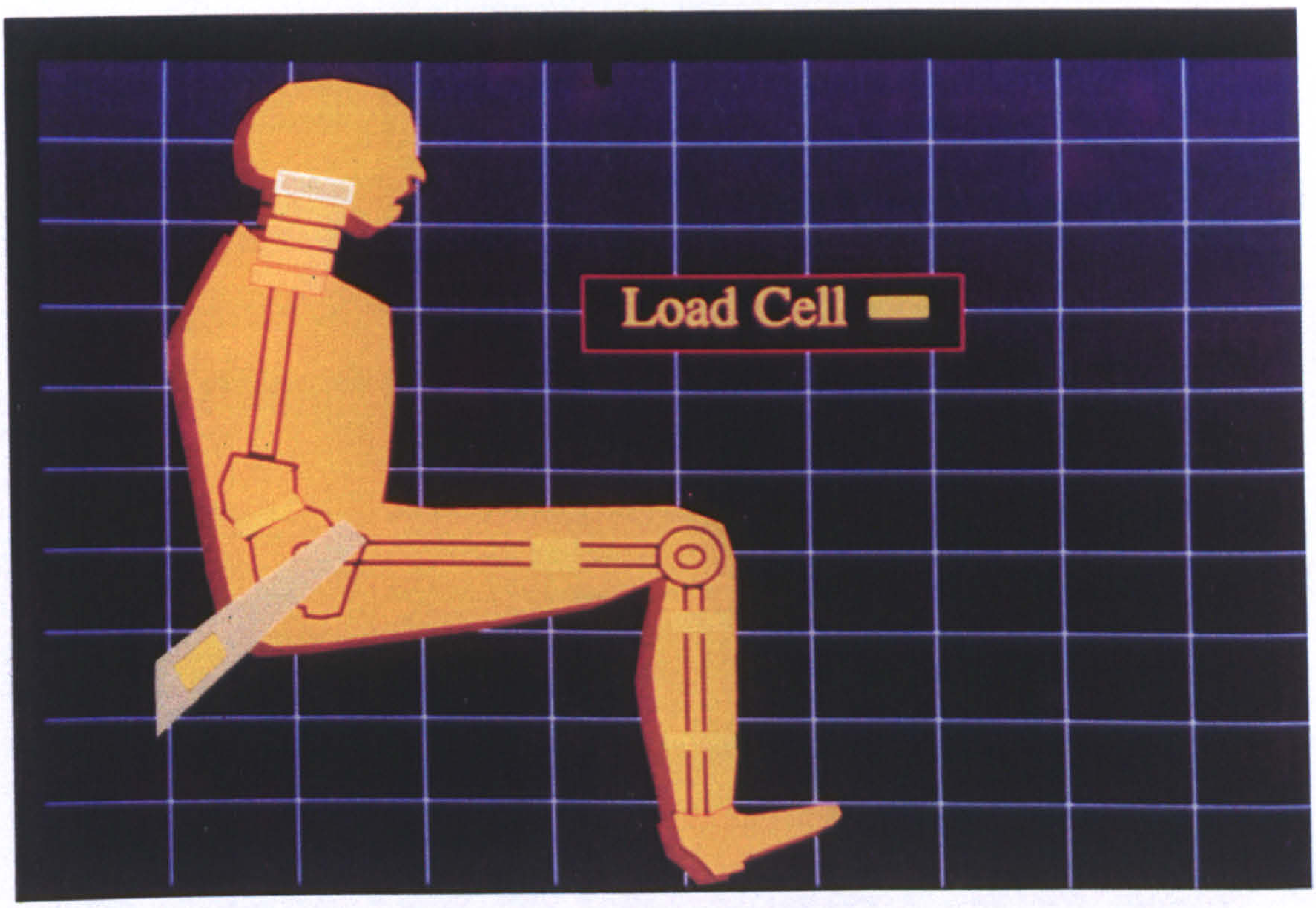

Fig. 9e Location of Load Cells within the Dummy

Brace Position

Brace position refers to the position adopted by the dummy at the time of impact.

B = braced

U = unbraced

Leg Position

Leg position refers to the position of the dummy's lower limbs.

LF = legs forward at an angle of 20° to a vertical line drawn through the knee.

LB = legs back at an angle of 11.5° to a vertical line drawn through the knee.

Seat Pitch

Two seat pitches were used 32" and 28"

Velocity

Velocity refers to the velocity of the sled at impact, measured in metres per second.

Flail

Flail refers to the behaviour of the lower limbs as seen on the high speed video recordings. If the lower limbs were thrown forwards and upwards causing hyperextension of the knee, then flailing was said to have occurred.

In some impacts, particularly those associated with a 28" seat pitch, it was difficult to decide whether flailing had occurred as opposed to the legs sliding forwards, after impact (a much lower energy phenomenon). These results were categorised with the letter 'P'.

Channels 3-32

The loads recorded in each of the transducers were plotted against time. The resulting graphs were analyzed and the peak loads were recorded. In some channels there was more than one peak and in these instances the value of the larger peak was recorded. The time at which the peak load occurred after impact is designated by the letter 'T'.

Analysis of the recordings from the right and left knee clevis units was not practical in terms of a single peak. During the course of the impact multiple peak loads were recorded and these were of differing polarity. Accordingly the data from channels 1, 2, 6 and 7 has not been analyzed in terms of peak loads.

Channel 3

Right Tibia Upper My

- the bending moment recorded about the y-axis in the right tibia upper load cell
- knee extension produced a negative output.

Channel 4

Right Tibia Lower My

- the bending moment recorded about the y-axis in the right tibia lower load cell
- knee extension produced a negative output.

Channel 5

Right Tibia Lower Fz

- the axial force recorded in the right tibia lower load cell
- tibial compression produced a negative output.

Channel 8

Left Tibia Upper My

- the bending moment about the y-axis recorded in the left tibia upper load cell
- knee extension produced a negative output.

Channel 9

Left Tibia Lower My

- the bending moment about the y-axis recorded in the lower left tibia lower load cell
- knee extension produced a negative output.

Channel 10

Left Tibia Lower Fz

- the axial force recorded in the left tibia lower load cell
- tibial compression produced a negative output.

Channel 11

Right Femur Fx

- the femoral shear load in the x-axis
- downward force on the thigh produced a positive signal

Channel 12

Right Femur My

- the bending moment about the y-axis recorded in the right femoral load cell
- upward movement of the pelvis or knee relative to the femoral load cell produced a negative output.

Channel 13

Right Femur Fz

- the axial load recorded in the right femoral load cell
- axial compression produced a negative output.

Channel 14

Left Femur Fx

- the shear load recorded in the left femoral load cell
- a downward force on the thigh produced a positive output

Channel 15

Left Femur My

- the bending moment about the y-axis recorded in the left femoral load cell
- upward movement of the pelvis or knee relative to the femoral load cell produced a negative output.

Channel 16

Left Femur Fz

- the axial load recorded in the left femoral load cell
- axial compression produced a negative output.

Channel 17

Right Femur Fy

- the shear force recorded in the y-axis in the right femoral load cell
- a lateral force produced a negative output.

Channel 18

Right Femur Mx

- the bending moment recorded about the x-axis in the right femoral load cell
- a force exerted medially on the right knee produced a negative output.

Channel 19

Right Femur Mz

- the axial rotation moment recorded in the right femoral load cell
- external rotation force produced a negative output.

Channel 20

Left Femur Fy

- the femoral shear load recorded in the y-axis in the left femoral load cell
- a force exerted laterally on the left knee produced a positive output.

Channel 21

Left Femur Mx

- the bending moment recorded about the x-axis in the left femoral load cell
- a force exerted laterally on the left knee produced a negative output.

Channel 22

Left Femur Mz

- the axial rotation moment recorded in the left femoral load cell
- external rotation produced a negative output.

Channel 23

Lumbar Fx

- the shear load recorded in the lumbar load cell

Channel 24

Lumbar My

- the moment recorded about the y-axis in the lumbar load cell
- forward flexion produced a positive output.

Channel 25

Lumbar Fz

- the axial load recorded in the lumbar load cell
- axial compression produced a negative output.

Channel 26

Vehicle G

- the peak G recorded in the vehicle accelerometer

Channel 27

Head Gx

- the peak acceleration recorded in the head in the x-axis

Channel 28

HIC

- the head injury criterion

Channel 29

Head Gz

- the peak acceleration recorded in the head in the z-axis

Channel 31

Lap belt

- the peak load recorded in the load cell which was mounted in series with the lap belt
- tension produced a negative output

Channel 32

Head Gy

- the peak acceleration recorded in the head in the y-axis

Channel 33 and 34

Left and Right Femur Resultant

- the resultant bending moment acting on each femur was computed from the bending moments recorded in the x and y-axis according to the equation $C^2 = A^2 + B^2$

PASSENGER BRACE POSITION STUDY										CHANNEL 3	
RUN No.	CAL. FILE	SETUP	BRACE POSITION	LEG POSITON	SEAT PITCH	VELOCITY (m/s)	FLAIL	COMMENTS FROM VIDEO TAPE	RUN No.	Rt TIB U/My (Nm)	T (ms)
3682	3674	A	B	LF	32	12.2	YES	RIGHT KNEE STOP BENT	3682	-133	153
3684	3674	A	B	LF	32	12.27	YES	RIGHT KNEE STOP BENT	3684	-133	149
3693	3674	A	B	LF	32	12.2	YES	RIGHT KNEE STOP BENT	3693	-75	153
3704	3674	A	B	LF	32	12.35	YES	LEFT KNEE STOP BENT	3704	-59	153
3681	3674	B	B	LB	32	12.2	NO	LEFT LEG SLIDE	3681	29	133
3683	3674	B	B	LB	32	12.2	NO	LEFT LEG SLIDE	3683	34	128
3694	3674	B	B	LB	32	12.12	NO	LEFT LEG SLIDE	3694	25	143
3705	3674	B	B	LB	32	12.35	NO	LEFT LEG SLIDE	3705	33	120
3677	3674	C	U	LF	32	12.27	YES	RIGHT KNEE STOP BENT	3677	-131	158
3688	3674	C	U	LF	32	12.27	YES	BOTH KNEE STOPS BENT	3688	-132	153
3691	3674	C	U	LF	32	12.2	YES	LEFT KNEE STOP BENT RIGHT KNEE STOP FRACTURE	3691	-122	153
3706	3674	C	U	LF	32	12.35	YES	BOTH KNEE STOPS BENT	3706	-93	158
3676	3674	D	U	LB	32	12.5	YES	RIGHT KNEE STOP BENT	3676	-132	164
3687	3674	D	U	LB	32	12.2	YES	BOTH KNEE STOPS BENT	3687	-111	168
3692	3674	D	U	LB	32	12.27	YES	RIGHT KNEE STOP BENT	3692	-70	168
3707	3674	D	U	LB	32	12.42	YES	LEFT KNEE STOP BENT	3707	-61	172
3675	3674	E	B	LF	28	12.5	P	BOTH LEGS SLIDE	3675	-136	102
3690	3674	E	B	LF	28	12.27	NO	BOTH LEGS SLIDE	3690	-136	112
3695	3674	E	B	LF	28	12.27	P	BOTH LEGS SLIDE	3695	-87	100
3702	3674	E	B	LF	28	12.27	P	BOTH LEGS SLIDE	3702	-124	112
3674	3674	F	B	LB	28	12.42	NO	BOTH LEGS SLIDE FORWARDS	3674	-61	117
3689	3674	F	B	LB	28	12.2	NO		3689	-46	120
3698	3674	F	B	LB	28	12.27	NO		3698	-40	120
3703	3674	F	B	LB	28	12.27	NO	BOTH LEGS SLIDE	3703	-9	117
3680	3674	G	U	LF	28	12.35	P	RIGHT LEG SLIDE	3680	-134	102
3686	3674	G	U	LF	28	12.27	NO		3686	-136	96
3697	3674	G	U	LF	28	12.35	YES		3697	-112	100
3700	3674	G	U	LF	28	12.35	P	LEG SLIDE	3700	-104	120
3678	3674	H	U	LB	28	12.2	NO	BOTH LEGS SLIDE	3678	-82	112
3685	3674	H	U	LB	28	12.27	NO		3685	-81	123
3698	3674	H	U	LB	28	12.27	P	LEFT LEG FLAIL	3698	-34	128
3701	3674	H	U	LB	28	12.35	YES		3701	-49	175
									MEAN		
									B/LF/32	-100.00	
									B/LB/32	30.25	
									U/LF/32	-119.50	
									U/LB/32	-93.50	
									B/LF/28	-120.75	
									B/LB/28	-39.00	
									U/LF/28	-121.50	
									U/LB/28	-61.50	

	CHANNEL 4		CHANNEL 5		CHANNEL 8		CHANNEL 9		CHANNEL10		CHANNEL 11		CHANNEL12	
RUN No.	Rt TIB L/My (Nm)	T (ms)	Rt TIB L/Fz (N)	T (ms)	Lt TIB U/My (Nm)	T (ms)	Lt TIB L/My (Nm)	T (ms)	LT TIB L/ Fz (N)	T (ms)	Rt FEMUR Fx (N)	T (ms)	Rt FEMUR My (Nm)	T (ms)
3682	-42	153	906	133	-125	158	24	133	689	138	755	148	-91	153
3684	-43	153	872	128	-100	158	35	128	669	133	637	148	-116	153
3693	-27	153	850	133	-91	138	22	128	599	133	597	153	-57	117
3704	-34	148	342	128	-100	158	25	133	652	138	138	153	-86	143
3681	-21	133	-1688	133	18	123	7	123	-655	123	-1305	133	-167	133
3683	-15	138	-1455	138	21	128	9	128	-693	123	-1270	128	-158	123
3694	-11	153	-1250	148	18	117	7	107	-700	128	-1089	153	-144	153
3705	-17	133	-1512	133	16	117	8	110	-678	117	-1373	128	-169	117
3677	-25	153	746	138	-125	158	9	117	597	143	444	158	-148	158
3688	-28	153	702	138	-125	153	27	117	668	143	322	153	-162	153
3691	-23	153	675	138	-120	153	33	117	691	138	246	153	-120	153
3706	-19	158	827	143	-82	163	16	158	421	153	208	158	-84	153
3676	-34	168	838	148	-123	170	-34	175	735	148	582	163	-126	163
3687	-30	180	587	154	-121	178	-34	180	652	153	357	178	-107	180
3692	-18	170	752	153	-103	173	-28	173	647	153	417	163	-53	178
3707	-17	175	628	153	-74	170	-20	180	650	153	317	173	-43	128
3675	-34	102	-595	117	-138	102	-29	102	-395	133	-750	123	-96	117
3690	-36	107	-622	117	-139	107	-37	107	-996	153	-721	123	-100	123
3695	-19	112	-203	77	-117	102	-24	117	-156	92	-522	128	-75	128
3702	-60	117	-680	117	-109	96	-56	112	-944	163	-563	123	-88	123
3674	-18	123	-1219	138	-69	117	-20	138	-1221	138	-862	138	-106	138
3689	-18	133	-1329	123	-80	117	-16	138	-813	133	-1058	128	-140	123
3698	-26	133	-1407	128	-30	117	-7	185	-606	123	-1177	128	-147	128
3703	-7	128	-760	148	-34	138	-9	143	-451	117	-695	133	-100	128
3680	-33	108	-247	123	-136	102	-33	107	-555	185	-378	133	-54	128
3686	-39	92	-844	107	-138	97	-35	97	-606	112	-711	112	-108	107
3697	-26	97	-174	77	-116	97	-26	195	-284	198	-334	133	-52	128
3700	-52	117	-398	128	-97	117	-50	117	-504	173	-302	138	-55	133
3678	-24	112	-747	158	-83	117	-18	138	-1054	133	-647	153	-83	153
3685	-22	123	-859	143	-91	128	-21	123	-867	143	-763	163	-97	163
3696	-9	133	-279	117	-43	128	-12	133	-998	170	-250	135	-41	128
3701	-11	193	-307	123	-46	185	-11	190	277	168	-224	143	-48	173
MEAN														
B/LF/32	-36.50		742.50		-104.00		26.50		652.25		531.25		-86.25	
B/LB/32	-16.00		-1476.25		18.25		7.75		-681.50		-1259.25		-159.50	
U/LF/32	-23.75		737.50		-113.00		21.25		593.75		305.00		-129.13	
U/LB/32	-24.75		701.25		-105.25		-29.00		671.00		418.25		-84.13	
B/LF/28	-37.25		-525.00		-125.75		-36.50		-637.25		-639.00		-89.75	
B/LB/28	-17.25		-1178.75		-53.28		-13.00		-772.75		-948.00		-124.50	
U/LF/28	-37.50		-415.75		-121.75		-36.00		-487.25		-431.25		-85.37	
U/LB/28	-16.50		-548.00		-65.75		-15.50		-799.00		-471.00		-86.75	

TABLE 7

Experiment 1 - Gx Impacts

	CHANNEL 13		CHANNEL 14		CHANNEL 15		CHANNEL 16		CHANNEL 17		CHANNEL 18		CHANNEL19	
RUN No.	Rt FEMUR Fz (N)	T (ms)	Lt FEMUR Fx (N)	T (ms)	Lt FEMUR My (Nm)	T (ms)	Lt FEMUR Fz (N)	T (ms)	Rt FEMUR Fy (N)	T (ms)	Rt FEMUR Mx (Nm)	T (ms)	Rt FEMUR Mz (Nm)	T (ms)
3682	1355	131	-455	123	-129	159	1025	138	296	138	-115	138	-42	107
3684	1416	131	-311	117	-82	158	1081	133	387	133	-128	133	-34	107
3693	1333	133	-233	117	-89	143	970	133	216	153	-128	138	-31	112
3704	1098	128	-408	117	-85	163	1025	138	371	158	-228	153	-43	112
3681	1125	111	-689	123	-90	121	872	107	-80	112	-15	205	-63	117
3683	1026	112	-617	123	-82	123	897	107	-56	107	14	208	-61	117
3694	911	117	-698	138	-91	128	891	112	-72	112	-18	153	-71	123
3705	1031	102	-574	117	-82	117	812	107	-48	100	-15	112	-66	107
3677	1008	143	348	158	-128	158	944	107	152	143	-28	148	-11	123
3688	1124	143	361	158	-131	128	985	148	155	163	-44	153	-14	153
3691	1125	112	341	158	-123	158	1031	143	232	168	-61	153	-14	153
3706	1148	148	133	235	-100	168	675	153	186	190	-95	153	-26	185
3676	1200	146	382	173	-115	170	1029	107	-163	153	-58	153	-25	123
3687	941	112	360	178	-111	180	930	107	-189	163	-89	163	-38	123
3692	1123	148	254	168	-115	175	989	100	-258	158	-92	158	-29	185
3707	1114	107	284	178	-64	170	981	100	-205	158	-139	163	-33	128
3675	-877	101	-689	128	-93	128	-1200	107	86	173	-41	107	-29	112
3690	-901	117	-998	138	-124	153	-1210	107	140	117	-21	128	-32	117
3695	-371	128	-729	133	-92	138	-992	100	258	158	-128	153	-40	117
3702	-372	112	-853	159	-130	158	-785	163	128	133	-45	163	-52	112
3674	426	97	-971	143	-134	148	-528	138	88	138	-15	133	-42	123
3689	750	100	-698	138	-102	133	-591	117	56	123	-16	123	-54	117
3698	380	107	-623	128	-94	128	-300	100	101	133	-21	133	-51	117
3703	840	107	-655	128	-106	117	-312	92	99	133	-24	158	-68	117
3680	-586	102	-547	149	-78	173	-909	107	-98	163	-19	170	-15	128
3686	-916	92	-529	112	-88	112	-1165	97	-65	148	26	97	-26	107
3697	-846	100	-385	120	-59	133	-1538	97	-84	163	-57	168	-28	128
3700	-302	117	-456	164	-67	168	-665	100	-60	188	-60	180	-31	143
3678	-442	123	-511	158	-70	156	-388	117	-37	107	19	112	-35	123
3685	-324	166	-511	163	-69	159	-590	123	-75	185	15	123	-38	158
3699	538	102	-912	170	-116	164	-780	175	-191	168	59	188	-25	133
3701	762	117	434	193	-40	138	-252	97	-164	173	-145	175	-39	138
MEAN														
B/LF/32	1300.00		-351.75		-98.25		1052.50		326.09		-161.84		-37.50	
B/LB/32	1023.25		-644.00		-86.25		868.00		-66.08		-17.39		-65.25	
U/LF/32	1100.75		-295.75		-120.50		895.12		188.11		-58.24		-16.25	
U/LB/32	1094.50		320.00		-101.25		938.37		211.66		-101.55		-31.25	
B/LF/28	-630.25		-817.25		-109.75		-1046.75		148.76		-53.17		-38.25	
B/LB/28	-594.00		-738.75		-109.00		-405.50		88.26		-21.01		-53.75	
U/LF/28	-662.50		-479.25		-73.00		-1110.13		-79.30		-40.62		-25.00	
U/LB/28	-516.50		-592.00		-73.75		-518.15		-101.72		-44.52		-34.25	

TABLE 7

Experiment 1 - Gx Impacts

	CHANNEL 20		CHANNEL 21		CHANNEL 22		CHANNEL 23		CHANNEL 24		CHANNEL 25		CHANNEL 26	
RUN No.	Lt FEMUR Fy (N)	T (ms)	Lt FEMUR Mx (Nm)	T (ms)	Lt FEMUR Mz (Nm)	T (ms)	LUMBAR Fx (N)	T (ms)	LUMBAR My (Nm)	T (ms)	LUMBAR Fz (N)	T (ms)	VEHICLE G	T (ms)
3682	-401	158	278	153	85	123	6678	128	163	168	4473	128	15.8	72
3684	-447	158	342	148	77	120	6065	123	174	168	3883	128	16.1	72
3693	-444	158	389	148	56	117	5638	128	160	168	3886	133	15.9	72
3704	-373	128	269	153	83	125	6148	128	149	173	4352	133	16.2	72
3681	-82	210	21	123	87	123	9271	131	476	143	5067	128	15.7	72
3683	138	178	14	123	100	128	8987	133	443	143	5398	133	15.7	72
3694	184	148	25	120	77	120	7890	133	398	138	4904	128	15.4	72
3705	163	178	31	120	80	117	9011	123	420	138	5212	128	16	72
3677	260	163	118	168	29	168	3856	175	218	195	3757	168	16.3	72
3688	368	163	132	165	30	138	3599	175	142	180	4259	168	16.3	72
3691	401	220	149	163	32	160	3245	180	174	220	4215	163	15.6	72
3708	340	164	218	168	55	148	3300	133	155	195	3251	163	16	72
3676	267	168	124	168	12	133	3879	128	211	200	2721	173	17.6	72
3687	319	175	153	175	33	140	4190	138	179	215	2943	138	15.7	72
3692	433	168	193	173	24	153	3533	200	224	200	3516	185	15.7	72
3707	435	168	196	173	38	143	3600	138	159	133	3043	143	15.5	72
3675	-308	117	169	168	103	140	6383	133	264	138	5019	128	17.3	70
3690	-435	153	64	175	92	130	6656	133	319	158	5447	133	16.2	72
3695	-261	168	138	168	104	133	5552	138	165	143	5416	133	15.6	72
3702	-626	168	81	185	121	143	6501	143	299	163	5136	138	16	72
3674	-312	148	40	148	109	153	7219	143	491	153	4405	133	16.6	70
3689	-225	117	-19	120	112	143	7734	138	459	158	5624	133	15.9	72
3696	-257	107	-12	120	109	128	8375	133	504	158	5387	133	16.1	72
3703	-312	123	25	97	123	133	7244	138	357	158	4981	133	16.2	72
3680	-275	112	223	183	88	153	3744	158	203	158	3426	138	16.1	72
3686	-280	112	-46	153	92	146	5509	128	265	153	4398	128	15.4	72
3697	-371	102	80	180	81	148	3752	138	171	153	3477	138	16	72
3700	-312	97	-46	158	82	148	3959	168	214	168	3429	143	16.1	72
3678	-153	117	17	117	121	153	5251	163	362	158	3473	138	15.8	72
3685	-157	117	-25	163	108	153	5618	164	411	168	3787	138	16	72
3698	-672	185	96	175	88	153	4231	173	311	178	3074	158	16.2	72
3701	-274	97	127	185	90	150	3397	133	150	133	2972	143	16.2	72
MEAN														
B/LF/32	-433.02		350.94		75.25		6132.35		161.50		4148.50			
B/LB/32	141.59		24.28		86.00		8789.75		434.25		5145.25			
U/LF/32	352.56		166.27		36.50		3500.00		172.25		3870.50			
U/LB/32	371.27		181.87		26.75		3800.00		193.25		3055.75			
B/LF/28	-401.27		116.52		105.00		6273.00		261.75		5254.50			
B/LB/28	-285.74		24.28		113.25		7643.00		452.75		5099.25			
U/LF/28	-320.53		87.10		85.75		4241.00		213.25		3682.50			
U/LB/28	-269.03		53.02		101.75		4624.25		308.50		3326.50			

TABLE 7

Experiment 1 - Gx Impacts

	CHANNEL 27		CHANNEL 28	CHANNEL 29		CHANNEL 31		CHANNEL32		CHANNEL 33	CHANNEL 34
RUN No	HEAD Gx	T (ms)	HIC	HEAD Gz	T (ms)	Lt LAPBELT (N)	T (ms)	HEAD Gy	T (ms)	Lt Femur Result (Nm)	Rt Femur Result (Nm)
3682	-72	168	154	-30	128	-9870	123	-2	235	302	120
3684	-58	163	118	-28	123	-8910	117	2	180	364	141
3693	-64	168	126	-26	133	-8920	128	-6	220	411	136
3704	-55	163	118	-29	128	-8820	123	3	195	289	234
3681	-27	190	275	-40	133	-9880	128	-3	205	86	163
3683	-26	200	242	-40	128	-9680	128	-4	200	83	154
3694	-23	200	251	-40	133	-9400	128	-3	183	92	140
3705	-33	173	197	-41	128	-10400	128	-2	215	87	164
3677	-67	193	514	-46	175	-8000	117	15	188	164	150
3688	-75	190	575	-44	185	-8360	112	-9	183	176	171
3691	-63	185	603	-38	183	-7860	112	-27	200	186	140
3706	-100	185	546	-36	180	-7720	117	-8	210	237	124
3676	-71	183	459	-35	178	-8930	117	-8	185	173	122
3687	-98	185	410	-28	173	-7860	117	-5	200	190	104
3692	-57	180	586	-38	180	-8280	112	-21	180	218	98
3707	-78	175	357	-34	175	-8600	112	-9	180	216	152
3675	-86	163	282	-34	128	-5440	143	-4	168	172	93
3690	-59	178	180	-36	133	-6700	153	-8	175	123	95
3695	-28	183	157	-31	138	-5410	107	-4	225	143	136
3702	-71	163	230	-32	133	-6730	117	5	170	129	83
3674	-120	163	523	-32	128	-6310	107	6	163	139	103
3689	-85	168	315	-37	138	-6800	112	-4	168	104	138
3696	-59	168	323	-38	138	-7600	128	-2	143	95	143
3703	-85	163	233	-34	133	-7330	133	6	170	105	98
3680	-114	180	590	-38	170	-5970	107	-12	180	235	43
3686	-73	178	499	-56	168	-5340	107	9	178	93	100
3697	-90	175	532	-31	153	-4200	153	5	173	84	50
3700	-147	183	683	-45	173	-6090	112	6	190	80	65
3678	-101	175	672	-52	163	-6600	112	-5	180	68	71
3685	-107	173	589	-50	170	-6850	112	16	173	70	90
3698	-78	180	681	-41	168	-5900	112	-11	173	147	83
3701	-67	185	531	-35	173	-7080	112	6	190	130	158
MEAN											
B/LF/32			129.00			-9130.00				341.50	157.75
B/LB/32			241.25			-9840.00				87.00	155.25
U/LF/32			559.50			-7965.00				190.75	146.25
U/LB/32			453.00			-8417.50				199.25	118.50
B/LF/28			212.25			-6070.00				141.75	101.75
B/LB/28			348.50			-7010.00				110.75	120.00
U/LF/28			576.00			-5400.00				123.00	64.50
U/LB/28			613.25			-6607.50				103.75	100.50

TABLE 7

Experiment 1 - Gx Impacts

7.9.2 High Speed Video

All impacts were recorded on a NAC 200 high speed video camera system recording at 200 fields per second. Subsequent review of these high speed video recordings proved most informative. However, review of such recordings remains subjective. The comments given below are my own subjective interpretations of the video recordings and can be viewed in conjunction with Figs. 10, 10a, 11, 11a, 12, 13, 14, 15, 16, 17.

1. Flailing behaviour was seen to occur in some impact tests. Flailing refers to the behaviour of the lower limbs when, following impact, they are thrown forwards and upwards causing hyperextension of the knee joint. This flailing was a high energy phenomenon and was often associated with deformation of the knee stops (see Fig.19).

2. Flailing behaviour was most marked at a 32" seat pitch and was seen to occur in all positions except the braced legs back position. (see Fig. 11).

3. In a braced legs back position no flailing occurred. On impact the lower limbs were seen to slide forwards to the vertical position where further progress was halted. On the left side the lower leg was seen to slide slightly forwards of the vertical. This was a late phenomenon and no contact occurred with the back of the forward seat. (see Figs. 10, 10a, 11, 11a).

4. At a 28" seat pitch flailing behaviour was observed in all of the positions tested except a braced legs back position. In a braced legs back position the lower limbs were seen to slide forwards to a position just forward of the vertical (see Fig.14).

5. At a 28" seat pitch flailing behaviour was seen in all of the other positions tested, however the proximity of the forward seat appeared to limit the forward movement of the lower legs and accordingly hyperextension of the knee joint was not always seen. Instances when the lower legs were thrown forwards but hyperextension of the knee joint did not occur or when hyperextension of only one knee joint occurred were described as partial flailing (see Figs. 14 - 17).

HIGH SPEED VIDEO RECORDINGS - Experiment 1 (-Gx Impacts)

Fig. 10 Run No. 3681 - Braced/Legs Back, 32" Seat Pitch

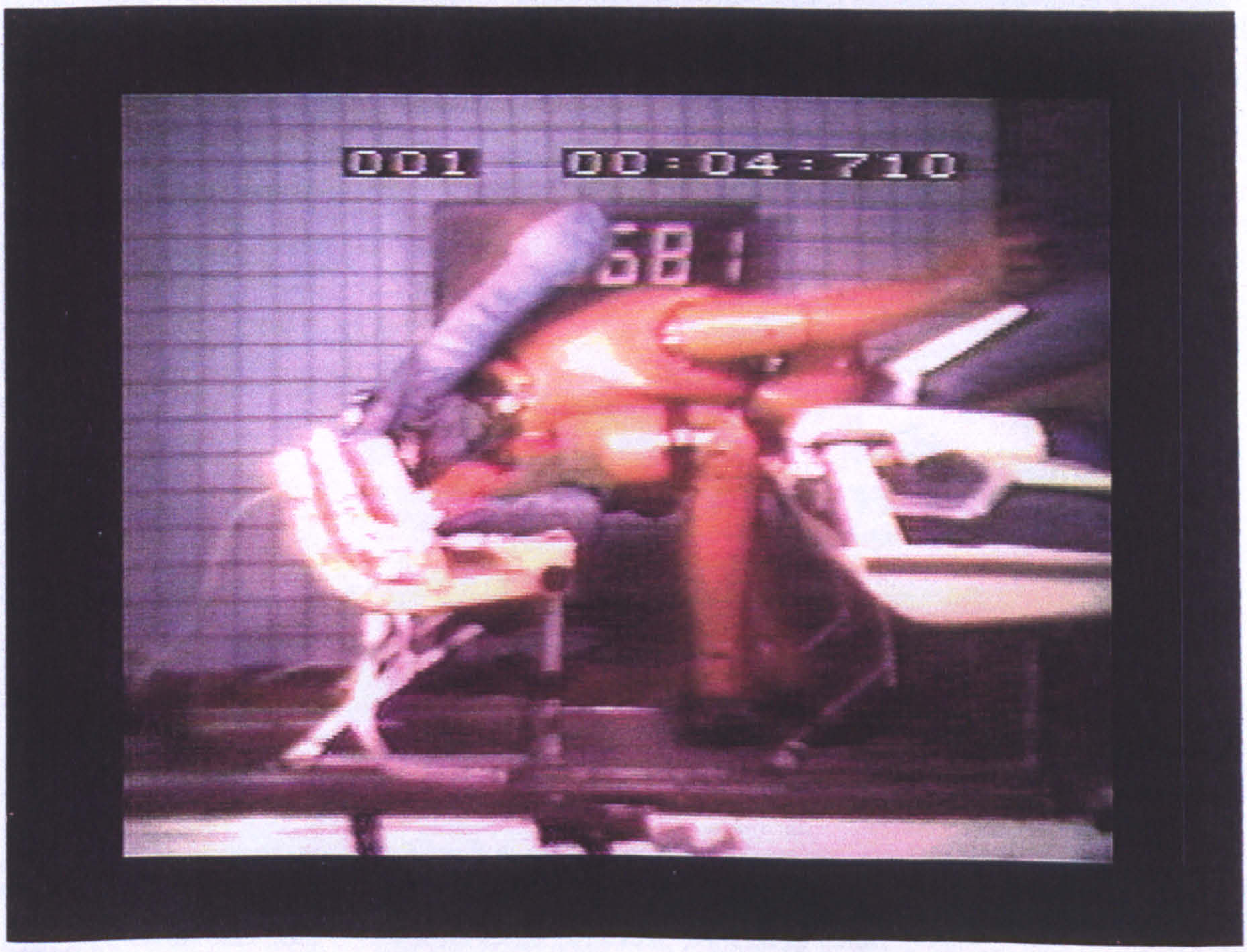

Fig. 10a Run No. 3681 - Braced/Legs Back, 32" Seat Pitch
- 100 ms after impact

Fig. 11 Run No. 3684 - Braced/Legs Forward, 32" Seat Pitch

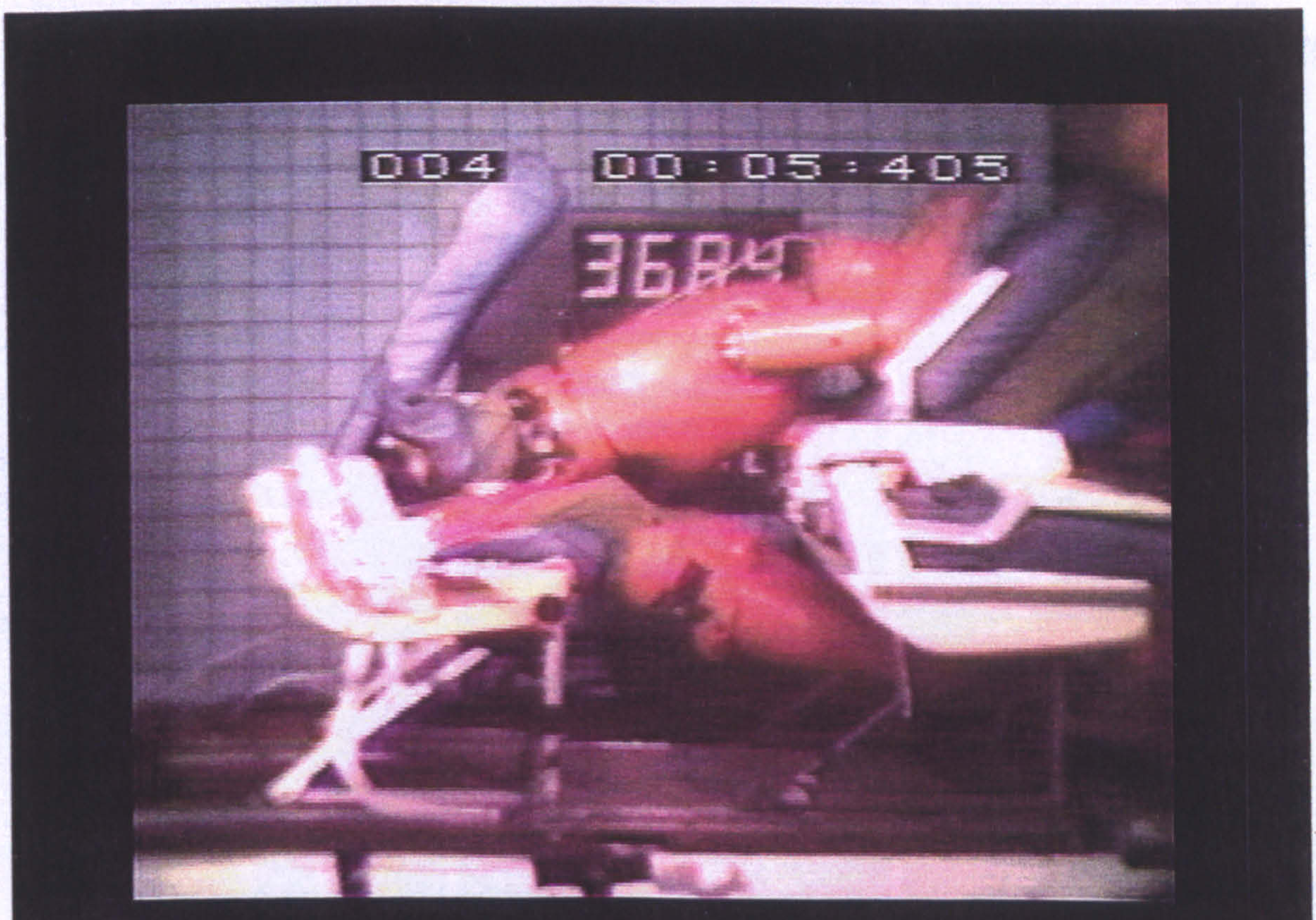

Fig. 11a Run No. 3684 - Braced/Legs forward, 32" Seat Pitch
- 100 ms after impact

HIGH SPEED VIDEO RECORDINGS - Experiment 1 (-Gx Impacts)

Fig. 12 Run No. 3676 - Unbraced/Legs Back, 32" Seat Pitch

Fig. 13 Run No. 3688 - Unbraced/Legs Forward, 32" Seat Pitch

HIGH SPEED VIDEO RECORDINGS - Experiment 1 (-Gx Impacts)

Fig. 14 Run No. 3674 - Braced/Legs Back, 28" Seat Pitch

Fig. 15 Run No. 3695 - Braced/Legs Forward, 28" Seat Pitch

HIGH SPEED VIDEO RECORDINGS - Experiment 1 (-Gx Impacts)

Fig. 16 Run No. 3678 - Unbraced/Legs Back, 28" Seat Pitch

Fig. 17 Run No. 3680 - Unbraced/Legs Forward, 28" Seat Pitch

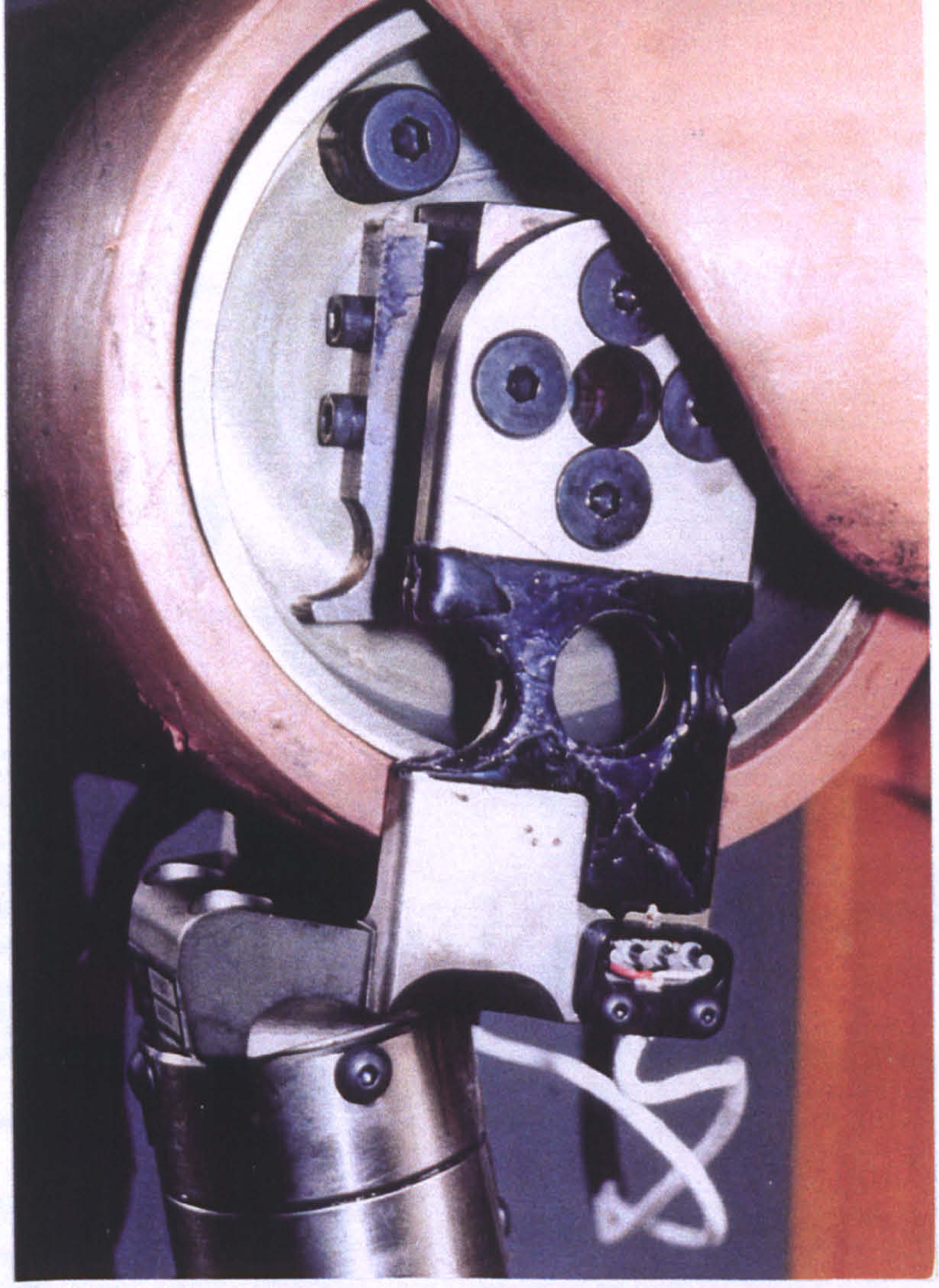

Fig. 18 Knee assembly with metal stop in situ

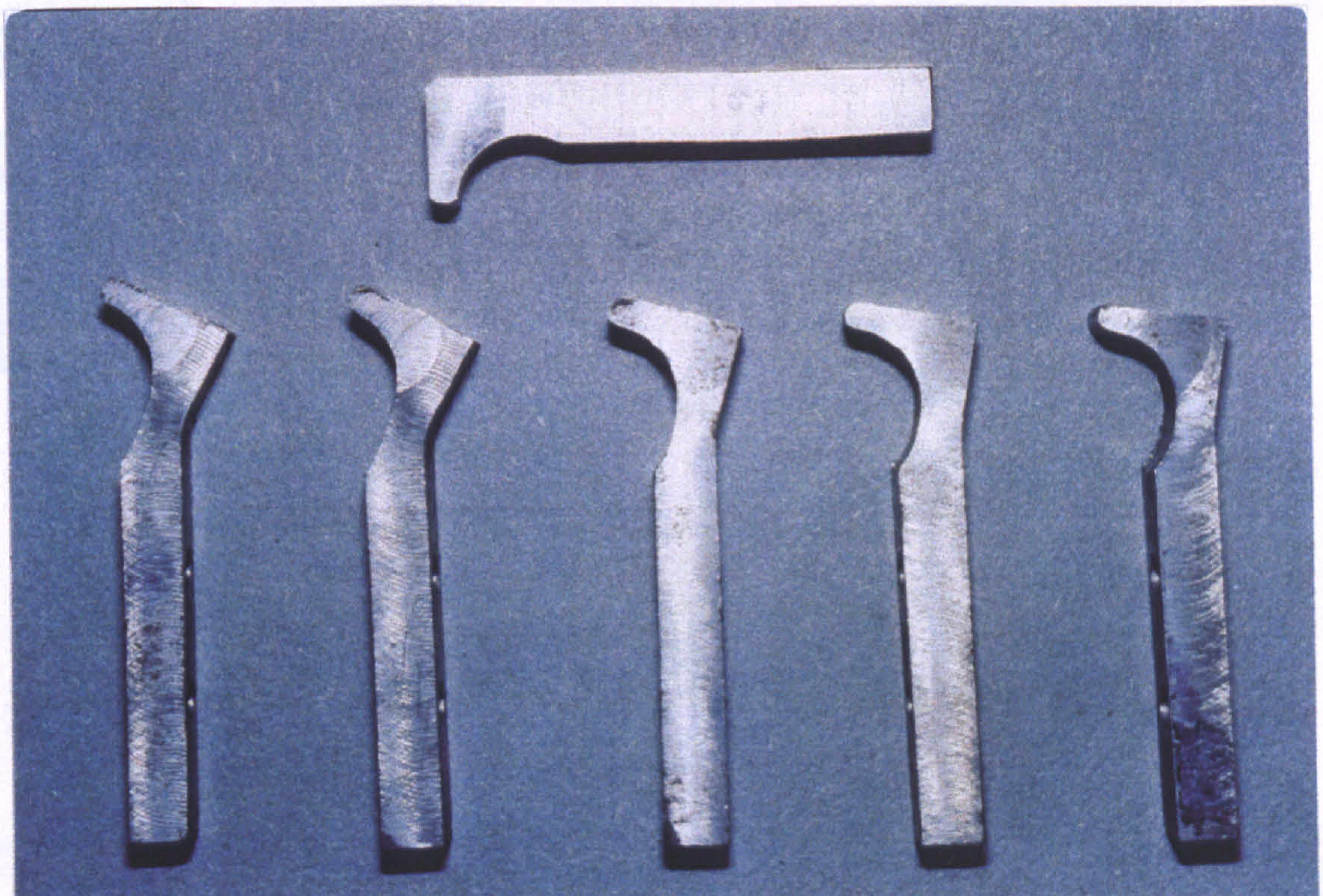

Fig. 19 Deformation of metal knee stops with round stop

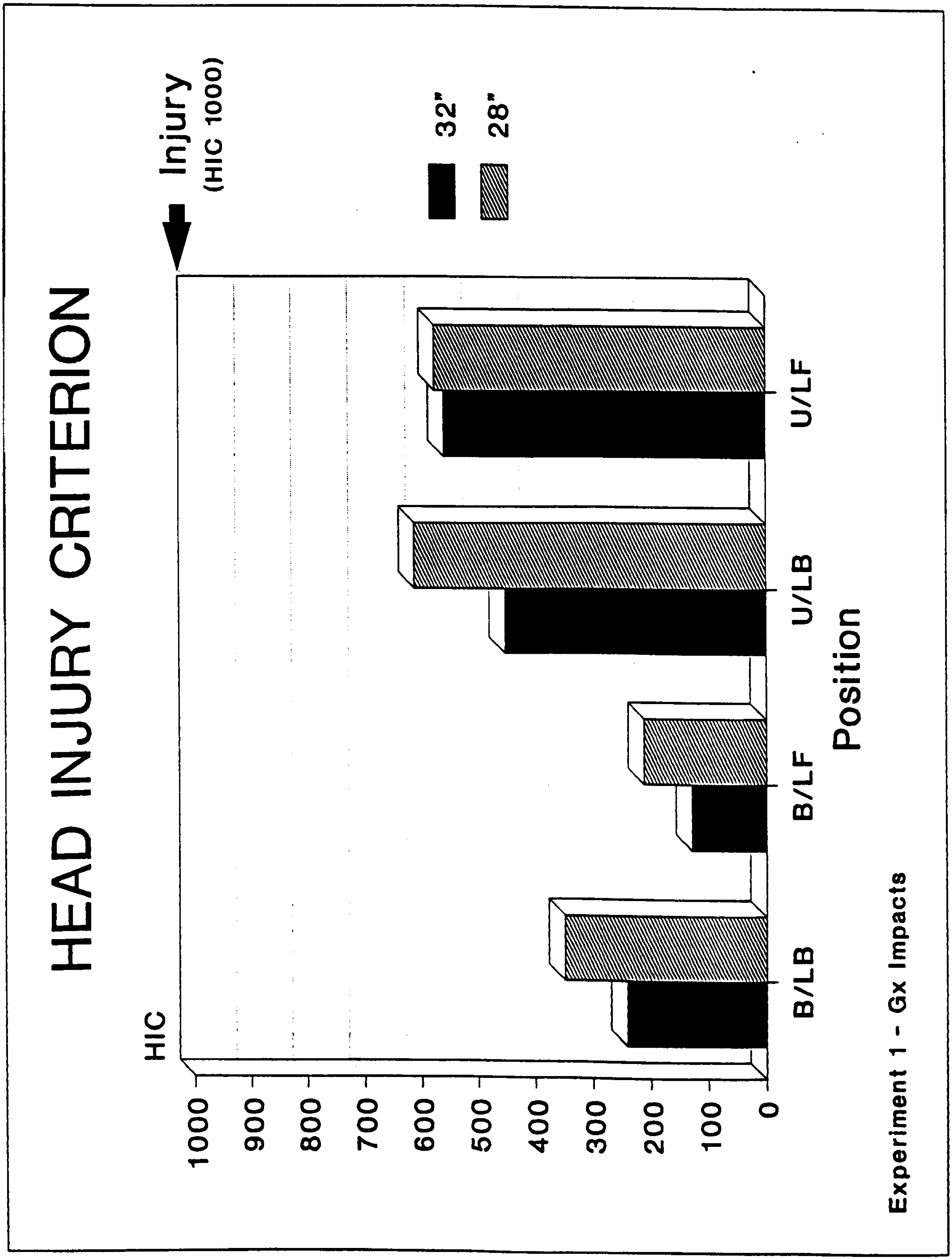

Fig. 20 Head Injury Criterion - Gx Impacts

7.10 STATISTICAL ANALYSIS AND DISCUSSION

The results of Experiment 1 (including statistical analysis) are discussed below:

Key to tables: Position B/LB Braced, legs back
Position U/LB Unbraced, legs back
Position B/LF Braced, legs forward
Position U/LF Unbraced, legs forward

*	$p<0.05$
**	$p<0.01$
***	$p<0.001$

7.10.1 Head

Head Injury Criterion (see Fig. 20)

Table 8 HIC

Source of Variation	Degrees of Freedom	Sums of Squares	Mean Squares	F Value	Sig
B	3	873951.	291317.	63.1831	***
S	1	67436.3	67436.3	14.6261	***
O	3	27850.1	9283.36	2.0135	NS
BS	3	21334.6	7111.53	1.5424	NS
Residual	21	96824.2	4610.67		

Position	B/LB	U/LB	B/LF	U/LF	Mean	
28"	348.50	613.25	212.25	576.00	437.50	)
32"	241.25	453.00	129.00	559.50	345.69	) HIC
Mean	294.88	533.12	170.63	567.75	391.59	)

Positions U/LB and U/LF > Positions B/LB and B/LF (***)
Position B/LB > Position B/LF (**)

The head injury criterion is the industry standard for assessing head injury potential (16).

A HIC value of 1000 is defined as the injury threshold [AS 8049] and represents the point at which 16% of individuals will suffer a significant brain injury (16).

In this experiment all the HIC values recorded were below 1000.

The significance of HIC values under 1000 is unknown and therefore one can only refer to the data in qualitative terms.

HIC values were higher at a 28" seat pitch (mean 438) than at a 32" seat pitch (mean 346). This difference is statistically significant ($p<0.001$).

It is suggested that the HIC values were higher at a shortened 28" seat pitch because the head impacts with the meal tray. At a 28" seat pitch the head will impact with a different area of the meal tray than at a 32" seat pitch. Different areas of the meal tray have different energy absorbing capacities and at a 28" seat pitch the head impacts with a more rigid area, e.g. the edge of the tray.

HIC values were found to be higher in the unbraced positions.

In an unbraced position the dummy is more upright. Therefore, the head accelerates over a greater distance before impacting with the seat ahead. This will cause an increase in the HIC value recorded as the velocity change on impact will be greater

The increased potential for head injury associated with an unbraced position was noted in the late 1980's by Chandler (6).

With the dummy in a braced position, HIC values were higher in a legs back position (mean 295) compared to a legs forward position (mean 171). However the values involved are well below the injury threshold and therefore, although this difference is statistically significant, it is probably not relevant in terms of injury.

7.10.2 Lap Belt

Lap Belt Tension (see Fig. 21a)

Table 9 Lap Belt Tension

Source of Variation	Degrees of Freedom	Sums of Squares	Mean Squares	F Value	Sig
B	3	0.120369E+8	0.401230E+7	13.9220	***
S	1	0.528906E+8	0.528906E+8	183.521	***
O	3	0.174768E+7	582558.	2.0214	NS
BS	3	0.177104E+7	590346.	2.0484	NS
Residual	21	0.605217E+7	288199.		

Position	B/LB	U/LB	B/LF	U/LF	Mean
28"	7010.00	6607.50	6070.00	5400.00	6271.88
32"	9840.00	8417.50	9130.00	7985.00	8843.13
Mean	8425.00	7512.50	7600.00	6692.50	7557.50

Position B/LB > Positions B/LF and U/LF (***)

Position B/LB > Position U/LB (**)

Positions U/LB and B/LF > Position U/LF (**)

Human tolerance to lap belt forces in an impact was investigated by Lewis and Stapp. In their experiments loads of up to 19kN were sustained with only soft tissue injury. However, the impact velocities used were relatively low (7.32 m/s to 8.84 m/s) (23).

In the M1 Kegworth accident, large numbers of pelvic injuries were seen and it was suggested that these injuries were related to the wearing of a lap belt. Subsequent impact tests indicated that passengers experienced lap belt loads of approximately 9kN during the impact (33).

Therefore injury would appear to occur with lap belt loads between 9kN and 19kN. This variation is at least in part due to the effects of variations in belt elasticity, belt stitching, seat stiffness and the duration of the impact pulse, amongst other factors.

All the loads recorded during this experiment approach or exceed the lower

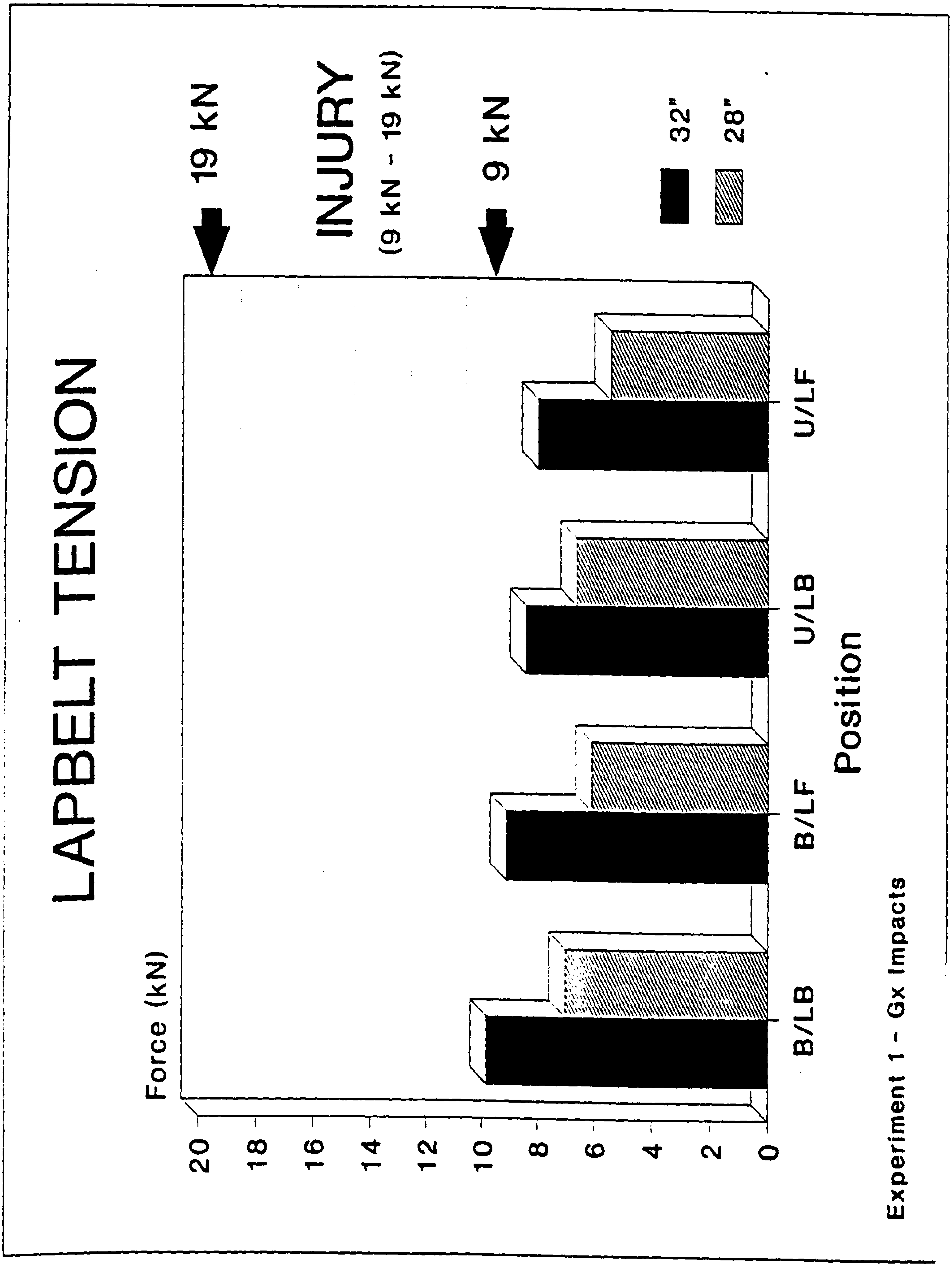

Fig. 21a Lap Belt Tension - Gx Impacts

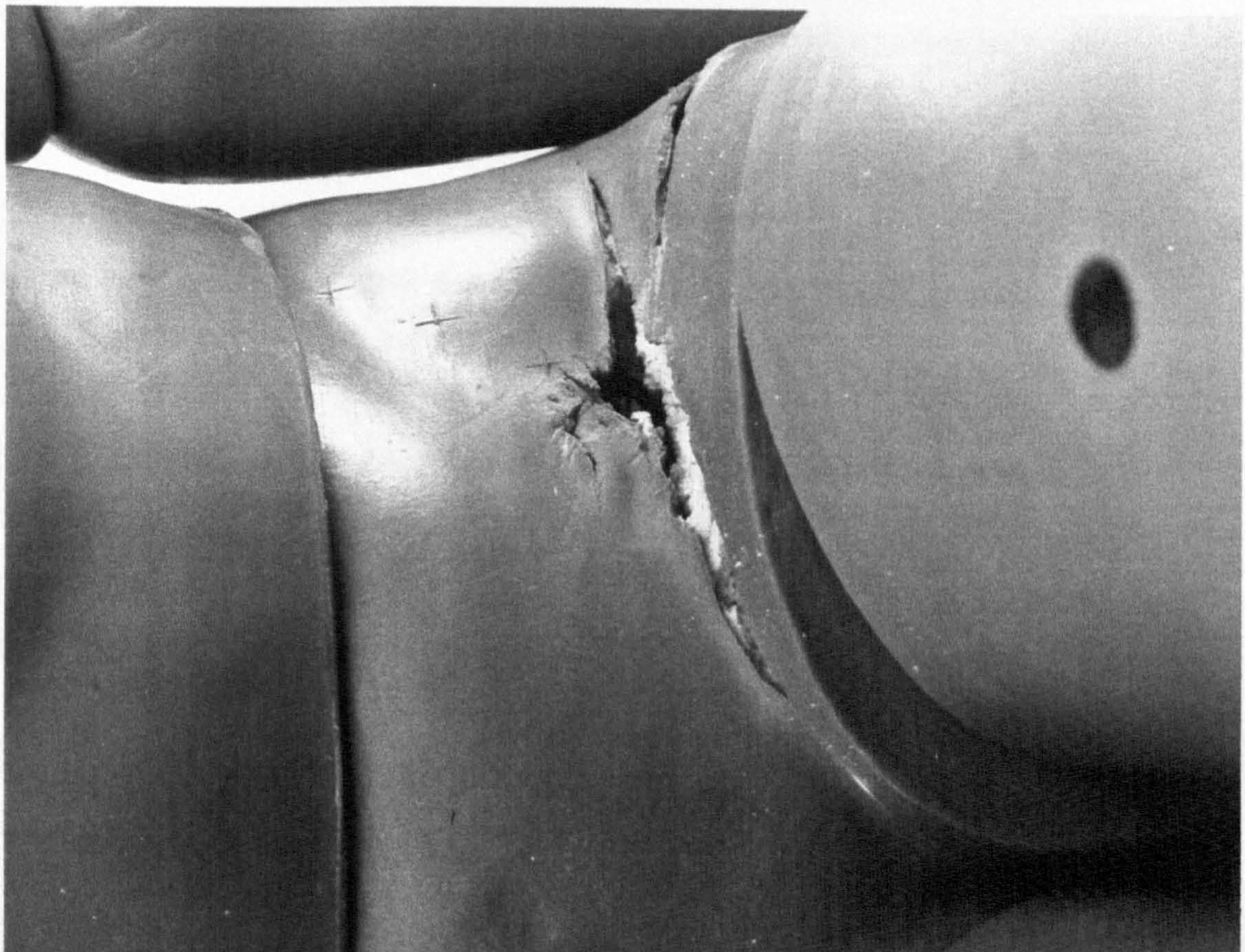

Fig. 21b Damage due to lap belt

limit of this range and indeed, lap belt forces caused damage to the skin overlying the dummy pelvis (Fig. 21b). This damage was repaired initially using masking tape. Unfortunately, no new pelvis soft tissue component was available due to both time and financial considerations.

The highest lap belt loads were associated with a braced legs back position (mean 8.4kN) and these loads were higher than in any of the other positions. This is statistically significant.

In a braced legs back position flailing of the lower limbs does not occur and the lower leg is relatively static. It is suggested that the increased loads seen in the lap belt are related to the lower limb remaining in a relatively fixed position and acting as a strut or lever.

Rowles in 1991 found a similar effect during impact simulation of the M1 Kegworth accident (33).

The lowest lap belt loads were associated with an unbraced legs forward position.

7.10.3 Lumbar Spine

Lumbar Spine Shear Load (see Fig. 22)

Table 10 Lumbar Fx

Source of Variation	Degrees of Freedom	Sums of Squares	Mean Squares	F Value	Sig
B	3	0.969812E+8	0.323271E+8	112.980	***
S	1	156101.	156101.	0.5456	NS
O	3	0.300667E+7	0.100222E+7	3.5027	*
BS	3	0.496888E+7	0.165629E+7	5.7886	**
Residual	21	0.600875E+7	286131.		

Position	B/LB	U/LB	B/LF	U/LF	Mean	
28"	7643.00	4624.25	6273.00	4241.00	5695.31	)
32"	8789.75	3800.50	6132.25	3500.00	5555.63	) N
Mean	8216.37	4212.38	6202.63	3870.50	5625.47	)

Seat pitch 28": Position B/LB > Positions U/LB, B/LF and U/LF (***)
Position B/LF > Positions U/LB and U/LF (***)

Seat pitch 32": Position B/LB > Positions U/LB, B/LF and U/LF (***)
Position B/LF > Positions U/LB and U/LF (***)

Order effect: linear

Melvin et al (29) have estimated that for a 50th percentile Hybrid III dummy, the injury threshold for shear loads in the lumbar spine is 10.7kN.

Therefore whilst the loads recorded in this experiment are high, all are below this estimated injury threshold.

Analysis of the lumbar spine shear loads revealed a linear order effect ($p < 0.05$). It is suggested that this effect was due to seat deformation and loss of elasticity in the lap belt from repeated impacts.

An interaction was shown to exist between brace position and seat pitch ($p < 0.01$).

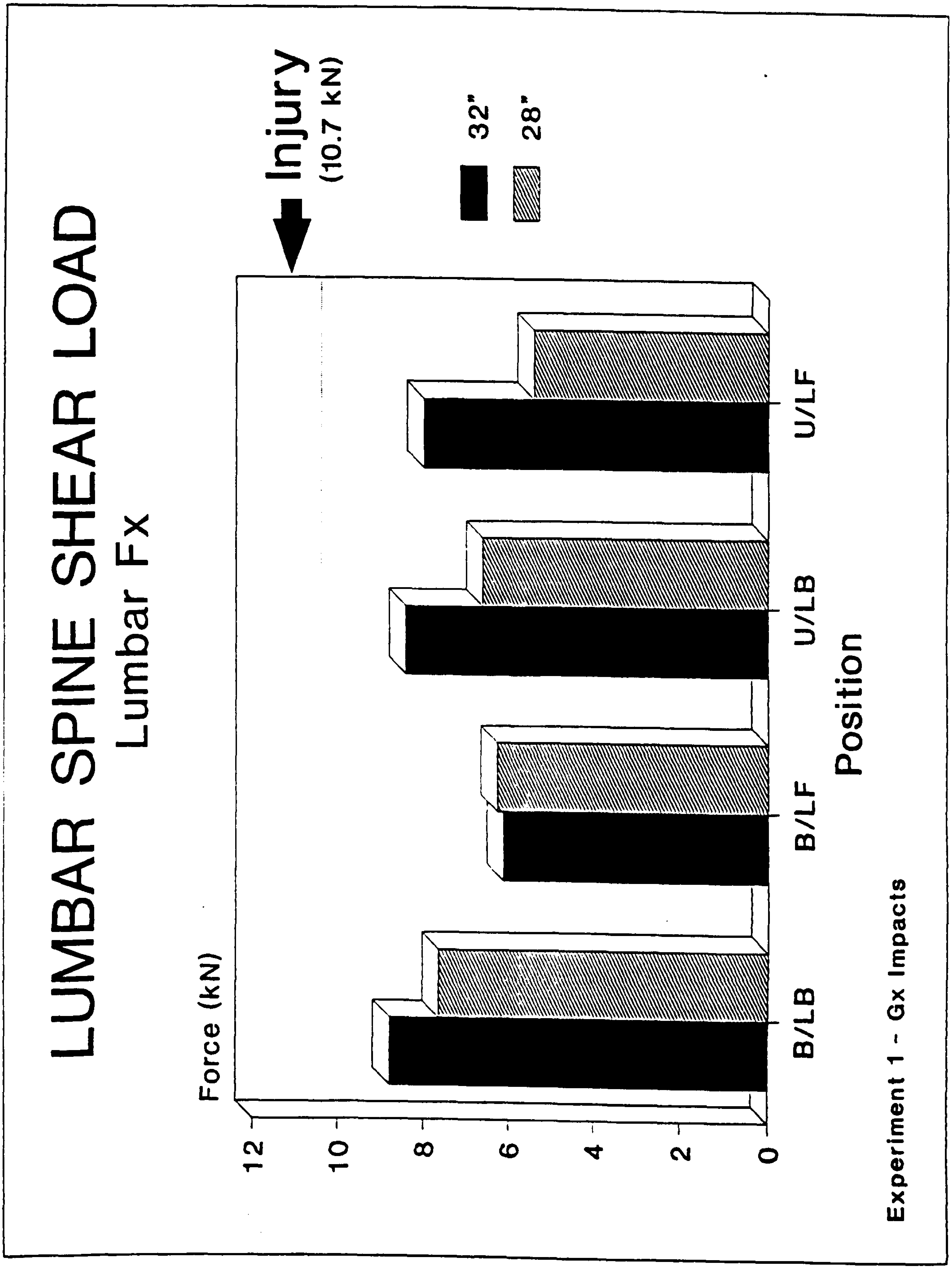

Fig. 22 Lumbar Spine Shear Load - Gx Impacts

There was no significant effect of seat pitch on lumbar spine shear load.

There was a significant effect of brace position on lumbar spine shear load ($p<0.001$).

At a 32" seat pitch the highest loads were associated with a braced legs back position (mean 8.8kN). This difference is statistically significant ($p<0.001$).

The loads recorded in the braced positions were higher than in either of the unbraced positions. These differences are statistically significant ($p<0.001$).

Similar effects were seen at a 28" seat pitch.

The reduction in lumbar spine shear loads associated with an unbraced position is difficult to explain in terms of any single factor.

Lumbar loads were highest in a braced legs back position. In a braced legs back position the lower limbs do not flail. This results in reduced movement in the pelvis which may be reflected in increased lumbar spine loads.

Lumbar Forward Flexion Bending Moment

Lumbar My (see Fig. 23)

Table 11 Lumbar My

Source of Variation	Degrees of Freedom	Sums of Squares	Mean Squares	F Value	Sig
B	3	318043.	106014.	37.8221	***
S	1	37812.5	37812.5	13.4902	**
O	3	21130.1	7043.37	2.5128	NS
BS	3	12899.2	4299.75	1.5340	NS
Residual	21	58862.4	2802.97		

Position	B/LB	U/LB	B/LF	U/LF	Mean	
28"	452.75	308.50	261.75	213.25	309.06	)
32"	434.25	193.25	161.50	172.25	240.31	) Nm
Mean	443.50	250.88	211.63	192.75	274.69	)

Position B/LB > Positions U/LB, B/LF and U/LF (***)
Position U/LB > Position U/LF (*)

Melvin et al (29) have estimated that for a 50th percentile Hybrid III dummy, the injury threshold for a forward flexion spinal bending moment is 1235Nm.

All the loads recorded in this experiment are below this estimated injury threshold.

A significant effect of seat pitch was observed ($p<0.01$) with higher loads being recorded at a 28" seat pitch (mean 309N) as compared to a 32" seat pitch (mean 240N) ($p<0.01$).

The reason for this difference is uncertain.

A significant effect of brace position was observed ($p<0.001$).

The highest bending moments were associated with a braced legs back position (mean 444N) and these loads were higher than in any of the other positions. These differences are statistically significant ($p<0.001$).

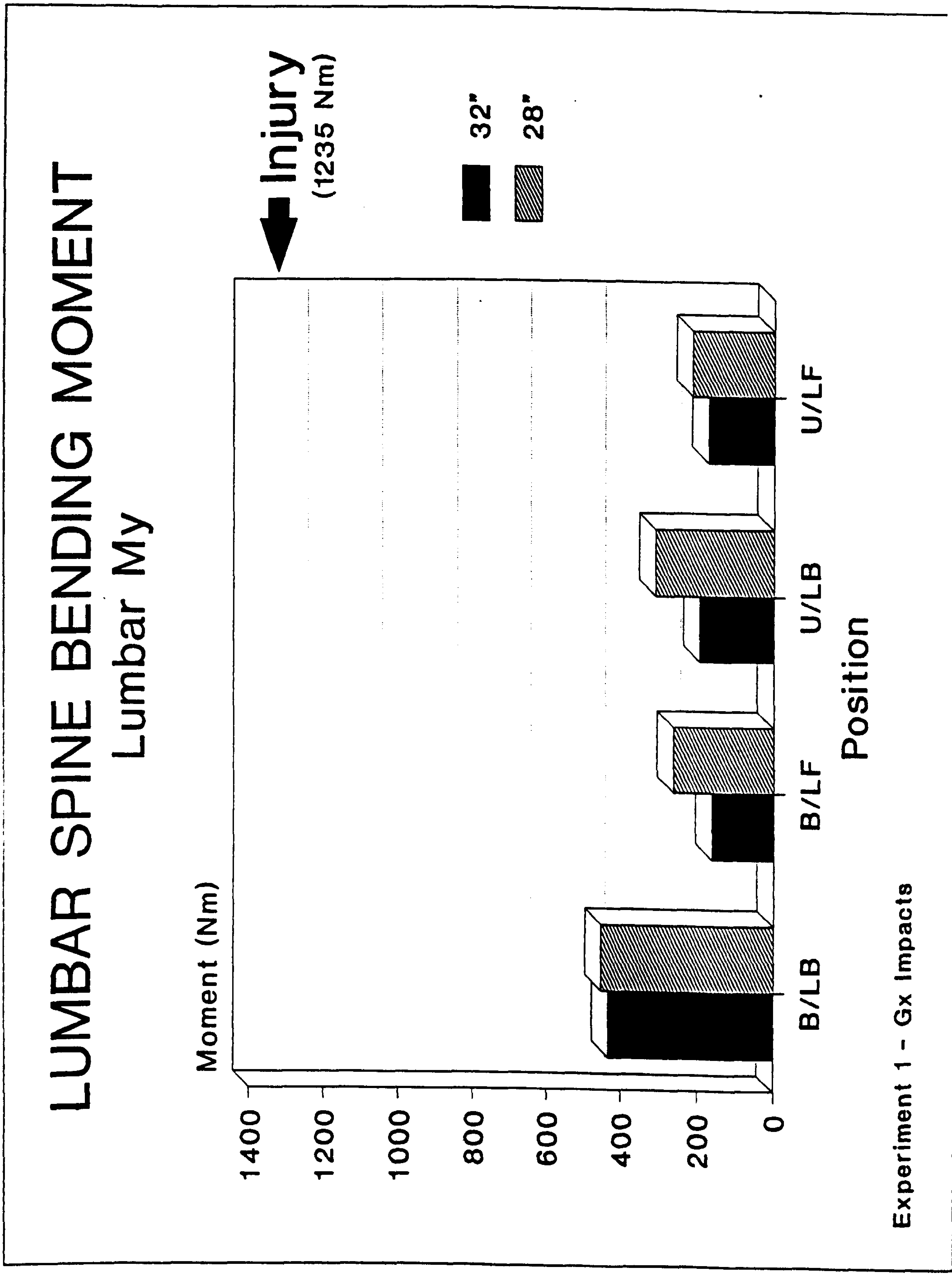

Fig. 23 Lumbar Spine Forward Flexion Bending Moments
- Gx Impacts

The loads recorded in an unbraced legs back position were higher than in an unbraced legs forward position and this difference is statistically significant ($p<0.05$).

The reason for these differences is not clear.

Lumbar Spine Axial Loads

Lumbar Fz (see Fig. 24)

Table 12 Lumbar Fz

Source of Variation	Degrees of Freedom	Sums of Squares	Mean Squares	F Value	Sig
B	3	0.183937E+8	0.613123E+7	50.5097	***
S	1	652939.	652939.	5.3790	*
O	3	966627.	322209.	2.6544	NS
BS	3	0.201506E+7	671688.	5.5334	**
Residual	21	0.254913E+7	121387.		

Position	B/LB	U/LB	B/LF	U/LF	Mean	
28"	5099.25	3326.50	5254.50	3682.50	4340.69	)
32"	5145.25	3055.75	4148.50	3870.50	4055.00	) N
Mean	5122.25	3191.13	4701.50	3776.50	4197.84	)

Seat pitch 28": Positions B/LB and B/LF > Positions U/LB and U/LF (***)

Seat pitch 32": Position B/LB > Positions U/LB, B/LF and U/LF (***)
Position B/LF > Position U/LB (***)
Position U/LF > Position U/LB (**)

The axial loads recorded in the lumbar spine are all in tension.

Melvin et al have estimated that for a 50th percentile Hybrid III dummy, the injury threshold for a tension load in the lumbar spine is 12kN (29).

All the loads recorded are below this injury threshold.

An interaction was noted between brace position and seat pitch ($p<0.01$).

There was a significant effect of brace position on lumbar spine axial loads ($p<0.001$).

At a 32" seat pitch the highest loads were associated with a braced legs back position (mean 5145N) and these loads were higher than in any of the other

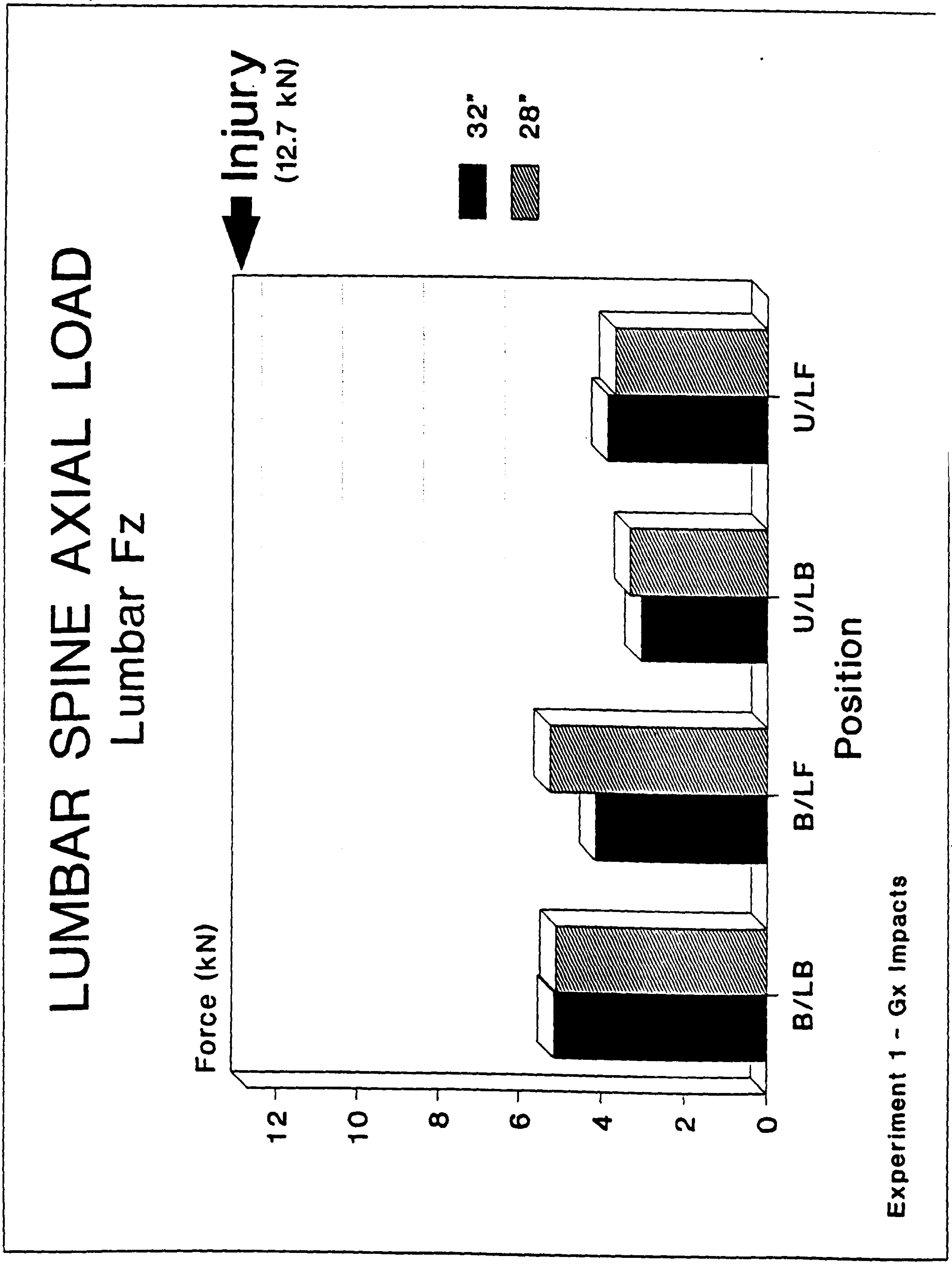

Fig. 24 Lumbar Spine Axial Loads - Gx Impacts

positions including the braced legs forward position (mean 4148N). This difference is statistically significant ($p<0.001$).

It is suggested that the increased loads associated with a braced position are due to the position of the torso at the time of impact. With the torso inclined forwards, impact forces will be transmitted axially along the spinal column producing tension loads.

7.10.4 Lower Limbs

Femoral Axial Load (see Fig. 25)

Table 13 Femur Fz

Right

Source of Variation	Degrees of Freedom	Sums of Squares	Mean Squares	F Value	Sig
B	3	136157.	45385.6	1.1169	NS
S	1	0.223714E+7	0.223714E+7	55.0546	***
O	3	50109.3	16703.1	0.4111	NS
BS	3	80794.1	26931.4	0.6628	NS
Residual	21	853334.	40634.9		

Position	B/LB	U/LB	B/LF	U/LF	Mean		
28"	594.00	516.50	630.25	662.50	600.81	)	
32"	1023.25	1094.50	1300.00	1100.75	1129.63	)	N
Mean	808.63	805.50	965.13	881.63	865.22	)	

Left

Order effect: non-linear

Analysis adjusted for time

Source of Variation	Degrees of Freedom	Sums of Squares	Mean Squares	F Value	
Linear run	1	70733.1	70733.1	3.8887	NS
Quadratic run	1	73745.67	73745.6	4.0543	NS
B (adjusted)	3	804712.	268237.	14.7468	***
S (adjusted)	1	275543.	275543.	15.1485	***
O (adjusted)	3	373903.	124634.	6.8520	**
BS (adjusted)	3	643678.	214559.	11.7958	***
Residual	19	345601.	18189.5		

Means adjusted for order

Position	B/LB	U/LB	B/LF	U/LF	Mean		
28"	405.50	516.13	1046.75	1110.13	769.63	)	
32"	868.00	936.37	1052.50	895.12	938.00	)	N
Mean	636.75	726.25	1049.63	1002.63	853.81	)	

Seat pitch 28": Positions B/LB and U/LB < Positions B/LF and U/LF (***)

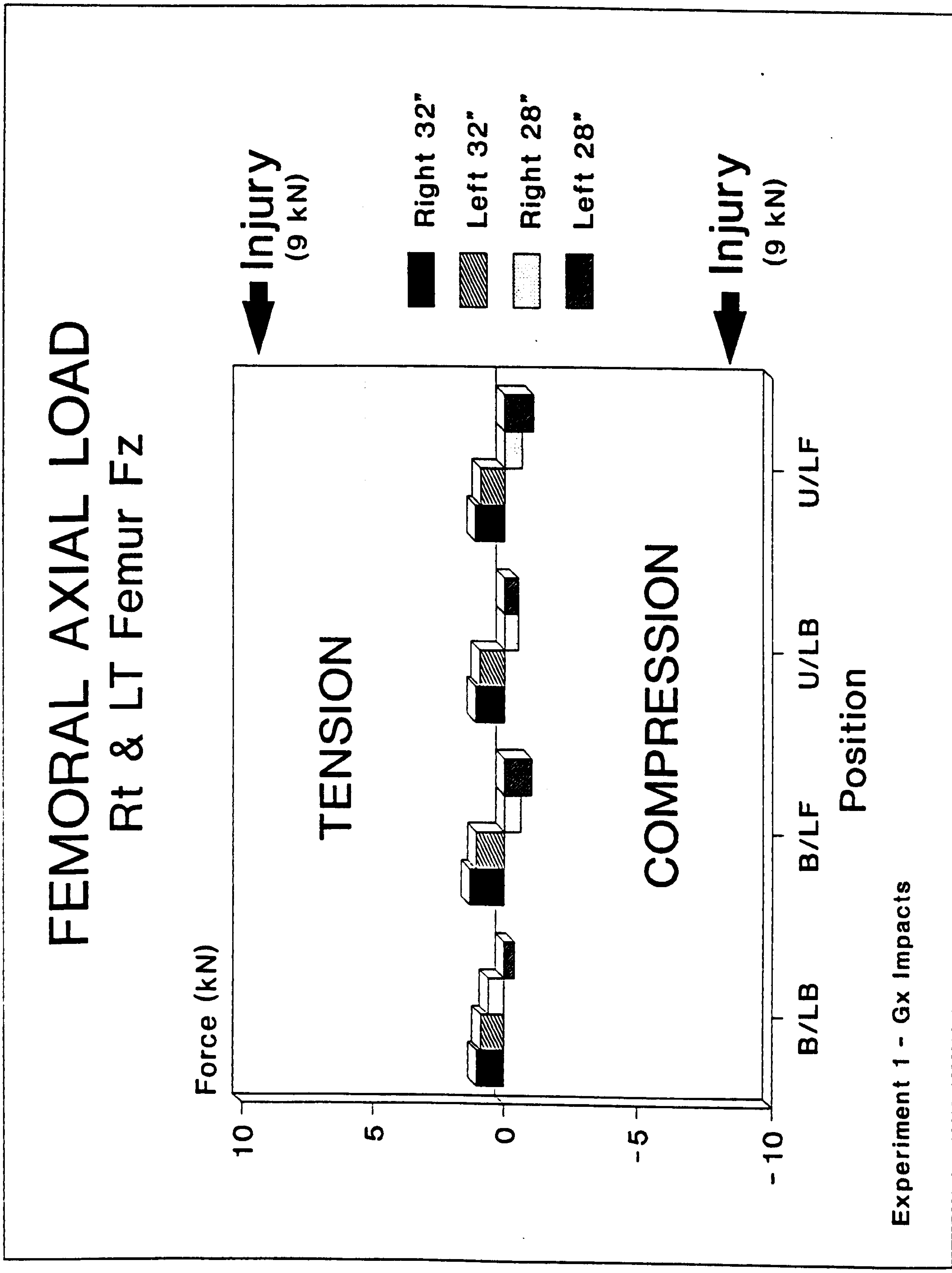

Fig. 25 Femoral Axial Load - Gx Impacts

Right Femur Fz

There was a significant effect of seat pitch on right femoral axial loads ($p<0.001$). At a 32" seat pitch the mean load recorded was 1130N and this was a tension load. At a 28" seat pitch the mean load recorded was 601N and this was a compression load.

There was no significant effect of brace position on femoral axial loads.

Left Femur Fz

A significant non-linear order effect was observed in relation to femoral axial load ($p<0.01$).

An interaction was observed between brace position and seat pitch ($p<0.001$).

There was a significant effect of seat pitch ($p<0.001$).

At a 32" seat pitch the mean load recorded in the left femur was 938N and this was a tension load.

At a 28" seat pitch the mean load recorded in the left femur was 770N and this was a compression load.

A statistically significant effect of brace position was observed ($p<0.001$).

At a 28" seat pitch the loads recorded in both the legs back positions (i.e. upright and braced forward) were lower than in either of the legs forward positions. This effect was statistically significant ($p<0.001$).

Discussion of Femoral Axial Load

A significant non-linear order effect was observed on the left side. It is suggested that this order effect was related to deformation of the back of the forward seat due to repeated impacts.

The increase in compressive axial loads seen at a 28" seat pitch is related to knee contact with the forward seat.

On impact the dummy translates forwards until the slack in the lap belt is taken up. At a 28" seat pitch the knees impact with the seat ahead and compressive loading occurs. At a 32" seat pitch no knee contact occurs with the back of the seat ahead. This was confirmed by review of the high speed video. Therefore only tension loads were recorded in the femur.

The injury threshold for dynamic compressive axial loading of the femur is at 8.68kN (31).

The injury threshold for a tension load applied to the femur is difficult to predict but should be in the region of 8kN.

Therefore all the loads recorded are below the injury threshold.

Higher loads were associated with adopting a legs back position on the left side at a 28" seat pitch. The reason for this is not clear.

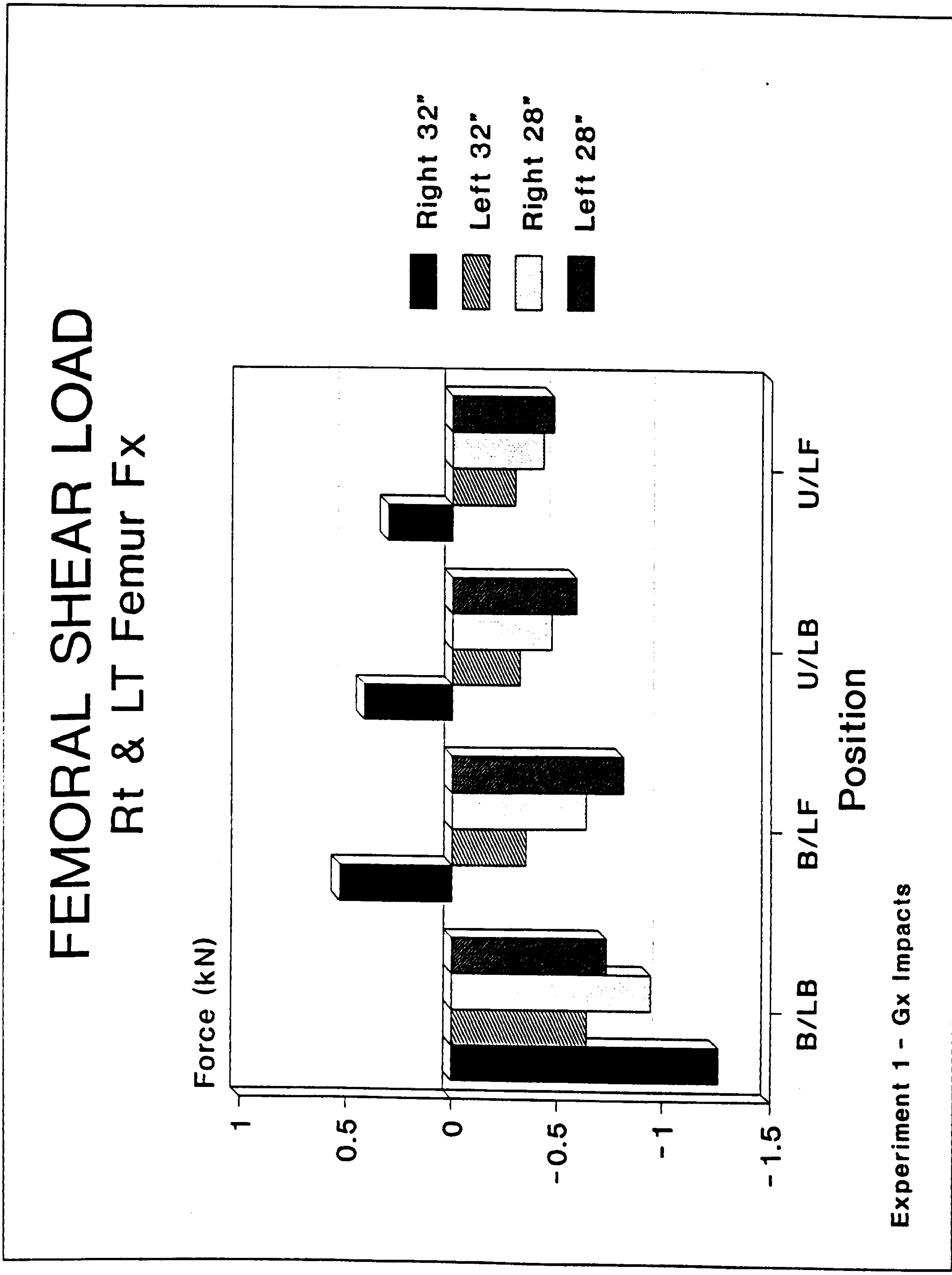

Fig. 26 Femoral Shear Load - Gx Impacts

Femoral Shear Loads

Femur Fx (See Fig. 26)

Table 14 Femur Fx

Right

Source of Variation	Degrees of Freedom	Sums of Squares	Mean Squares	F Value	Sig
B	3	0.263353E+7	877843.	36.7113	***
S	1	300.125	300.125	0.0126	NS
O	3	344895.	114965.	4.8078	*
BS	3	254116.	84705.5	3.5424	*
Residual	21	502154.	23912.1		

Position	B/LB	U/LB	B/LF	U/LF	Mean		
28"	948.00	471.00	639.00	431.25	622.31	)	
32"	1259.25	418.25	531.25	305.00	628.44	)	N
Mean	1103.62	444.63	585.13	368.13	625.38	)	

Seat pitch 28": Position B/LB > Positions U/LB, B/LF and U/LF (**)
Seat pitch 32": Position B/LB > Positions U/LB, B/LF and U/LF (***)

Order effect: linear

Left

Source of Variation	Degrees of Freedom	Sums of Squares	Mean Squares	F Value	
B	3	435776.	145259.	9.1189	***
S	1	513845.	513845.	32.2577	***
O	3	43203.1	14401.0	0.9041	NS
BS	3	152054.	50684.5	3.1818	*
Residual	21	334517.	15929.4		

Position	B/LB	U/LB	B/LF	U/LF	Mean		
28"	736.75	592.00	817.25	479.25	656.31	)	
32"	644.00	320.00	351.75	295.75	402.88	)	N
Mean	690.38	456.00	584.50	387.50	529.59	)	

Seat pitch 28": Positions B/LB and B/LF > Position U/LF (**)
Position B/LF > Position U/LB (*)

Seat pitch 32": Position B/LB > Positions U/LB, B/LF and U/LF (**)

Right Femur Fx

A linear order effect was observed ($p<0.05$). It is suggested that this order effect was related to deformation of the seat and loss of elasticity in the lap belt due to repeated impacts.

An interaction was noted between brace position and seat pitch ($p<0.05$).

There was a statistically significant effect of brace position on femoral shear loads in the x-axis ($p<0.001$).

At a 32" seat pitch the highest femoral shear loads were associated with a braced legs back position (mean 1259N) and these loads were higher than in any of the other brace positions. This difference is statistically significant ($p<0.001$).

A similar pattern was seen at a 28" seat pitch ($p<0.01$).

The direction of the applied shear load was reversed in the braced/legs back position at a 32" seat pitch when compared to the other positions.

Left Femur Fx

No order effect was observed.

An interaction was noted between brace position and seat pitch ($p<0.05$).

A statistically significant effect of brace position was observed on femoral shear loads in the x-axis ($p<0.001$).

At a 32" seat pitch the highest shear loads were associated with a braced legs back position (mean 690N) and these values were higher than in any of the other positions. This difference was statistically significant ($p<0.01$).

At a 28" seat pitch the highest loads were associated with a braced legs forward position (mean 817N).

Discussion

See Discussion of Femoral Shear Loads.

Femur Fy (See Fig. 27)

Table 15 Femur Fy

Right

Source of Variation	Degrees of Freedom	Sums of Squares	Mean Squares	F Value	Sig
B	3	4.62972	1.54324	12.6413	***
S	1	2.18813	2.18813	17.9237	***
O	3	0.770569	0.256856	2.1040	NS
BS	3	1.77744	0.592481	4.8532	*
Residual	21	2.56367	0.122080		

Back-transformed means

Position	B/LB	U/LB	B/LF	U/LF	Mean		
28"	88.26	101.72	148.76	79.30	112.13	)	
32"	66.08	211.66	326.09	188.11	189.17	)	N
Mean	81.25	156.11	234.33	129.94		)	

Seat pitch 28": Positions B/LB < Position B/LF (*)
Seat pitch 32": Position B/LB < Positions U/LB, B/LF and U/LF (***)

Left

Source of Variation	Degrees of Freedom	Sums of Squares	Mean Squares	F Value	
B	3	2.25121	0.750402	8.4022	***
S	1	0.217652E-1	0.217652E-1	0.2437	NS
O	3	0.831341	0.277114	3.1028	*
BS	3	1.20146	0.400486	4.4842	*
Residual	21	1.87552	0.893106E		

Back-transformed means

Position	B/LB	U/LB	B/LF	U/LF	Mean		
28"	285.74	269.03	401.27	320.53	332.81	)	
32"	141.59	371.27	433.02	352.56	315.90	)	N
Mean	205.03	322.14	424.88	342.65		)	

Seat pitch 32": Position B/LB < Positions U/LB, B/LF and U/LF (***)

Order effect: linear

Right Femur Fy

No significant order effect was observed.

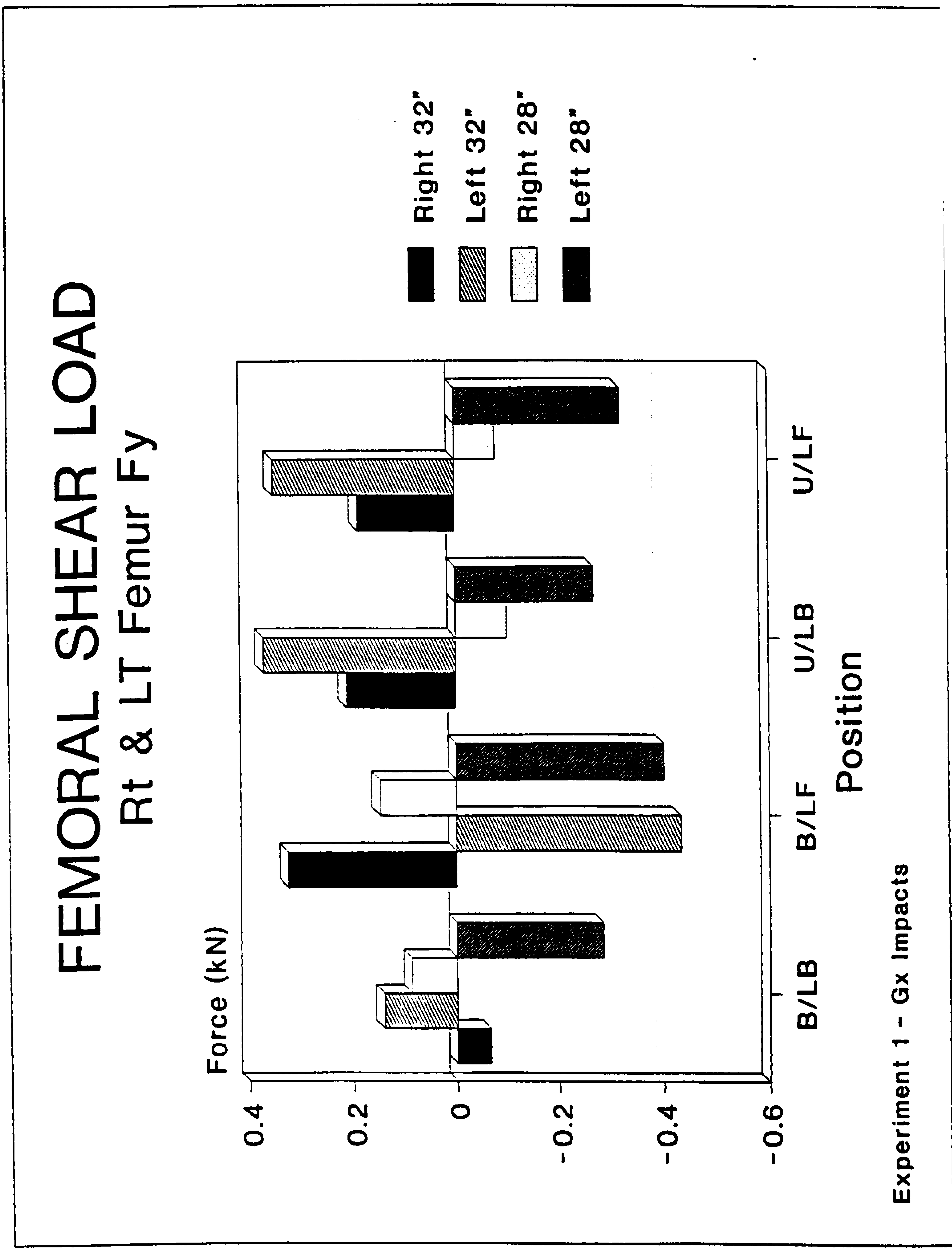

Fig. 27 Femoral Shear Load - Gx Impacts

An interaction was noted between brace position and seat pitch ($p < 0.05$).

A significant effect of brace position was observed on shear loads recorded in the y-axis ($p < 0.001$).

At a 32" seat pitch the lowest shear loads were associated with a braced legs back position (mean 66N) and these loads were lower than in any of the other positions. This difference is statistically significant ($p < 0.001$).

At a 28" seat pitch the loads recorded in a braced legs back position (mean 88N) were lower than those recorded in a braced legs forward position (mean 148N). This difference is statistically significant ($p < 0.05$).

Left Femur Fy

A linear order effect was observed ($p < 0.05$).

It is suggested that the order effect was related to seat deformation and loss of elasticity in the lap belt due to repeated impacts.

An interaction was noted between brace position and seat pitch ($p < 0.05$).

A significant effect of brace position on shear loads in the y-axis was observed ($p < 0.001$).

At a 32" seat pitch the lowest shear loads were associated with a braced legs back position (mean 142N). These loads were lower than in any of the other positions. This difference is statistically significant ($p < 0.001$).

Discussion

See Discussion of Femoral Shear Loads.

Discussion of Femoral Shear Loads

Injury thresholds for a shear load applied to the human femur are difficult to predict.

It should be noted that the highest shear loads in the x-axis were recorded in the braced legs back position. This contrasts with the loads recorded in the y-axis which were lowest in this position.

In a braced legs back position, flailing of the lower limbs did not occur. Therefore, the orientation of the femoral load cell relative to the front seat spar remains constant during the impact. In the other positions, flailing of the lower limbs may occur. Flailing of the lower limbs is associated with axial rotation of the limb about the hip joint. Such rotation changes the orientation of the femoral load cell relative to the front seat spar. Therefore, it is suggested that in the presence of flailing, rotation of the limb occurs, the orientation of the femoral load cell relative to the front seat spar is altered and loads are detected in the y-axis load cell as opposed to the x-axis load cell.

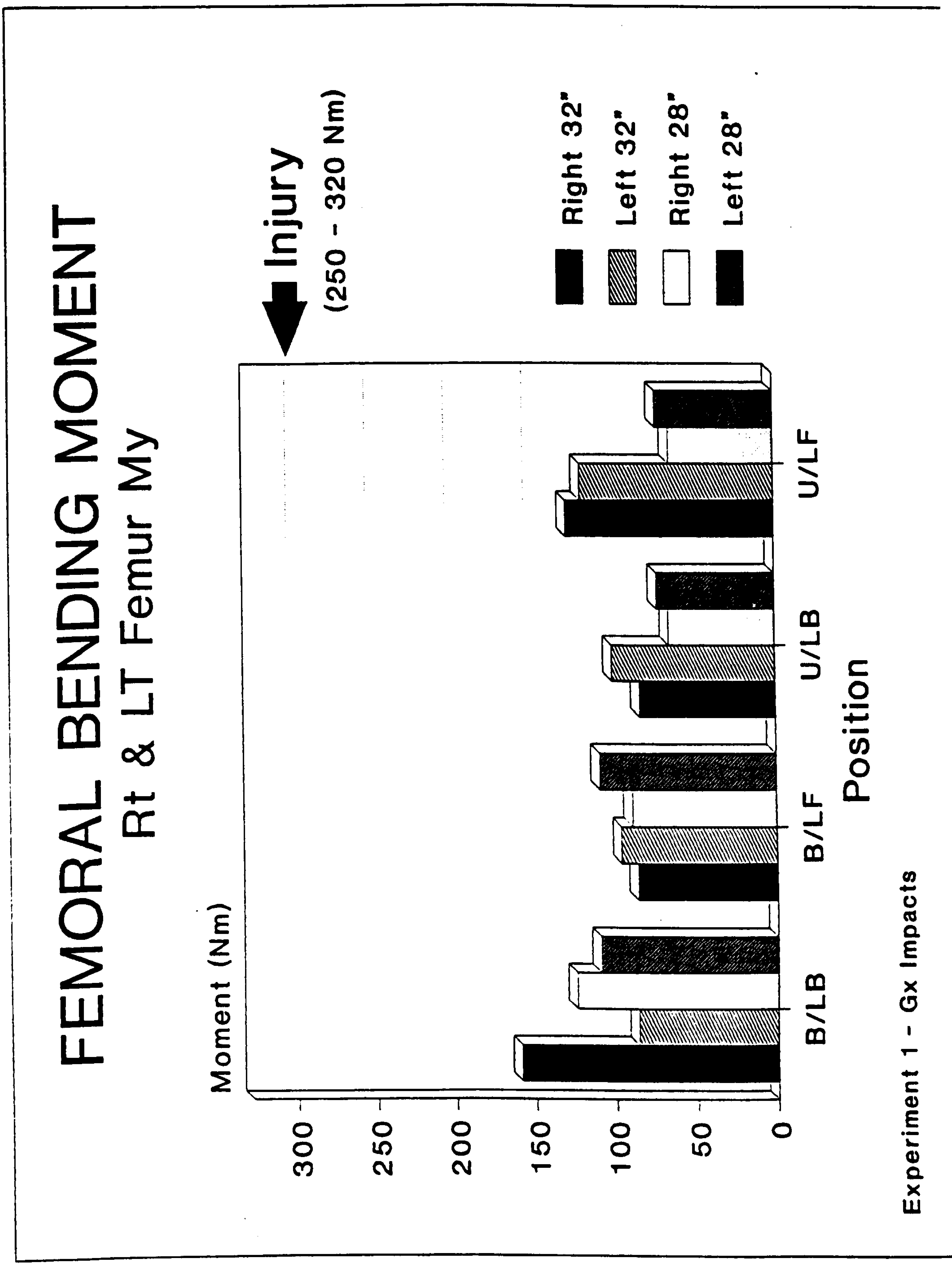

Fig. 28 Femoral Bending Moment - Gx Impacts

Femoral Bending Moments

Femur My (See Fig. 28)

Table 16 Femur My

Right

Order effect: non-linear

Analysis adjusting for order

Source of Variation	Degrees of Freedom	Sums of Squares	Mean Squares	F Value	Sig
Linear Run	1	4869.58	4869.58	11.3348	**
Quadratic Run	1	227.653	227.653	0.5299	NS
B (adjusted)	3	19984.0	6661.35	15.5055	***
S (adjusted)	1	6243.58	6243.58	14.5330	**
O (adjusted)	3	3231.57	1077.19	2.5073	NS
BS (adjusted)	3	4755.75	1585.25	3.6899	*
Residual	19	8162.65	429.613		

Means adjusted for order

Position	B/LB	U/LB	B/LF	U/LF	Mean	
28"	124.50	66.75	89.75	65.37	86.60)	
32"	159.50	84.13	86.25	129.13	114.75)	Nm
Mean	142.00	75.44	88.00	97.25	100.67)	

Seat pitch 28": Position B/LB > Positions U/LB and U/LF (***)
Position B/LB > Position B/LF (*)

Seat pitch 32": Position B/LB > Positions U/LB and B/LF (***)
Position U/LF > Positions U/LB and B/LF (**)

Left

Source of Variation	Degrees of Freedom	Sums of Squares	Mean Squares	F Value	
B	3	994.094	331.365	0.8953	NS
S	1	750.781	750.781	2.0285	NS
O	3	1768.34	589.448	1.5926	NS
BS	3	6673.84	2224.61	6.0106	**
Residual	21	7772.41	370.115		

Position	B/LB	U/LB	B/LF	U/LF	Mean	
28"	109.00	73.75	109.75	73.00	91.38)	
32"	86.25	101.25	96.25	120.50	101.06)	Nm
Mean	97.63	87.50	103.00	96.75	96.22)	

Right Femur My

A non-linear order effect was observed the effect of which was lost after adjusting for quadratic run.

An interaction was noted between brace position and seat pitch ($p<0.05$).

A statistically significant effect of seat pitch was observed ($p<0.01$) with higher loads being recorded at a 32" seat pitch (mean 115Nm) as compared to 28" seat pitch (mean 87Nm).

A statistically significant effect of brace position on femoral bending moments in the y-axis in the right femur was observed ($p<0.001$).

At a 32" seat pitch the highest bending moments were associated with a braced legs back position (mean 160Nm) and these loads were higher than in the unbraced legs back and braced legs forward positions. These differences are statistically significant ($p<0.001$).

At a 28" seat pitch a similar effect was observed.

Left Femur My

No significant effect of brace position or seat pitch was observed.

Overall, the mean bending moment recorded in the y-axis in the left femur was 91Nm.

Discussion

See Discussion of Femoral Bending Moments.

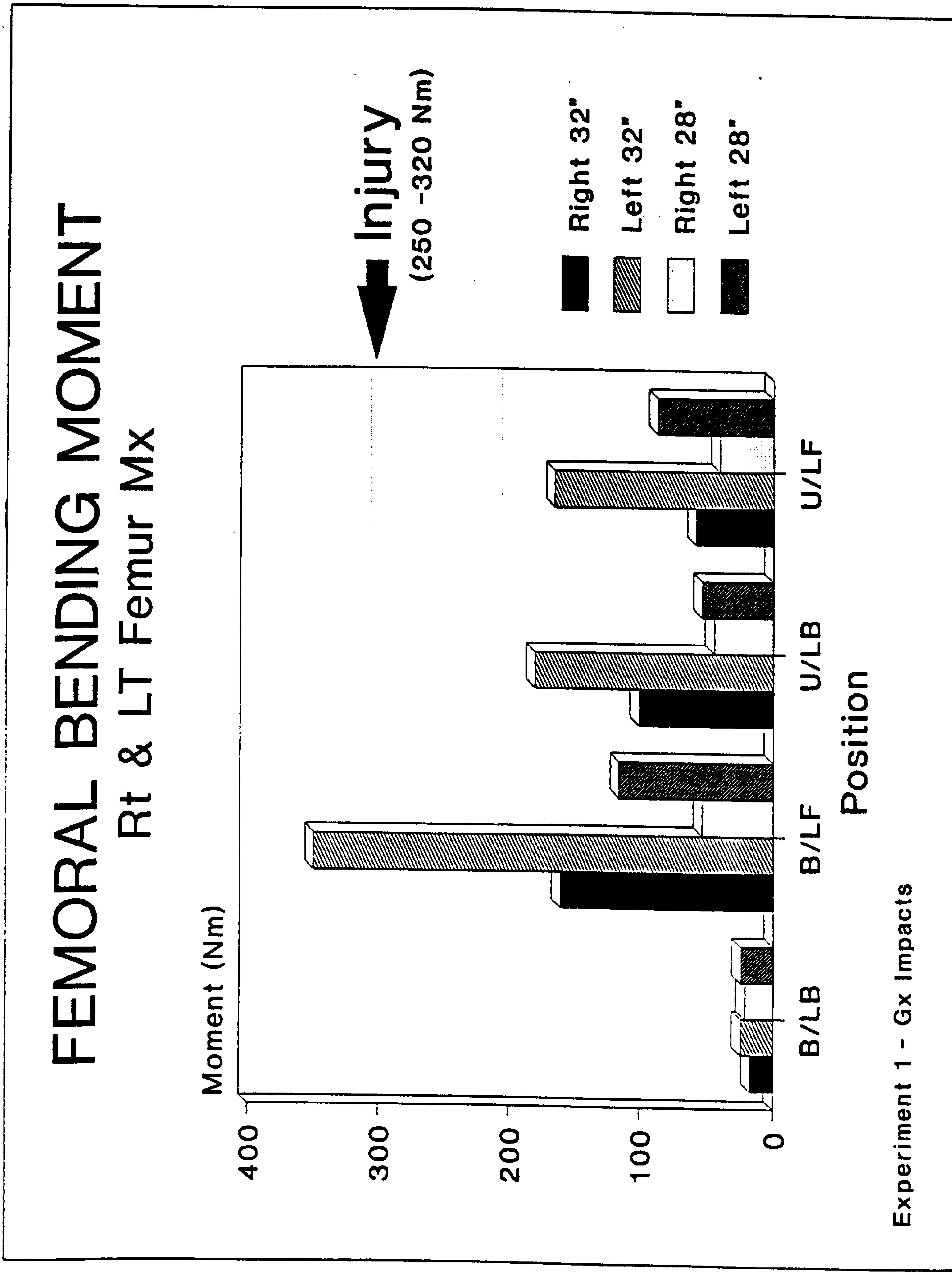

Fig. 29 Femoral Bending Moment - Gx Impacts

Femur Mx (See Fig. 29)

Table 17 Femur Mx

Right

Source of Variation	Degrees of Freedom	Sums of Squares	Mean Squares	F Value	Sig
B	3	11.1511	3.71703	22.3917	***
S	1	2.22333	2.22333	13.3936	**
O	3	4.14600	1.38200	8.3253	***
BS	3	1.94651	0.648835	3.9086	*
Residual	21	3.48600	0.166000		

Back-transformed means

Position	B/LB	U/LB	B/LF	U/LF	Mean		
28"	21.01	44.52	53.17	40.62	46.26	)	
32"	17.39	101.55	161.84	58.24	78.37	)	Nm
Mean	20.40	71.77	99.01	51.91		)	

Seat pitch 28": Positions B/LB < Positions U/LB, B/LF and U/LF (*)
Seat pitch 32": Position B/LB < Positions U/LB, B/LF and U/LF (***)
Position U/LF < Positions U/LB and B/LF (**)

Order effect: linear

Left

Source of Variation	Degrees of Freedom	Sums of Squares	Mean Squares	F Value	
B	3	19.6810	6.56034	23.8241	***
S	1	4.44520	4.44520	16.1429	***
O	3	0.965277	0.321759	1.1685	NS
BS	3	1.86137	0.620457	2.2532	NS
Residual	21	5.78268	0.275366		

Back-transformed means

Position	B/LB	U/LB	B/LF	U/LF	Mean		
28"	24.28	53.02	116.52	87.10	84.18	)	
32"	24.28	181.87	350.94	166.27	177.39	)	Nm
Mean	26.79	108.36	223.16	132.80		)	

Position B/LB < Positions U/LB, B/LF and U/LF (***)
Position U/LB < Position B/LF (*)

Right Femur Mx

A linear order effect was observed ($p<0.001$) and an interaction was noted between brace position and seat pitch ($p<0.05$).

A statistically significant effect of seat pitch on femoral bending moments in the x-axis was observed ($p<0.01$) with higher moments being recorded at a 32" seat pitch (mean 78Nm) as compared to a 28" seat pitch (mean 46Nm).

A statistically significant effect of brace position was observed ($p<0.001$).

At a 32" seat pitch the lowest bending moments were associated with a braced legs back position (mean 17Nm) and these loads were lower than in any of the other positions ($p<0.001$).

A similar effect was observed at a 28" seat pitch ($p<0.05$).

Left Femur Mx

A statistically significant effect of seat pitch on femoral bending moments in the x-axis was observed ($p<0.001$) with higher moments recorded at a 32" seat pitch (mean 177Nm) as compared to a 28" seat pitch (mean 84Nm).

A statistically significant effect of brace position was observed ($p<0.001$).

The lowest loads were associated with a braced legs back position (mean 27Nm) and these were lower than in any other position ($p<0.001$).

Very high loads were associated with a braced legs forward position at a 32" seat pitch (mean 351Nm).

Discussion

See Discussion of Femoral Bending Moments.

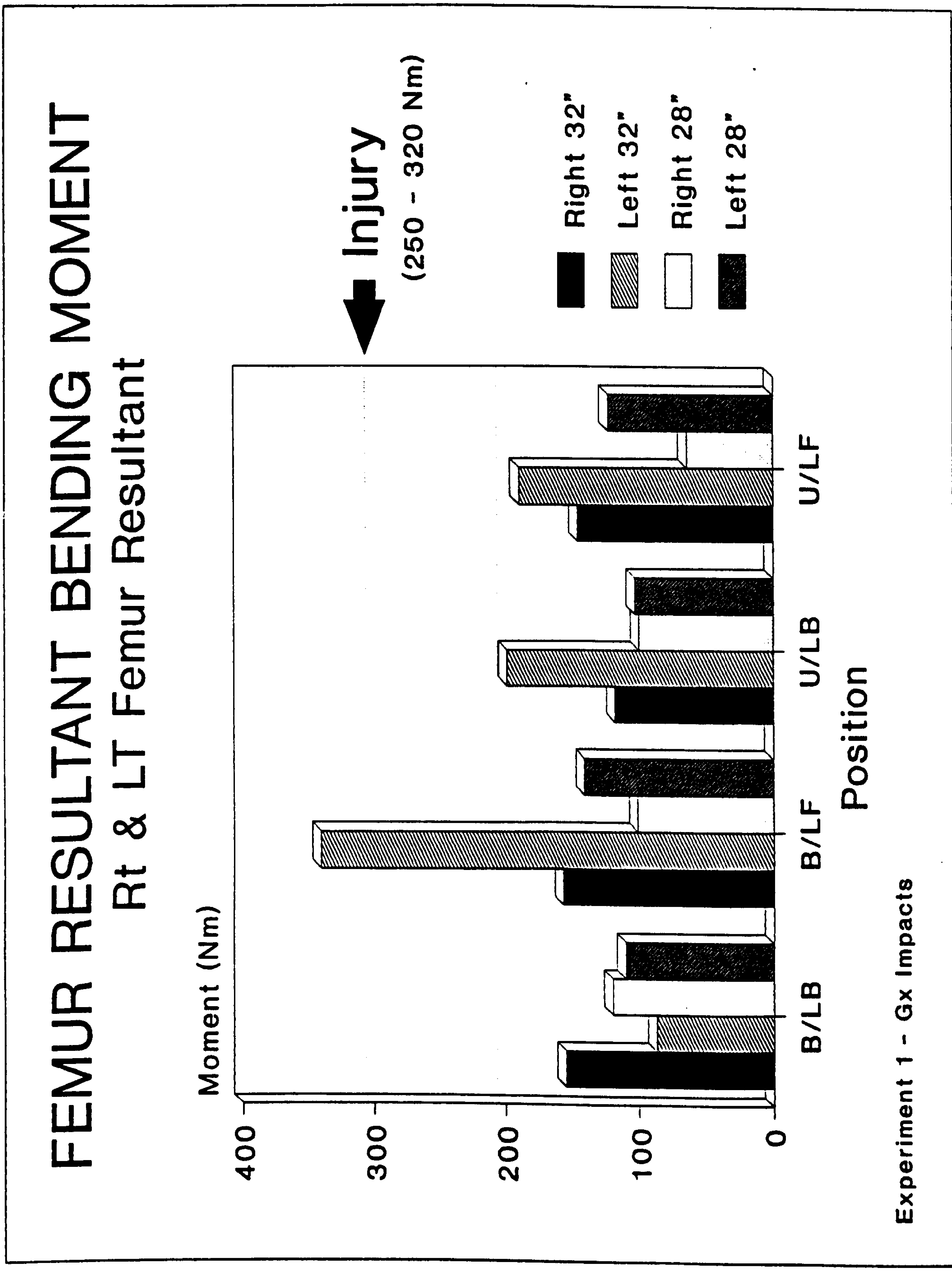

Fig. 30a Femur Resultant Bending Moment - Gx Impacts

Femur Resultant Bending Moment (See Fig. 30a)

Table 18 Femur Resultant Bending Moment

Right

Source of Variation	Degrees of Freedom	Sums of Squares	Mean Squares	F Value	Sig
B	3	5828.62	1942.87	2.2457	NS
S	1	18240.5	18240.5	21.0839	***
O	3	3098.13	1032.71	1.1937	NS
BS	3	4530.75	1510.25	1.7457	NS
Residual	21	18167.9	865.137		

Position	B/LB	U/LB	B/LF	U/LF	Mean	
28"	120.00	100.50	101.75	64.50	96.69	)
32"	155.25	118.50	157.75	146.25	144.44	) Nm
Mean	137.63	109.50	129.75	105.38	120.56	)

Left

Source of Variation	Degrees of Freedom	Sums of Squares	Mean Squares	F Value	
B	3	83689.8	27896.6	16.1093	***
S	1	57545.3	57545.3	33.2303	***
O	3	2176.84	725.615	0.4190	NS
BS	3	50803.6	16934.5	9.7791	***
Residual	21	36365.9	1731.71		

Position	B/LB	U/LB	B/LF	U/LF	Mean	
28"	110.75	103.75	141.75	123.00	119.81	)
32"	87.00	199.25	341.50	190.75	204.63	) Nm
Mean	98.88	151.50	241.63	156.88	162.22	)

Seat pitch 32": Position B/LF > Positions B/LB, U/LB and U/LF (***)
Position B/LB < Position U/LB (***)
Position B/LB < Position U/LF (**)

Right Femur Resultant Bending Moment

A statistically significant effect of seat pitch on right femur resultant bending moment was observed ($p<0.001$) with higher loads recorded at a 32" seat pitch (mean 144Nm) as compared to a 28" seat pitch (mean 97Nm).

No significant effect of brace position was observed.

Left Femur Resultant Bending Moment

An interaction was noted between brace position and seat pitch ($p < 0.001$).

A statistically significant effect of seat pitch was observed ($p < 0.001$) with higher loads recorded at a 32" seat pitch (mean 205Nm) as compared to a 28" seat pitch (mean 120Nm).

A statistically significant effect of brace position was observed ($p < 0.001$).

The highest loads were associated with a braced legs forward position (mean 191Nm) and these loads were higher than in any of the other positions ($p < 0.001$).

Discussion

See Discussion of Femoral Bending Moments.

Discussion of Femoral Bending Moments

Order effects were observed in the bending moments recorded in the right femur about the x-axis and y-axis. The order effects were linear and it is suggested that the effects were related to deformation of the seat and loss of elasticity in the lap belt as a result of repetitive loading.

Differences are noted between the behaviour of the right and left femur. On the high speed video these differences manifested as a tendency for the left leg to slide forward more readily than the right, on impact.

The bending moments are lower in both the y-axis and the x-axis (and the resultant) at a 28" seat pitch. At a 28" seat pitch knee contact occurs with the back of the seat ahead. Therefore energy will be absorbed by axial compression of the femur.

In the x-axis the highest bending moments on the right side were associated with a braced legs back position. (On the left side no effect of brace position was observed.) This contrasts with the y-axis where the lowest femoral bending moments were associated with a braced legs back position.

In the braced legs back position the lower legs do not flail. Consequently the orientation of the femoral load cell relative to the front seat spar and lap belt remain constant. In all the other positions flailing may occur and review of the high speed video reveals that the limb rotates about the hip joint during flailing. Consequently the orientation of the femoral load cell relative to the front seat spar and lap belt are changed and it is suggested that in the flailing situation this change in orientation causes bending moments to be recorded preferentially in the x-axis load cell.

This behaviour would explain why the resultant femoral bending moments, in both legs, are relatively uniform (with the exception of the left leg, braced legs forward position, 32" seat pitch).

Weber (28) predicted that for a bending load applied to the femur, the load to failure was on average 233Nm in the male and 165Nm in the female. Messerer (28) produced comparable figures with the value of 310Nm in the male and 180Nm in the female. Both of these loads were applied statically. Mather has shown that when bones are loaded dynamically, the load to failure increases. In his experiments the energy to failure increased by up to 48% when bones were loaded dynamically (27). Martens similarly showed that the dynamic load to failure for a torque load applied to the femur was 16 to 24% greater than the comparable static value (25).

St-Laurent recently defined a dynamic bending load to failure of 320Nm for the frangible femoral component in a motorcyclist anthropometric test device (36).

Therefore it would seem that the injury threshold for the human femur when loaded in a bending configuration under dynamic conditions lies in the range of 250Nm-320Nm.

High loads were recorded in the left femur in a braced legs forward position at a 32" seat pitch. The mean load recorded (342Nm) was above the injury threshold. Whilst high loads were seen in all of the other positions the loads recorded in this particular configuration are the only ones which are above the injury threshold. The result appears to be anomalous. However, review of subsequent computer simulations revealed that foot entrapment produces high bending moments in the human femur. It is possible that a degree of foot entrapment may have occurred on the left side which remained hidden from view of the high speed video camera being the side most distant from the camera lens.

It is suggested that bending loads may be responsible for femoral fractures in seated occupants involved in an aircraft accident with a similar impact pulse.

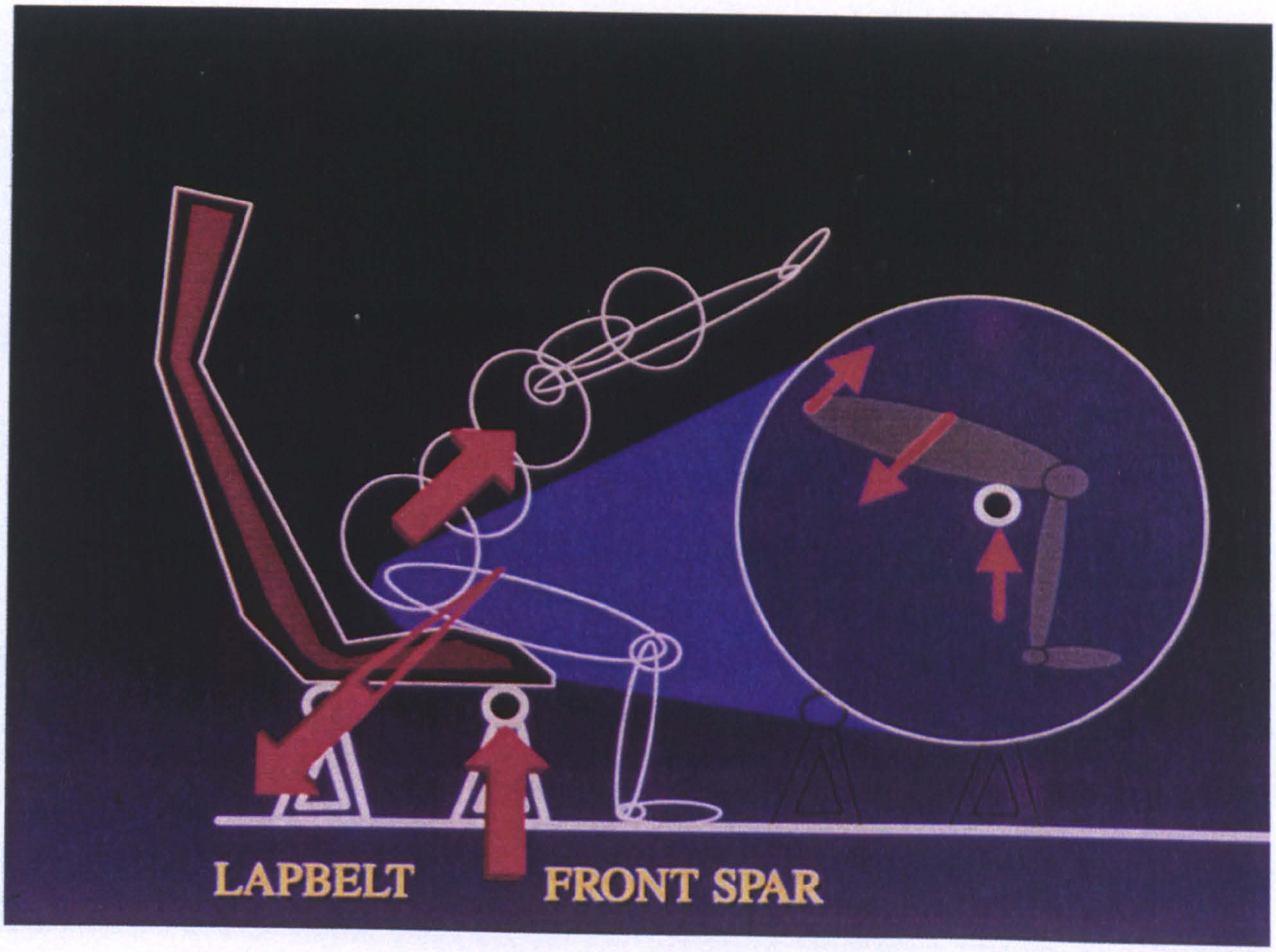

Fig. 30b Femoral Bending Moment - No Flail

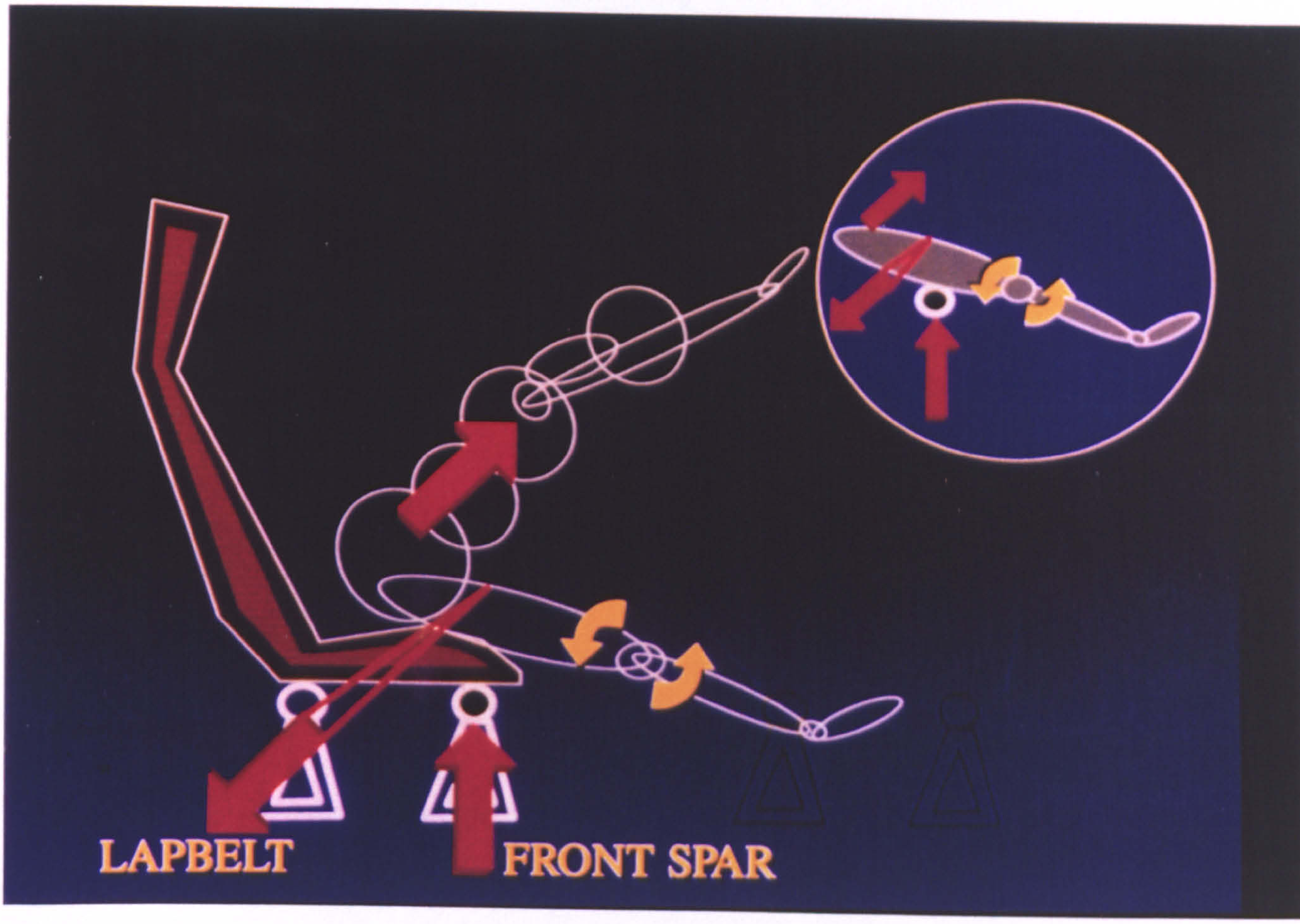

Fig. 30c Femoral Bending Moment - Flail

The bending moments appeared to result from forward flexion of the upper torso around the lap belt and involved the front seat spar. This produced a bending moment in a three point configuration (see Fig. 30b). In addition, in the non flailing situation, the lower leg will act as a strut. This was reflected in the increased axial compressive loads seen in the lower leg when flailing did not occur.

When flailing occurs a further downward moment is created just proximal to the knee as a result of hyperextension of the knee and consequent deformation of the knee stop (see Figs. 11, 11a, 18, 19, 30c).

Femoral Torque

Femur Mz (See Fig. 31)

Table 19 Femur Mz

Right

Source of Variation	Degrees of Freedom	Sums of Squares	Mean Squares	F Value	Sig
B	3	6330.62	2110.21	62.8239	***
S	1	0.500000	0.500000	0.0149	NS
O	3	616.125	205.375	6.1143	**
BS	3	436.250	145.417	4.3293	*
Residual	21	705.375	33.5893		

Position	B/LB	U/LB	B/LF	U/LF	Mean	
28"	53.75	34.25	38.25	25.00	37.81	)
32"	65.25	31.25	37.50	16.25	37.56	) Nm
Mean	59.50	32.75	37.88	20.63	37.69	)

Seat pitch 28": Position B/LB > Positions U/LB, B/LF and U/LF (***)
Positions U/LB and B/LF > Position U/LF (*)

Seat pitch 32": Position B/LB > Positions U/LB, B/LF and U/LF (***)
Positions U/LB and B/LF > Position U/LF (**)

Order effect: linear

Left

Source of Variation	Degrees of Freedom	Sums of Squares	Mean Squares	F Value	
B	3	8688.34	2896.11	25.4188	***
S	1	16425.8	16425.8	144.1667	***
O	3	682.094	227.365	1.9955	NS
BS	3	2930.59	976.865	8.5738	***
Residual	21	2392.66	113.936		

Position	B/LB	U/LB	B/LF	U/LF	Mean	
28"	113.25	101.75	105.00	85.75	101.44	)
32"	86.00	26.75	75.25	36.50	56.13	) Nm
Mean	99.63	64.25	90.13	61.13	78.78	)

Seat pitch 28": Positions B/LB, U/LB and B/LF > Position U/LF (*)

Seat pitch 32": Positions B/LB and B/LF > Positions U/LB and U/LF (***)
Positions U/LB and B/LF > Position U/LF (**)

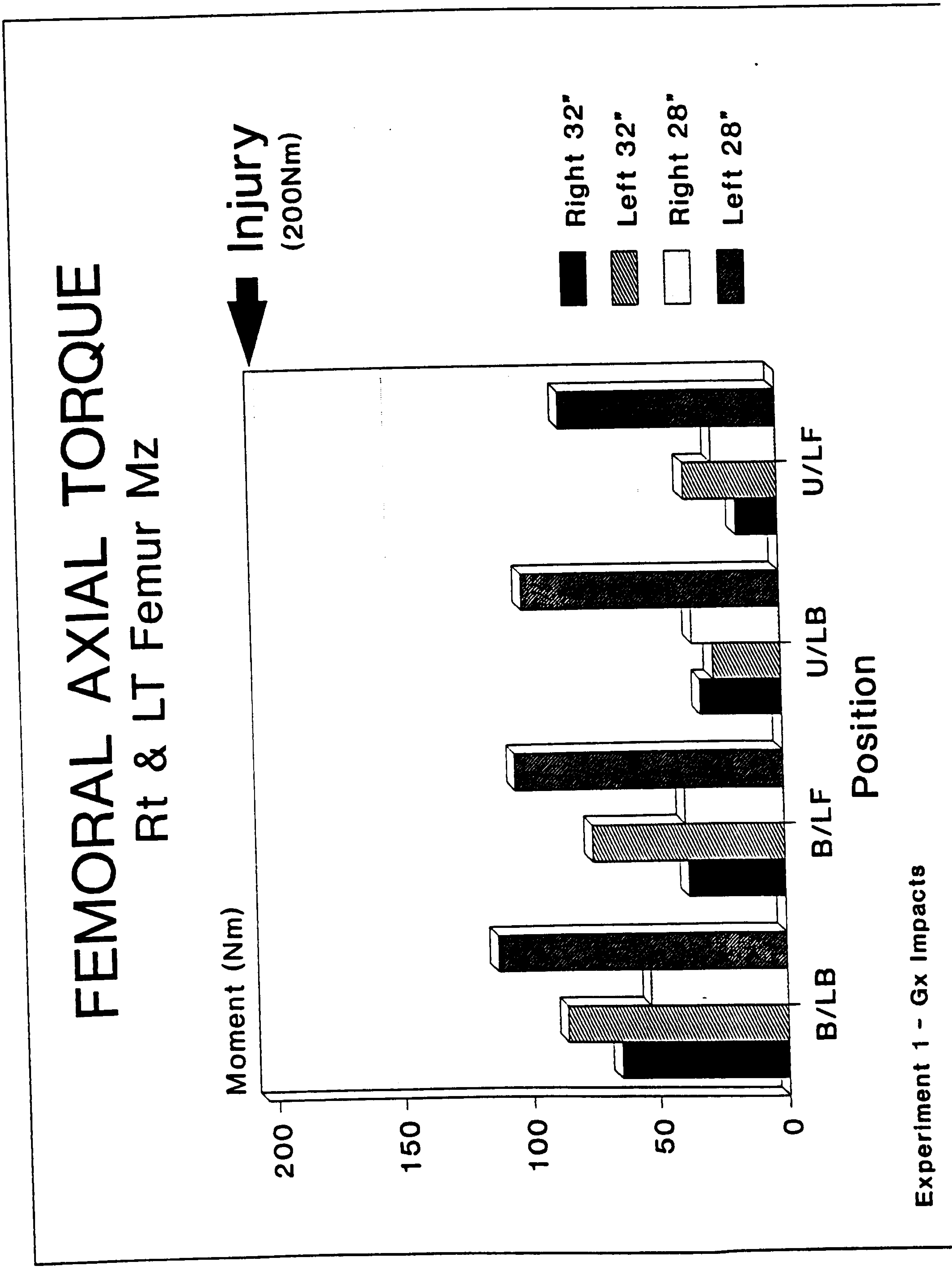

Fig. 31 Femoral Torque - Gx Impacts

Right Femur Mz

A linear order effect was observed ($p < 0.01$) and an interaction was noted between brace position and seat pitch ($p < 0.01$).

No significant effect of seat pitch was observed.

A significant effect of brace position on right femoral torque was observed ($p < 0.001$).

At a 32" seat pitch the highest torques were associated with a braced legs back position (mean 65Nm) and these loads were higher than in any of the other positions.

A similar effect was observed at a 28" seat pitch.

Left Femur Mz

An interaction was noted between brace position, seat pitch and left femoral torque ($p < 0.001$).

A statistically significant effect of brace position on left femoral torque was observed ($p < 0.001$).

At a 32" seat pitch the highest loads were associated with a braced legs back position (mean 113Nm) and these loads were significantly higher than in either the unbraced legs back or unbraced legs forward positions ($p < 0.001$).

Discussion of Femoral Torque

A linear order effect was observed on the right side. It is suggested that this effect was related to seat deformation and loss of elasticity in the lap belt due to repeated impacts.

In the braced legs back position the lower limbs do not flail. In all the other positions there is a tendency for flailing to occur.

If flailing occurs then the lower limbs rotate about the hip joint and any rotational moments will produce rotation around this joint.

In the non-flail situation such rotational moments produce a torsional load in the femoral load cell because the lower leg will act as a strut. This would account for the increased torsional loads associated with a braced legs back position.

Martens et al defined the injury threshold for dynamic torsional loading of the femur at 204Nm for males (25). St-Laurent et al defined a dynamic torsional load to failure of 192Nm for the frangible femoral component of a motorcyclist anthropometric test device (36). Therefore the injury threshold would appear to lie at about 200Nm for the adult male.

All the loads recorded are below the injury threshold.

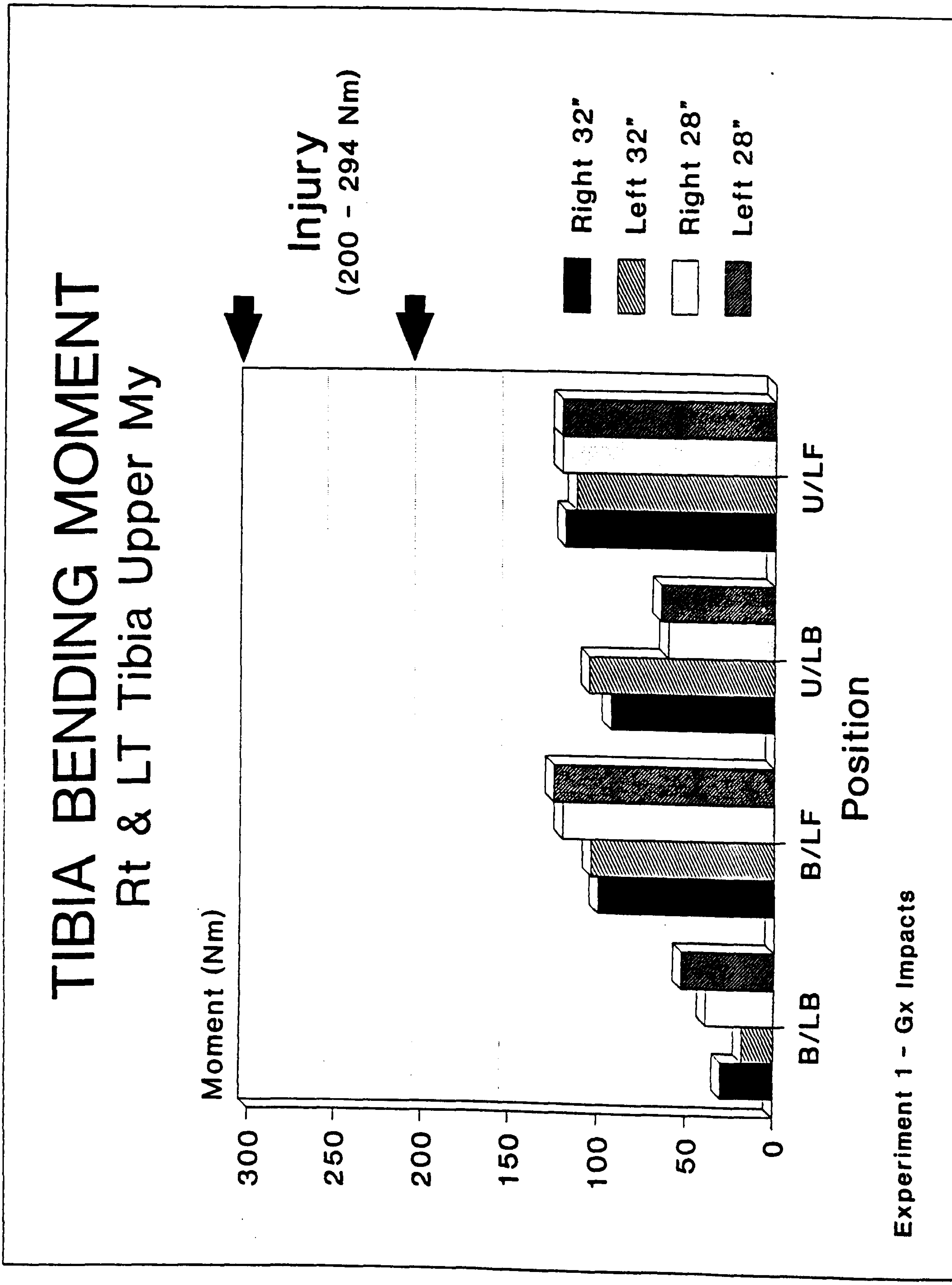

Fig. 32 Tibia Bending Moment - Gx Impacts

Tibia

Tibial Bending Moment (See Fig. 32)

Table 20(a) Tibia upper My

Right

Source of Variation	Degrees of Freedom	Sums of Squares	Mean Squares	F Value	Sig
B	3	35966.3	11988.8	51.5936	***
S	1	0.125000	0.1250000	0.0005	NS
O	3	9573.75	3191.25	13.7335	***
BS	3	3070.13	1023.38	4.4041	*
Residual	21	4879.75	232.369		

Position	B/LB	U/LB	B/LF	U/LF	Mean	
28"	39.00	61.50	120.75	121.50	85.69)	
32"	30.25	93.50	100.00	119.50	85.81)	Nm
Mean	34.63	77.50	110.38	120.50	85.75)	

Seat pitch 28": Position B/LB < Positions U/LB, B/LF and U/LF (***)
Position U/LB < Positions B/LF and U/LF (***)

Seat pitch 32": Position B/LB < Positions U/LB, B/LF and U/LF (***)
Position U/LB < Position U/LF (*)

Order effect: linear

Left

Source of Variation	Degrees of Freedom	Sums of Squares	Mean Squares	F Value	
B	3	34567.3	11522.4	90.6342	***
S	1	338.000	338.000	2.6587	NS
O	3	6340.75	2113.58	16.6252	***
BS	3	6331.75	2110.58	16.6016	***
Residual	21	2669.75	127.131		

Position	B/LB	U/LB	B/LF	U/LF	Mean
28"	53.25	65.75	125.75	121.75	91.63
32"	18.25	105.25	104.00	113.00	85.13
Mean	35.75	85.50	114.88	117.38	88.38

Seat pitch 28": Positions B/LB and U/LB < Positions B/LF and U/LF (***)
Seat pitch 32": Position B/LB < Positions U/LB, B/LF and U/LF (***)

Order effect: linear

Right Tibia Upper My

A linear order effect was observed ($p<0.001$).

An interaction was noted between brace position and seat pitch ($p<0.05$).

No significant effect of seat pitch was observed.

A statistically significant effect of brace position on bending moments recorded in the right upper tibia was observed ($p<0.001$).

At a 32" seat pitch the lowest bending moments were associated with a braced legs back position (mean 30Nm) and these loads were lower than in any of the other positions. This difference is statistically significant ($p<0.001$).

A similar effect was observed at a 28" seat pitch.

Left Tibia Upper My

A linear order effect was observed ($p<0.001$) and an interaction was observed between brace position and seat pitch ($p<0.001$).

No significant effect of seat pitch was observed.

A statistically significant effect of brace position on bending moments recorded in the left upper tibia was observed ($p<0.001$).

At a 32" seat pitch the lowest tibial bending moments were associated with a braced legs back position (mean 36Nm) and these loads were lower than in any of the other positions. This difference is statistically significant ($p<0.001$).

Discussion

See Discussion of Tibial Bending Moments.

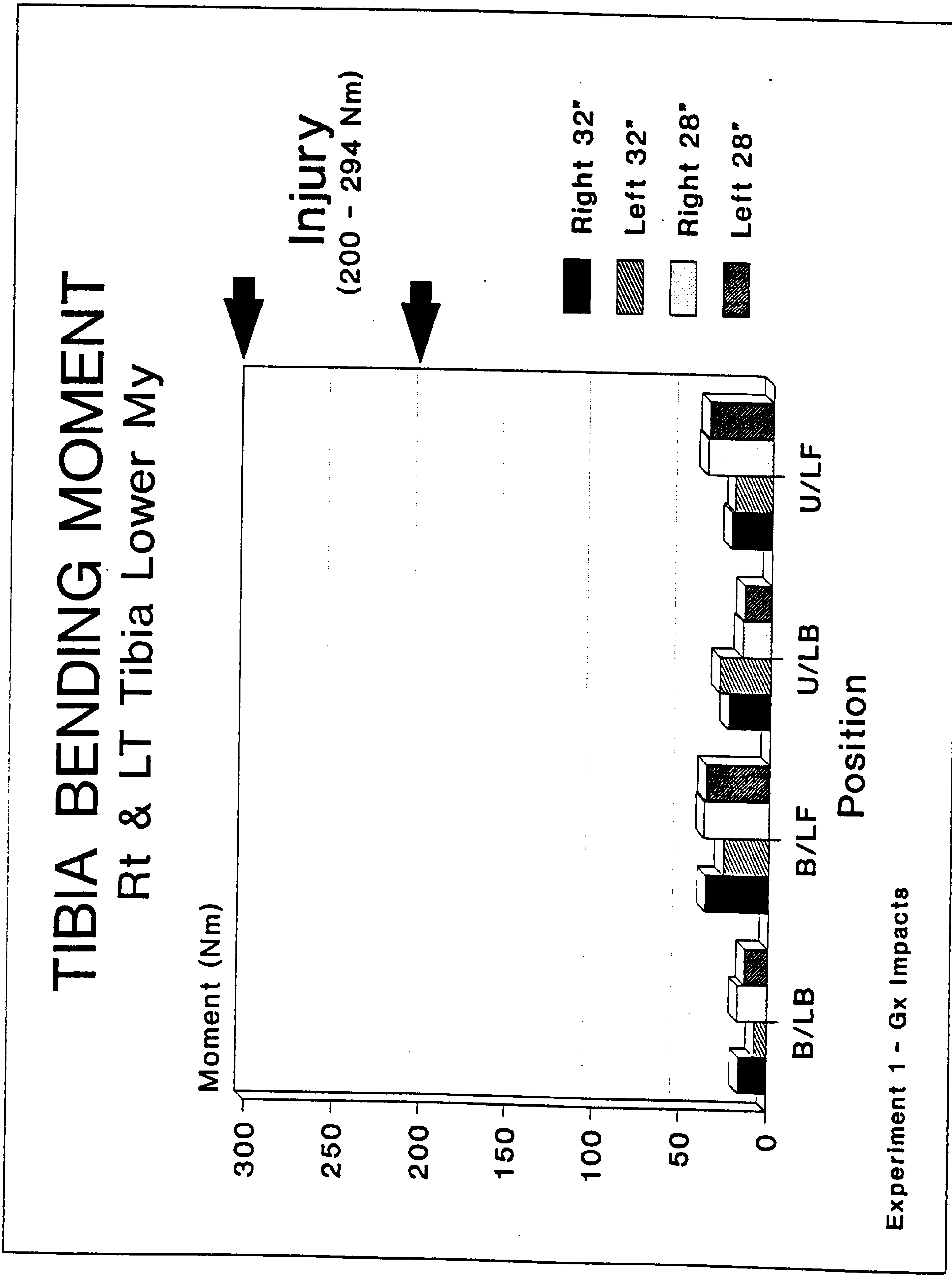

Fig. 33 Tibia Bending Moment - Gx Impacts

Tibia Lower My (See Fig. 33)

Table 20(b) Tibia lower My

Right

Source of Variation	Degrees of Freedom	Sums of Squares	Mean Squares	F Value	Sig
B	3	2050.38	683.458	8.8344	***
S	1	28.1250	28.1250	0.3635	NS
O	3	441.375	147.125	1.9017	NS
BS	3	490.375	163.458	2.1129	NS
Residual	21	1624.62	77.3631		

Position	B/LB	U/LB	B/LF	U/LF	Mean	
28"	17.25	16.50	37.25	37.50	27.13	)
32"	16.00	24.75	36.50	23.75	25.25	) Nm
Mean	16.63	20.63	36.88	30.63	26.19	)

Position B/LB < Position B/LF (***)
Position B/LB < Position U/LF (**)
Position U/LB < Position B/LF (**)
Position U/LB < Position U/LF (*)

Left

Source of Variation	Degrees of Freedom	Sums of Squares	Mean Squares	F Value	
B	3	2109.63	703.208	10.2170	***
S	1	136.125	136.125	1.9778	NS
O	3	217.125	72.3750	1.0515	NS
BS	3	918.625	306.208	4.4489	*
Residual	21	1445.37	68.8274		

Position	B/LB	U/LB	B/LF	U/LF	Mean	
28"	13.00	15.50	36.50	36.00	25.25	)
32"	7.75	29.00	26.50	21.25	21.13	) Nm
Mean	10.38	22.25	31.50	28.63	23.19	)

Seat pitch 28": Positions B/LB and U/LB < Positions B/LF and U/LF (**)
Seat pitch 32": Position B/LB < Positions U/LB, B/LF and U/LF (*)

Right Tibia Lower My

The mean load recorded overall was 26Nm.

A significant effect of brace position was observed on bending moments recorded in the right lower tibia ($p<0.001$).

The lowest loads were associated with a braced legs back position (mean 16Nm).

Left Tibia Lower My

The mean load recorded overall was 23Nm.

An interaction was noted between brace position and seat pitch ($p<0.05$).

A significant effect of brace position was observed ($p<0.001$).

At a 32" seat pitch the lowest loads were associated with a braced legs back position.

A similar effect was noted at a 28" seat pitch.

Discussion

See Discussion of Tibial Bending Moments.

Discussion of Tibial Bending Moments

Weber defined that the load to failure for a bending moment applied to the human tibia was 180Nm in the male and 125Nm in the female (28). Messerer defined the comparable values 207Nm in the male and 124Nm in the female (28).

Both of these loads were applied statically and it has been shown that when a bone is loaded dynamically, the loads to failure are increased (27) (25).

St-Laurent et al defined a dynamic bending load to failure of 294Nm for the tibial component in a motorcyclist anthropometric test device (36).

Therefore the injury threshold for a dynamic bending load applied to the tibia lies in the range of 200Nm to 294Nm.

All the loads recorded in this experiment are below the injury threshold.

The lowest bending moments were associated with a braced legs back position. In this position flailing of the lower limbs is prevented.

Tibial Axial Load

Table 21 Tibia lower Fz (see Fig. 34)

Right

Source of Variation	Degrees of Freedom	Sums of Squares	Mean Squares	F Value	Sig
B	3	0.308957E+7	0.102986E+7	22.3277	***
S	1	490050.	490050.	10.6245	**
O	3	328601.	109534.	2.3747	NS
BS	3	35592.2	11864.1	0.2572	NS
Residual	21	968617.	46124.6		

Position	B/LB	U/LB	B/LF	U/LF	Mean	
28"	1178.75	548.00	525.00	415.75	666.88)	
32"	1476.25	701.25	742.50	737.50	914.38)	N
Mean	1327.50	624.62	633.75	576.63	790.63)	

Position B/LB > Positions U/LB, B/LF and U/LF (***)

Order effect: linear

Left

Source of Variation	Degrees of Freedom	Sums of Squares	Mean Squares	F Value	
B	3	197040.	65679.9	1.2682	NS
S	1	4777.53	4777.53	0.0922	NS
O	3	204598.	68199.4	1.3169	NS
BS	3	67778.1	22592.7	0.4362	NS
Residual	21	0.108758E+7	51789.5		

Position	B/LB	U/LB	B/LF	U/LF	Mean	
28"	772.75	799.00	637.25	487.25	674.06)	
32"	681.50	671.00	652.25	593.75	649.62)	N
Mean	727.12	735.00	644.75	540.50	661.84)	

Right Tibia Lower Fz

A significant effect of seat pitch was observed ($p<0.01$) with higher loads recorded at a 32" seat pitch (mean 914N) as compared to a 28" seat pitch (mean 667N).

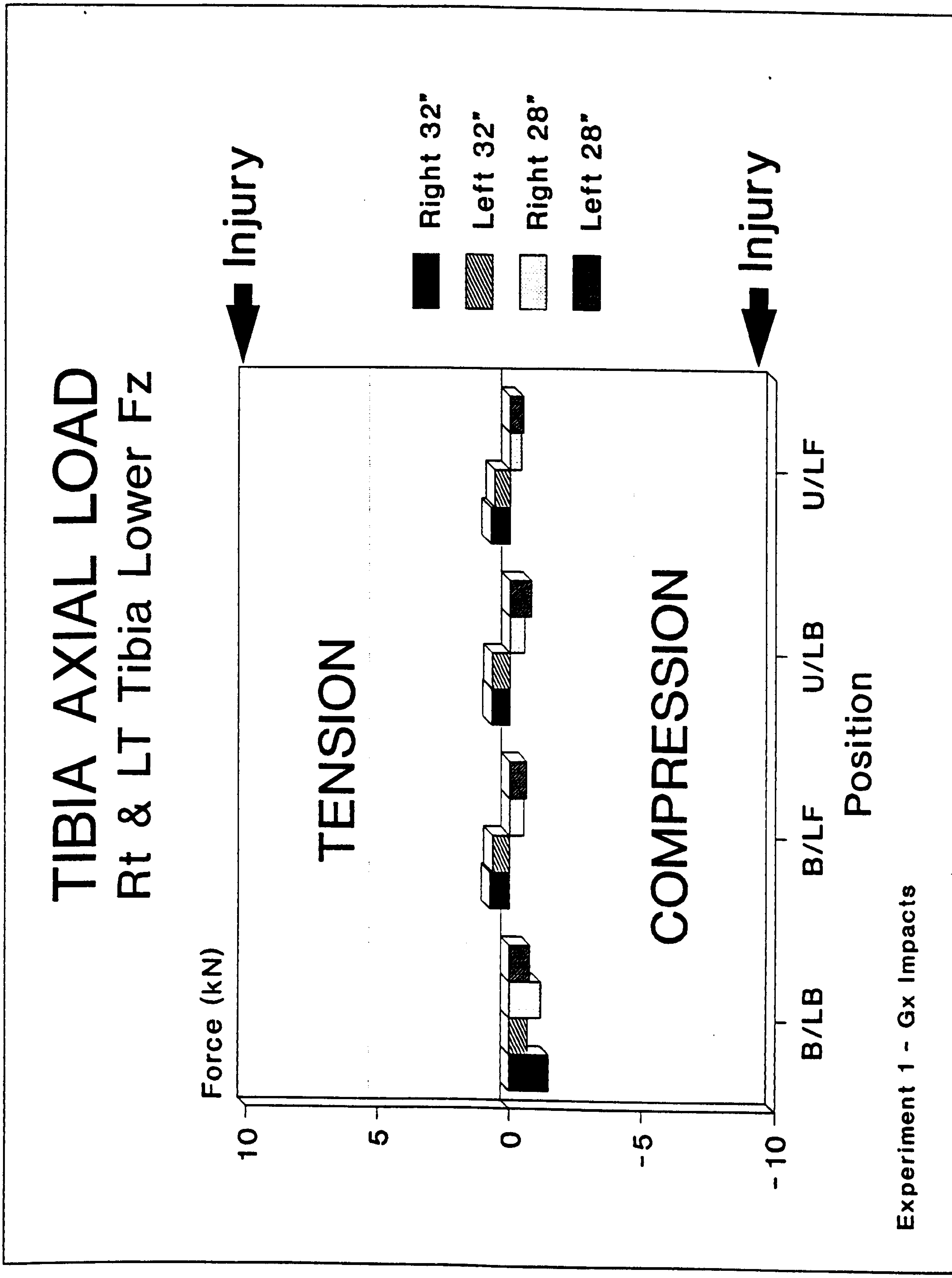

Fig. 34 Tibia Axial Load - Gx Impacts

A statistically significant effect of brace position on tibial axial loads was observed ($p < 0.001$). The highest loads were associated with a braced legs back position (mean 1327Nm) and these loads were higher than in any of the other positions ($p < 0.001$).

Left Tibia Lower Fz

No significant effect was observed.

Discussion of Tibial Axial Loads

On the right side the highest axial compressive loads were associated with a braced legs back position. In this position the lower limbs do not flail. On impact the foot slides forwards until the lower leg reaches a vertical position where friction is maximal (confirmed in later computer modelling) and further movement stops. Consequently forward kinetic energy is converted into axial loading of the tibia.

On the left side there was a tendency for the left leg to slide forward slowly after impact. This effect dissipated energy. Hence no statistically meaningful differences were found between the brace positions on the left side.

Messerer predicted a mean load to failure for a compression load applied axially to the tibia of 10.36kN in the male and 7.49kN in the female (28). These loads were applied statically. It has been shown that the load to failure for a dynamic load applied to the bone is greater than the corresponding static value (27) (25). Therefore it would appear that the injury threshold for a compressive load applied axially to the human tibia lies above the 10kN level.

Culver et al have shown that the static load to failure for the ankle ligament occurs at the 3kN level (9).

Again all the loads recorded in this experiment are below these injury thresholds.

7.11 SUMMARY

High Speed Video Recording

Review of the high speed video recordings revealed that flailing of the lower limbs did not occur when the dummy was placed in a braced legs back position. Instead of flailing, the lower limbs were seen to slide from a position behind the knee to a position just forward of the knee. Forward motion of the lower limbs being arrested due to friction between the shoes and carpet which was maximal in this position.

In the other positions flailing occurred and the lower limbs were seen to fly forwards into the back of the seat ahead. This resulted in damage to the artificial skin covering the lower limbs of the dummy. In addition the knees were seen to hyperextend which resulted in damage to the metal stop in the knee mechanism (see Fig.19).

Head

The risk of head injury, as indicated by the Head Injury Criterion, is reduced by adopting a braced position. This finding parallels the results of earlier research performed at CAMI. There is little difference in terms of head injury risk between a braced legs back position and a braced legs forward position.

Pelvis

The injury threshold for lap belt loads applied to the pelvis is between 9 kN and 19 kN. This wide range makes interpretation of the test data difficult. However, at a 32" seat pitch the lap belt loads recorded, approach the lower limit of this range irrespective of the brace position adopted.

At a 28" seat pitch the lap belt loads recorded were lower as knee contact occurred with the back of the forward seat.

The highest loads were associated with a braced legs back position. The mean load was 9840N and this compares with a value of 9130N in the braced legs forward position.

Therefore passengers involved in an impact aircraft accident are at risk of pelvic injury due to lap belt loading. If the lower limbs are placed in a legs back position then this risk may be increased slightly.

Lumbar Spine

The poor biofidelity of the lumbar spine in the Hybrid III dummy makes interpretation of the test data difficult.

The forward flexion spinal bending moments and the spinal axial loads appeared to be well below the estimated injury thresholds. However, the lumbar spine shear loads recorded in this experiment approach the estimated injury threshold. The highest lumbar spine shear loads were associated with a braced legs back position.

Therefore there appears to be a risk of injury due to shear forces applied to the lumbar spine. The risk is greatest when the passenger adopts a braced legs back position.

Lower Limbs

Femur

At a 32" seat pitch the axial loads recorded in the femoral load cell were tension loads. This suggests that knee contact does not occur with the forward seat. This suggestion was confirmed by review of the high speed video.

At a 28" seat pitch compressive axial loads were recorded suggesting that knee contact had occurred with the back of the forward seat. This was confirmed by review of the high speed video. Even when knee contact occurred, the axial loads recorded were well below the predicted threshold of 8.7 kN.

Regulations relating to the dynamic performance testing of aircraft seats stipulate a maximum figure of 10kN for axial loads recorded in the femur. The results of this experiment suggest that axial loading of the femur is not a significant injury mechanism. Such a recommendation would appear to be unnecessary.

The femoral bending moments recorded in both femurs indicate that a bending mechanism may be involved in the production of femoral fractures in an impact aircraft accident.

The resultant femoral bending moments approached the injury threshold in all of the positions tested.

In the left femur, loads exceeding the injury threshold were recorded in a braced legs forward position at a 32" seat pitch. Subsequent computer analysis has suggested that this effect may be related to foot entrapment. Such entrapment was difficult to visualise on the high speed video as the left side was the most distant from the camera lens.

Bending moments appear to be applied to the femur as a result of the forward and upward movement of the torso, the downward force caused by the lap belt and the upward force produced by the front seat spar. In the flailing situation a further bending moment is produced distal to the front seat spar (see Fig. 30(b) and 30(c)).

Tibia

The injury threshold for a bending moment applied to the human tibia is above 200Nm. The loads recorded in the braced legs forward position, unbraced legs back position and unbraced legs forward position are all significantly higher than those recorded in a braced legs back position.

In a braced legs back position the lower limbs do not flail. Forward motion is arrested due to friction between the foot and the floor which is greatest in this position. Increased axial compressive loads are produced in the tibia but these remain well below the predicted injury threshold.

7.12 CONCLUSIONS

1. The risk of head injury is reduced if the passenger adopts a braced position.

2. The risk of pelvic injury due to the lap belt is significant and is largely unaltered by the position that the passenger adopts at the time of impact.

3. There is a risk of lumbar spine injury. The shear forces recorded approached the injury threshold when the occupant adopted a braced position and were highest when the occupant adopted a braced legs back position.

4. Axial loading of the femur due to knee contact with the back of the forward seat does not appear to be a significant injury mechanism even at a shortened 28" seat pitch.

5. Femoral bending appears to be a significant injury mechanism which might produce femoral shaft fracture. The loads involved appear to vary little with brace position. However, very high bending moments may be produced in the femur if foot entrapment occurs.

6. A braced legs back position prevents flailing of the lower limbs. If flailing is prevented then reduced bending moments are seen in the tibia. In addition there is no tendency for the knee joints to hyperextend and there is a reduced chance of soft tissue injury as a result of contact with the back of the forward seat.

7. If flailing does not occur then, increased axial compressive loads are produced in the tibia. Such loads <u>do not</u> approach the predicted injury threshold.

8. EXPERIMENT 2 - Vertical (+Gz IMPACT)

8.1 OBJECTIVE

To compare the values obtained from the transducers fitted to the dummy, for four dummy positions during a predominantly vertical +Gz impact.

8.2 IMPACT PULSE

The impact pulse measured on the vehicle was similar to the FAA -14G pulse specified in Aerospace Standard 8089.

Min G. = 14
Min Vt (m/s) = 10.67 (35 ft/s)
Max tr (s) = 0.08

Vt = Impact velocity
tr = rise time

8.3 TEST FIXTURE

8.3.1 Seat

A multiple row test fixture (two rows of three seats in each row) was used to best evaluate head and knee impact conditions.

Undamaged or minimally damaged seat rows were taken from the Kegworth accident (G-OBME).

The seats were subjected to non destructive testing by the RAF (including magnetic particle analysis) prior to the experiment.

The seats were Weber Aircraft Forward Facing Passenger Seats (Specification NAS 809 Type 1).

Two rows of seats were mounted onto the test vehicle.

The seats were mounted on a ramp which gave an impact angle of 30° from the vertical (i.e. the test floor was placed at 60° to the horizontal) (see Fig.35).

The joint at which the seats were attached to the floor rails was reinforced with a metal block (see Fig.6) to minimise the risk of the seats becoming detached during testing.

Panelling was removed from the arm rest of the outside seats to facilitate recording of displacement data.

A suitable floor was constructed and this was carpeted.

The seats were mounted at a 32" seat pitch, which represented the seat pitch most widely used in G-OBME. Preliminary experiments revealed no evidence of contact with the seat ahead associated with this test fixture. Accordingly in view of the relative rigidity of the ramp and the difficulty in changing seat pitch on such a fixture, it was decided to use a single seat pitch of 32" and no anthropomorphic test dummy was placed in the seat in front of the experimental model.

8.3.2 Dummy

A 50% Hybrid III anthropomorphic test dummy was used as the experimental model.

The dummy was clothed in form fitting cotton stretch garments with mid-thigh length pants and size 11 E shoes weighing 11.6N (2.6 lbs).

The shoes had a smooth leather sole and the coefficient of friction of the shoe on the carpeted floor was determined prior to the experiment (Fig. 8).

8.4 INSTRUMENTATION

The transducers were allocated channels in the following manner.

RECORDING CHANNELS

Channel	Transducer	Excitation	Gain	Recording
1	R TIBIA L Clevis	10v	500	DATALAB
2	R TIBIA R Clevis	10v	500	DATALAB
3	R TIBIA U/My	10v	500	DATALAB
4	R TIBIA L/My	10v	500	DATALAB
5	R TIBIA L/Fz	10v	500	DATALAB
6	L TIBIA L Clevis	10v	500	DATALAB
7	L TIBIA R Clevis	10v	500	DATALAB
8	L TIBIA U/My	10v	500	DATALAB
9	L TIBIA L/My	10v	500	DATALAB
10	L TIBIA L/Fz	10v	500	DATALAB
11	R FEMUR Fx	10v	500	DATALAB
12	R FEMUR My	10v	500	DATALAB
13	R FEMUR Fz	10v	500	DATALAB
14	L FEMUR Fx	10v	500	DATALAB
15	L FEMUR My	10v	500	DATALAB
16	L FEMUR Fz	10v	500	DATALAB
17	R FEMUR Fy	10v	500	DATALAB
18	R FEMUR Mx	10v	500	DATALAB
19	R FEMUR Mz	10v	500	DATALAB
20	L FEMUR Fy	10v	500	DASH16

EXPERIMENT 2 - +Gz IMPACT

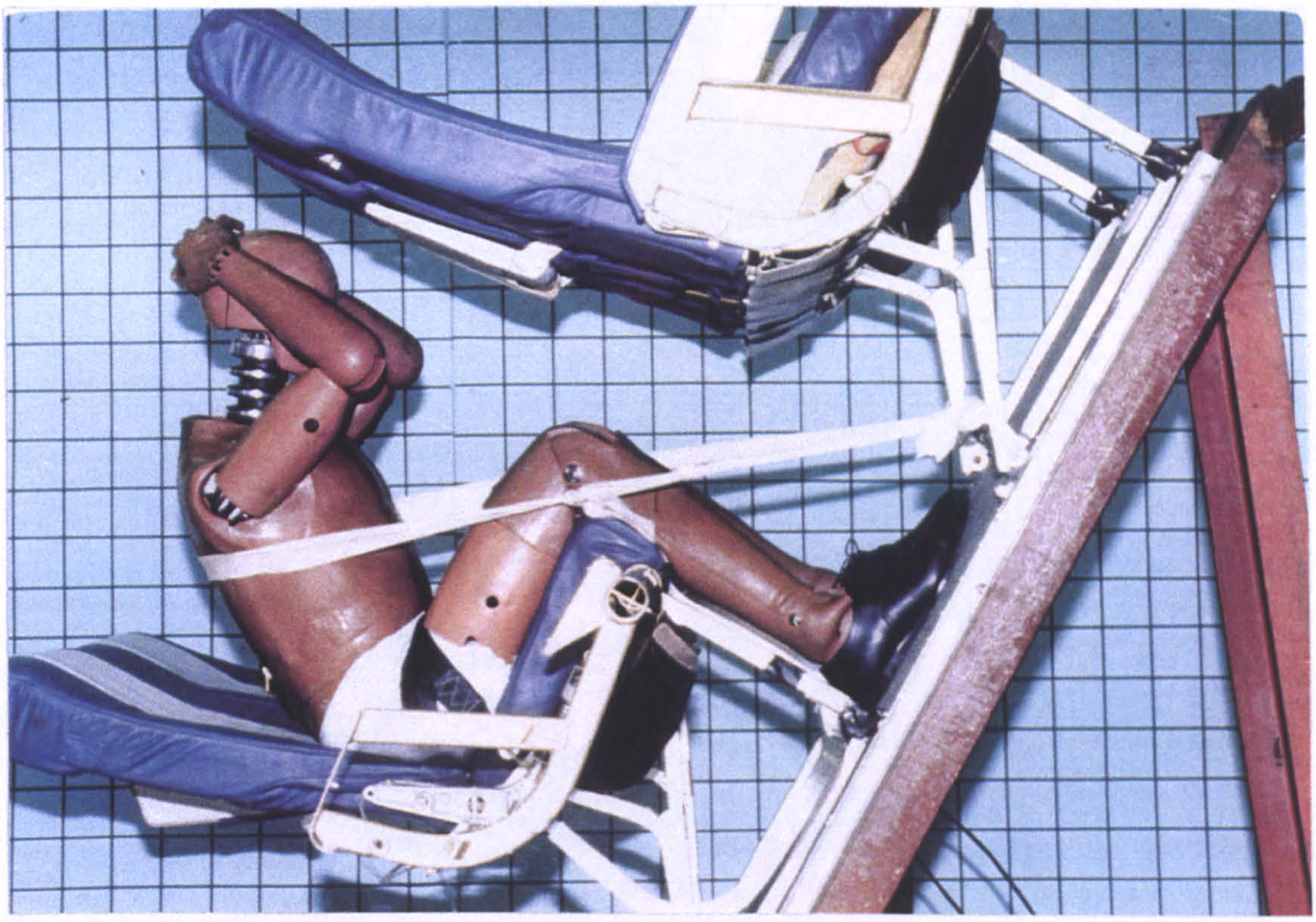

Fig. 35 Experiment 2 - Braced/Legs Back Position

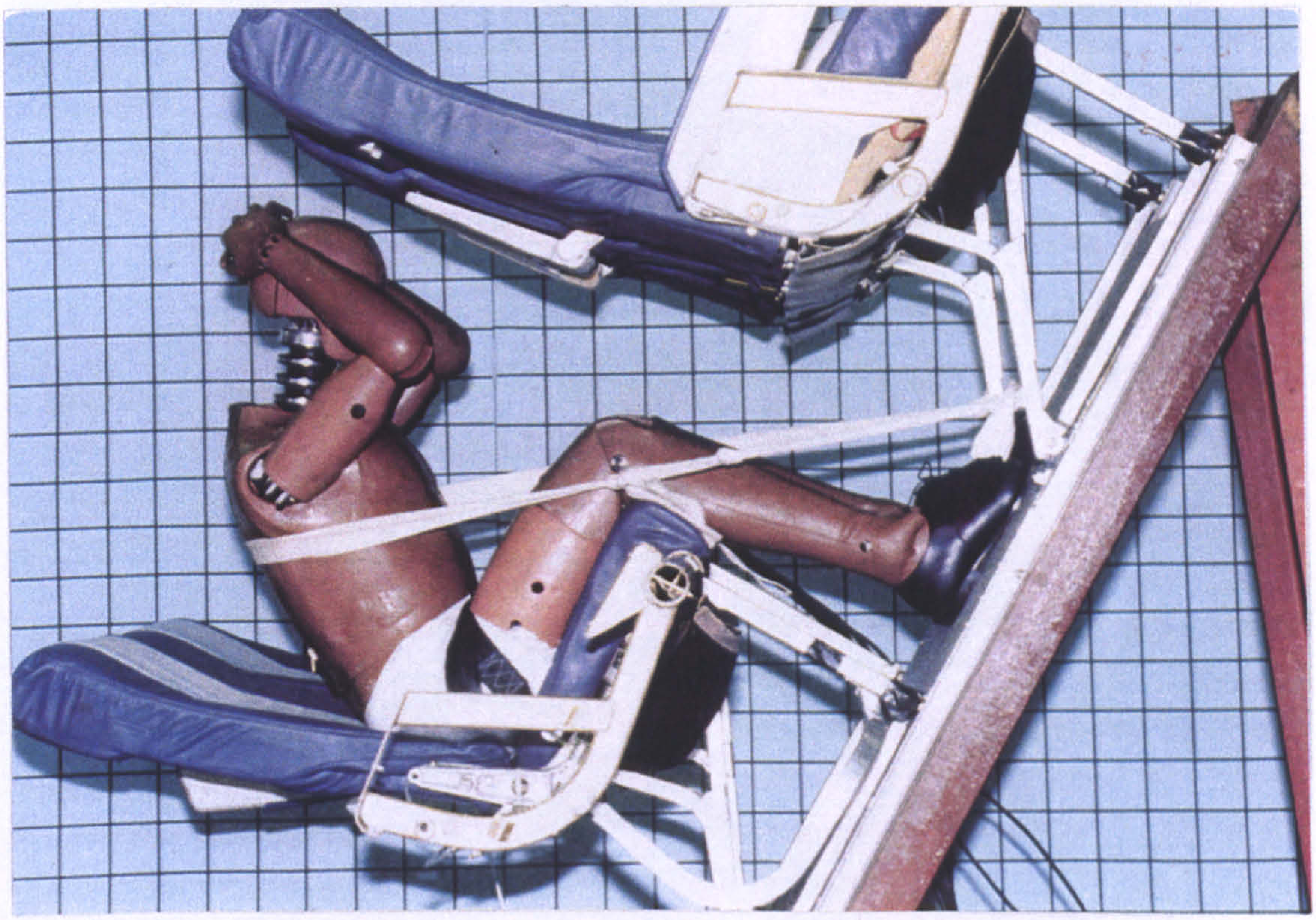

Fig. 36 Experiment 2 - Braced/Legs Forward Position

EXPERIMENT 2 - +Gz IMPACTS

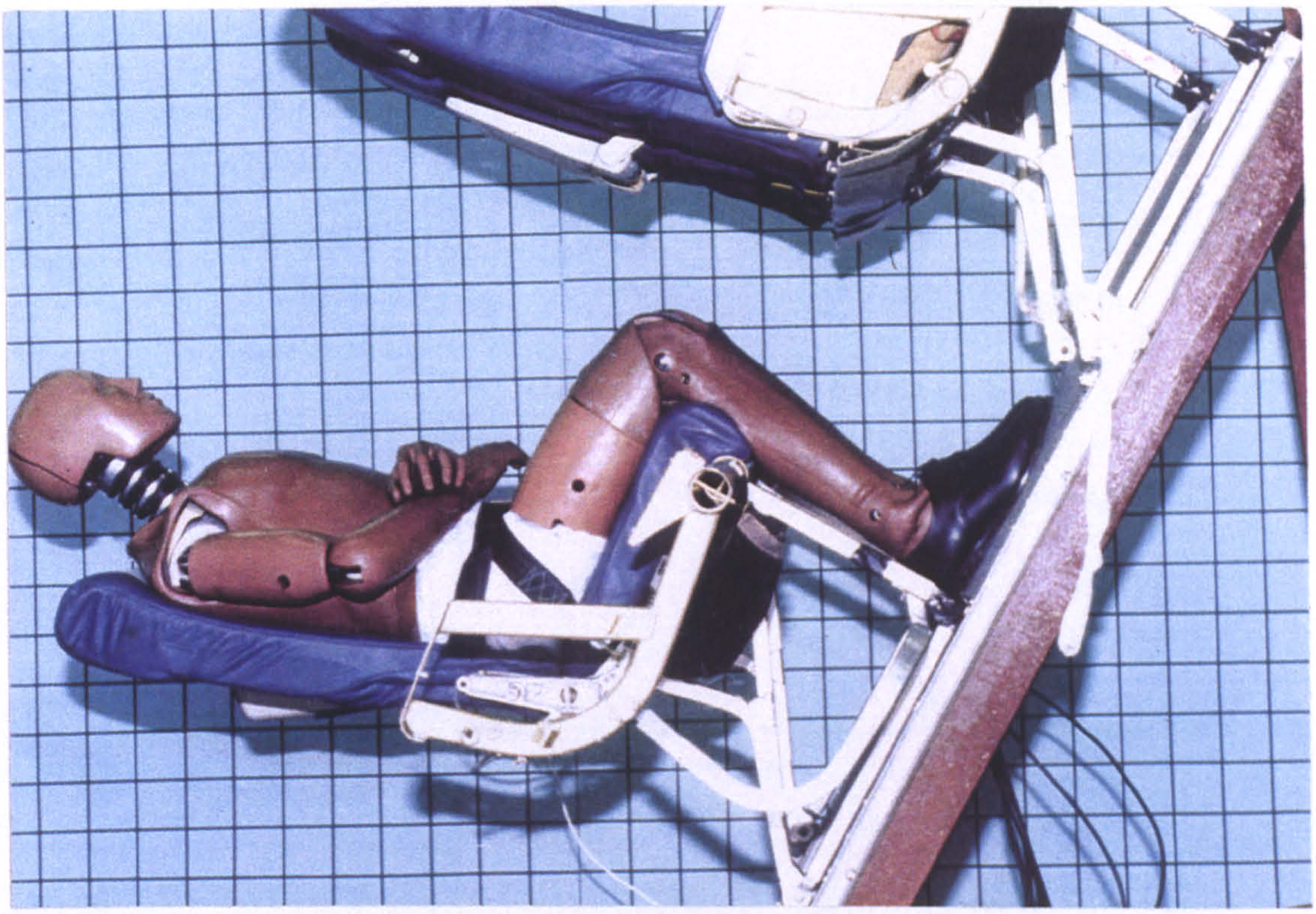

Fig. 37 Experiment 2 - Unbraced/Legs Back Position

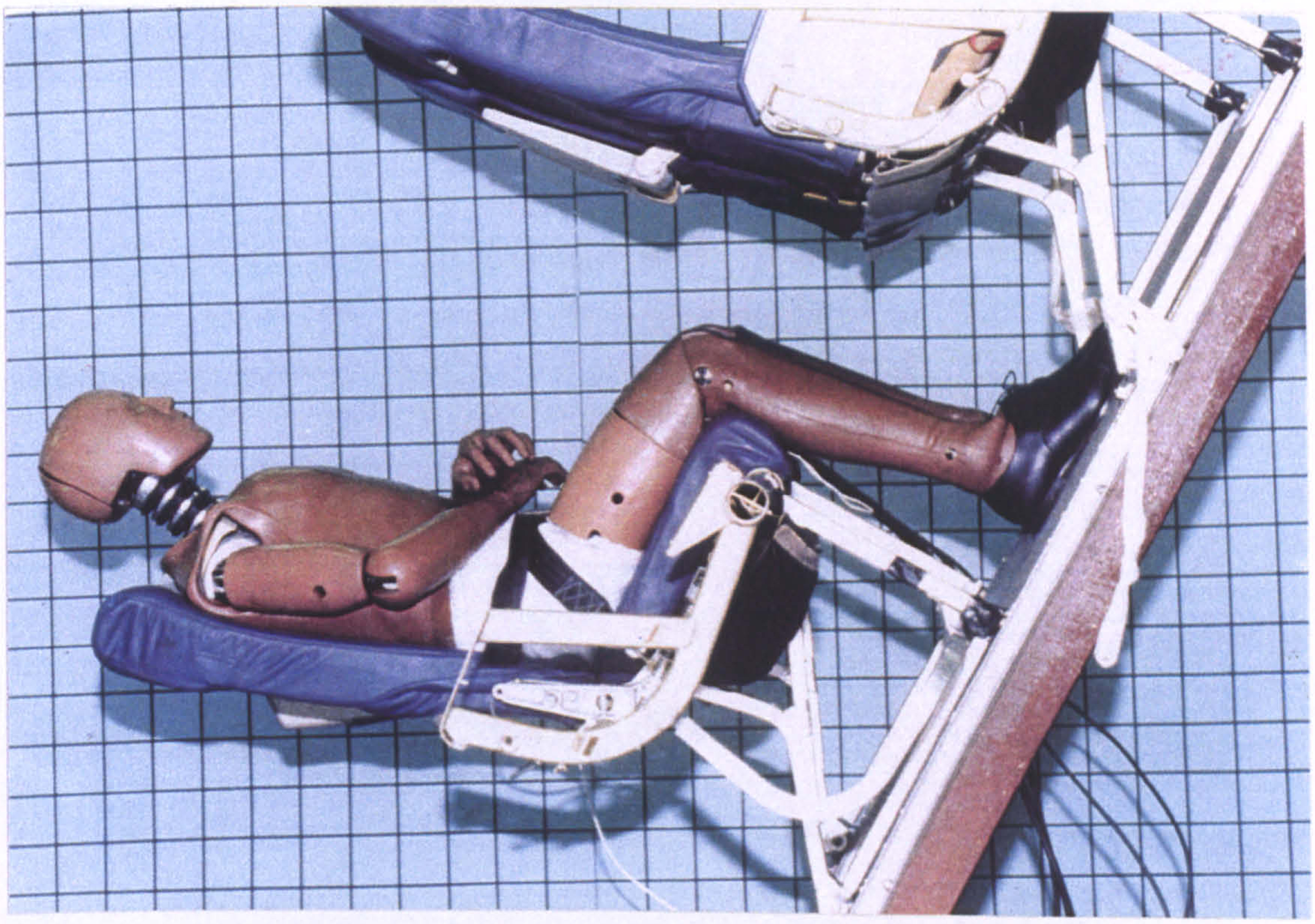

Fig. 38 Experiment 2 - Unbraced/Legs Forward Position

Channel	Transducer	Excitation	Gain	Recording
21	L FEMUR Mx	10v	500	DASH16
22	L FEMUR Mz	10v	500	DASH16
23	LUMBAR Fx	10v	500	DASH16
24	LUMBAR My	10v	500	DASH16
25	LUMBAR Fz	10v	500	DASH16
26	VEHICLE G	4V	1200	DASH16
27	HEAD Gx	10V	500	DASH16
28	TRIAXIAL HEAD			
29	HEAD Gz	10V	500	PORTAX
31	L LAPBELT	Piezo		PORTAX
32	HEAD Gy	10v	500	PORTAX
33	R FEMUR RESULT			
34	L FEMUR RESULT			

All impacts were recorded on a NAC 200 high speed video camera system operating at 200 fields per second.

8.5 EXPERIMENTAL VARIABLES

The experiment compared the values obtained from the transducers fitted to the dummy, for four dummy positions at a 32" seat pitch.

The experimental variables were:

1) Brace position - braced
- unbraced

2) Lower leg position - forward
- backward

The four dummy positions used are illustrated in Figs. 35, 36, 37, 38.

In the braced position the dummy was flexed forwards so that the head rested on the back of the seat ahead. This position could only be achieved by placing a sling around the upper torso. During the acceleration phase of the impact test, there was invariably some movement of the dummy's head away from the seat in front (Fig.39).

The hands were placed on the head and were held in position by interlocking the fingers.

In the unbraced position the dummy was sat upright.

Two lower limb positions were identified.

In the first the lower legs were placed 20° forwards of a vertical line drawn from the tilted "floor" through the knee.

In the second the legs were placed 11.5° behind a vertical line drawn from the tilted "floor" through the knee.

Both positions represented a comfortable seating position.

8.6 TEST PROCEDURE

The 50th percentile instrumented Hybrid III dummy was located in the second row (from the front) in the centre of the three seat positions.

The dummy was placed in the seat in a standard way, with the back and buttocks against the seat back.

The friction of the limb joints was set so that the weight of the limb was barely restrained when extended horizontally.

The knees were separated by approximately 100mm (4").

The seat was placed in its normal "upright" position.

The dummy was placed in one of four different brace positions; torso forward/back and feet forward/back at one seat pitch only (32").

The lapbelt tension was set using a spring balance to a tension of 70N (15 lbs) which represents a firm but not uncomfortable level.

Before the test vehicle was winched into position and the triggering device was armed.

The vehicle was released and the impact recorded.

After each test, all equipment was assessed for damage.

8.7 RANDOMIZATION

The tests were randomized to minimise linear order effects and each run was repeated 4 times.

The experiment was randomized according to the following schedule:

A - Legs forward } Braced
B - Legs back }

C - Legs forward } Unbraced
D - Legs back }

Orientation -Gx/+Gz
Run

1 A

2 B

3 C

4 D

5 B

6 D

7 A

8 C

9 C

10 A

11 D

12 B

13 D

14 C

15 B

16 A

8.8 ANALYSIS OF RESULTS

The raw data was entered into a computer. The data was manipulated using software developed by the Institute of Aviation Medicine, Farnborough, based upon the Asyst programme.

It was at this level that the calibration data for the load cells and accelerometers was added to allow the information to be expressed in the correct units.

8.8.1 Zero-ing of Recordings

A zero level for each set of data was obtained by sampling the data between the trigger point and the point of impact.

When the data recording equipment is triggered the vehicle is in its coast phase. The impact point is 1 metre from the trigger point.

Therefore at a mean velocity of 12.7 m/s this represents 78 m/s.

With a sampling rate of 5000 samples per second this represents 400 counts between data recording trigger point and impact.

Therefore counts 10-110 were taken and the average obtained.

This value was then taken as the zero point.

8.8.2 Statistical Analysis

This study was designed to compare the effect of different passenger brace positions on injury arising from impact. Impact decelerations of -14Gx were conducted with the dummy placed in 4 positions; torso forward (=braced) or upright (=unbraced) with legs either forward or back. Each brace position was repeated four times. Measurements were made of tibial loads, femoral loads, lumbar loads, head injury criterion (HIC) and lap belt loads.

The maximum absolute value of each load measurement during the impact was subjected to analysis. The method of analysis of variance (ANOVA) was used with factors as given below.

Factor	Number of levels	Description
B	4	Brace Position
O	4	Order of replications

Transformation was not required for any variable in this analysis.

8.9 RESULTS

The results of the impact tests performed in Experiment 2 are contained in the following tables. A key explaining the organisation of the tables can be found in Appendix 1 and for clarity is included below.

8.9.1 Result Tables

Key to Result Tables

Run No.

The run no. is the unique number given to each impact test. The first run in Experiment 2 was 3709 and the last run was 3725. Run 3721 was repeated due to failure of the triggering mechanism.

Cal. File

This is the number of the calibration file used to interpret the data from each test run.

Set Up

This refers to the configuration used during each test.

A - Braced/Legs forward	)	
	)	
B - Braced/Legs back	)	
	)	32" seat pitch
C - Unbraced/Leges forward	)	
	)	
D - Unbraced/Legs back	)	

Brace Position

Brace position refers to the position adopted by the dummy at the time of impact.

B = braced

U = unbraced

Leg Position

Leg position refers to the position of the dummy's lower limbs.

LF = legs forward at an angle of 20° to a vertical line drawn through the knee.

LB = legs back at an angle of 11.5° to a vertical line drawn through the knee.

Velocity

Velocity refers to the velocity of the sled at impact, measured in metres per second.

Flail

Flail refers to the behaviour of the lower limbs as seen on the high speed video recordings. If the lower limbs were thrown forwards and upwards causing hyperextension of the knee, then flailing was said to have occurred.

In some impacts, particularly those associated with a 28" seat pitch, it was difficult to decide whether flailing had occurred as opposed to the legs sliding forwards, after impact (a much lower energy phenomenon). These results were categorised with the letter 'P'.

CHANNELS 3-32:

The loads recorded in each of the transducers were plotted against time. The resulting graphs were analyzed and the peak loads were recorded. In some channels there was more than one peak and in these instances the value of the larger peak was recorded. The time at which the peak load occurred after impact is designated by the letter 'T'.

Analysis of the recordings from the right and left knee clevis units was not practical in terms of a single peak. During the course of the impact multiple peak loads were recorded and these were of differing polarity. Accordingly the data from channels 1, 2, 6 and 7 has not been analyzed in terms of peak loads.

Channel 3

Right Tibia Upper My

- the bending moment recorded about the y-axis in the right tibia upper load cell
- knee extension produced a negative output.

Channel 4

Right Tibia Lower My

- the bending moment recorded about the y-axis in the right tibia lower load cell
- knee extension produced a negative output.

Channel 5

Right Tibia Lower Fz

- the axial force recorded in the right tibia lower load cell
- tibial compression produced a negative output.

Channel 8

Left Tibia Upper My

- the bending moment about the y-axis recorded in the left tibia upper load cell
- knee extension produced a negative output.

Channel 9

Left Tibia Lower My

- the bending moment about the y-axis recorded in the lower left tibia lower load cell

- knee extension produced a negative output.

Channel 10

Left Tibia Lower Fz

- the axial force recorded in the left tibia lower load cell
- tibial compression produced a negative output.

Channel 11

Right Femur Fx

- the femoral shear load in the x-axis
- downward force on the thigh produced a positive signal

Channel 12

Right Femur My

- the bending moment about the y-axis recorded in the right femoral load cell
- upward movement of the pelvis or knee relative to the femoral load cell produced a negative output.

Channel 13

Right Femur Fz

- the axial load recorded in the right femoral load cell
- axial compression produced a negative output.

Channel 14

Left Femur Fx

- the shear load recorded in the left femoral load cell
- a downward force on the thigh produced a positive output

Channel 15

Left Femur My

- the bending moment about the y-axis recorded in the left femoral load cell
- upward movement of the pelvis or knee relative to the femoral load cell produced a negative output.

Channel 16

Left Femur Fz

- the axial load recorded in the left femoral load cell
- axial compression produced a negative output.

Channel 17

Right Femur Fy

- the shear force recorded in the y-axis in the right femoral load cell
- a lateral force produced a negative output.

Channel 18

Right Femur Mx

- the bending moment recorded about the x-axis in the right femoral load cell
- a force exerted medially on the right knee produced a negative output.

Channel 19

Right Femur Mz

- the axial rotation moment recorded in the right femoral load cell
- external rotation force produced a negative output.

Channel 20

Left Femur Fy

- the femoral shear load recorded in the y-axis in the left femoral load cell
- a force exerted laterally on the left knee produced a positive output.

Channel 21

Left Femur Mx

- the bending moment recorded about the x-axis in the left femoral load cell
- a force exerted laterally on the left knee produced a negative output.

Channel 22

Left Femur Mz

- the axial rotation moment recorded in the left femoral load cell
- external rotation produced a negative output.

Channel 23

Lumbar Fx

- the shear load recorded in the lumbar load cell

Channel 24

Lumbar My

- the moment recorded about the y-axis in the lumbar load cell
- forward flexion produced a positive output.

Channel 25

Lumbar Fz

- the axial load recorded in the lumbar load cell
- axial compression produced a negative output.

Channel 26

Vehicle G

- the peak G recorded in the vehicle accelerometer

Channel 27

Head Gx

- the peak acceleration recorded in the head in the x-axis

Channel 28

HIC

- the head injury criterion

Channel 29

Head Gz

- the peak acceleration recorded in the head in the z-axis

Channel 31

Lap belt

- the peak load recorded in the load cell which was mounted in series with the lap belt
- tension produced a negative output

Channel 32

Head Gy

- the peak acceleration recorded in the head in the y-axis

Channel 33 and 34

Left and Right Femur Resultant

- the resultant bending moment acting on each femur was computed from the bending moments recorded in the x and y-axis according to the equation $C^2 = A^2 + B^2$

8.9.2 High Speed Video

1. Flailing of the lower limbs did not occur.

2. When the dummy was in a braced position the upper torso was seen to flex further forwards on impact striking the back of the seat ahead. In an upright position forward flexion of the torso did occur after impact but was less marked (see Figs. 39 and 41).

	CHANNEL 27	CHANNEL 28	CHANNEL 29	CHANNEL 31		CHANNEL32	CHANNEL 33	CHANNEL 34
RUN No.	HEAD Gx	HIC	HEAD Gz	Lt LAPBELT (N)	T (ms)	HEAD Gy	Rt Femur Result	Lt Femur Result
3709	-32	93	-15	-1007	215	7.7	99	68
3715	-20.2	52	11.1	-1240	220	-2.5	63	73
3718	-24.3	77	-15.5	-1080	205	-3.1	101	98
3725	-28.9	78	-17.8	-1780	185	-4.6	84	90
3710	-16.5	61	-14.9	-1610	195	-6.6	81	54
3713	-20	48	-11	-1670	210	1.8	73	66
3720	-31.2	55	12	-1040	225	-2.1	56	48
3724	-44.9	85	-15.8	-2290	185	-8.6	14	18
3711	-3.5	35	21.7	-265	332	-10.5	7	18
3716	-5.2	34	21.1	-92	240	1.5	10	18
3717	-5.7	34	22.4	-181	250	1.5	15	23
3723	-5.6	43	24.4	-273	250	1.2	13	21
3712	-4.7	35	21.4	-49	230	0.9	15	22
3714	-4.9	36	22	-152	250	1.3	14	17
3719	-5.6	34	21.9	-158	245	-0.7	18	20
3722	-5.4	46	25.1	-410	240	2.3	84	85
MEAN								
B/LF		75.00		-1276.75			86.75	82.25
B/LB		62.25		-1652.50			56.00	46.50
U/LF		36.50		-202.75			11.25	20.00
U/LB		37.75		-192.25			32.75	36.00

TABLE 22

Experiment 2 - Gz Impacts

HIGH SPEED VIDEO RECORDINGS - Experiment 2 +Gz Impacts

Fig. 39 Run No. 3713 - Braced/Legs Back Position

Fig. 40 Run No. 3709 - Braced/Legs Forward Position

<u>**HIGH SPEED VIDEO RECORDINGS - Experiment 2 +Gz Impacts**</u>

Fig. 41 Run No. 3712 - Unbraced/Legs Back Position

Fig. 42 Run No. 3716 - Unbraced/Legs Forward Position

8.9.2 High Speed Video

1. Flailing of the lower limbs did not occur.

2. When the dummy was in a braced position the upper torso was seen to flex further forwards on impact striking the back of the seat ahead. In an upright position forward flexion of the torso did occur after impact but was less marked (see Figs. 39 and 41).

8.10 STATISTICAL ANALYSIS AND DISCUSSION

The results of Experiment 2 (including statistical analysis) are discussed below:

Key to tables:	Position B/LB	Braced, legs back
	Position U/LB	Unbraced, legs back
	Position B/LF	Braced, legs forward
	Position U/LF	Unbraced, legs forward

*	$p<0.05$
**	$p<0.01$
***	$p<0.001$

8.10.1 Head

Head Injury Criterion (See Fig. 43)

Table 23 HIC

Source	Sums of Squares	Df	Mean Squares	F Ratio	Sig
B	4297.2500	3	1432.41667	14.687	**
O	912.7500	3	304.2500	3.120	NS
Residual	877.7500	9	97.52778		
Total	6087.7500	15			

B/LB	U/LB	B/LF	U/LF	Mean	
62.25	37.75	75.00	36.50	52.88	HIC

Position B/LF > Positions U/LB and U/LF (**)
Position B/LB > Positions U/LB and U/LF (*)

The Head Injury Criterion is the industry standard for assessing head injury potential (16).

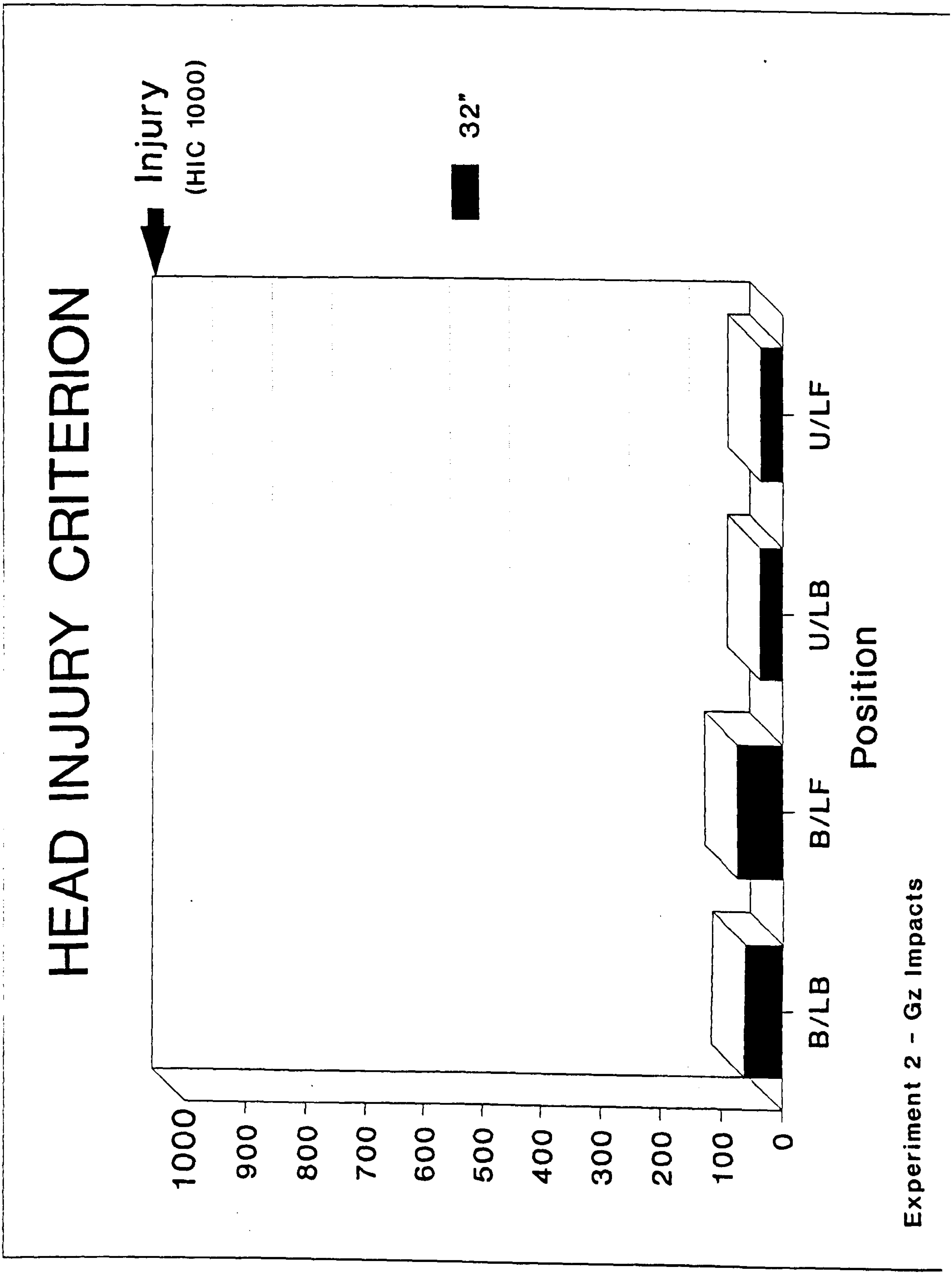

Fig. 43 Head Injury Criterion - Gz Impacts

A HIC value of 1,000 is defined as the injury threshold (13) and represents the point at which 16% of individuals will suffer a significant brain injury (16).

In this experiment all the HIC values recorded were below 1,000.

The significance of HIC values under 1,000 is unknown and therefore one can only refer to the data in qualitative terms.

Higher HIC values were recorded in a braced legs forward position (mean 75) and a braced legs back position (mean 62) when compared to each of the unbraced positions. These differences are statistically significant.

It is suggested that higher HIC values were seen in the braced positions due to the upper torso flexing further forwards on impact, striking the back of the seat ahead. In the upright position such forward flexion of the torso did not occur (see Figs. 41 and 42).

8.10.2 Lap Belt

Lap Belt Tension (See Fig. 44)

Table 24 Lap Belt Tension

Source	Sums of Squares	Df	Mean Squares	F Ratio	Sig
B	6705019.68750	3	2235006.56250	40.340	**
O	743403.68750	3	247801.22917	4.473	*
Residual	498635.56250	9	55403.95139		
Total	7947058.93750	15			

B/LB	U/LB	B/LF	U/LF	Mean	
1652.50	192.25	1276.75	202.75	831.06	) N

Positions B/LB and B/LF > Positions U/LB and U/LF (***)

Order effect: linear

A linear order effect was observed ($p<0.05$). It is suggested that this order effect was related to seat deformation and loss of elasticity in the lap belt as a result of repetitive loading.

Discussion of Lap Belt Tension Loads

Human tolerance to lap belt forces in an impact was investigated by Lewis and Stapp (23). In their experiments loads of up to 19kN were sustained with only soft tissue injury. However the impact velocities that were used were relatively low (7.32 m/s to 8.84 m/s).

In the M1 Kegworth accident, large numbers of pelvic injuries were seen. It was suggested that these injuries were related to the wearing of a lap belt. Subsequent impact tests indicated that passengers had experienced lap belt loads of approximately 9kN (33).

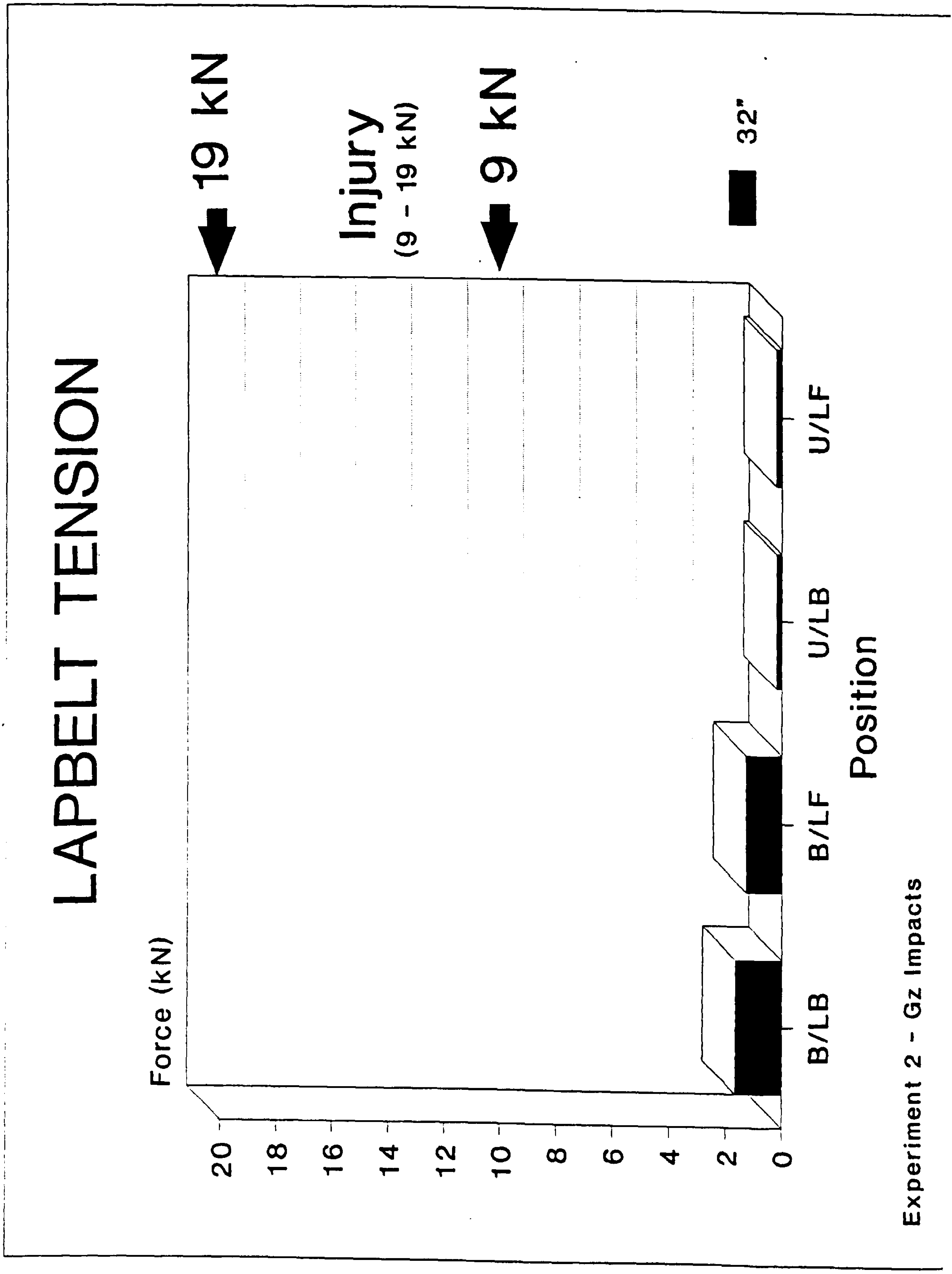

Fig. 44 Lap Belt Tension - Gz Impacts

Therefore for lap belt loads, the injury threshold would appear to lie between 9 and 19kN.

All the loads recorded during this experiment were below the lower limit of this range.

The highest loads were associated with a braced position and the loads in both braced positions were significantly higher than in either of the unbraced positions ($p<0.001$). In a vertical impact, with the dummy in a braced position, the upper torso moves forward on impact generating increased lap belt loads.

8.10.3 Lumbar Spine

Lumbar Spine Shear Load (See Fig. 45)

Table 25 Lumbar Fx

Source	Sums of Squares	Df	Mean Squares	F Ratio	Sig
B	15969202.00	3	5323067.33330	15.552	**
O	3582389.00	3	1194129.66670	3.489	NS
Residual	3080455.00	9	342272.77778		
Total	22632046.00	15			

B/LB	U/LB	B/LF	U/LF	Mean	
2034.00	4039.50	2026.00	4016.50	3029.00	) N

Positions B/LB and B/LF < Positions U/LB and U/LF (**)

Melvin et al estimated that for a 50th percentile Hybrid III dummy, the injury threshold for shear loads in the lumbar spine is 10.7kN (29).

All the shear loads recorded in this experiment were well below this injury threshold.

A significant effect of brace position on lumbar spine shear loads was observed ($p<0.01$).

The highest loads were associated with an unbraced position and these loads were significantly higher than those recorded in the braced positions ($p<0.01$).

In a vertical impact situation, with the dummy in a braced position, the upper torso will flex forwards on impact causing a forward flexion moment in the lumbar spine. In an unbraced position, such forward flexion will be less marked (Figs. 41 and 42) and higher shear loads will be recorded.

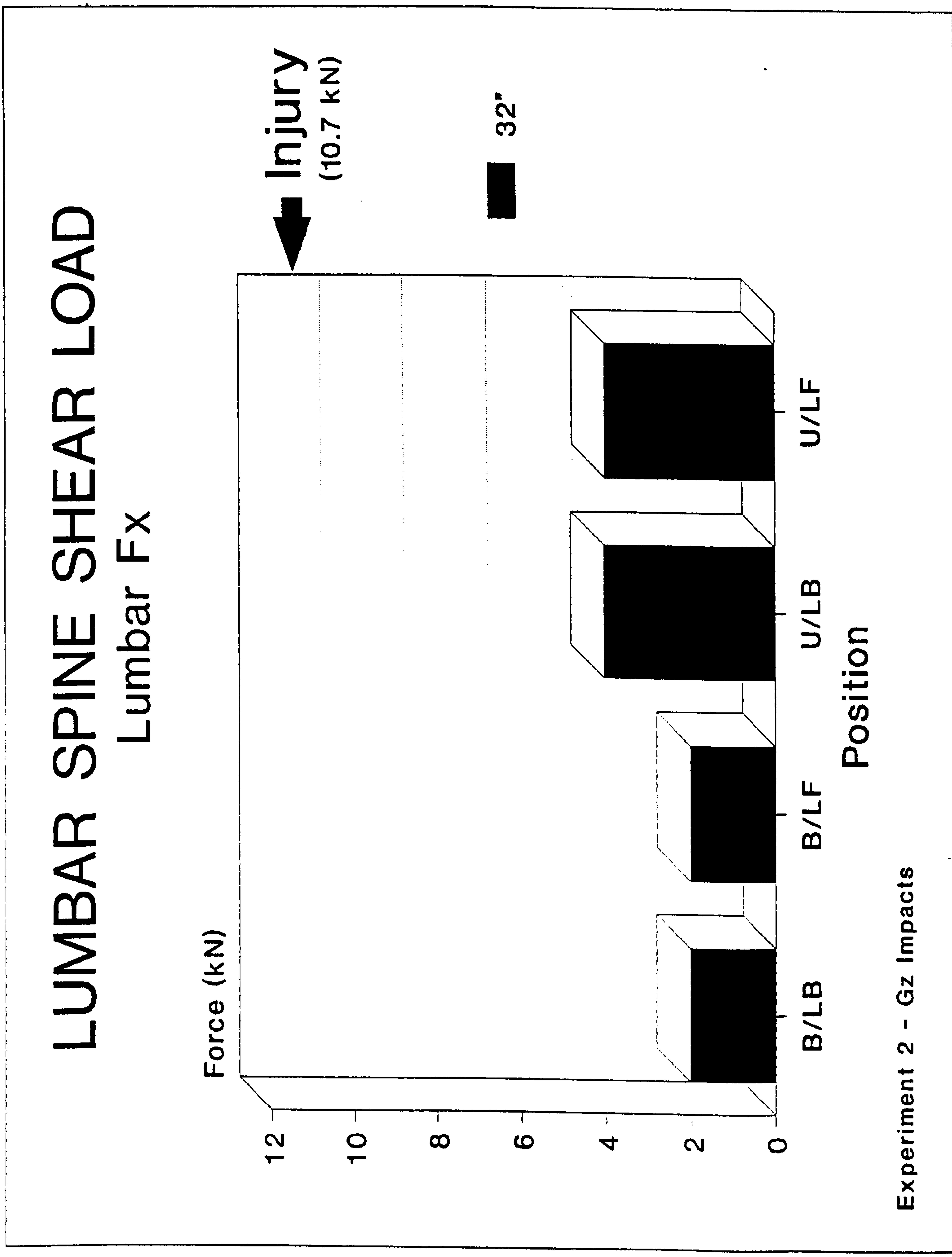

Fig. 45 Lumbar Spine Shear Load - Gz Impacts

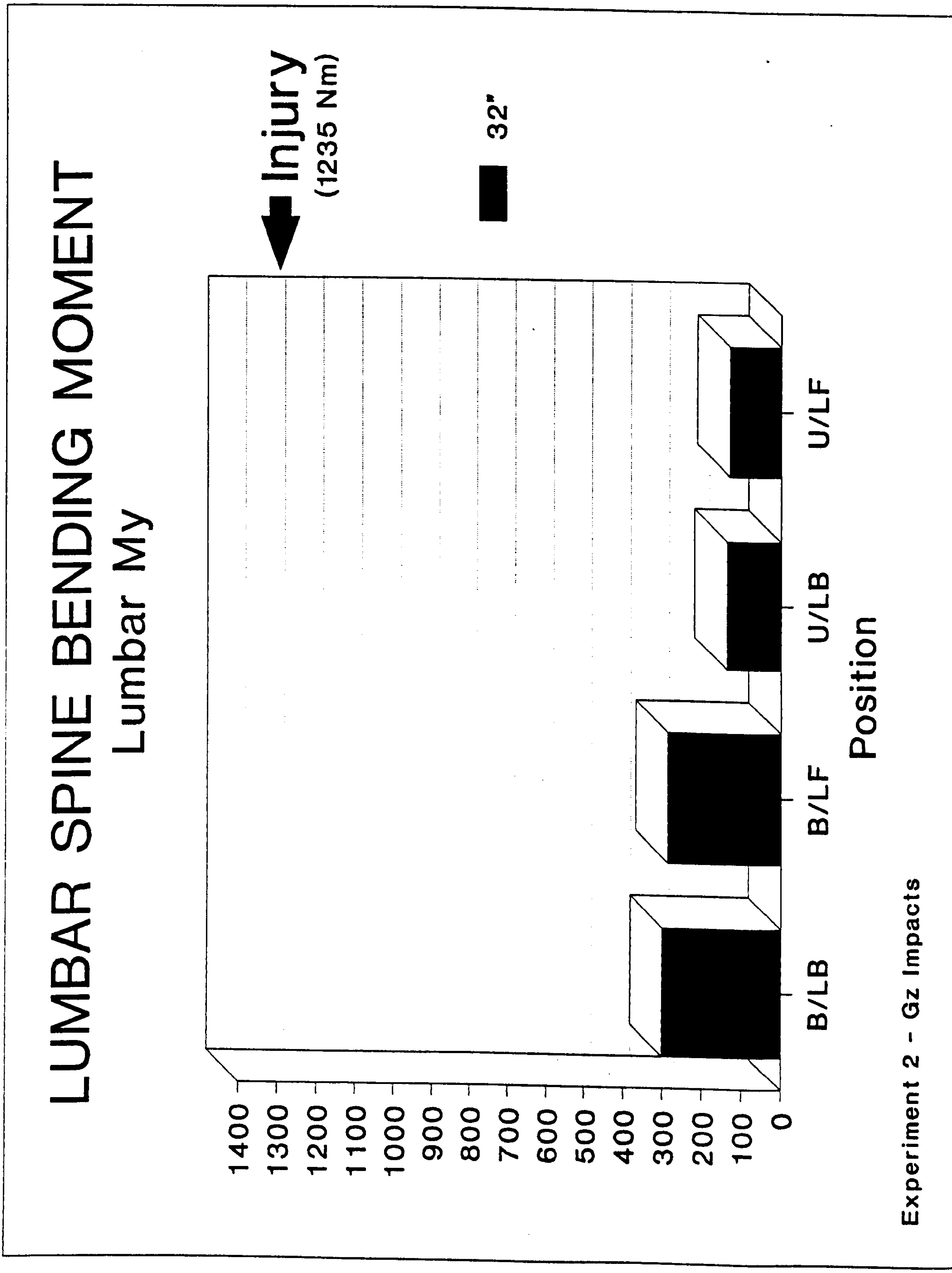

Fig. 46 Lumbar Forward Flexion Bending Moment - Gz Impacts

Lumbar Forward Flexion Bending Moment

Lumbar My (See Fig. 46)

Table 26 Lumbar My

Source	Sums of Squares	Df	Mean Squares	F Ratio	Sig
B	103217.500	3	34405.83333	40.584	**
O	1063.500	3	354.500	0.418	NS
Residual	7630.00	9	847.77778		
Total	111911.00	15			

B/LB	U/LB	B/LF	U/LF	Mean	
301.50	137.50	287.25	130.75	214.25	) N

Positions B/LB and B/LF > Positions U/LB and U/LF (***)

Melvin et al estimated that for a 50th percentile Hybrid III dummy, the injury threshold for a forward flexion spinal bending moment is 1235Nm (29).

All the loads recorded in this experiment were below this injury threshold.

A significant effect of brace position on the lumbar forward flexion bending moment was observed ($p<0.01$).

The highest bending moments were associated with a braced position and the loads were higher than those recorded in the unbraced positions ($p<0.001$).

In a vertical impact, the dummy in a braced position will flex further forwards on impact and this will be reflected in increased lumbar spine forward flexion bending moments. In an unbraced position, higher axial compressive loads would be expected.

Lumbar Spine Axial Loads

Lumbar Fz (See Fig. 47)

Table 27 Lumbar Fz

Source	Sums of Squares	Df	Mean Squares	F Ratio	Sig
B	16547622.7500	3	5515874.2500	17.597	**
O	6734426.2500	3	2244808.7500	7.161	**
Residual	2821176.7500	9	313464.08333		
Total	26103225.7500	15			

B/LB	U/LB	B/LF	U/LF	Mean	
3690.50	5886.50	3610.50	5429.00	4654.13	) N

Positions U/LB and U/LF > Positions B/LB and B/LF (**)

Order effect: linear

The axial loads recorded in the lumbar spine are all compressive.

Melvin et al have estimated that for a 50th percentile Hybrid III dummy, the injury threshold for a compressive load applied to the lumbar spine, is 7kN (29).

A significant linear order effect was observed ($p<0.01$) and it is suggested that this was due to deformation of the seat structure and seat padding due to repeated impacts.

A significant effect of brace position on lumbar axial loads was observed ($p<0.01$).

The highest loads were associated with an unbraced position and the loads in both the unbraced positions were significantly higher than in the braced positions ($p<0.01$).

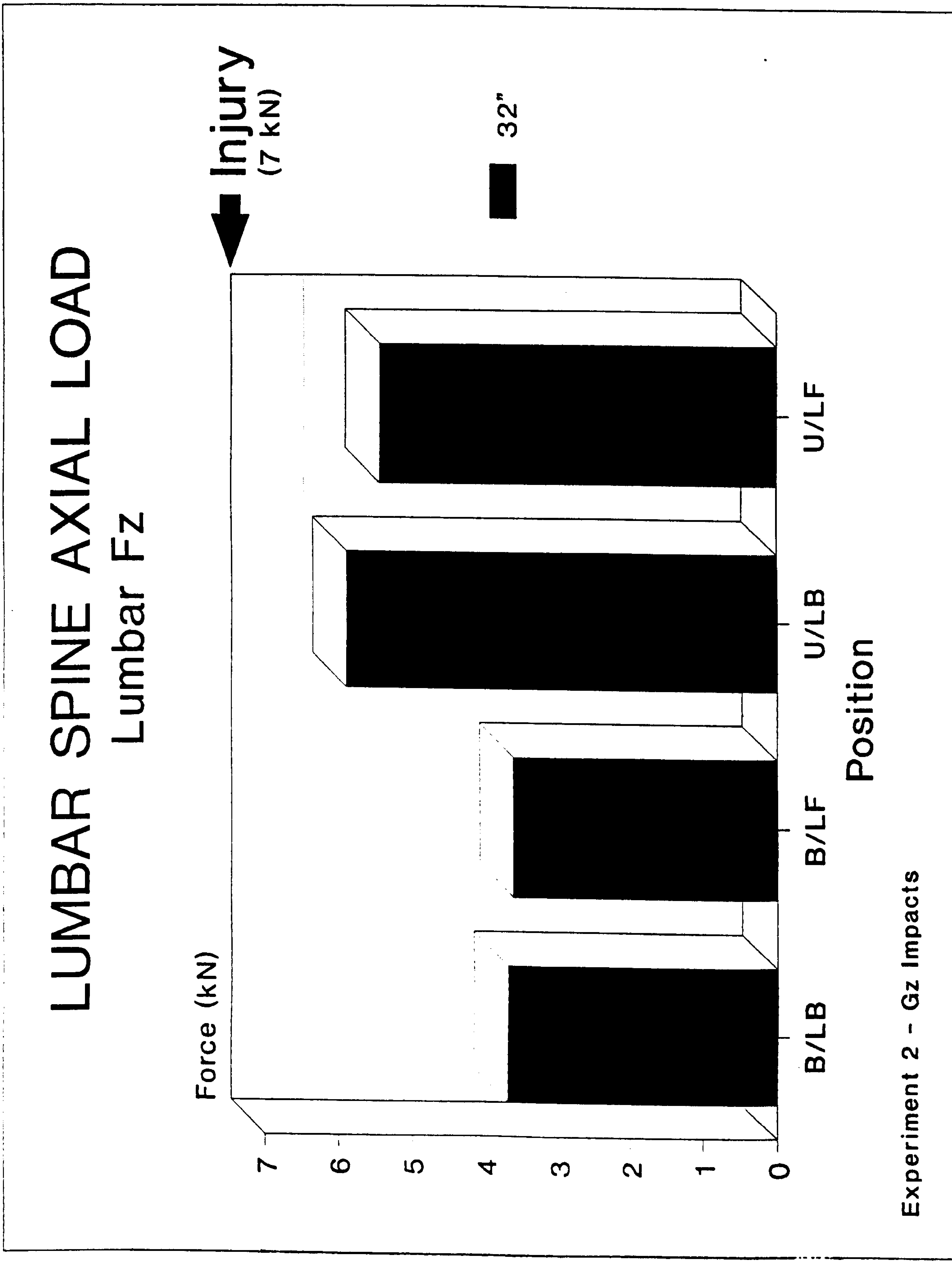

Fig. 47 Lumbar Spine Axial Loads - Gz Impacts

It is suggested that the increased axial compressive loads seen in association with an unbraced position are due to the impact forces being directed axially to the spine. With the dummy in a braced position, a vertical impact will produce forward flexion of the torso causing increased forward flexion bending moments in the lumbar spine rather than axial compressive loads.

8.10.4 Lower Limbs

Femoral Axial Loads (See Fig. 48)

Table 28 Femur Fz

Right

Source	Sums of Squares	Df	Mean Squares	F Ratio	Sig
B	15992.2500	3	5330.7500	7.586	**
O	10484.7500	3	3494.91667	4.973	*
Residual	6324.7500	9	702.7500		
Total	32801.7500	15			

B/LB	U/LB	B/LF	U/LF	Mean
339.25	275.25	303.00	255.00	293.12

Position B/LB > Positions U/LB and U/LF (**)
Order effect: Linear

Left

Source	Sums of Squares	Df	Mean Squares	F Ratio	Sig
B	20171.18750	3	6723.72917	5.196	*
O	11213.18750	3	3737.72917	2.889	NS
Residual	11645.06250	9	1293.89583		
Total	43029.43750	15			

B/LB	U/LB	B/LF	U/LF	Mean
401.75	380.75	333.75	313.00	357.31

Position B/LB > Position U/LF (*)

Right Femur Fz

A linear order effect was observed ($p<0.05$).

A significant effect of brace position on right femoral axial loads was observed ($p<0.01$).

All the loads recorded were tension loads.

The highest loads were associated with a braced legs back position and these loads were higher than in any of the unbraced positions ($p<0.001$).

The mean load recorded in a braced legs back position was 339N.

Left Femur Fz

A significant effect of brace position on left femoral axial loads was observed ($p<0.05$).

All the loads recorded were tension loads.

The loads recorded in a braced legs back position were significantly higher than in an unbraced legs forward position ($p<0.05$).

The mean load recorded in a braced legs back position was 402N.

Discussion of Femoral Axial Loads

A significant linear order effect was observed on the right side. It is suggested that this was related to loss of elasticity in the lap belt due to repetitive loading.

All the loads recorded were tension loads indicating that significant knee contact did not occur with the back of the forward seat.

The highest loads were associated with a braced legs back position. The reason for this is not clear.

The injury threshold for a tension load applied to the human femur is approximately 9kN. Consequently injury is very unlikely.

Femoral Shear Loads

Femur Fx (See Fig. 49)

Table 29 Femur Fx

Right

Source	Sums of Squares	Df	Mean Squares	F Ratio	Sig
B	768303.18750	3	256101.06250	90.776	**
O	6508.68750	3	2169.56250	0.769	NS
Residual	25391.06250	9	2821.22917		
Total	800202.93750	15			

B/LB	U/LB	B/LF	U/LF	Mean
556.25	142.00	595.00	134.50	356.94

Positions B/LB and B/LF > Positions U/LB and U/LF (***)

Left

Source	Sums of Squares	Df	Mean Squares	F Ratio	Sig
B	545249.18750	3	181749.72917	54.475	**
O	4966.68750	3	1655.56250	0.496	NS
Residual	30027.56250	9	3336.39583		
Total	580243.43750	15			

B/LB	U/LB	B/LF	U/LF	Mean
490.00	136.25	519.25	135.75	320.31

Positions B/LB and B/LF > Positions U/LB and U/LF (***)

Right Femur Fx

A significant effect of brace position on right femoral shear loads was observed ($p<0.01$).

The highest shear loads were recorded in the braced positions and these loads were higher than in either of the unbraced positions. This effect is statistically significant ($p<0.001$).

Left Femur Fx

Findings were similar to the right femur.

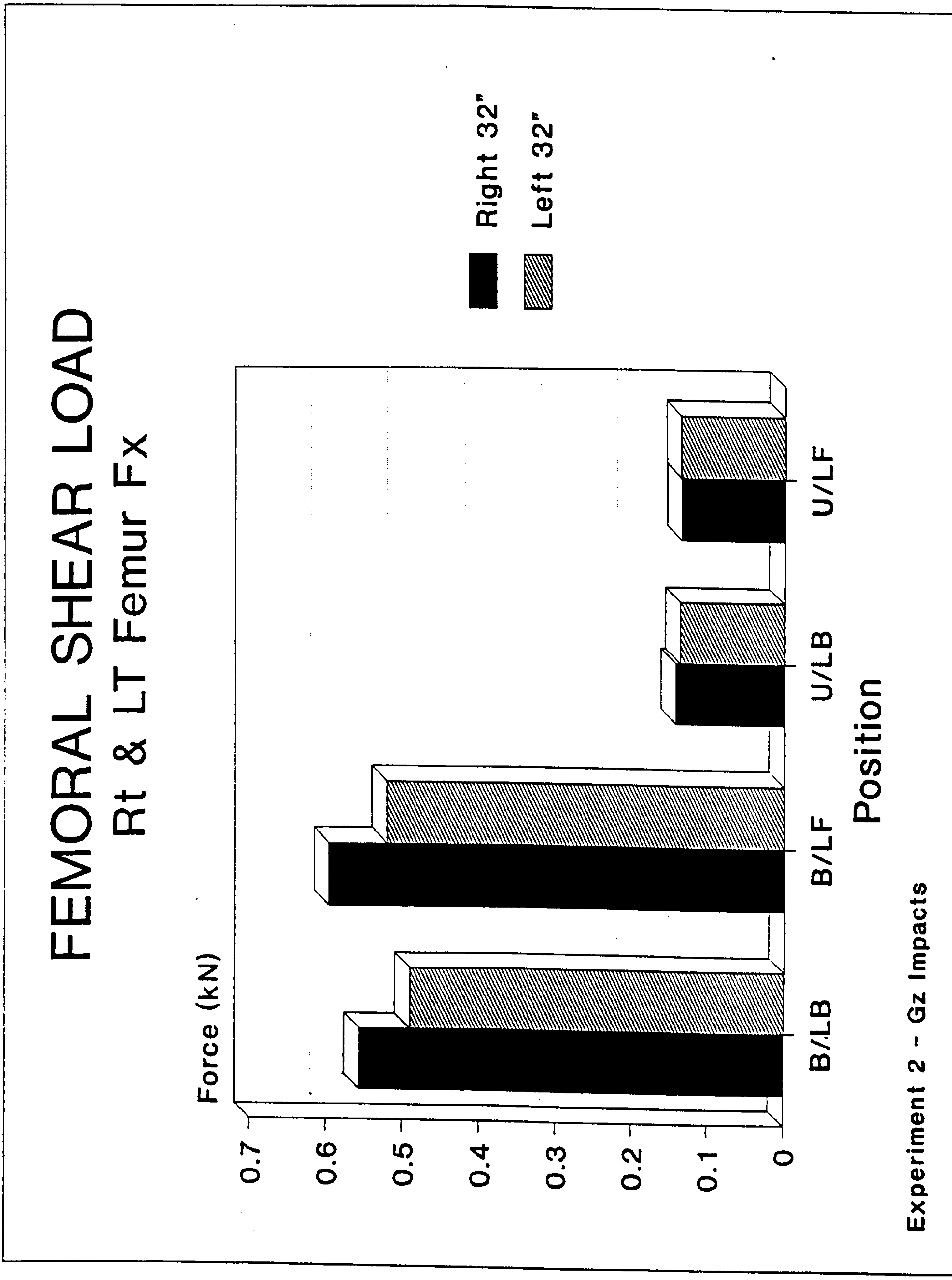

Fig. 49 Femoral Shear Loads (Fx) - Gz Impacts

Discussion

See Discussion of Femoral Shear Loads.

Femur Fy (See Fig. 50)

Table 30 Femur Fy

Right

Order effect: non-linear

Analysis adjusting for order

Source	Sums of Squares	Df	Mean Squares	F Ratio	Sig
Linear run	1.01	1	1.01	0.016	NS
Quadratic run	2791.33	1	2791.33	45.687	***
B (adjusted)	3033.25	3	1011.08	16.545	**
O (adjusted)	1084.67	3	361.56	5.918	*
Residual	427.68	7	61.10		
Total	7337.94	15			

Means adjusted for order

B/LB	U/LB	B/LF	U/LF	Mean
64.91	43.58	51.45	22.32	45.56

Position B/LB > Position U/LF (***)

Position B/LB > Position U/LB (*)

Position B/LF > Position U/LF (**)

Position U/LB > Position U/LF (*)

Left

Source	Sums of Squares	Df	Mean Squares	F Ratio	Sig
B	47499.68750	3	15833.22917	7.617	**
O	11936.68750	3	3978.89583	1.914	NS
Residual	18708.06250	9	2078.67361		
Total	78144.43750	15			

B/LB	U/LB	B/LF	U/LF	Mean
118.50	50.75	175.00	40.50	96.19

Position B/LF > Positions U/LB and U/LF (*)

Right Femur Fy

A non-linear order effect was observed ($p < 0.05$). This was adjusted for in the statistical analysis.

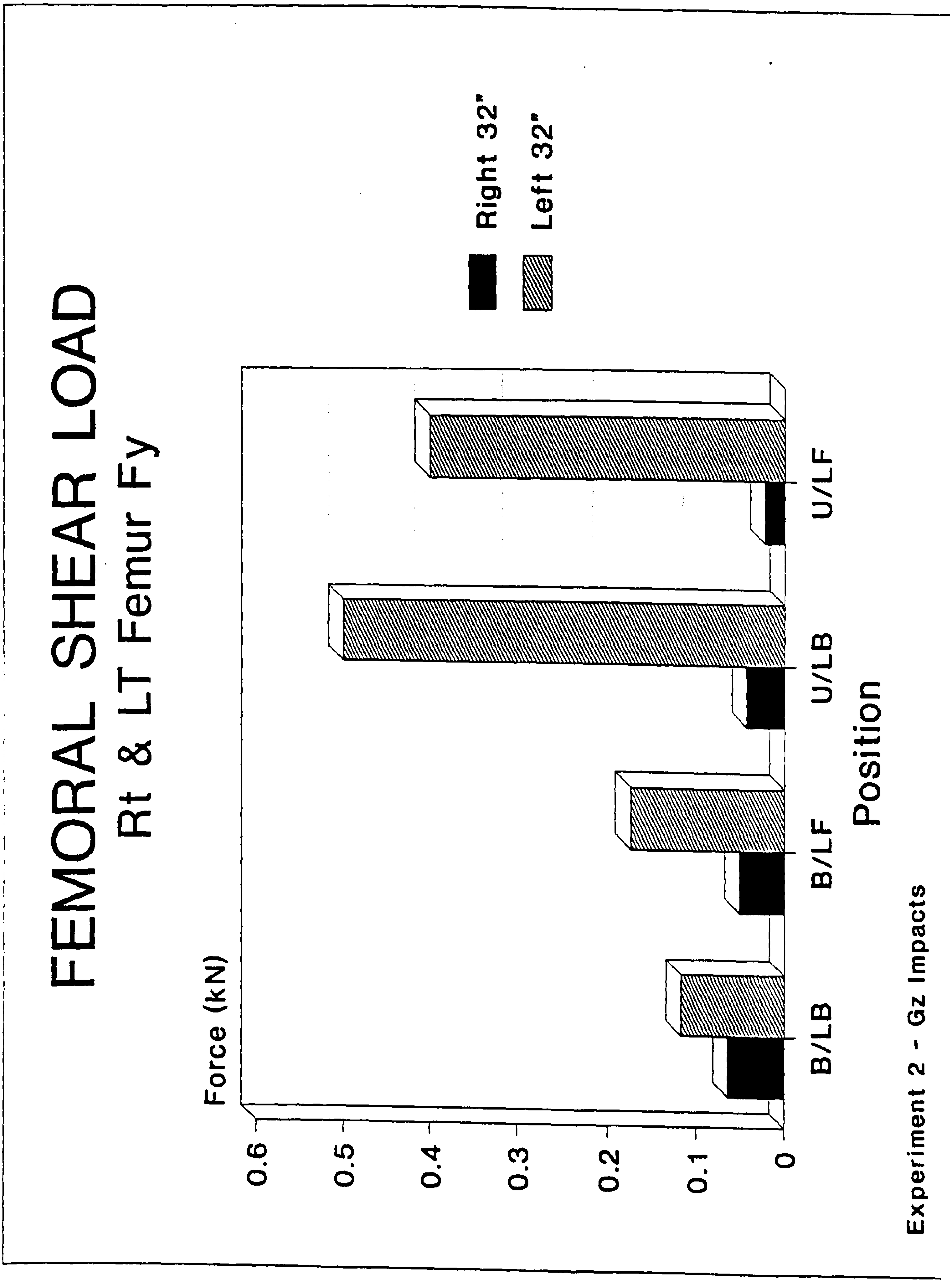

Fig. 50 Femoral Shear Loads (Fy) - Gz Impacts

A significant effect of brace position on right femur shear load was observed ($p<0.01$).

The highest shear loads were associated with a braced legs back position and these were significantly higher than in the unbraced legs forward position ($p<0.001$) and the unbraced legs back position ($p<0.05$).

Left Femur Fy

A significant effect of brace position on left femur shear load was observed ($p<0.01$).

The highest loads were associated with a braced legs forward position and these loads were higher than in either of the unbraced positions ($p<0.05$).

Discussion of Femoral Shear Loads

Injury thresholds for a shear load applied to the human femur are difficult to predict.

The highest loads were associated with adopting a braced position. The reason for this is not clear.

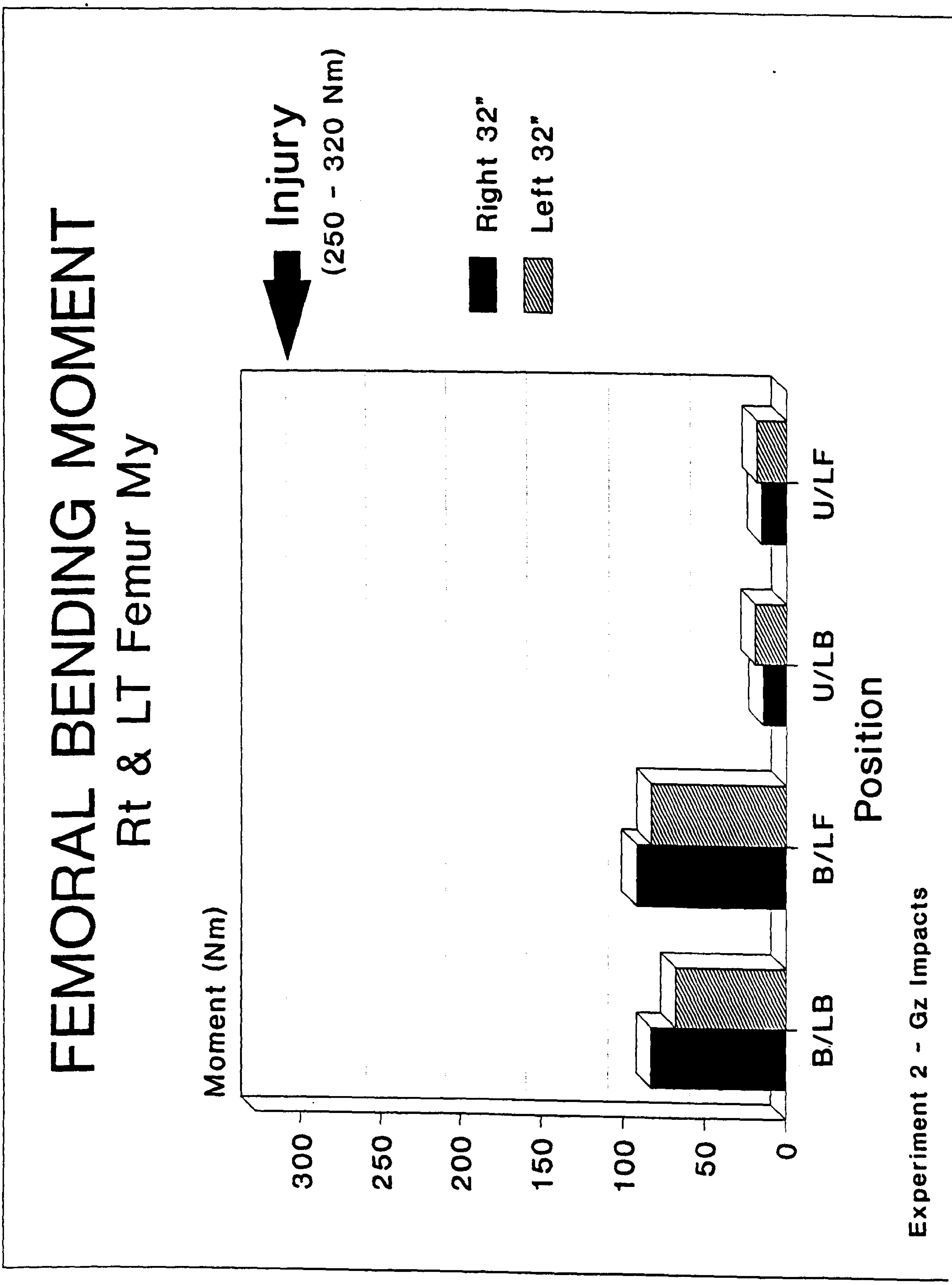

Fig. 51 Femoral Bending Moment (My) - Gz Impacts

Femoral Bending Moments

Femur My (See Fig. 51)

Table 31 Femur My

Right

Source	Sums of Squares	Df	Mean Squares	F Ratio	Sig
B	21324.500	3	7108.16667	62.474	**
O	229.500	3	76.500	0.672	NS
Residual	1024.00	9	113.77778		
Total	22578.00	15			

B/LB	U/LB	B/LF	U/LF	Mean
83.50	14.75	92.25	15.50	51.50

Positions B/LB and B/LF > Positions U/LB and U/LF (***)

Left

Source	Sums of Squares	Df	Mean Squares	F Ratio	Sig
B	13378.68750	3	4459.56250	52.841	**
O	222.18750	3	74.06250	0.878	NS
Residual	759.56250	9	84.39583		
Total	14360.43750	15			

B/LB	U/LB	B/LF	U/LF	Mean
68.25	19.50	83.00	18.00	47.19

Positions B/LB and B/LF > Positions U/LB and U/LF (***)
Position B/LF > Position B/LB (*)

Right Femur My

A significant effect of brace position on right femoral bending moments was observed ($p<0.01$).

The bending moments in the y-axis were higher in the braced positions than in the unbraced positions. This difference is statistically significant ($p<0.001$).

The mean load recorded in a braced legs back position was 84Nm and in a braced forward position 92Nm.

Left Femur My

A significant effect of brace position on left femoral bending moments was observed ($p<0.01$).

The highest loads were associated with a braced position and these loads were higher than in any of the unbraced positions ($p<0.001$).

The mean load recorded in a braced legs back position was 68Nm and in a braced legs forward position 83Nm.

Discussion

See Discussion of Femoral Bending Moments.

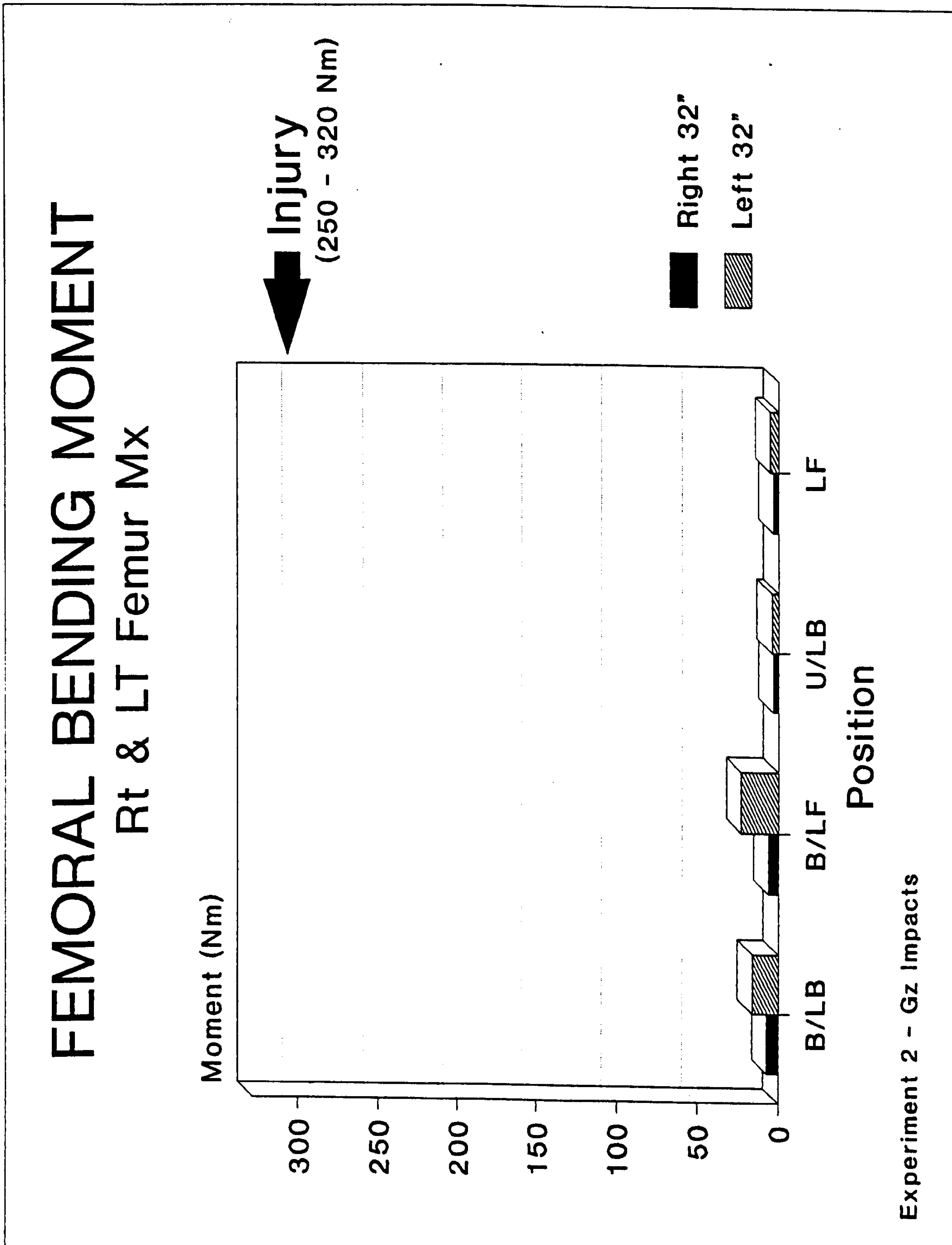

Fig. 52 Femoral Bending Moment (Mx) - Gz Impacts

Right and Left Femur Mx

Femur Mx (See Fig. 52)

Table 32 Femur Mx

Right

Source	Sums of Squares	Df	Mean Squares	F Ratio	Sig
B	52.2500	3	17.41667	9.646	**
O	15.2500	3	5.08333	2.815	NS
Residual	16.2500	9	1.80556		
Total	83.7500	15			

B/LB	U/LB	B/LF	U/LF	Mean
7.25	3.25	6.00	3.00	4.88

Position B/LB > Positions U/LB and U/LF (**)
Position B/LF > Positions U/LB and U/LF (*)

Left

Source	Sums of Squares	Df	Mean Squares	F Ratio	Sig
B	961.500	3	320.500	4.242	*
O	487.500	3	162.500	2.151	NS
Residual	680.00	9	75.55556		
Total	2129.00	15			

B/LB	U/LB	B/LF	U/LF	Mean
16.25	5.00	23.00	4.75	12.25

Position B/LF > Positions U/LB and U/LF (*)

Right Femur Mx

The mean bending moment recorded in the x-axis in the right femur was 5Nm.

The loads associated with a braced position were higher than in either of the unbraced positions. This difference is statistically significant.

Left Femur Mx

The mean bending moment recorded in the x-axis in the left femur was 12Nm.

The highest loads were associated with a braced legs forward position and these loads were higher than in either of the unbraced positions. This difference is statistically significant ($p<0.05$).

Discussion

See Discussion of Femoral Bending Moments.

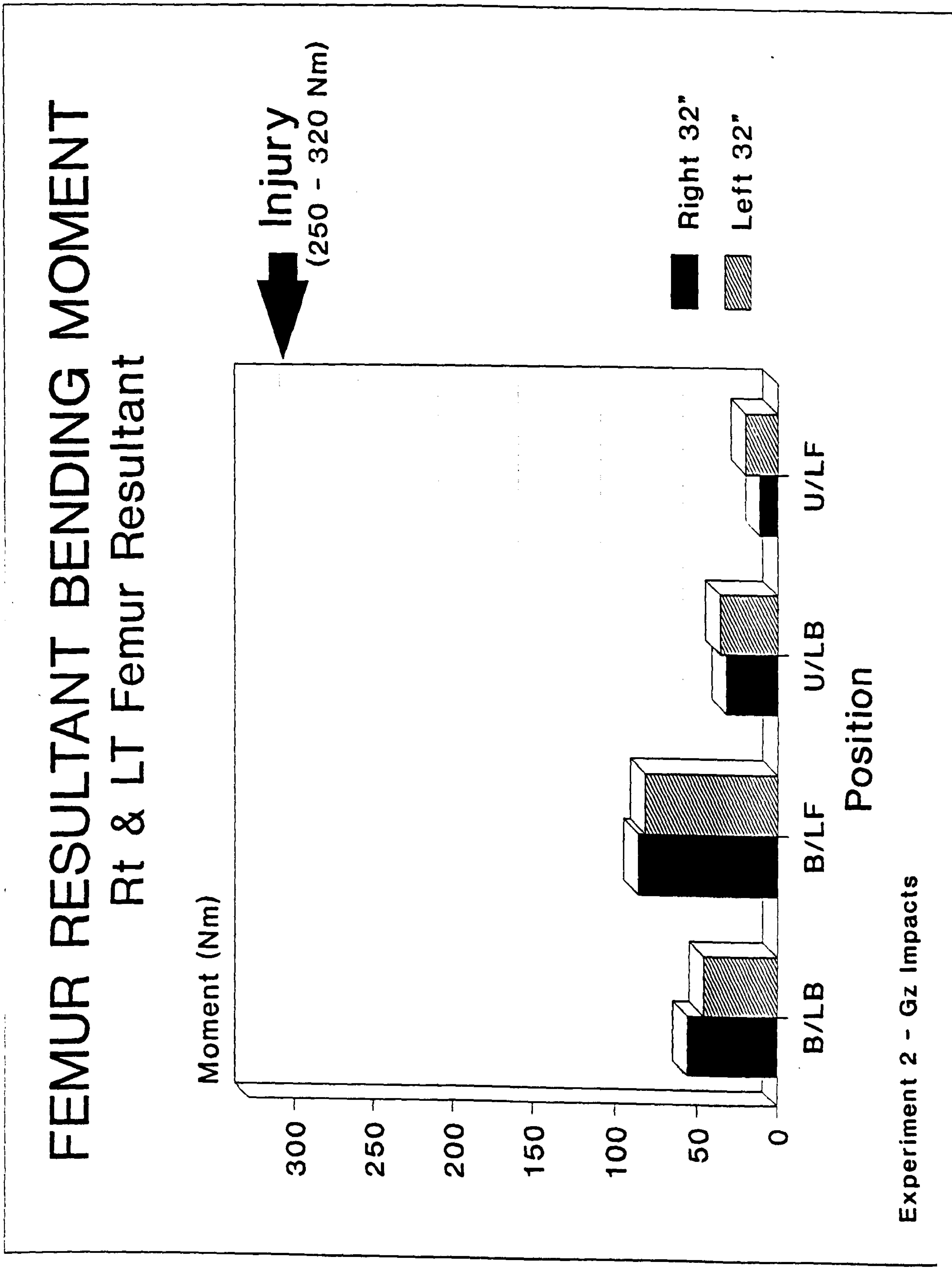

Fig. 53 Femur Resultant Bending Moment - Gz Impacts

Femur Resultant Bending Moment

Femur Resultant Bending Moment (See Fig. 53)

Table 33 Femur Resultant Bending Moment

Right

Source	Sums of Squares	Df	Mean Squares	F Ratio	Sig
B	12567.18750	3	4189.06250	5.469	*
O	256.68750	3	85.56250	0.112	NS
Residual	6893.56250	9	765.95139		
Total	19717.43750	15			

B/LB	U/LB	B/LF	U/LF	Mean
56.00	32.75	86.75	11.25	46.69

Position B/LF > Position U/LF (**)

Left

Source	Sums of Squares	Df	Mean Squares	F Ratio	Sig
B	8360.68750	3	2786.89583	5.333	*
O	376.68750	3	125.56250	0.240	NS
Residual	4703.06250	9	522.56250		
Total	13440.43750	15			

B/LB	U/LB	B/LF	U/LF	Mean
46.50	36.00	82.25	20.00	46.19

Position B/LF > Positions U/LB and U/LF (*)

Right Femur Resultant Bending Moment

A significant effect of brace position on the right femur resultant bending moment was observed ($p<0.05$).

The highest loads were associated with a braced legs forward position (mean 87Nm).

Left Femur Resultant Bending Moment

A significant effect of brace position on the left femur resultant bending moment was observed ($p<0.05$).

The highest loads were associated with adopting a braced legs forward position (mean 82Nm).

Discussion

See Discussion of Femoral Bending Moments.

Discussion of Femoral Bending Moments

Weber predicted that for a bending load applied to the femur, the load to failure was on average 233Nm in the male and 165Nm in the female (28). Messerer produced comparable figures with the value of 310Nm in the male and 180Nm in the female (28). These loads were applied statically. Mather has shown that when bones are loaded dynamically, the load to failure increases. In his experiments he showed that the energy to failure may increase by 48% under dynamic loading conditions (27). Martens similarly showed that the dynamic load to failure for a torsional load applied to the femur was 16-24% greater than comparable static values (25).

St-Laurent recently defined a dynamic bending load to failure of 320Nm for the frangible femoral component in a motorcyclist anthropometric test device (36).

In this experiment the mean resultant bending moment in the left femur was 47Nm and in the right femur 87Nm. Therefore injury would seem to be very unlikely.

The highest bending moments were associated with adopting a braced position. It is suggested that this was due to the upper torso flexing further forwards on impact. Forward flexion of the torso around the lap belt introduces a bending load into the femur as a result of the downward force created by the lap belt and the upward force created by the front seat spar. (See Fig. 30b)

Femoral Torque

Femur Mz (See Fig. 54)

Table 34 Femur Mz

Right

Source	Sums of Squares	Df	Mean Squares	F Ratio	Sig
B	1341.00	3	447.00	15.443	**
O	101.500	3	33.83333	1.169	NS
Residual	260.500	9	28.94444		
Total	1703.00	15			

B/LB	U/LB	B/LF	U/LF	Mean
29.00	6.50	19.50	8.00	15.75

Position B/LB > Positions U/LB and U/LF (**)
Position B/LF > Positions U/LB and U/LF (*)
Position B/LB > Position B/LF (*)

Left

Source	Sums of Squares	Df	Mean Squares	F Ratio	Sig
B	352.7500	3	117.58333	4.719	*
O	304.7500	3	101.58333	4.077	*
Residual	224.2500	9	24.91667		
Total	881.7500	15			

B/LB	U/LB	B/LF	U/LF	Mean
24.00	17.00	30.00	21.50	23.13

Position B/LF > Position U/LB (*)

Order effect: linear

Right Femur Mz

A significant effect of brace position on right femoral torque was observed ($p<0.01$).

The highest loads were associated with a braced position and these loads were higher than in either of the unbraced positions.

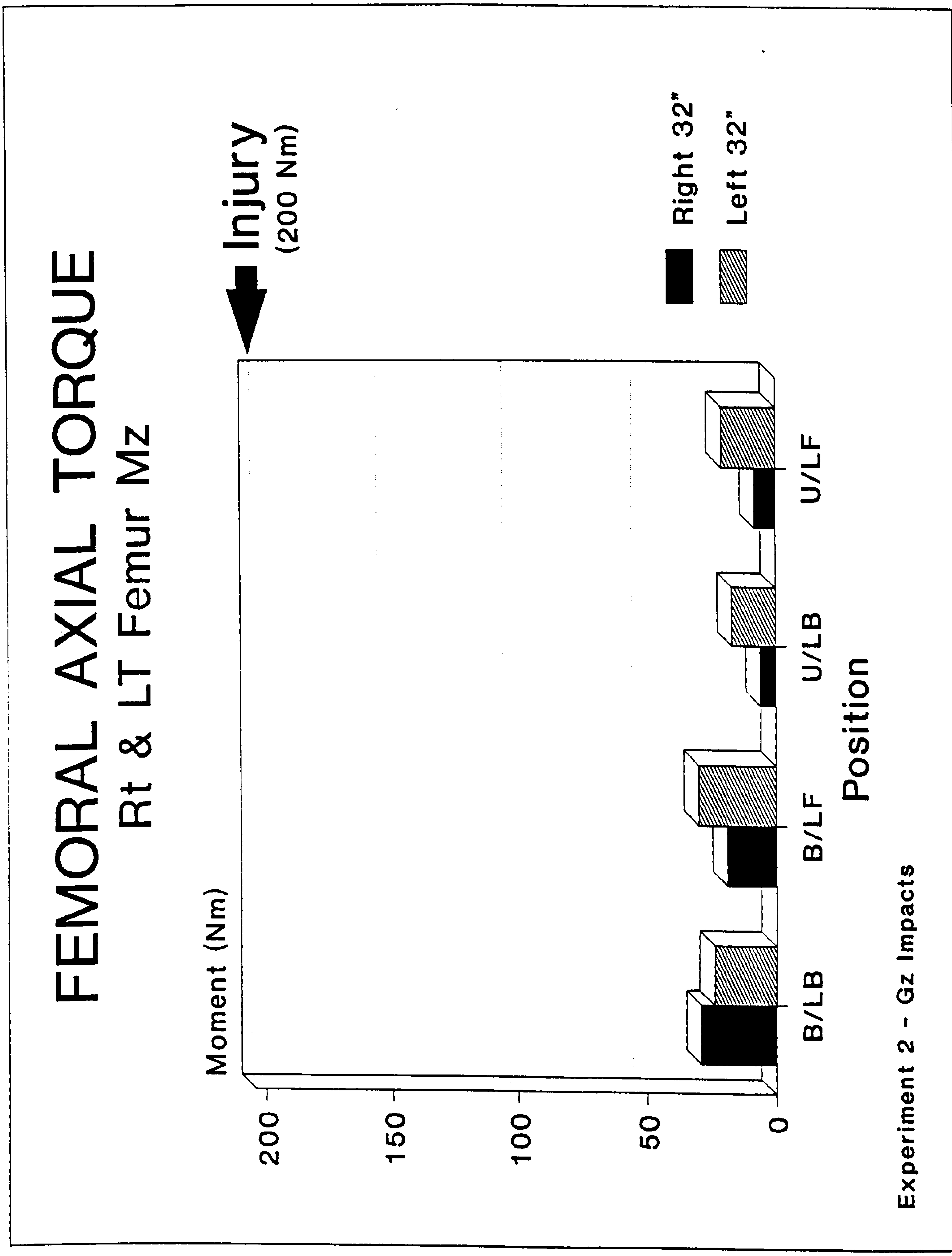

Fig. 54 Femoral Torque - Gz Impacts

Left Femur Mz

A linear order effect was observed ($p<0.05$).

A significant effect of brace position on left femoral torque was observed ($p<0.05$).

The highest loads were associated with a braced position.

Discussion of Femoral Torque

A linear order effect was observed on the left side. It is suggested that such an effect was related to seat deformation and loss of elasticity in the lap belt due to repeated impacts.

Martens et al defined the injury threshold for dynamic torsional loading of the femur at 204Nm for males (25). St-Laurent et al defined a dynamic torsional load to failure of 192Nm for the frangible femoral component in a motorcyclist anthropometric test device (36). Therefore the injury threshold would appear to lie between 192 and 204Nm for the adult male.

All the loads recorded in this experiment were well below the injury threshold and injury would seem to be very unlikely.

The highest loads were associated with adopting a braced position. The reason for this is not clear.

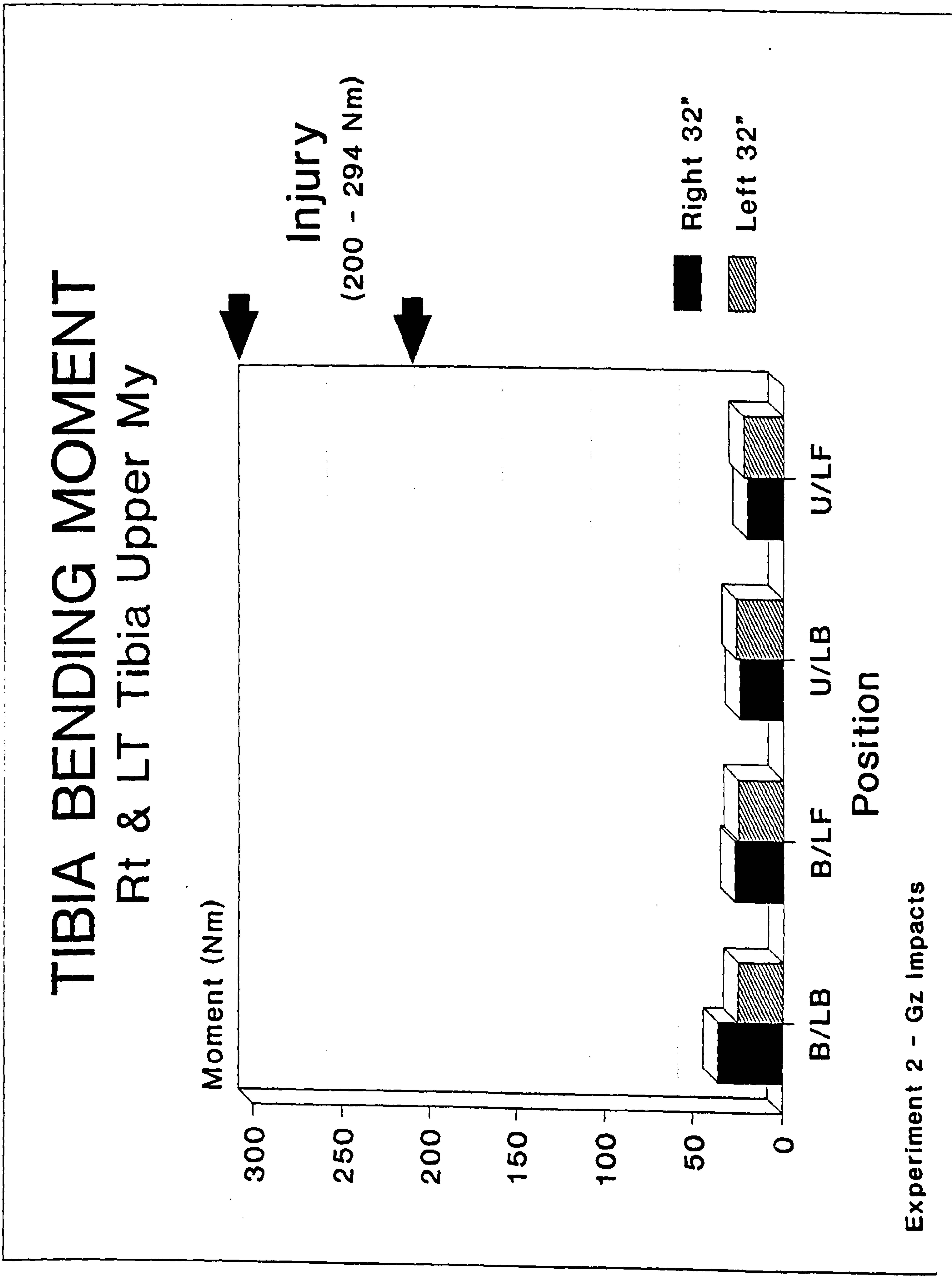

Fig. 55 Tibia Bending Moment (U/My) - Gz Impacts

Tibia

Tibial Bending Moment

Tibia Upper My (See Fig. 55)

Table 35 Tibia upper My

Right

Source	Sums of Squares	Df	Mean Squares	F Ratio	Sig
B	533.2500	3	177.7500	4.829	*
O	103.2500	3	34.41667	0.935	NS
Residual	331.2500	9	36.80556		
Total	967.7500	15			

B/LB	U/LB	B/LF	U/LF	Mean
36.00	24.50	27.75	20.25	27.13

Position B/LB > Position U/LF (*)

Left

Source	Sums of Squares	Df	Mean Squares	F Ratio	Sig
B	35.500	3	11.83333	1.401	NS
O	23.500	3	7.83333	0.928	NS
Residual	76.00	9	8.44444		
Total	135.00	15			

B/LB	U/LB	B/LF	U/LF	Mean
25.75	26.00	25.00	22.25	24.75

Right Tibia Upper My

A significant effect of brace position on tibial upper bending moments was observed ($p<0.05$).

The highest loads were associated with a braced legs back position.

Left Tibia Upper My

No significant effect of brace position was observed.

Discussion

See Discussion of Tibial Bending Moments.

Tibia Lower My (See Fig. 56)

Table 36 Tibia lower My

Right

Source	Sums of Squares	Df	Mean Squares	F Ratio	Sig
B	257.2500	3	85.7500	19.662	**
O	11.2500	3	3.7500	0.860	NS
Residual	39.2500	9	4.36111		
Total	307.7500	15			

B/LB	U/LB	B/LF	U/LF	Mean
12.25	3.75	12.00	4.50	8.13

Positions B/LB and B/LF > Positions U/LB and U/LF (**)

Left

Source	Sums of Squares	Df	Mean Squares	F Ratio	Sig
B	134.18750	3	44.72917	4.191	*
O	27.18750	3	9.06250	0.849	NS
Residual	96.06250	9	10.67361		
Total	257.43750	15			

B/LB	U/LB	B/LF	U/LF	Mean
12.50	6.75	9.25	4.75	8.31

Position B/LB > Position U/LF (*)

Right Tibia Lower My

A significant effect of brace position on right lower tibial bending moments was observed ($p<0.01$).

The highest loads were associated with adopting a braced position and these loads were higher than in either of the unbraced positions.

The difference is statistically significant ($p<0.01$).

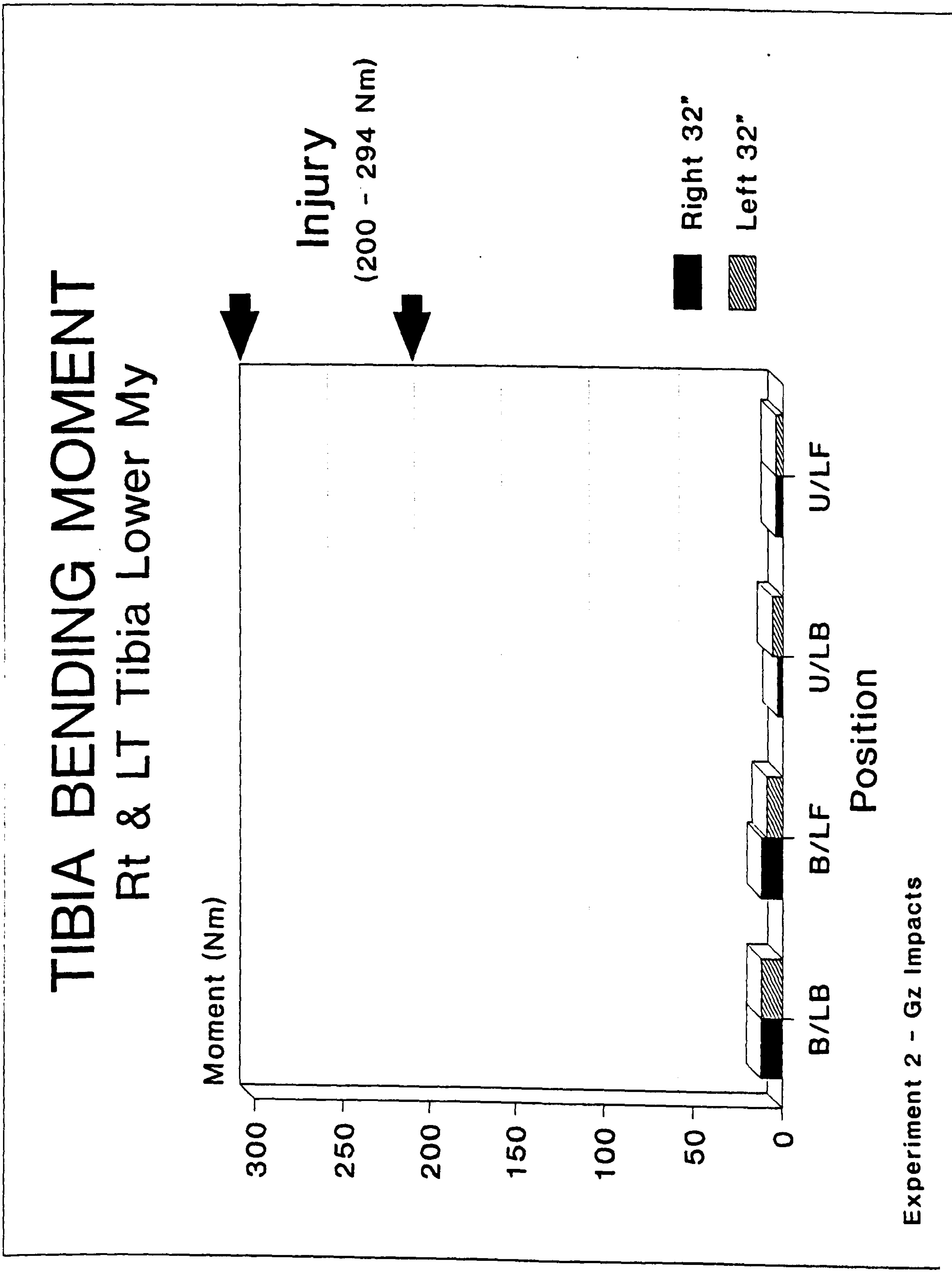

Fig. 56 Tibia Bending Moment (L/My) - Gz Impacts

Left Tibia Lower My

A significant effect of brace position on left lower tibial bending moments was observed ($p < 0.05$).

The highest loads were associated with adopting a braced legs back position.

Discussion

See Discussion of Tibial Bending Moments.

Discussion of Tibial Bending Moments

Weber defined that the load to failure for a bending moment applied to the human tibia was 180Nm in the male and 125Nm in the female (28). Messerer defined the comparable values of 207Nm in the male and 124Nm in the female (28).

Both of these loads were applied statically. It has been shown that when a bone is loaded dynamically the loads to failure are increased (27)(25).

St-Laurent et al defined a dynamic bending load to failure of 294Nm for the tibial component in a motorcyclist anthropometric test device (36).

In this experiment all the loads recorded are well below the injury threshold and injury would seem to be extremely unlikely.

Greater loads were recorded in the braced positions and this is attributable to the forward flexion of the dummy's upper torso which occurs during a vertical impact situation in this position.

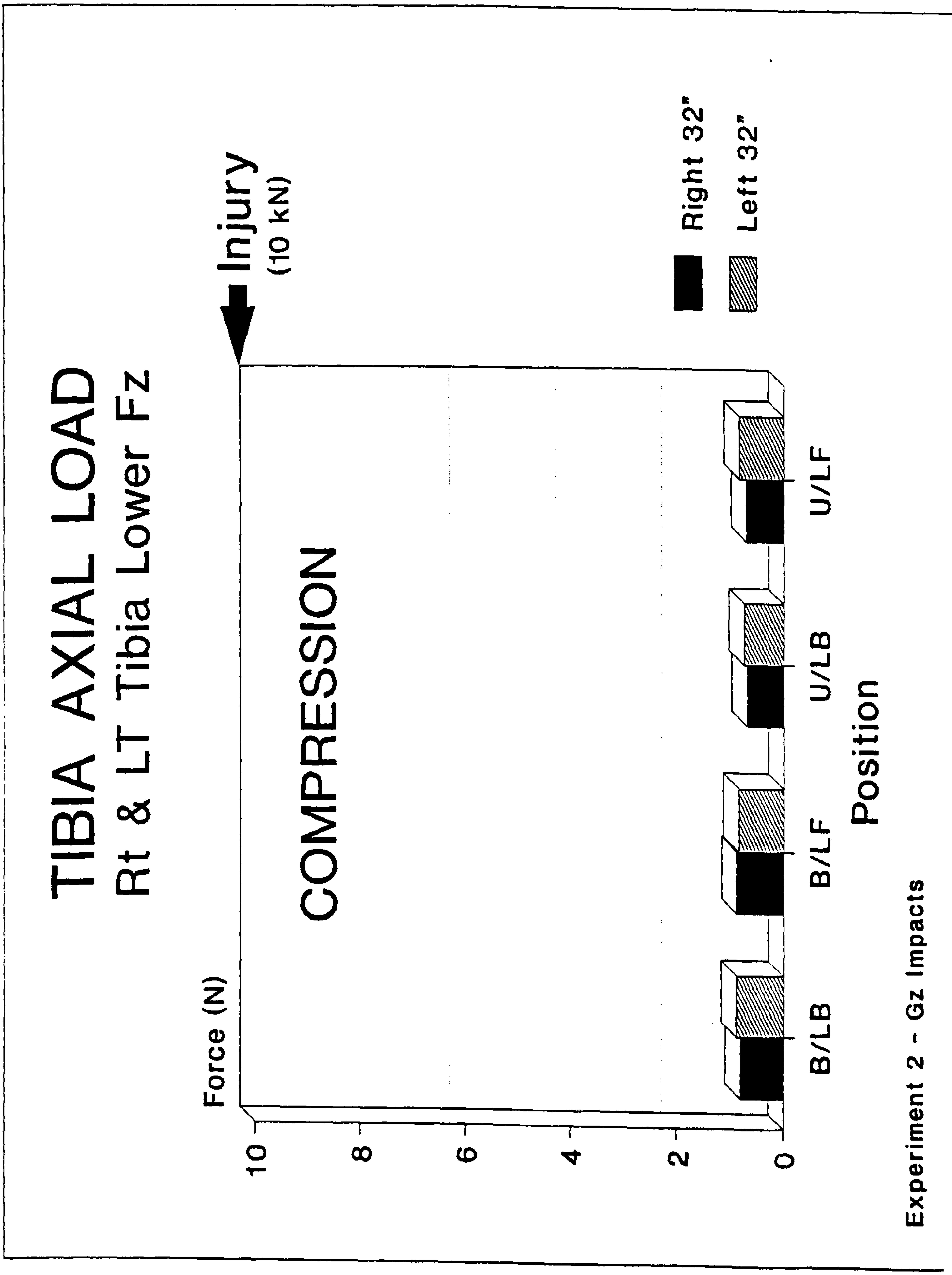

Fig. 57 Tibia Axial Load - Gz Impacts

Tibia Axial Load

Tibia Lower Fz (See Fig. 57)

Table 37 Tibia lower Fz

Right

Source	Sums of Squares	Df	Mean Squares	F Ratio	Sig
B	105957.2500	3	35319.08333	1.940	NS
O	37663.2500	3	12554.41667	0.690	NS
Residual	163855.2500	9	18206.13889		
Total	307475.7500	15			

B/LB	U/LB	B/LF	U/LF	Mean
818.25	689.75	885.00	702.50	773.87

Left

Source	Sums of Squares	Df	Mean Squares	F Ratio	Sig
B	48513.500	3	16171.16667	0.654	NS
O	69698.00	3	23232.66667	0.939	NS
Residual	222645.500	9	24738.38889		
Total	340857.00	15			

B/LB	U/LB	B/LF	U/LF	Mean
897.75	747.50	855.50	846.25	836.75

Right Tibia Lower Fz

No significant effect of brace position on tibial axial loading was observed.

Left Tibia Lower Fz

No significant effect of brace position on tibial axial loading was observed.

Discussion of Tibial Axial Loads

The mean axial compressive load recorded in the right tibia was 774N and in the left tibia 837N.

Messerer predicted a mean load to failure for a compression load applied axially to the tibia of 10.36kN in the male and 7.49kN in the female (28). These loads were applied statically. It has been shown that the load to failure for a dynamic load applied to a bone is greater than the corresponding static load (27)(25). Therefore it would appear that the injury threshold for a compressive load applied axially to the human tibia lies above the 10kN level.

Culver et al have shown that the static load to failure for the ankle ligaments occurs at 3kN (9).

In this experiment, all the loads recorded are well below these injury thresholds. Consequently injury is very unlikely.

8.11 SUMMARY

High Speed Video Recording

Review of the high speed video recordings revealed that when the dummy was placed in a braced position there was a tendency for the torso to flex further forwards on impact.

Head

The risk of head injury as indicated by the Head Injury Criterion appears to be minimal in any of the positions tested.

Pelvis

The risk of lap belt loads causing pelvic injury appears to be minimal in any of the positions tested.

Lumbar Spine

The poor biofidelity of the spine in the Hybrid III dummy makes it difficult to interpret the loads recorded in the lumbar spine load cell.

The shear loads and forward flexion spinal bending moments are all well below the estimated injury thresholds. However, the axial compressive loads are high and approach the estimated injury threshold. The loads are significantly higher in association with an unbraced position. In such an unbraced position the vertical impact forces will be transmitted directly through to the spine.

Lower Limbs

Femur

The loads recorded in the left and right femur are all well below their respective injury thresholds.

Tibia

The loads recorded in the left and right tibia are all well below their respective injury thresholds.

8.12 CONCLUSIONS

1. In the predominantly vertical impact simulated in this experiment, the forces generated in the head, lap belt and lower limbs were unlikely to cause injury.

2. In the predominantly vertical impact simulated in this experiment, the forces recorded in the lumbar spine were high. These loads were highest in an unbraced position.

MATHEMATICAL MODELLING

1. VALIDATION OF THE MATHEMATICAL MODEL

1.1 STAGE 1 - IMPACT TESTING

1.1.1 Objective

To provide data with which to validate a mathematical model developed by HW Structures Ltd.

1.1.2 Impact Pulse

The impact pulse measured on the vehicle was similar to the FAA 16G pulse specified in Aerospace Standard 8049.

Min G = 16
Min Vt (m/s) = 13.41 [44 ft/s]
Max tr (s) = 0.09

Vt = Impact velocity
tr = rise time

However, no floor deformation was introduced prior to the test. (The seat structure itself was not being tested and the purpose of providing floor deformation is to demonstrate that the seat/restraint system will remain attached to the airframe and perform properly, even though the aircraft and/or seat are severely deformed by the forces associated with a crash.)

The seat was aligned with 10 degrees of yaw to the right.

1.1.3 Test Fixture

Seat

A multiple row test fixture (two rows of three seats in each row) was used to best evaluate head and knee impact conditions. (Fig.58)

Undamaged or minimally damaged seat rows were taken from the Kegworth accident (G-OBME).

The seats were subjected to non destructive testing (including magnetic particle analysis) prior to the experiment.

The seats were Weber Aircraft Forward Facing Passenger Seats (Specification NAS 809 Type 1).

The seats were mounted onto the test vehicle. The joint at which the seats were attached to the floor rails was reinforced with a metal block (see Fig.6) to minimise the risk of the seats becoming detached during testing.

The seats were mounted facing forwards, i.e. in a -Gx orientation. In addition the seats were yawed 10° to the right.

Panelling was removed from the arm rest of the outside seats to facilitate use of the high speed video.

The seats were mounted at a 32" seat pitch, which represented the seat pitch most widely used in G-OBME.

A suitable floor was constructed and this was carpeted.

Fig. 58 Test Fixture with 10° yaw to the right

Dummy

A 50% Hybrid III anthropomorphic dummy was used as the experimental model.

The dummy was clothed in form fitting cotton stretch garments with mid-thigh length pants and size 11 E shoes weighing 11.6N (2.6 lbs).

The shoes had a smooth leather sole and the coefficient of friction of the shoe on the carpeted floor was determined prior to the experiment. (Fig.7)

1.1.4 Instrumentation

The instrumentation used was similar to that used in Experiments 1 and 2 with the exception of Channels 1, 2, 6, 7, 17, 20 (Table 38). Pelvic acceleration was measured in the Gx, Gy and Gz planes in order to allow closer correlation to the mathematical model.

Table 38 - Instrumentation

CH	LOCATION	MODEL	SER NO	EXC V	GAIN	FSD SI	UNIT	SENS mV/V
1	Upr R Tibia Mx	1583	411	10	500	395.5	Nm	2.96
2	Lwr R Tibia Fx	1584-A	411	10	500	11125	N	0.969
3	Upr R Tibia My	1583	423	10	500	395.5	Nm	2.96
4	Lwr R Tibia My	1584-A	411	10	500	395.5	Nm	2.902
5	Lwr R Tibia Fz	1584-A	411	10	500	11125	N	0.969
6	Upr L Tibia Mx	1583	415	10	500	395.5	Nm	2.889
7	Lwr L Tibia Fx	1584-A	410	10	500	11125	N	0.97
8	Upr L Tibia My	1583	415	10	500	395.5	Nm	2.889
9	Lwr L Tibia My	1584-A	410	10	500	395.5	Nm	2.958
10	Lwr L Tibia Fz	1584-A	410	10	500	11125	N	0.97
11	R Femur Fx	1914A	220	10	500	13350	N	1.906
12	R Femur My	1914A	220	10	500	339	Nm	1.502
13	R Femur Fz	1914A	220	10	500	22250	N	1.174
14	L Femur Fx	1914A	219	10	500	13350	N	1.917
15	L Femur My	1914A	219	10	500	339	Nm	1.501
16	L Femur Fz	1914A	219	10	500	22250	N	1.185
17	Pelvic Gx	7267A	BJ32	10	500	1500	G	-
18	R Femur Mx	1914A	220	10	500	339	Nm	1.499
19	R Femur Mz	1914A	220	10	500	339	Nm	2.653
20	Pelvic Gy	7267A	BJ32	10	500	1500	G	-
21	L Femur Mx	1914A	219	10	500	339	Nm	1.516
22	L Femur Mz	1914A	219	10	500	339	Nm	2.674
23	Lumbar Fx	1842	99	10	500	13350	N	0.934
24	Lumbar My	1842	99	10	500	565	Nm	1.719
25	Lumbar Fz	1842	99	10	500	13350	N	0.945
26	Vehicle Acc	PR9367	L0701	4	1200	50	G	0.514
27	Head Gx	7267A	BB61	10	500	1500	G	19.17
29	Head Gz	7267A	BB61	10	500	1500	G	20.655
30	Pelvic Gz	7267A	BJ32	10	500	1500	G	-
31	L Lap belt	300796	-	-	-	-	N	4Pc/N
32	Head Gy	7267A	BB61	10	500	1500	G	22.065

The transducers were allocated channels in the following manner.

RECORDING CHANNELS

Channel	Transducer	Excitation	Gain	Recording
1	R TIBIA U/Mx	10v	500	DL
2	R TIBIA L/Fx	10v	500	DL
3	R TIBIA U/My	10v	500	DL
4	R TIBIA L/My	10v	500	DL
5	R TIBIA L/Fz	10v	500	DL
6	L TIBIA U/Mx	10v	500	DL
7	L TIBIA L/Fx	10v	500	DL
8	L TIBIA U/My	10v	500	DL
9	L TIBIA L/My	10v	500	DL
10	L TIBIA L/Fz	10v	500	DL
11	R FEMUR Fx	10v	500	DL
12	R FEMUR My	10v	500	DL
13	R FEMUR Fz	10v	500	DL
14	L FEMUR Fx	10v	500	DL
15	L FEMUR My	10v	500	DL
16	L FEMUR Fz	10v	500	DL
17	Pelvic Gx	10v	500	DL
18	R FEMUR Mx	10v	500	DL
19	R FEMUR Mz	10v	500	DL
20	Pelvic Gy	10v	500	DASH16
21	L FEMUR Mx	10v	500	DASH16
22	L FEMUR Mz	10v	500	DASH16
23	LUMBAR Fx	10v	500	DASH16
24	LUMBAR My	10v	500	DASH16
25	LUMBAR Fz	10v	500	DASH16
26	VEHICLE G	4V	1200	DASH16
27	HEAD Gx	10V	500	DASH16
28	TRIAXIAL HEAD			
29	HEAD Gz	10V	500	PORTAX
31	L LAPBELT	Piezo		PORTAX
32	HEAD Gy	10v	500	PORTAX

All impacts were recorded on a NAC200 high speed video camera system operating at 200 frames per second.

1.1.5 Test Procedure

The 50th percentile instrumented Hybrid III dummy was located in the second row (from the front) in the centre of the three seat positions.

The dummy was placed in the seat in a uniform manner, with the back and buttocks against the seat back.

The friction of the limb joints was set so that the weight of the limb was barely restrained when extended horizontally.

The knees were separated by approximately 100mm (4").

The seat was placed in an upright position.

The dummy was placed in a braced position with the dummy leaned forwards so that the head rested on the back of the seat ahead. The feet were placed flat on the floor with the lower legs inclined rearwards at an angle of 11.5 degrees.

A second dummy - a 50th percentile (OGLE) dummy was placed in the forward seat row ahead of the Hybrid III dummy in a braced position.

The lapbelt tension was set using a spring balance to a tension of 70N (15 lbs) which represents a firm but not uncomfortable tightness.

Before each test the vehicle was winched into position and the triggering device was armed.

The vehicle was released and the impact recorded.

After each test, all equipment was assessed for damage.

1.1.6 Analysis of Results

The raw data was entered into a computer. The data was manipulated using software developed by the Institute of Aviation Medicine, Farnborough, based upon the Assyst programme.

It was at this level that the calibration data for the load cells and accelerometers were added to allow the information to be expressed in the correct units.

Zero-ing of Recordings:
A zero level for each set of data was obtained by sampling the data between the trigger point and the point of impact.

When the data recording equipment is triggered the vehicle is in its coast phase. The impact point is 1 metre from the trigger point. Therefore at a velocity of 12.7 m/s this represents 78ms.

With a sampling rate of 5000 samples per second this represents
400 counts between data recording trigger point and subsequent impact.

Therefore counts 10-110 were taken and the average obtained. This value was then taken as the zero point.

This technique minimised the effects of the small movements which occur in dummy position during the acceleration phase of the impact test run - a recognised limitation in deceleration sled facilities.

1.1.7 Results

The results of the impact tests performed are included in Table 40.

1.1.8 Conclusions

It was decided to correlate the mathematical model to run no. PB3673. The vehicle G recorded on this run was 17.2G and the vehicle velocity 12.42 m/s.

The vehicle G recorded is above the minimum G level described in Aerospace Standard 8049, however the vehicle velocity is slightly less at 12.42 m/s (Aerospace Standard AS8089 = 13.41 m/s).

Due to limitations in the track design, it was not possible to increase the vehicle velocity to the required level without producing a much larger increase in vehicle acceleration (see Table 39, Run 3670).

Therefore it was decided to accept a slightly reduced velocity.

Values from a single run were selected rather than mean values from several repeated test impacts as:

1. The impact pulse was closest to the 16G pulse described in Aerospace Standard 8049.

2. Time and financial pressures did not allow for either repetitive runs to be made in this area of the study nor for new seats to be used in the testing.

PASSENGER BRACE POSITION STUDY											
								CHANNEL 1		CHANNEL 2	
RUN No.	CAL. FILE	BRACE POSITION	LEG POSITON	SEAT PITCH	VELOCITY (m/s)	FLAIL	COMMENTS	Rt TIB U/Mx (Nm)	T (ms)	RtTIB L/Fx (N)	T (ms)
3670	3669	B	LB	32	13.25	NO	LEFT LEG SLIDE	-38	107	-295	117
3671	3669	B	LB	32	12.42	NO	"	-34	107	-241	117
3672	3669	B	LB	32	12.5	NO	"	53	148	-266	117
3673	3669	B	LB	32	12.42	NO	"	-40	112	-251	123

TABLE 39

	CHANNEL 3		CHANNEL 4		CHANNEL 5		CHANNEL 6		CHANNEL 7		CHANNEL 8	
RUN No.	Rt TIB U/My (Nm)	T (ms)	Rt TIB L/My (Nm)	T (ms)	Rt TIB L/Fz (N)	T (ms)	Lt TIB U/Mx (Nm)	T (ms)	Lt TIB L/Fx (N)	T (ms)	Lt TIB U/My (Nm)	T (ms)
3670	42	112	-15	133	-1536	123	26	112	-114	97	25	97
3671	37	112	-16	133	-1427	128	29	107	-132	107	18	92
3672	39	123	-12	138	-1544	123	24	112	258	225	-22	225
3673	35	123	-15	133	-1473	128	26	107	306	225	-32	225

TABLE 39

	CHANNEL 9		CHANNEL10		CHANNEL 11		CHANNEL12		CHANNEL 13		CHANNEL 14	
RUN No.	Lt TIB L/My (Nm)	T (ms)	LT TIB L/ Fz (N)	T (ms)	Rt FEMUR Fx (N)	T (ms)	Rt FEMUR My (Nm)	T (ms)	Rt FEMUR Fz (N)	T (ms)	Lt FEMUR Fx (N)	T (ms)
3670	10	102	-478	123	-1442	112	-169	123	1248	102	-556	112
3671	11	107	-472	116	-1372	128	-164	128	935	97	-513	112
3672	-15	225	-357	117	-1457	128	-177	128	945	107	-502	112
3673	-17	225	-212	112	-1362	128	-163	128	929	102	-470	112

TABLE 39

Validation of the Mathematical Model

	CHANNEL 15		CHANNEL 16		CHANNEL 17		CHANNEL 18		CHANNEL19		CHANNEL 20	
RUN No.	Lt FEMUR My (Nm)	T (ms)	Lt FEMUR Fz (N)	T (ms)	PELVIC Gx (G)	T (ms)	Rt FEMUR Mx (Nm)	T (ms)	Rt FEMUR Mz (Nm)	T (ms)	PELVIC Gy (G)	T (ms)
3670	-75	123	673	92	-21.2	102	-39	112	-43	138	-12	107
3671	-69	112	888	97	-16	97	-33	112	40	153	-8	117
3672	-64	112	851	102	-16.6	102	-40	128	64	148	-8	117
3673	-60	112	870	102	-17.1	102	-37	112	44	148	-9	112

TABLE 39

	CHANNEL 21		CHANNEL 22		CHANNEL 23		CHANNEL 24		CHANNEL 25		CHANNEL 26	
RUN No.	Lt FEMUR Mx (Nm)	T (ms)	Lt FEMUR Mz (Nm)	T (ms)	LUMBAR Fx (N)	T (ms)	LUMBAR My (Nm)	T (ms)	LUMBAR Fz (N)	T (ms)	VEHICLE G (G)	T (ms)
3670	75	123	66	117	9514	117	498	133	4945	123	19.9	67.1
3671	24	117	74	117	8599	117	430	138	4275	123	16.6	67.1
3672	27	123	59	123	9148	123	424	138	5240	128	17.2	72.2
3673	24	120	63	117	8813	123	401	138	4812	128	17.2	72.2

TABLE 39

	CHANNEL 27		CHANNEL 28	CHANNEL 29		CHANNEL 30		CHANNEL 31		CHANNEL 32	
RUN No.	HEAD Gx (G)	T (ms)	HIC	HEAD Gz (G)	T (ms)	PELVIC Gz (G)	T (ms)	Lt LAPBELT (N)	T (ms)	HEAD Gy (G)	T (ms)
3670	-77	168		-47	123	-13	138	-8800	112	-43	163
3671	-43	164		-37	123	-14	139	-8582	123	-25	117
3672	-55	158		-39	123	-12	143	-9388	128	-23	158
3673	-84	163		-38	123	-12	143	-8500	123	-45	168

1.2 STAGE 2 - CORRELATION OF THE MATHEMATICAL MODEL TO THE IMPACT TEST

1.2.1 Objective

To correlate the mathematical model developed by H W Structures with impact test PB3673.

1.2.2 The Mathematical Model

The baseline model was developed by H W Structures and was based upon MADYMO 3D version 4.3. MADYMO is a worldwide accepted engineering analysis programme developed by the TNO Crash Safety Research Centre for the simulation of systems undergoing large displacement. The programme has been designed especially for the study of the complex dynamic response of the human body and its environment under extreme loading conditions as occurs in crash situation.

MADYMO combines in one simulation programme the capabilities offered by the multibody approach (for the simulation of the gross motionless systems of a body connected by complicated kinematical joints) and the finite element method (for the simulation of structural behaviour).

1.2.3 Impact Pulse

The impact pulse used was based upon impact test run no. PB3673.

Velocity - 12.42 m/s
Vehicle G - 17.2G

It should be noted that the impact pulse differs from that stipulated in the FAA regulations regarding the dynamic performance testing of seats. Whilst the peak G is achieved, the impact velocity is reduced.

1.2.4 Test Fixture

Seat

The seat profile, mass and inertial properties were based upon data relating to the Weber seats used in the Boeing 737-400 G-OBME which crashed at Kegworth. These data had been acquired for a separate correlation study (33).

In addition, seat stiffness and lap belt restraint stiffness were determined using a new Weber 4000 triple row seat using a TriFilar method.

The seat profile was measured using a Stiefelmeyer electronic profile measuring machine (serial no. 30380187).

Seat back and seat cushion stiffness were determined using a ballasted dummy digital force gauge (manufactured by Salter, model EFG 500, serial no. 5806) and a dial test indicator (manufactured by Mercer, model 252). The values used or given in Reference 51.

The lap belt restraint stiffness was determined using a digital force gauge (manufactured by Salter, model EFG 500, serial no. 5806) strain gauge. The results were that the belts stiffened to 17% strain at 10kN.

Dummy

The dummy model was based upon a 50th percentile Hybrid III dummy data set.

1.2.5 Test Procedure

The model was correlated against impact test PB3673. The baseline model had a 0.54 friction coefficient between foot and floor, a 32" seat pitch and the occupant was in a braced position with a lower leg angle of 11.5° rearwards of the vertical. The angle of the seat belt to the horizontal was 65°. The distance from the front of the knee to the seat ahead was 187 mm.

1.2.6 Results

The peak injury values of the IAM sled test and the final baseline model are shown in the table below:

Table 40 Mathematical Model Compared to Impact Test

PARAMETER	RECORDED VALUES	
	Test - PB3673	Mathematical Model
HIC	258	295
Head Resultant Acceleration (Ar)	850 m/s²	674 m/s²
Pelvis Acceleration		
Resultant (Ar)	-	249 m/s²
Ax	-168 m/s²	-235 m/s²
Ay	-87 m/s²	-81 m/s²
Az	-118 m/s²	-101 m/s²
Lap Belt Load	8500N	7360N
Left Femur		
Fx	470N(shear)	1362N(shear)
Fz	870N(tensile)	1629N(tensile)
My	60Nm	180Nm
Right Femur		
Fx	1360N(shear)	1419N(shear)
Fz	929N(tensile)	1591N(tensile)
My	163Nm	178Nm
Left Lower Tibia		
Fx	306N(shear)	246N(shear)
Fy	-	135N
Fz	209N(compressive)	1633N(compressive)
Right Lower Tibia		
Fx	251N(shear)	276N(shear)
Fy	-	198N
Fz	1470N(compressive)	1608N(compressive)
Lumbar Fz	4800N(tensile)	4895N(tensile)

A comparison of the two impact pulses is given below.

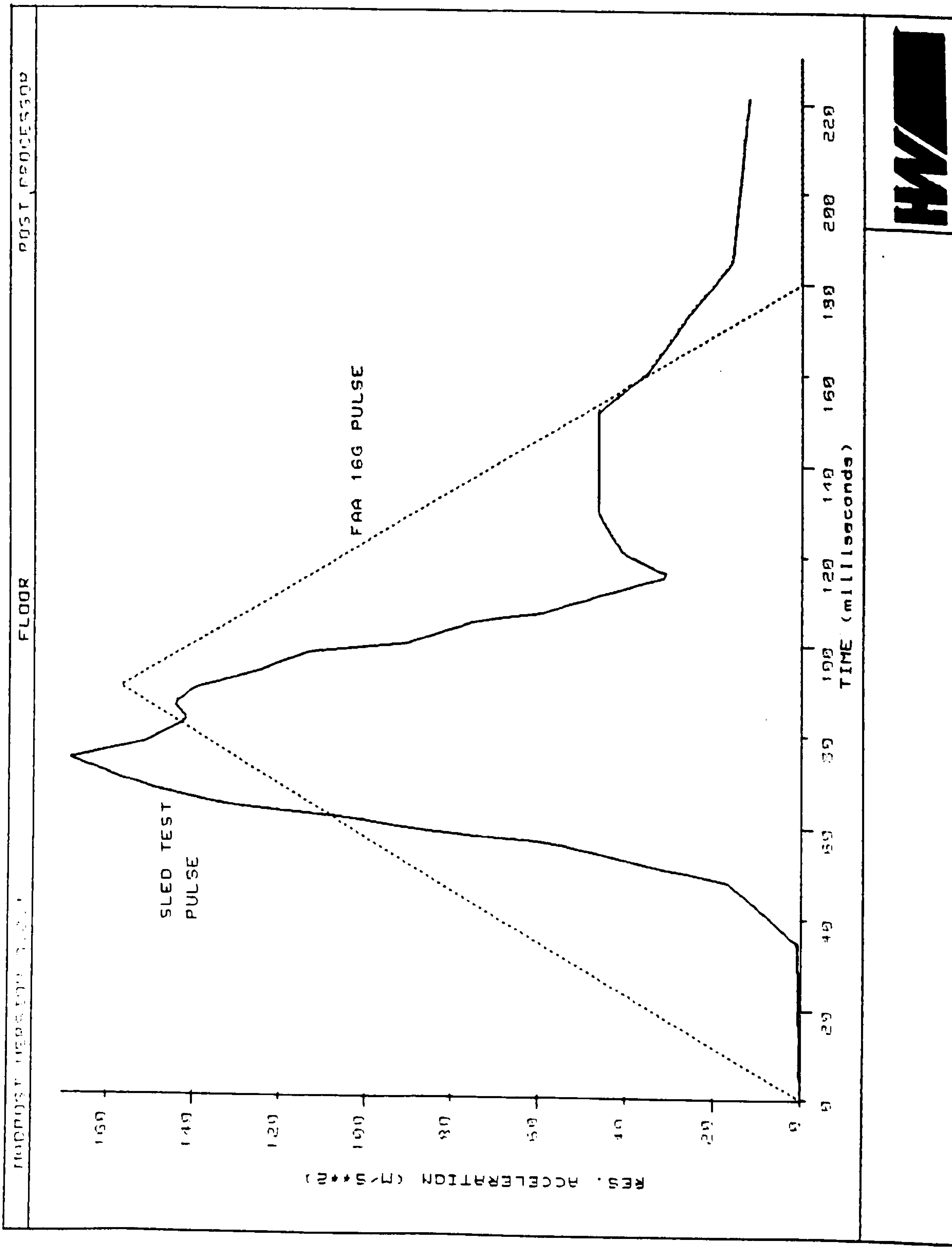

Fig. 59 Comparison of sled test pulse and FAA 16G pulse

1.2.7 Discussion

Table 40 compares the peak injury values established from the IAM sled test and the final baseline computer model. There are notable differences between test and analysis in the femurs and left tibia values. These differences are due to non-uniformity between the impact sled test and the computer model. Whilst efforts were made to minimise such differences, discrepancies did exist. The discrepancies are explained below:

1. Seats:

   In the impact test, a multiple row test fixture was used using seats from the Boeing 737-400 G-OBME. The front seat row was from the first row of the aircraft whereas the second row was from the rear of the aircraft. Therefore the configuration did not replicate exactly an actual twin row configuration as defined in the mathematical model. The effect was that the seat in front was offset to the right. In the mathematical model the seats which were based on an actual twin row configuration as used in G-OBME comparable with seat rows 15 and 16 on the right side of the wing box section.

2. Lap Belt:

   The manufacturers data specified that the lap belt would elongate by 20% at 2,200 lbs. Subsequent investigation revealed that the actual elongation was 17% at 2,200 lbs (within the manufacturers tolerance band). Furthermore, the same seat belt was used for two concurrent tests and the effect in the second test was to alter the elastic properties of the belt. It should be noted that a shortened length of belt was also used as the lap belt load cell was mounted in series. The most accurate correlation was with a strain of 11%.

3. Seat Cushion Stiffness:

   The cushions used in the impact test had been subjected to repeated impacts. Effectively instead of the dummy sitting on a "springy" cushion, the dummy was sitting on a more compressed surface. In the mathematical model the cushion stiffness was based on a new seat cushion.

4. Seat Back Stiffness:

   The breakover stiffness of the seat back in front has an effect on the timing of the head acceleration and the magnitude of the Head Injury Criterion. In the impact test situation seats were used for repetitive tests and consequently the breakover torque was affected and probably reduced.

5. Front Seat Luggage Bar:

   It became apparent through the simulation that the feet of the occupant can strike the luggage bar under the seat in front. This was particularly evident when flailing or sliding of the lower legs occurred. Under certain circumstances, foot entrapment under the luggage bar was also observed. On studying the video output from the sled test, it became clear that the luggage bar was not present in run PB3674 as it had been removed from the forward seat. The entrapment of the foot can cause severe knee hyperextension. Torques generated at the ankle and knee are sufficiently high to cause fracture of the foot, ankle or knee joint.

6. High Speed Film:

   No camera was available to monitor the left side of the sled during impact. Consequently it was difficult to observe the left femur during impact. In the computer simulation moderate sliding of the left femur occurred. This was attributable to the yaw position and the consequent 10° lateral deceleration.

1.2.8 Conclusion

In conclusion, this study has attempted to correlate a mathematical model to an individual impact test. Whilst some degree of correlation has been achieved, discrepancies do exist between the impact test and the mathematical model. Indeed only 6 of the 17 comparisons agreed within 10%.

The correlation might be improved by taking the mean values from 5 impact tests. For each test new seats and new lapbelt webbing should be used. Soft tissue damage to the pelvis should be repaired after each run.

Unfortunately, the necessary resources were not available to implement these changes for this study. In particular, new seats were not available for testing.

Despite the limitations in the level of correlation achieved, it was considered that a parametric study using the mathematical model would prove valuable.

2. MATHEMATICAL MODELLING - PARAMETRIC STUDY

2.1 OBJECTIVE

To assess the effect of various parameters on injury potential for the seated occupant in an impact aircraft accident.

2.2 METHOD

A mathematical model based upon MADYMO 3D (version 4.3) was correlated to an impact test performed at the RAF Institute of Aviation Medicine, Farnborough as previously described.

In the baseline model the foot to floor friction coefficient was 0.5, the seat pitch was 32" and the occupant was in a braced position with the lower legs positioned at an angle of 11.5° rearward of the vertical.

A parametric study was undertaken to compare the effects of the parameters listed below on occupant kinematics. Data output included assessment of the head acceleration, the axial lumbar spine load, the femoral axial and shear loads, the femoral bending and torsion moments, tibial axial and shear loads and tibial bending moments.

2.3 EXPERIMENTAL VARIABLES

1. Foot to floor friction
2. Seat pitch
3. Occupant lower leg angle
4. 16G FAA pulse

1. Foot to floor friction

In the baseline model the coefficient of friction between foot and floor was 0.5 which represented a shoe with a new smooth leather sole on a short pile carpet. The friction coefficient was increased in 0.05 increments to 0.7 which represented a shoe with a treaded rubber sole on a short pile carpet. The results obtained were compared.

2. Seat Pitch

In the baseline model the seat pitch was 32". In addition, seat pitches of 27", 30", 32", 34" and 36" were investigated. Upper torso angles changed to accommodate seat pitch. The results obtained were compared.

3. Occupant Lower Leg Angle

In the baseline model, the lower leg was positioned 11.5° rearward of the vertical. The position of the lower leg was varied between 11.5° rearward of the vertical and 8.5° forward of the vertical. The results obtained were compared.

4. FAA 16G Crash Pulse

The pulse used in the baseline and parametric study models was the actual acceleration time history recorded in impact test PB3673 carried out at the RAF Institute of Aviation Medicine. It is important to note that the required impact velocity and deceleration pulse as stipulated in the FAA guidelines for the dynamic performance testing of seats, was not achieved.

In the sled test an impact velocity of 12.4 m/s was attained but the 16G regulation required this to be at least 13.41 m/s. Although the minimum requirement of 16G peak deceleration within 0.09 second was achieved, the reduced impact velocity resulted in the sled test producing a less severe pulse in terms of the energy involved.

It was therefore decided to run the original baseline simulation with the two braced occupants both with the sled test acceleration time history and using the FAA 16G pulse in order to compare the results.

2.4 RESULTS

2.4.1 Floor Friction Coefficient

The occupant kinematics associated with increasing the coefficient of friction between foot and floor from 0.55 to 0.7 are illustrated in Figs. 60, 61, 62 and 63.

Table 41 records the effect of varying foot to floor friction on the loads measured in the occupant.

Table 41 The effect of floor friction coefficient.

PARAMETER	UNIT	FLOOR FRICTION COEFFICIENT				
		0.5 Baseline	0.55	0.6	0.65	0.7
HIC		295	294	292	295	306
Lap Belt Load	N	7360	7363	7368	7365	7373
Left Femur						
Fx	N	+1362	+1405	+1429	+1400	+1445
Fz	N	+1629	+1648	+1646	+1663	+1660
My	Nm	180	186	188	187	190
Right Femur						
Fx	N	+1419	+1437	+1452	+1447	+1473
Fz	N	+1591	+1604	+1602	+1613	+1612
My	Nm	178	181	180	182	182
Left Lower Tibia						
Fx	N	246	340	437	449	489
Fy	N	135	64	68	130	289
Fz	N	+1633	+1710	+1775	+1696	+1849
Right Lower Tibia						
Fx	N	276	362	444	438	475
Fy	N	198	166	131	215	239
Fz	N	+1608	+1635	+1665	+1546	+1861
Lumbar Fz	N	+4895	+4898	+4897	+4896	+4904

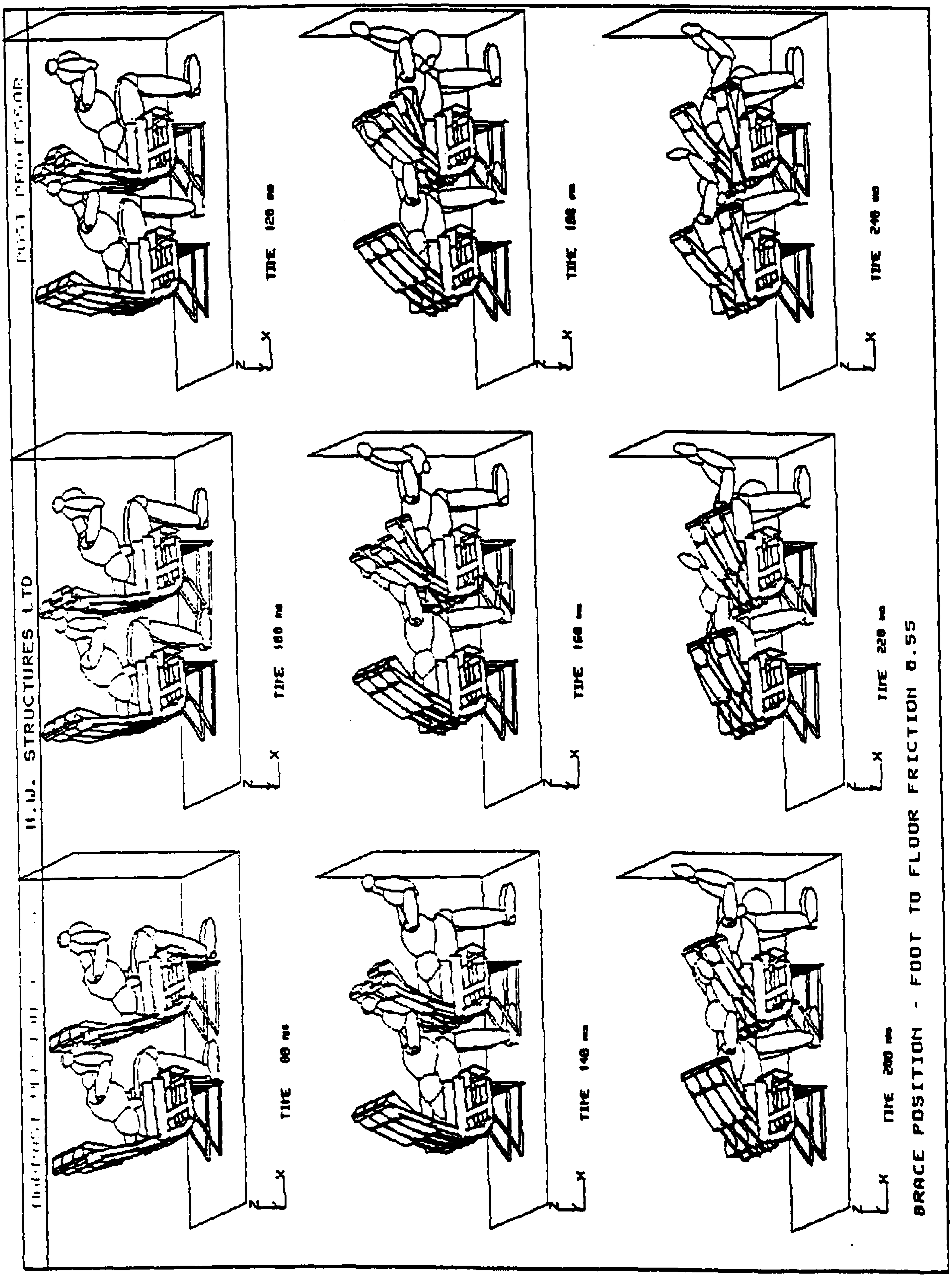

Fig. 60 Occupant Kinematics - Coefficient of Foot to Floor Friction 0.55

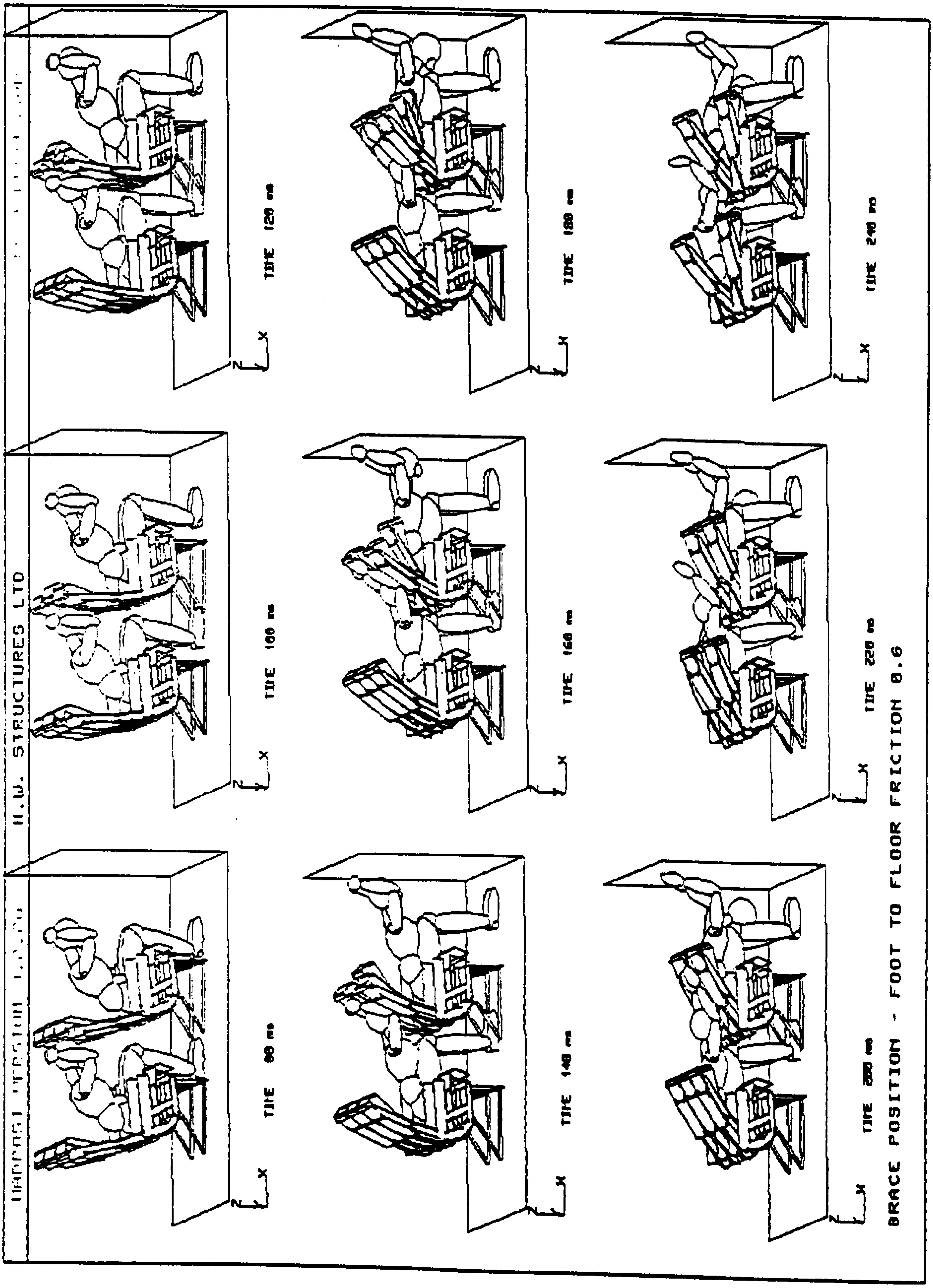

Fig. 61 Occupant Kinematics - Coefficient of Foot to Floor Friction 0.6

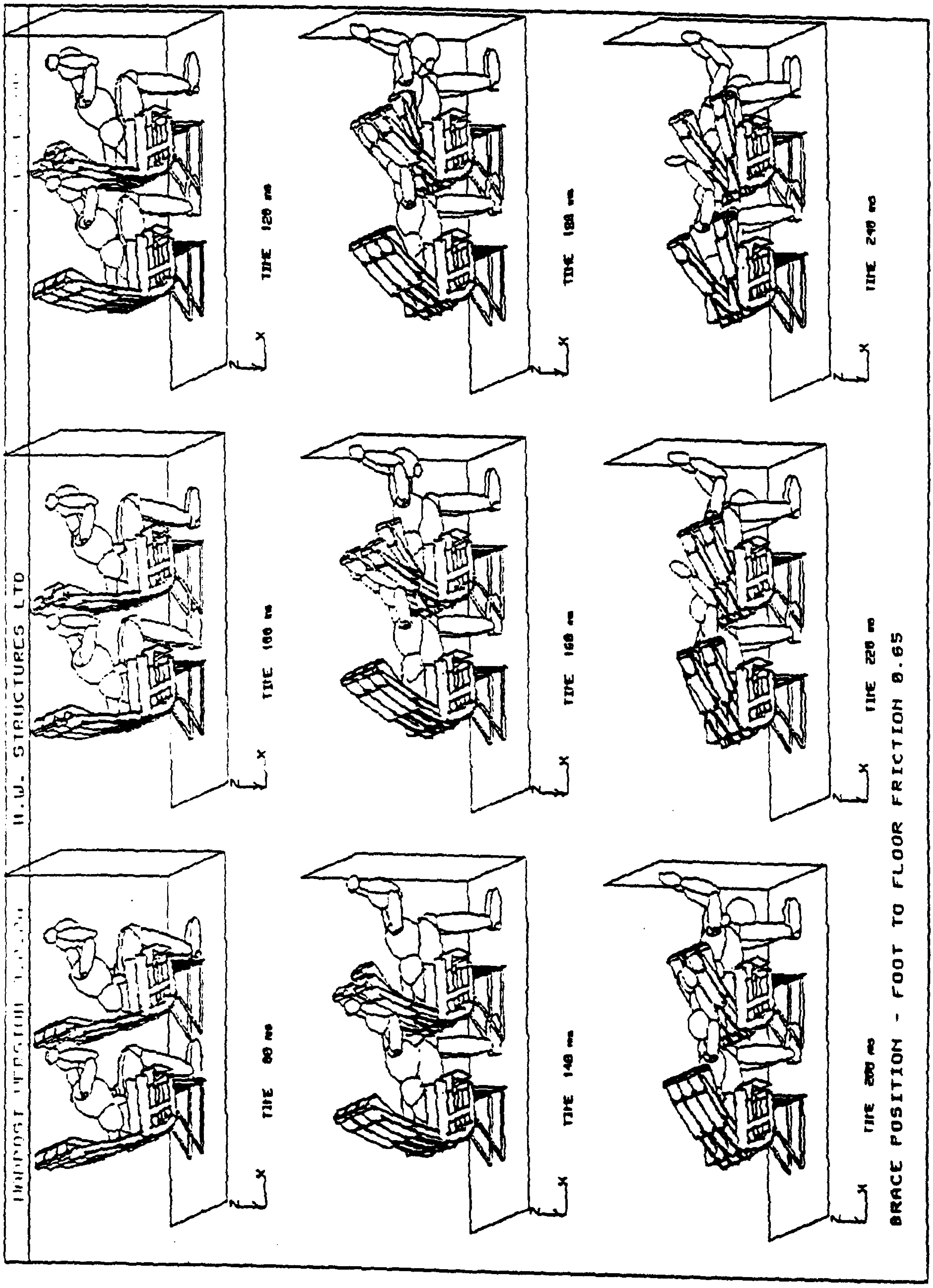

Fig. 62 Occupant Kinematics - Coefficient of Foot to Floor Friction 0.65

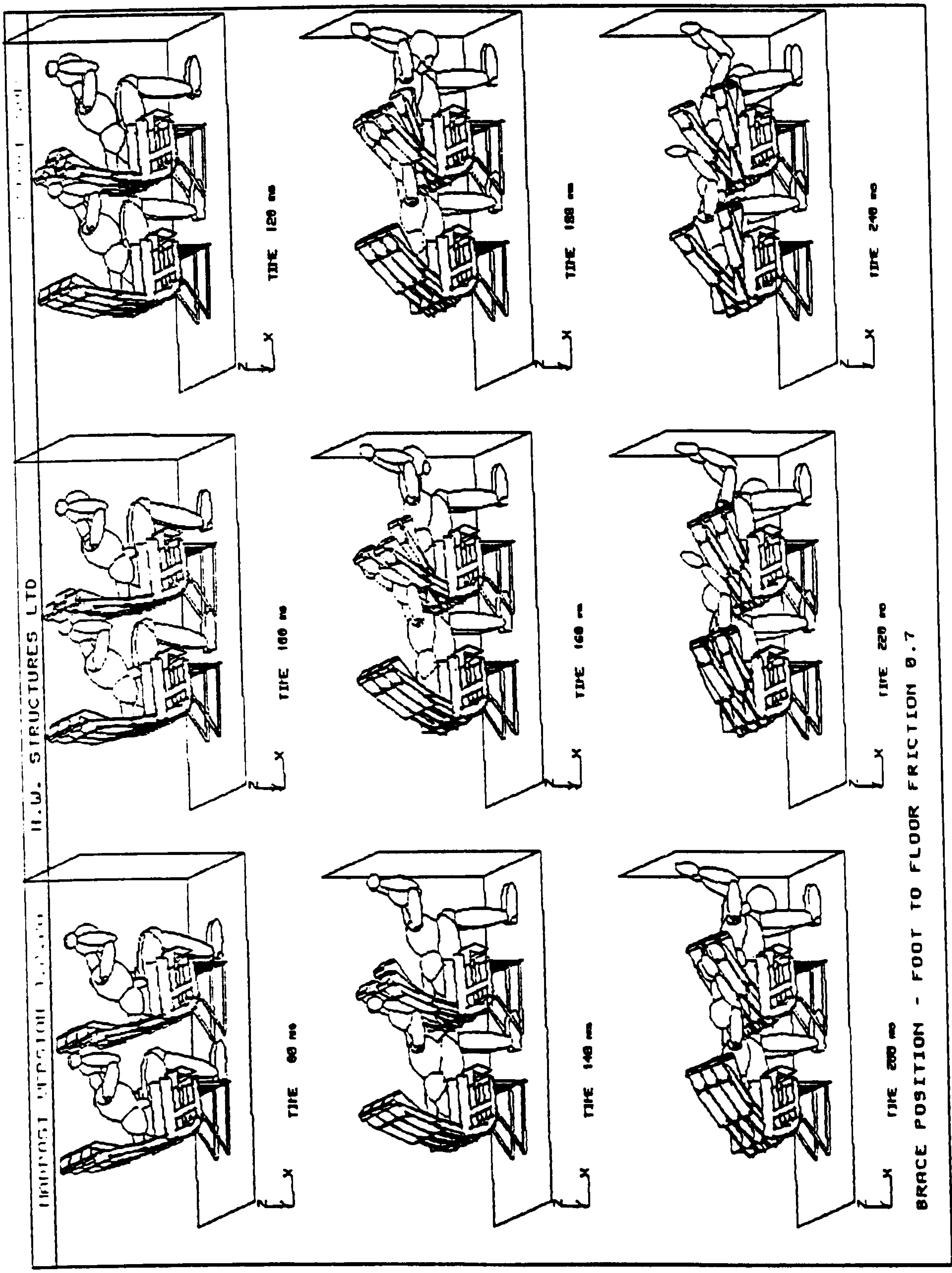

Fig. 63 Occupant Kinematics - Coefficient of Foot to Floor Friction 0.7

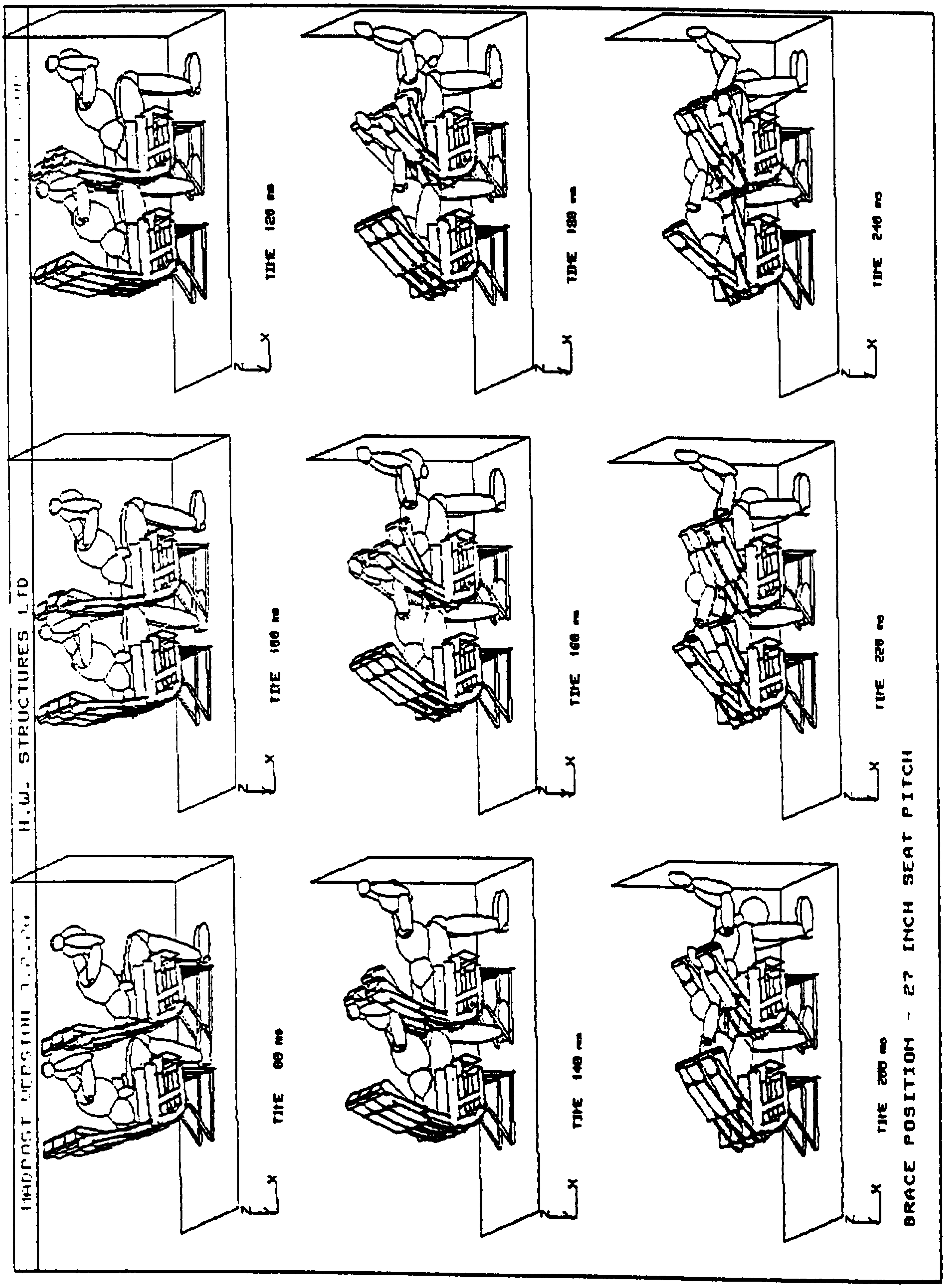

Fig. 64 Occupant Kinematics - 27 inch seat pitch

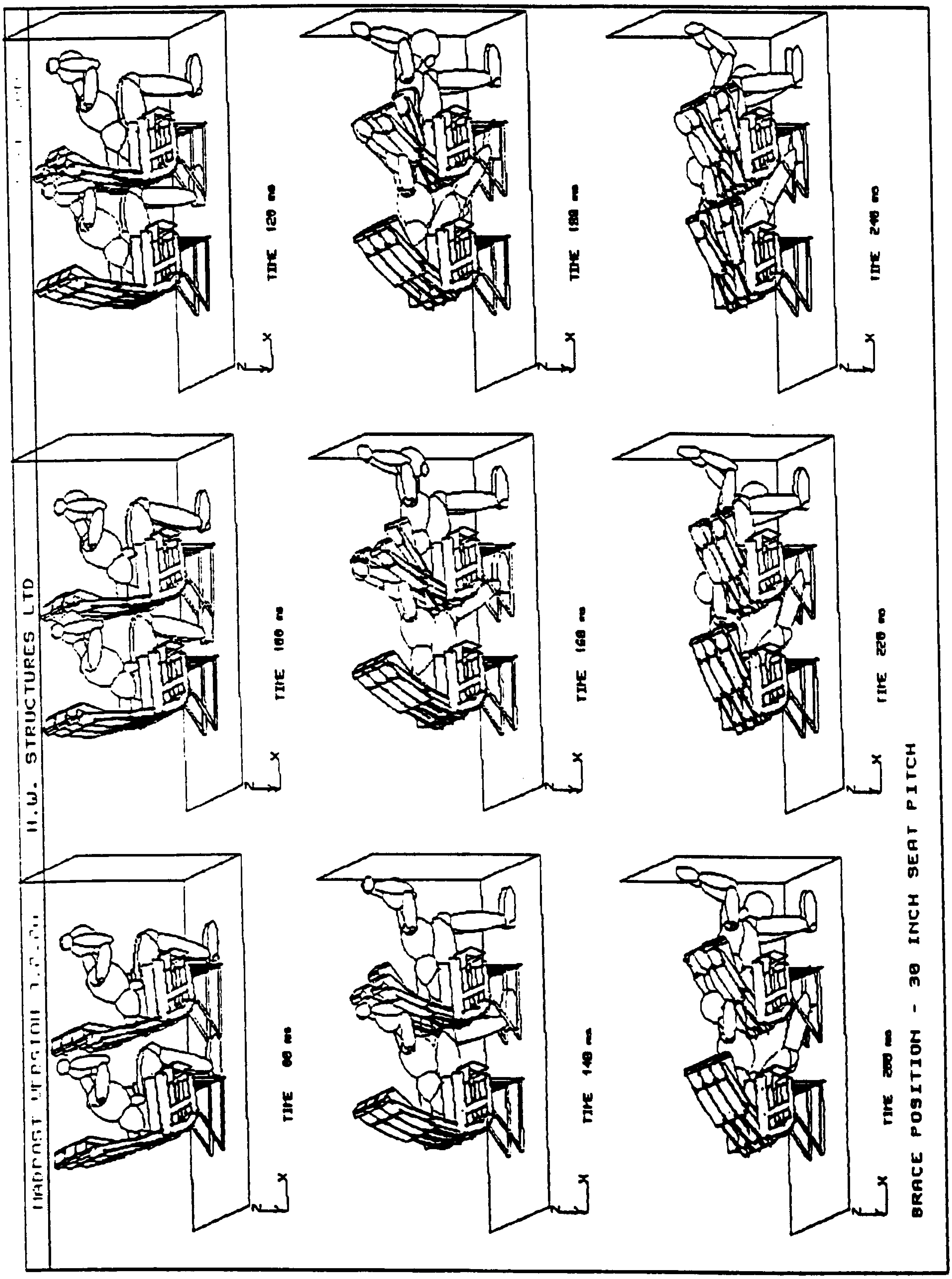

Fig. 65 Occupant Kinematics - 30 inch seat pitch

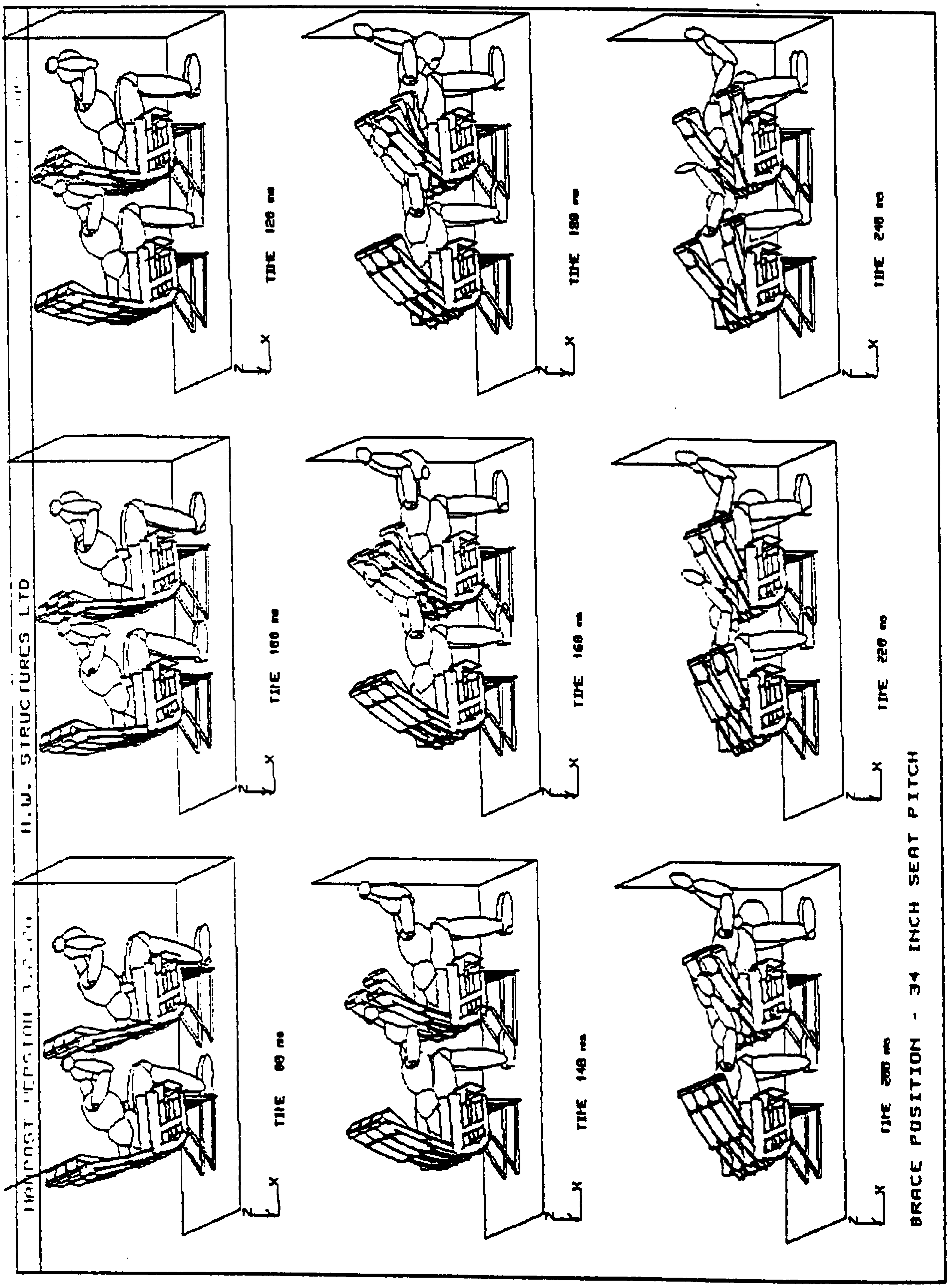

Fig. 66 Occupant Kinematics - 34 inch seat pitch

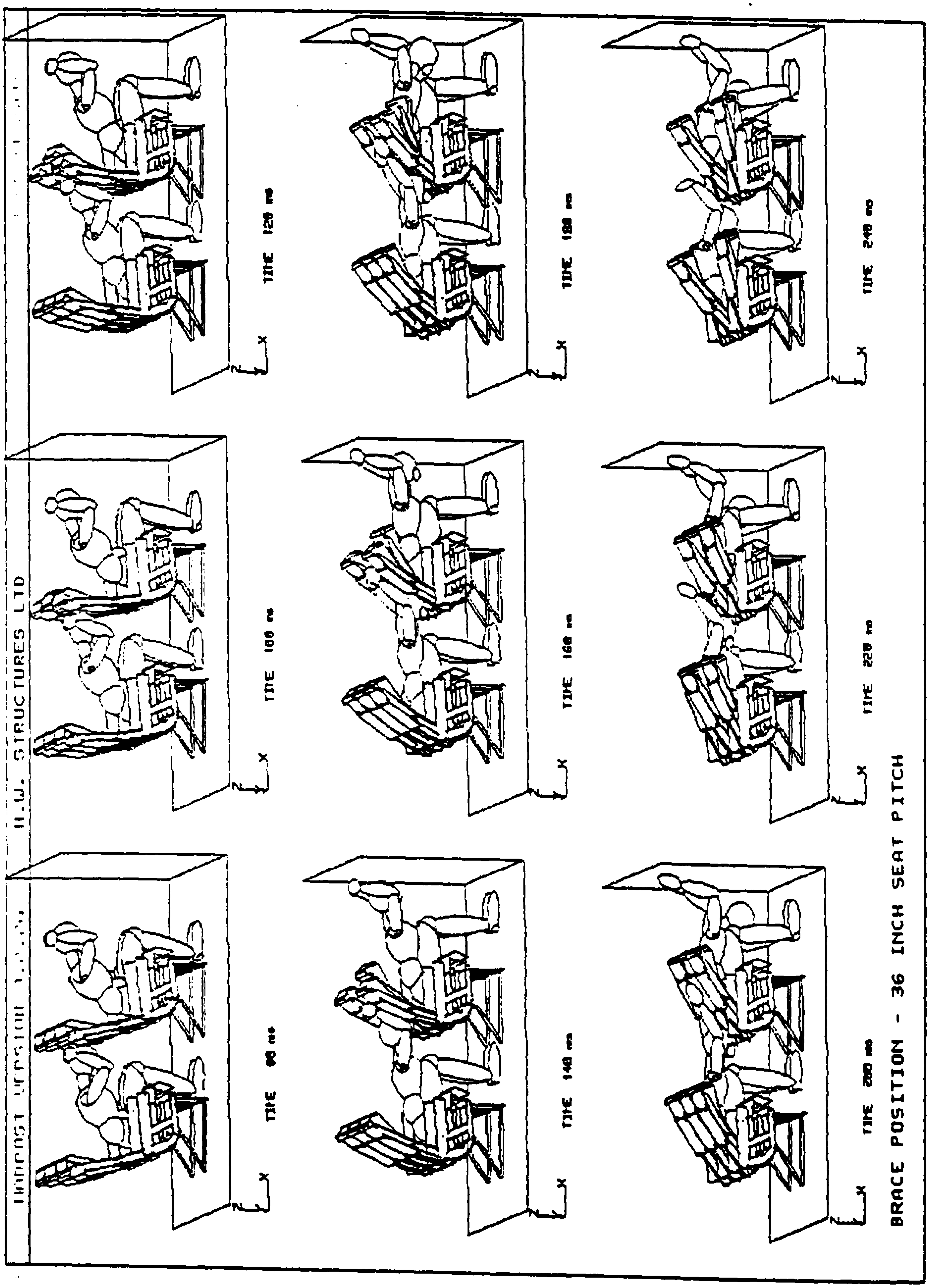

Fig. 67 Occupant Kinematics - 36 inch seat pitch

2.4.2 Seat Pitch

The occupant kinematics for different seat pitches are given in Figs. 64, 65, 66 and 67.

Table 42 records the effect of varying seat pitch on the loads measured in the occupant.

Table 42 The variation in loads measured in the occupant at different seat pitches.

PARAMETER	UNIT	SEAT PITCH				
		27"	30"	32" Baseline	34"	36"
HIC		384	433	295	586	520
Lap Belt Load	N	6660	7567	7360	7096	6873
Left Femur						
Fx	N	+1310	+1049	+1362	+1440	+1416
Fz	N	-2025	+2015	+1629	+1530	+1488
My	Nm	188	484	180	187	182
Right Femur						
Fx	N	+1072	+1047	+1419	+1498	+1430
Fz	N	-1844	+1694	+1591	+1476	+1421
My	Nm	174	457	178	186	175
Left Lower Tibia						
Fx	N	-564	-3258	246	375	420
Fy	N	283	-237	135	107	160
Fz	N	+1826	+1484	+1633	+1670	+1605
Right Lower Tibia						
Fx	N	-528	-1645	276	386	425
Fy	N	246	-98	198	170	178
Fz	N	+1749	+1464	+1608	+1679	+1547
Lumbar Fz	N	+5154	+4550	+4895	+5090	+5068

2.4.3 Lower Limb Position

The occupant kinematics for different lower limb positions are shown in Figs. 68, 69, 70 and 71.

Table 43 records the effect of varying lower leg positions on the loads measured in the occupant.

Table 43 The variation in loads measured in the occupant for different lower leg positions.

PARAMETER	UNIT	TIBIA ANGLE FROM VERTICAL				
		-11.5° Baseline	-6.5°	-1.5°	3.5°	8.5°
HIC		295	375	561	598	601
Lap Belt Load	N	7360	7338	7289	7258	7251
Left Femur						
Fx	N	+1362	-1084	-1518	-1705	-1533
Fz	N	+1629	+1602	+1720	+1842	+1593
My	Nm	180	143	-149	-130	-94
Right Femur						
Fx	N	+1419	-2626	-1615	-2399	-3007
Fz	N	+1591	+1560	+1627	+1807	+1802
My	Nm	178	220	292	221	150
Left Lower Tibia						
Fx	N	246	-811	-1425	-1202	-1293
Fy	N	135	-143	-151	-192	-199
Fz	N	+1633	+1186	+1607	+1816	+2441
Right Lower Tibia						
Fx	N	276	477	-3323	-2677	-2243
Fy	N	198	-530	-186	-313	-580
Fz	N	+1608	+1857	+3240	+2614	+1688
Lumbar Fz	N	+4895	+4838	+4719	+4796	+4944

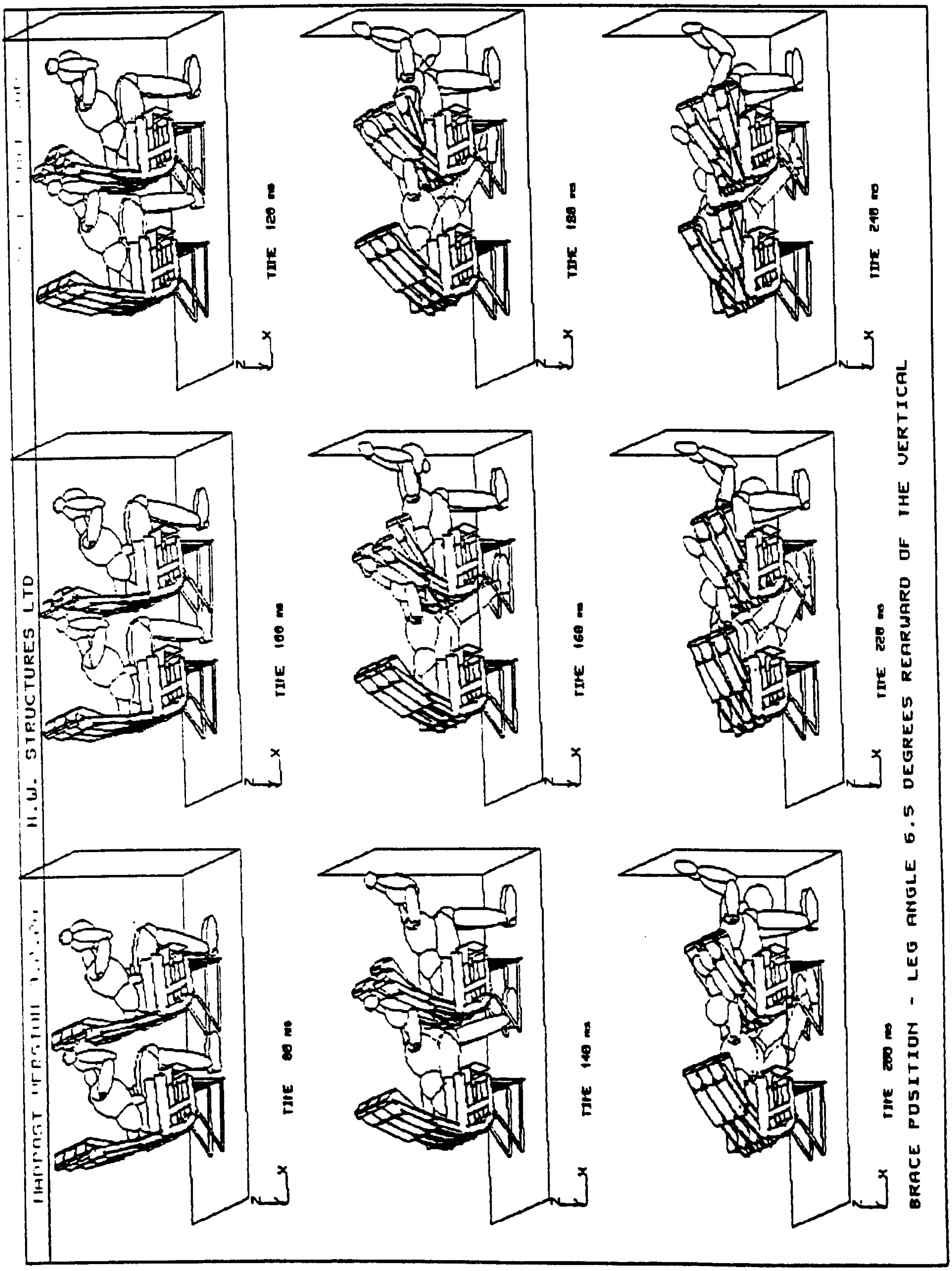

Fig. 68 Occupant Kinematics - Leg angle 6.5 degrees rearward of the vertical

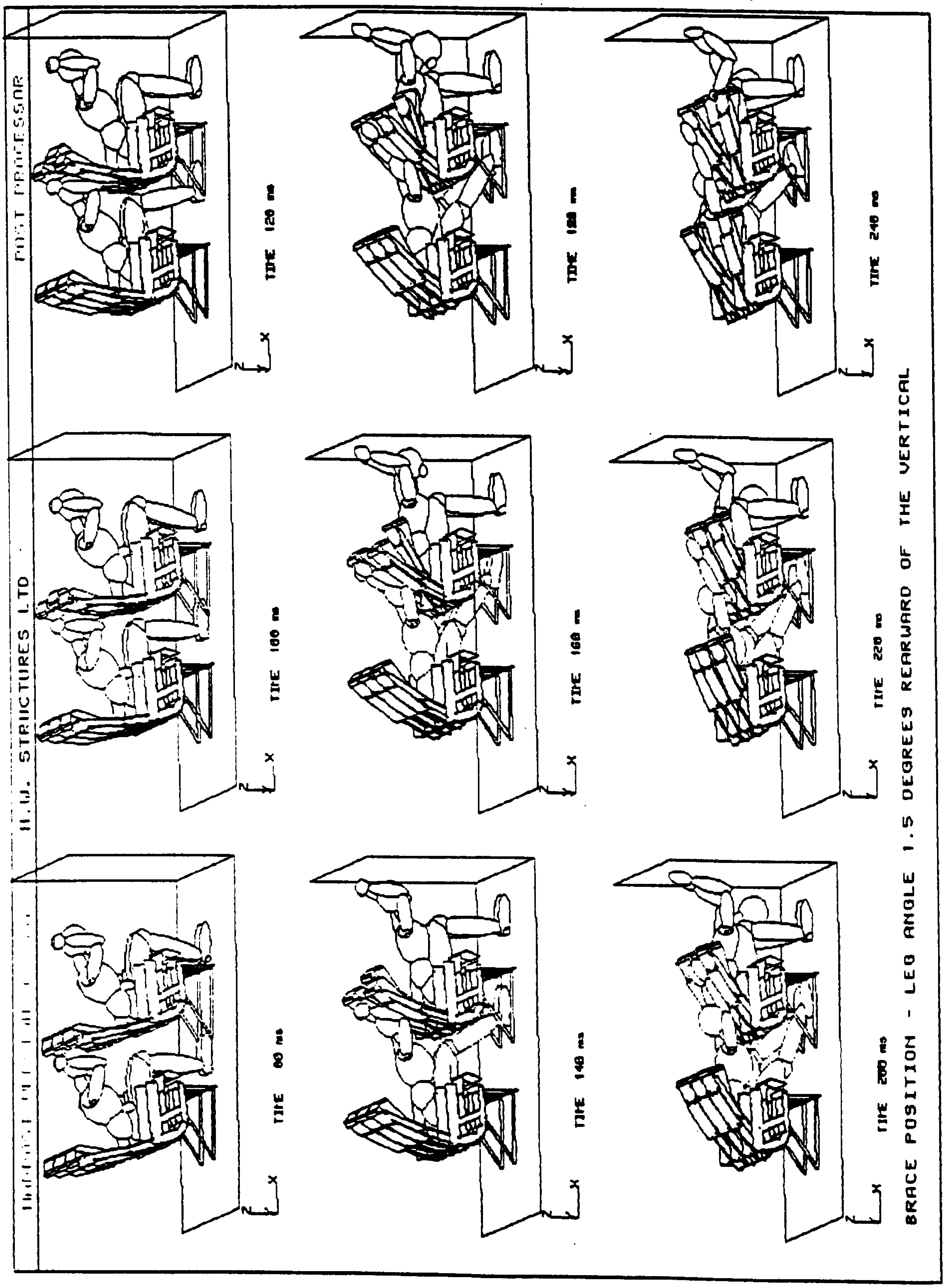

Fig. 69 Occupant Kinematics - Leg angle 1.5 degrees rearward of the vertical

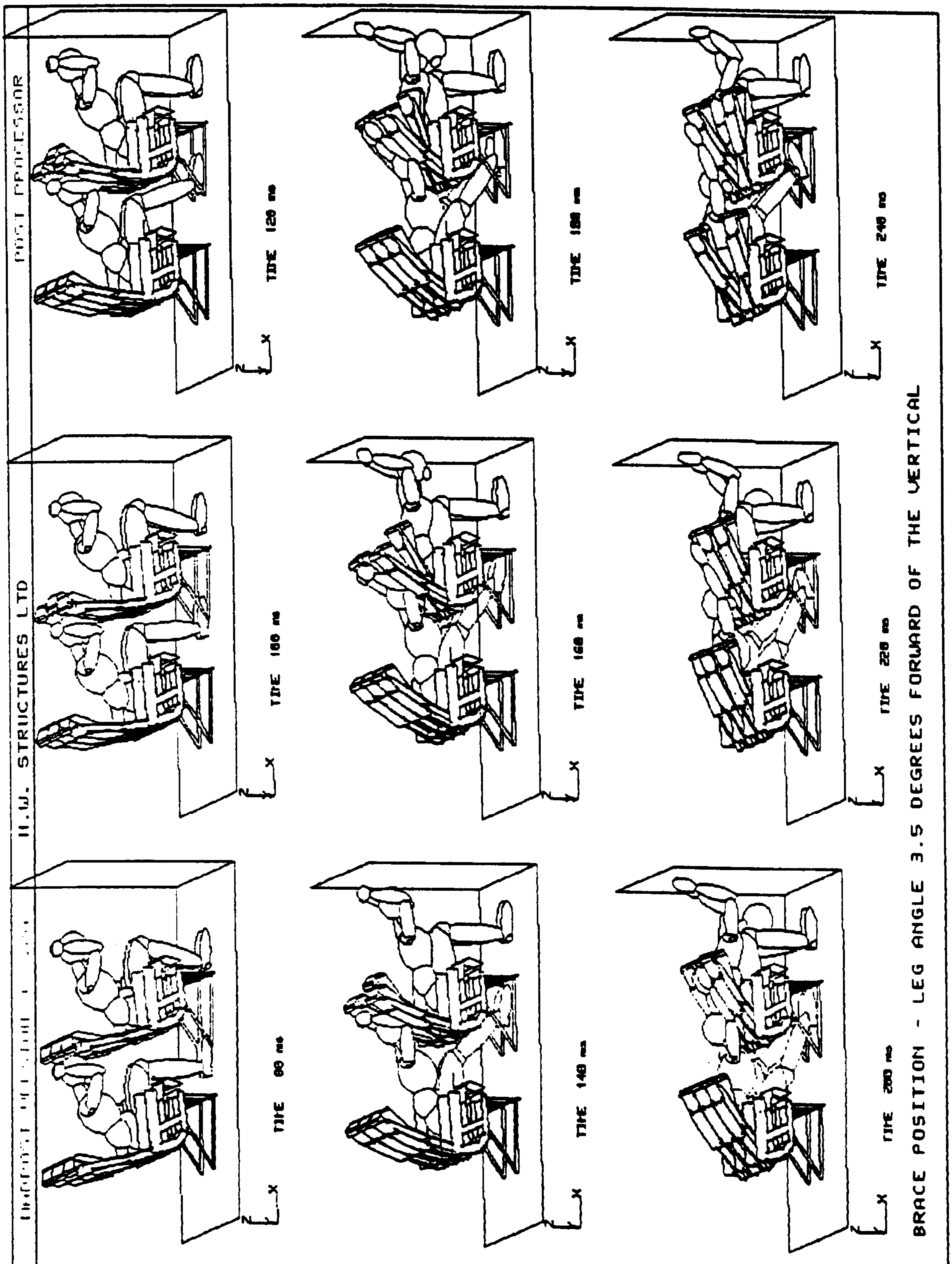

Fig. 70 Occupant Kinematics - Leg angle 3.5 degrees forward of the vertical

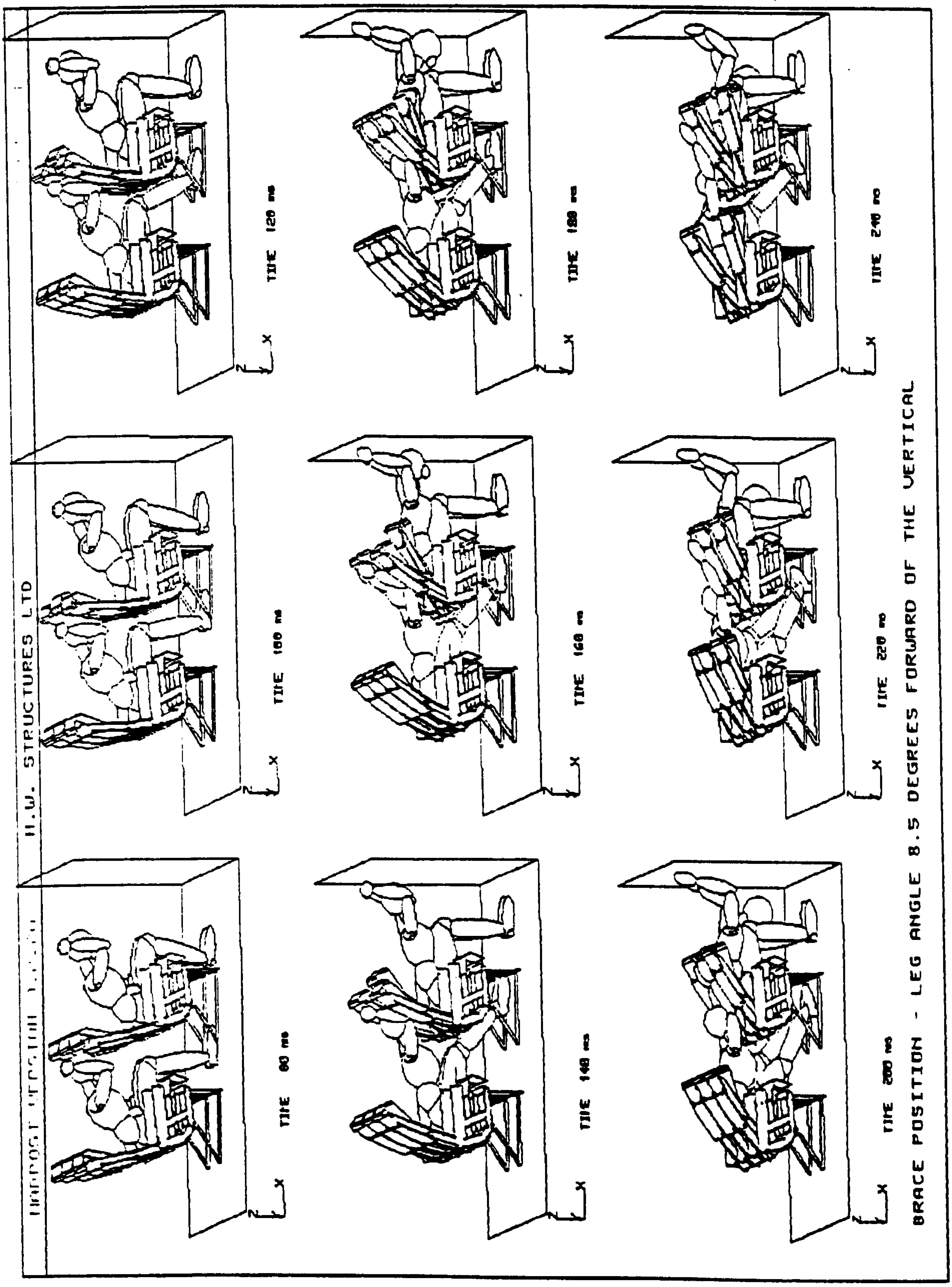

Fig. 71 Occupant Kinematics - Leg angle 8.5 degrees forward of the vertical

2.4.4 16G Pulse

Table 44 records the loads measured in the occupant during the baseline configuration (similarly impact test PB3674) and at the exact FAA 16G pulse (velocity 13.41 m/s).

Table 44 Comparison of loads measured in the occupant in baseline test and in FAA 16G pulse.

PARAMETER	UNIT	CONFIGURATION	
		Baseline (Simulation of Test PB3673)	16G Crash Pulse
HIC		295	871
Lap Belt Load	N	7360	7869
Left Femur			
Fx	N	-1362	-1639
Fz	N	-1629	-1508
My	Nm	180	229
Right Femur			
Fx	N	-1419	-1894
Fz	N	-1591	-1442
My	Nm	178	236
Left Lower Tibia			
Fx	N	246	346
Fy	N	135	267
Fz	N	1633	1859
Right Lower Tibia			
Fx	N	276	391
Fy	N	198	226
Fz	N	1608	2084
Lumbar Fz	N	-4895	-7483

2.5 DISCUSSION

2.5.1 Floor Friction Coefficient

<u>Head Injury Criterion</u>

Fig. 72 shows the variation of head injury criterion with foot to floor friction coefficient. There was no significant change in the head injury criterion with varying floor friction.

A HIC value of 1,000 is defined as the injury threshold and represents the point at which 16% of individuals will suffer a significant brain injury (16).

In this experiment all the HIC values calculated were well below 1,000.

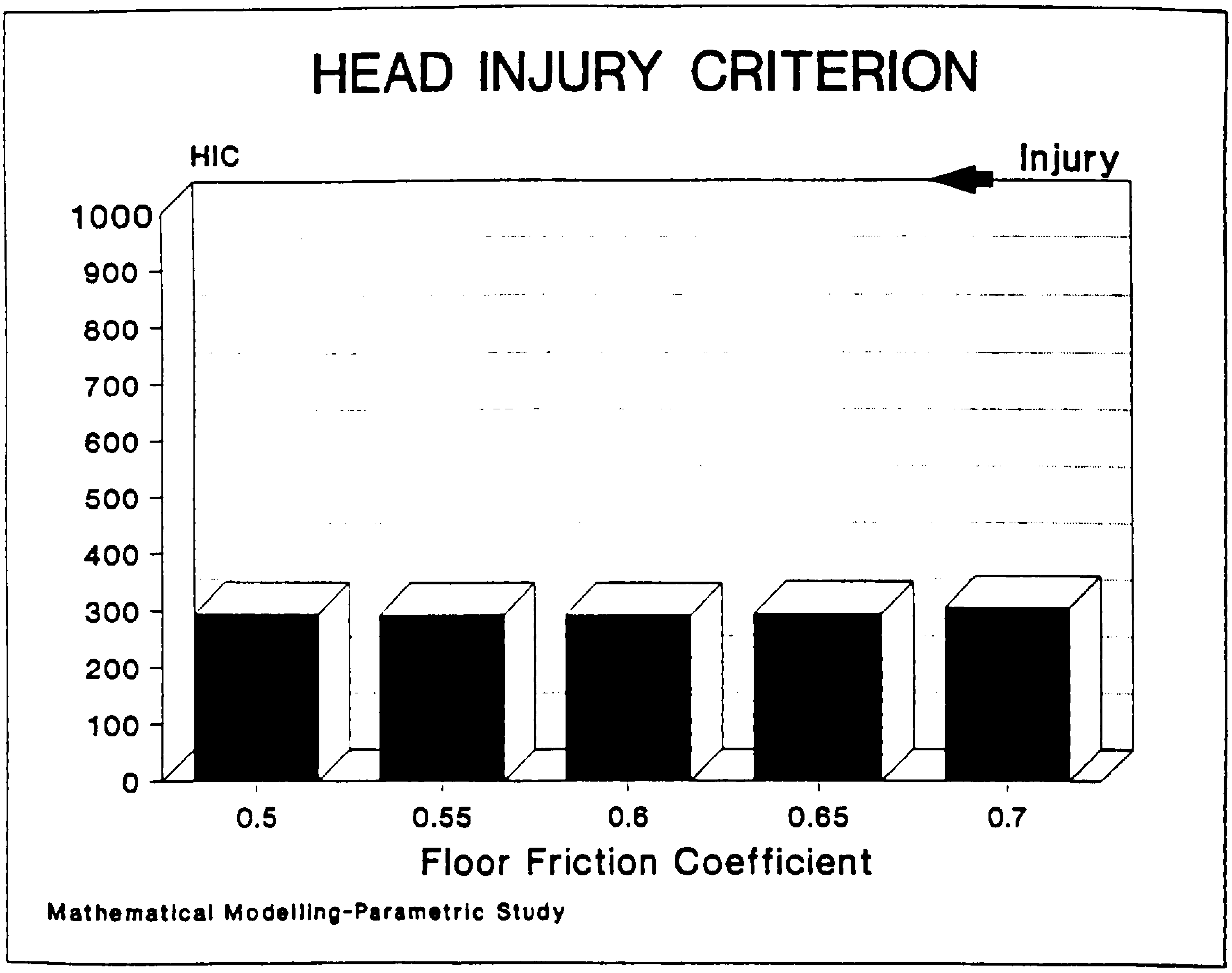

Fig. 72 Variation of Head Injury Criterion with Floor Friction Coefficient

Lap Belt Load

Fig. 73 shows the variation in lap belt load with foot to floor friction coefficient. Belt load decreased with increasing floor friction. This effect is small when compared to the overall loads measured and is not significant in terms of injury potential.

Human tolerance to lap belt forces in an impact is difficult to predict. The injury threshold has been estimated as occurring between 9 and 19kN (23) (33).

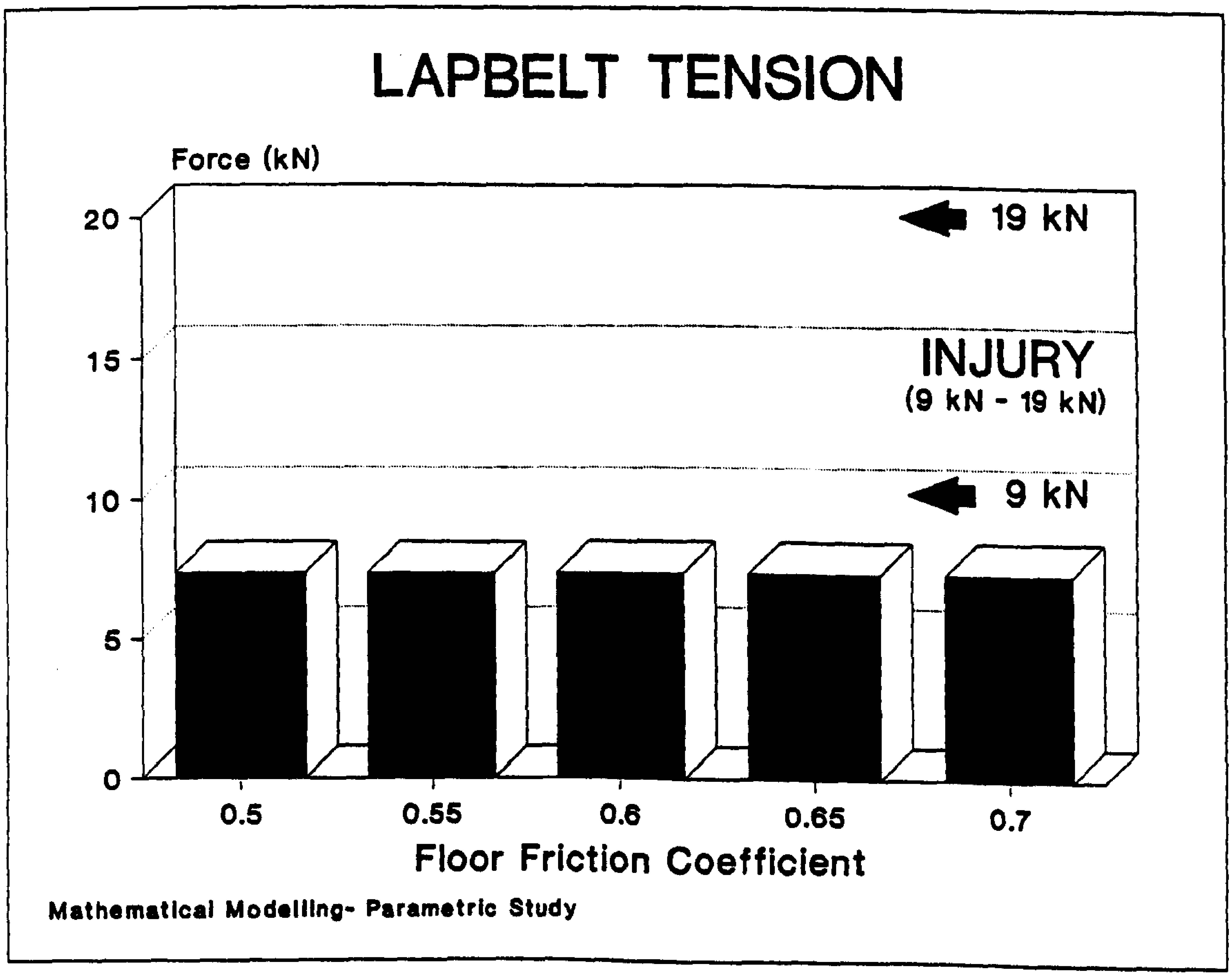

Fig. 73 Variation of Lap Belt Load with Floor Friction Coefficient

Lumbar Axial Load

Fig. 74 shows that there was little variation in the lumbar axial loads recorded for different foot to floor friction coefficients. All the loads recorded were in tension. The loads decreased slightly with increasing floor friction but the differences are small overall. A maximum load of 4904N was recorded which is below the estimated injury threshold of 12kN (29).

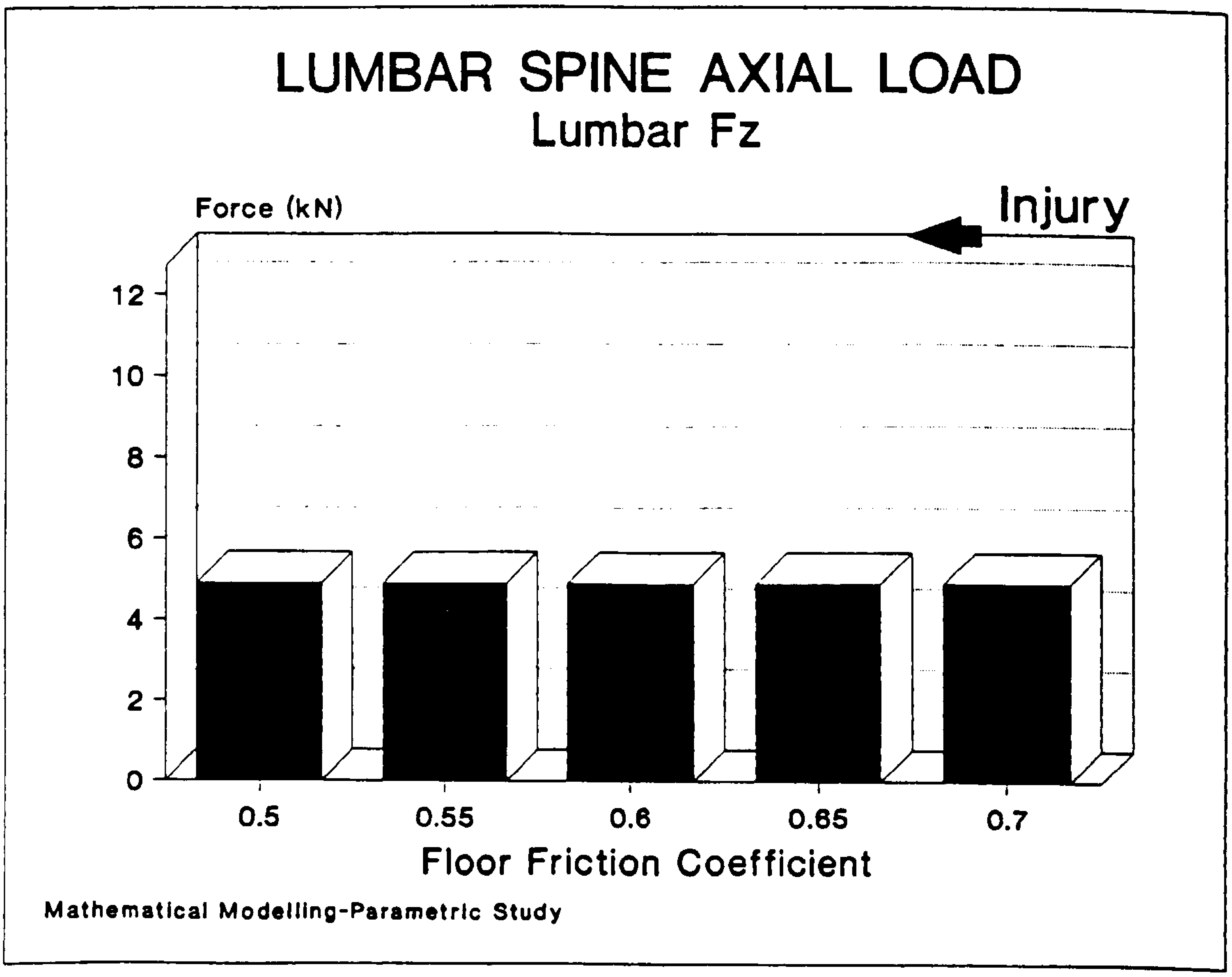

Fig. 74 Variation in Lumbar Axial Load with Floor Friction Coefficient

Femoral Axial Load

Fig. 75 shows the variation in femoral axial load with foot to floor friction. All the loads recorded were tensile as knee contact did not occur with the back of the forward seat.

The tensile loads increased with increasing foot to floor friction, however the effect was not significant in terms of injury potential. The peak load recorded was 1660N which remains well below the estimated injury threshold of 10kN (31). The data for comparison to the human is not available.

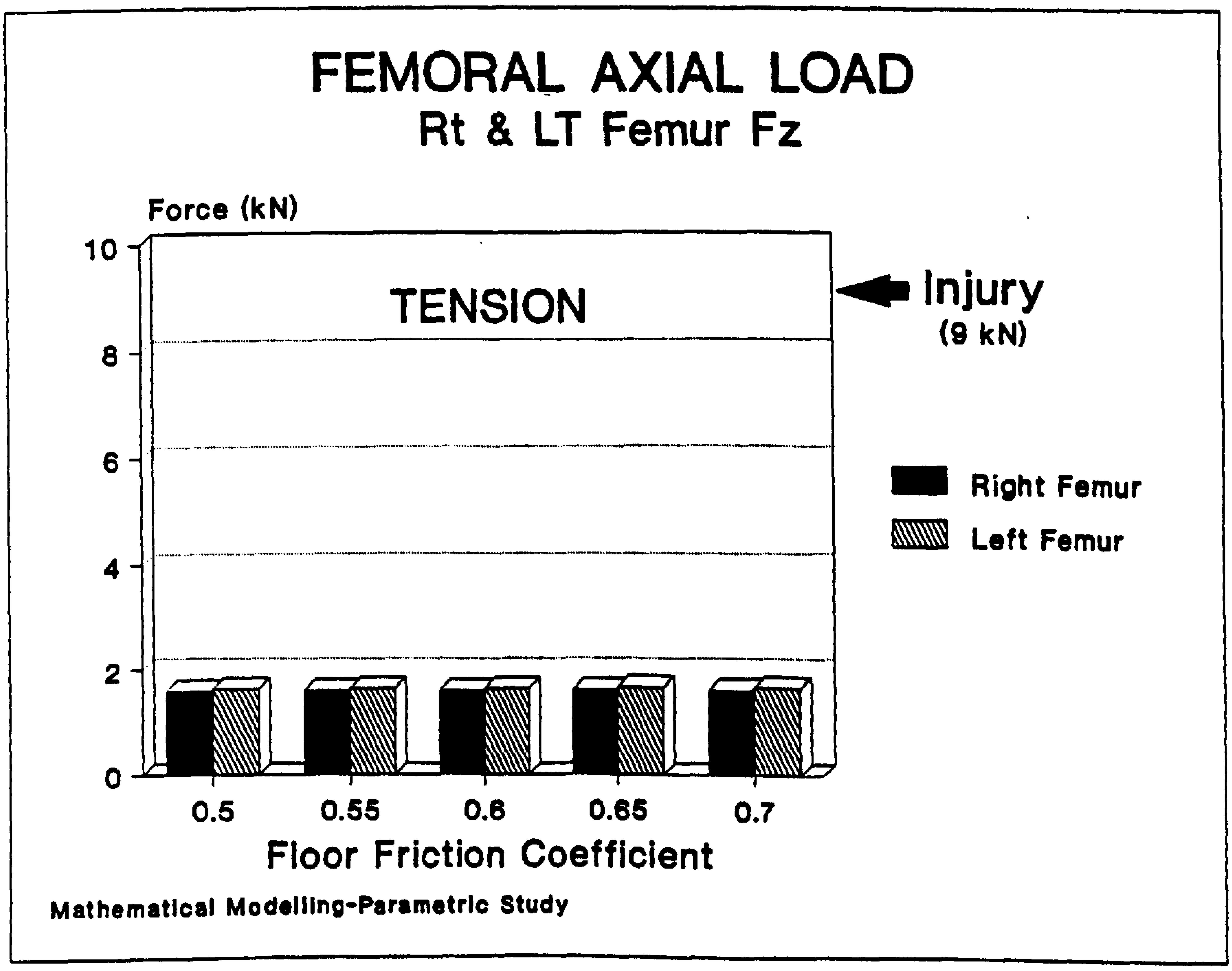

Fig. 75 Variation in Femoral Axial Load with Floor Friction Coefficient

Femoral Shear Load

Fig. 76 shows the variation in femoral shear load with different floor friction coefficients. Shear loads tended to increase with increasing foot to floor friction. The loads were greater on the left side and this reflects the lateral force component in the impact pulse.

Injury thresholds for a shear load applied to the human femur are difficult to predict as the data for comparison to the human is not available.

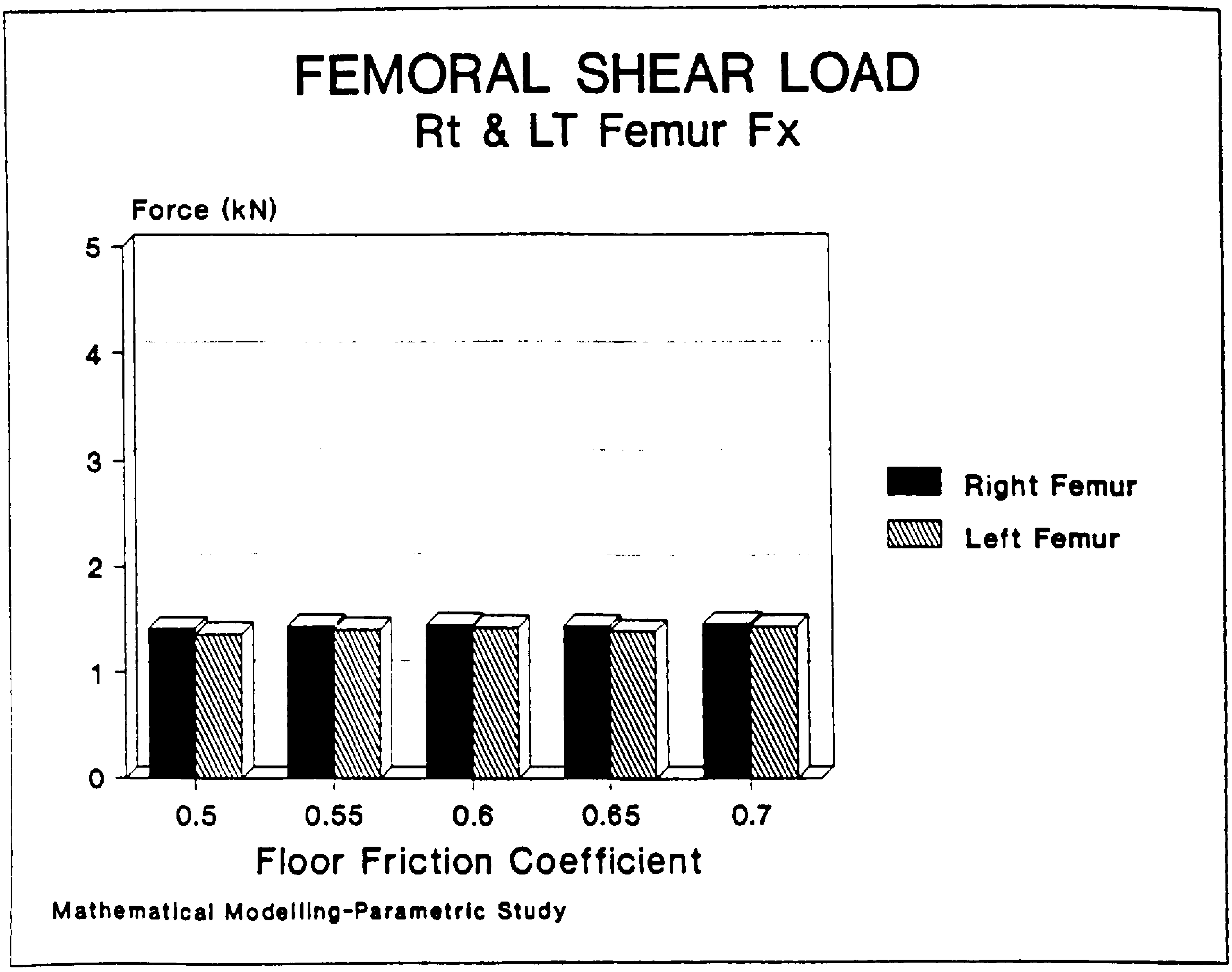

Fig. 76 Variation in Femoral Shear Load with Floor Friction Coefficient

Femoral Bending Moment

Fig. 77 shows the variation in femoral bending moment with increasing foot to floor friction. The femoral bending moment increased with foot to floor friction. However the differences were small compared to the overall loads recorded. The highest load recorded was 190Nm. This load is high but is below the injury range of 250Nm to 320Nm (36).

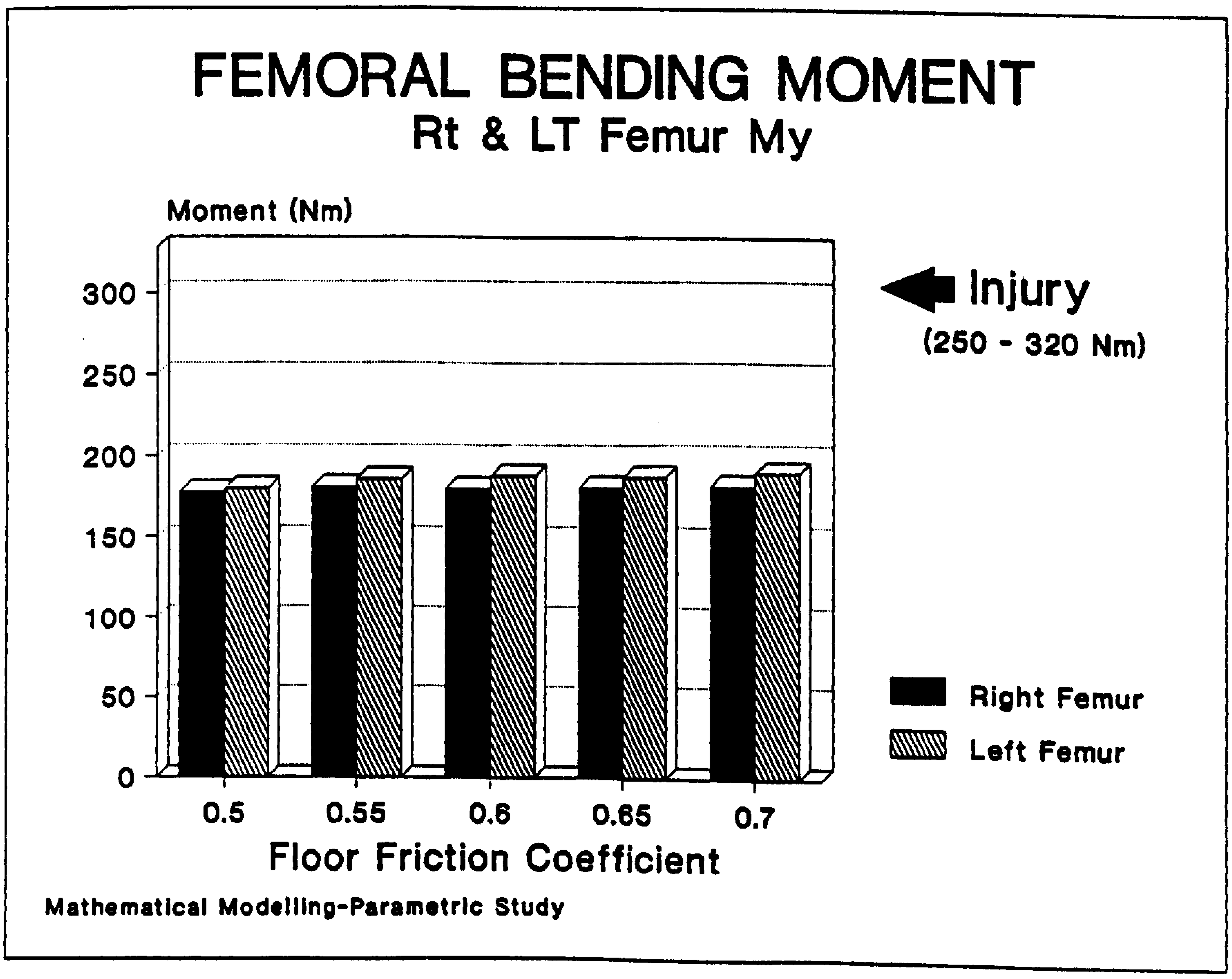

Fig. 77 Variation in Femoral Bending Moment with Foot to Floor Friction

Tibia Shear Load

Figs. 78 and 79 show the variation in tibial shear loads in the x-axis and y-axis with increasing foot to floor friction. The shear loads tended to increase with increasing foot to floor friction.

The significance of shear loads recorded in the tibia is difficult to predict, there is no comparable data available in the human.

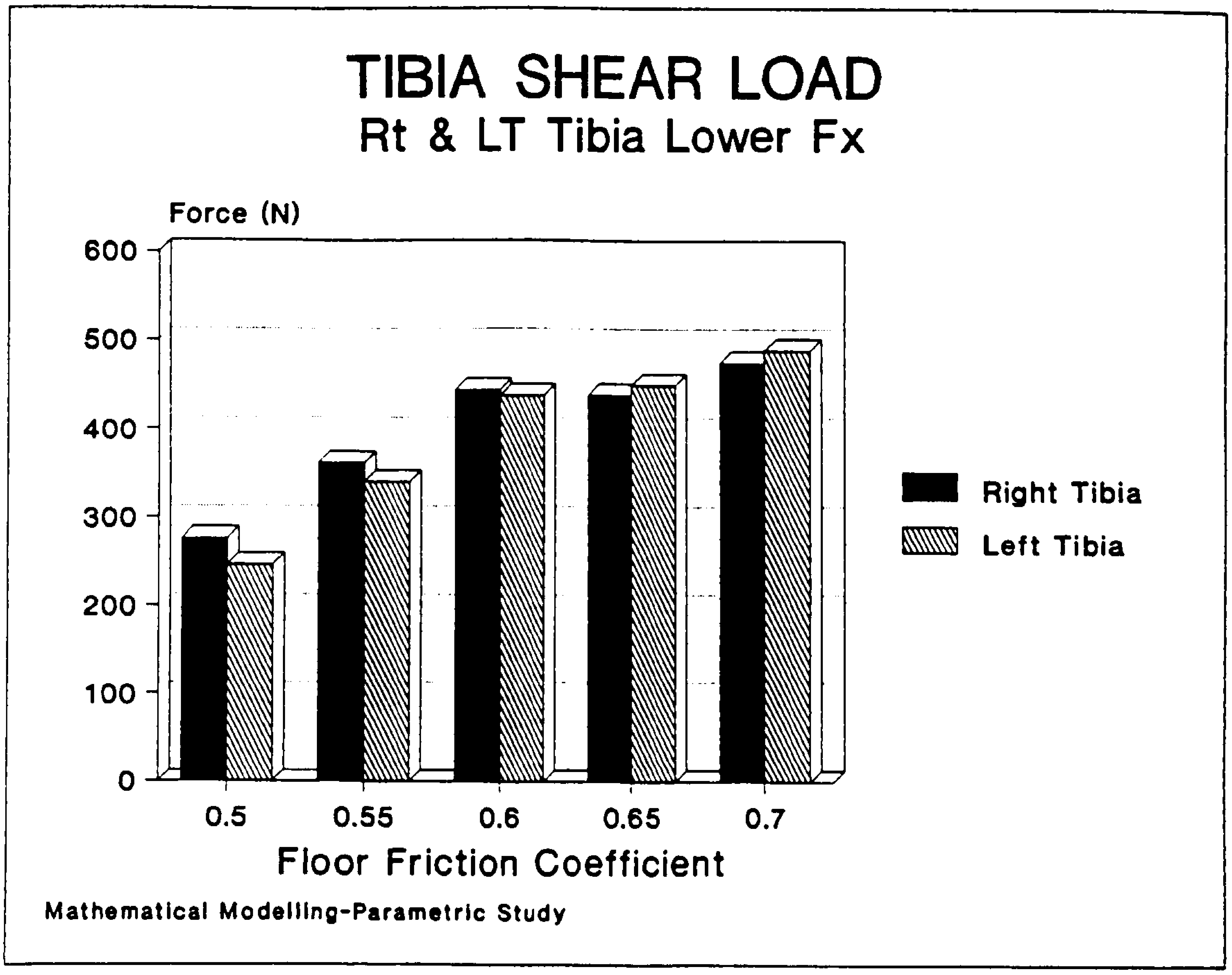

Fig. 78 Variation in Tibia Shear Load (Fx) - with Foot to Floor Friction

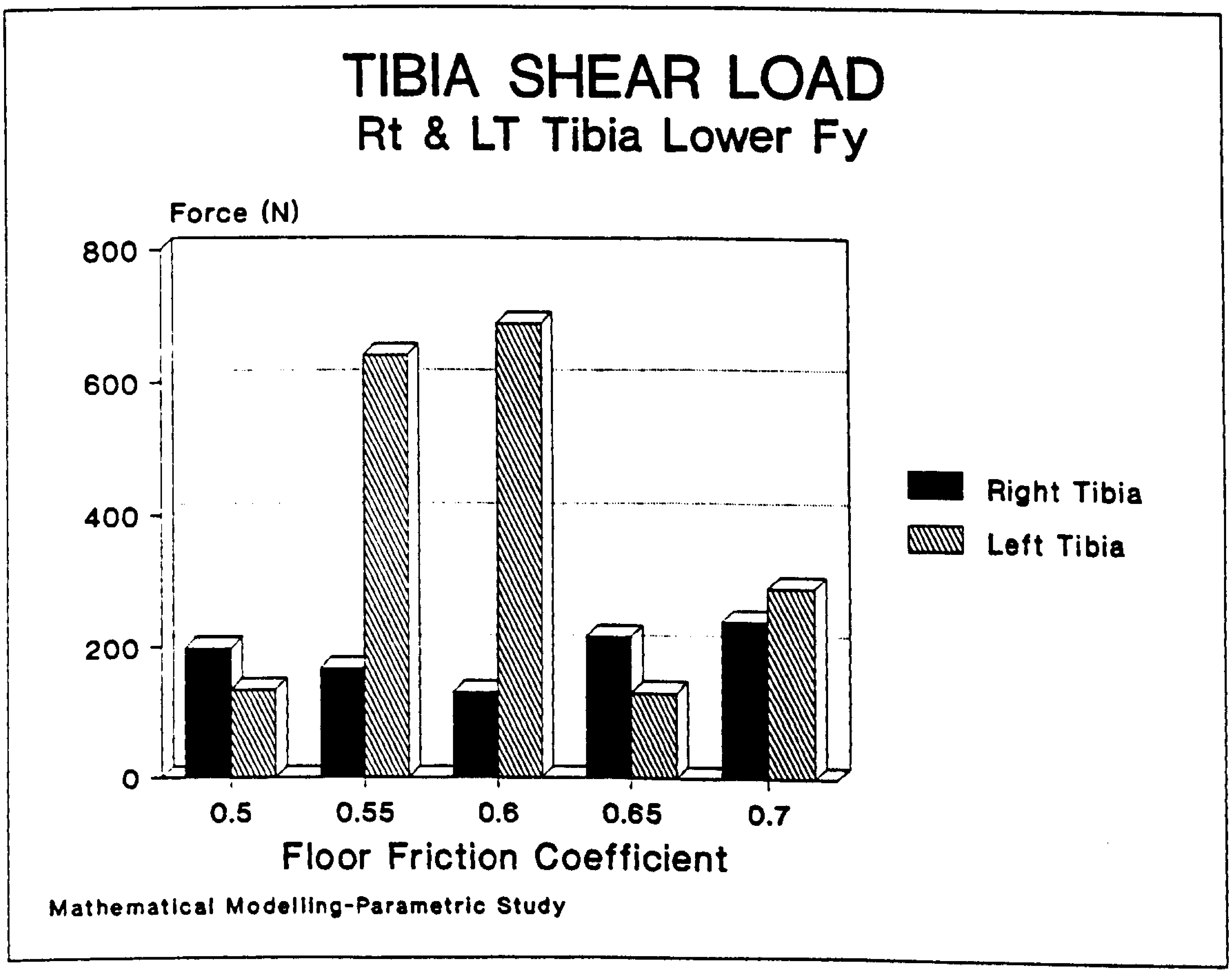

Fig. 79 Variation in Tibia Shear Load (Fy) with Foot to Floor Friction

Tibia Axial Load

Fig. 80 shows the small variation in tibial axial loads with increasing foot to floor friction. The maximum load occurred at a foot to floor friction coefficient of 0.7. The maximum load recorded was 4904N. This is well below the predicted injury threshold of 10.36kN in the male and 7.49kN in the female (28).

The maximum load was recorded at a maximum coefficient of floor friction. This was due to the lower leg showing less tendency to slide forwards on impact.

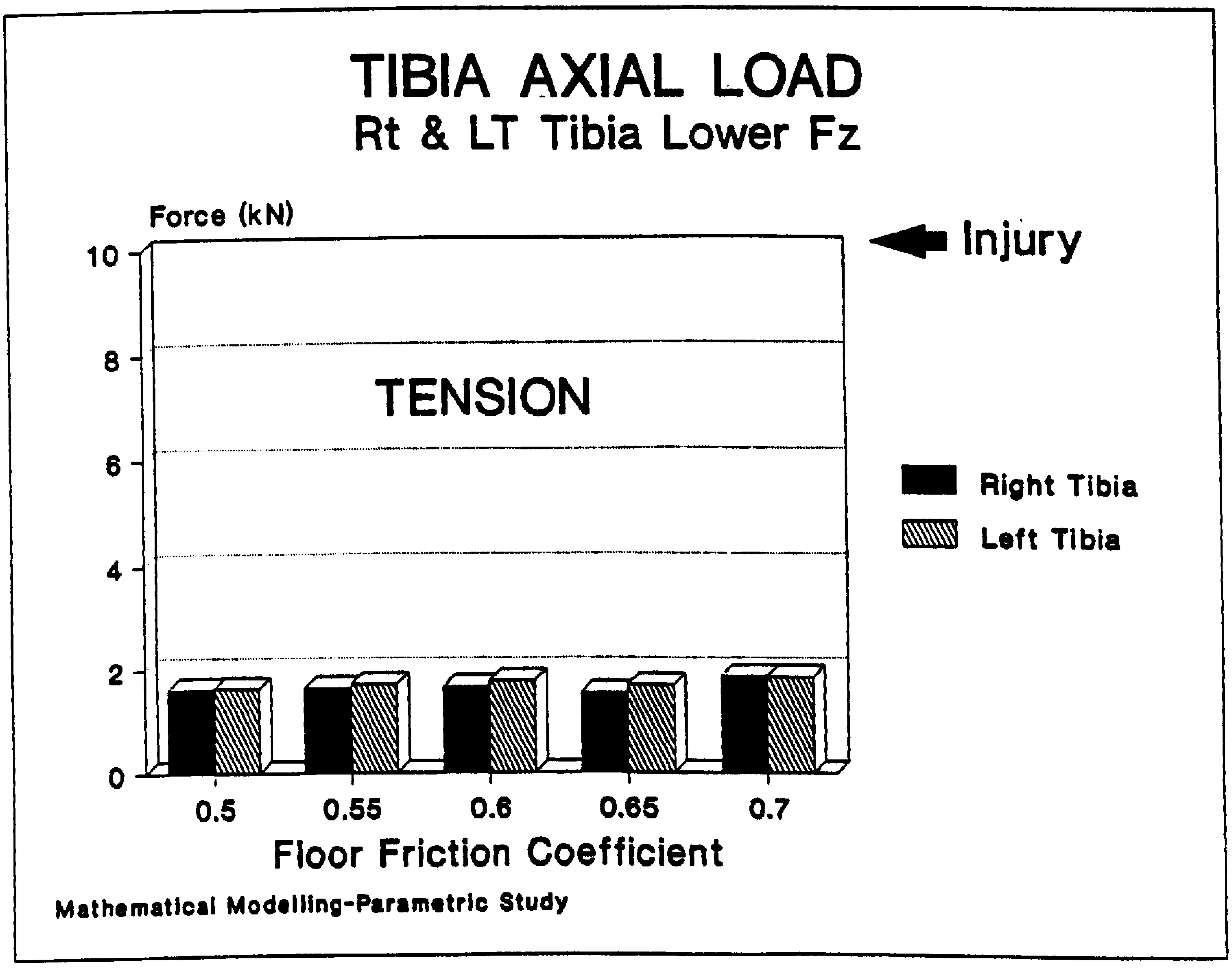

Fig. 80 Variation in Tibia Axial Load with Foot to Floor Friction

2.5.2 Seat Pitch

Head Injury Criterion

Fig. 81 shows the variation in the HIC value recorded for different seat pitches.

The HIC value varies according to which part of the seat against which the head impacts, reduced values being associated with impacts against the soft part of the seat and higher values being associated with impacts against the edge of the food/meal tray.

At a 27" and 30" seat pitch the dummy is in a more upright position. Therefore head acceleration occurs over an increased distance before impact with the seat ahead. The head strikes the upper edge of the food/meal tray and consequently the HIC values recorded are higher than those recorded at the baseline 32" seat pitch where the head strikes the middle of the food/meal tray.

At a 34" seat pitch the head strikes the lower edge of the food meal tray causing an increased HIC value compare with the baseline model.

At a 36" seat pitch the head strikes the softer part of the seat back below the meal tray.

A HIC value of 1,000 is defined as the injury threshold and represents the point at which 16% of individuals will suffer a significant brain injury (16).

In this experiment all the HIC values recorded were below 1,000.

The significance of HIC values under 1,000 is unknown.

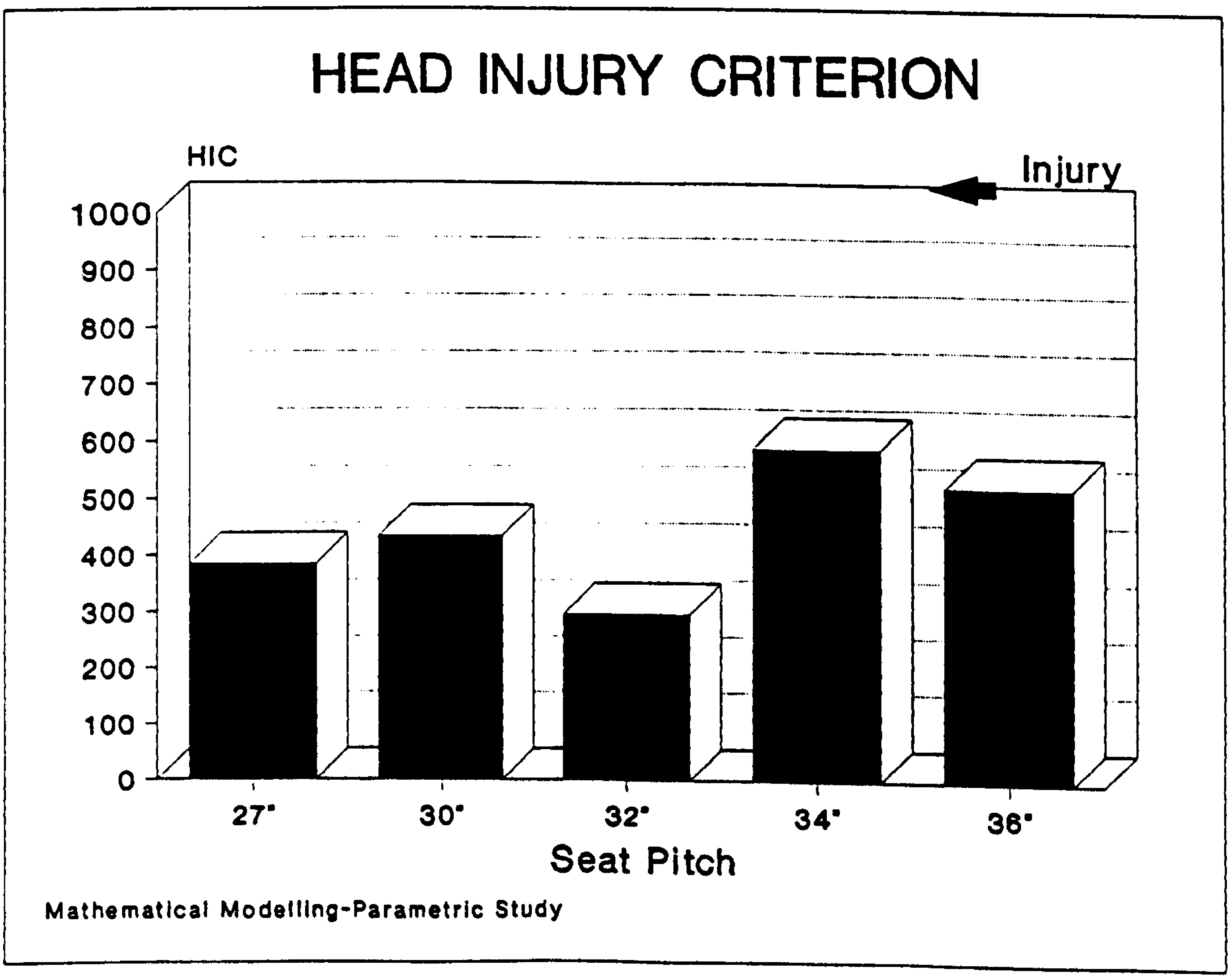

Fig. 81 Variation in Head Injury Criterion with Seat Pitch

Lap Belt Load

The lap belt loads associated with different seat pitches are shown in Fig. 82.

Reduced lap belt loads were seen at a 27" seat pitch due to the knees impacting with the back of the seat ahead.

Reduced lap belt loads were seen at a 34" and 36" seat pitch when compared to the baseline model. This may be due to a reduction in the upper torso angle causing reduced inertial forces on the upper and lower torso with a consequent decrease in the pelvic resultant acceleration.

Human tolerance to lap belt forces in an impact are difficult to predict but the injury range is between 9 and 19kN (23) (33). All the loads recorded were below the lower limit of this injury range.

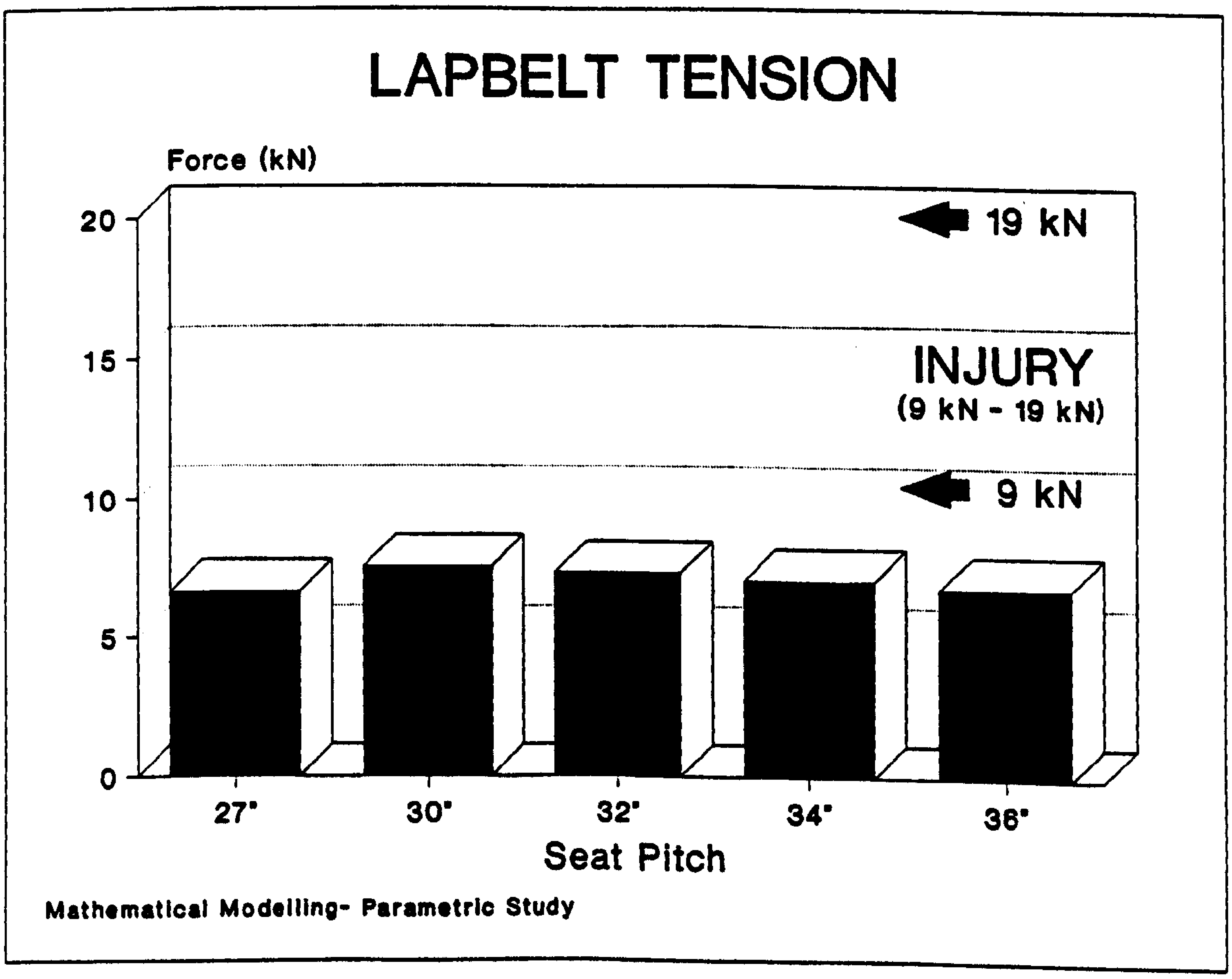

Fig. 82 Variation in Lap Belt Load with Seat Pitch

Lumbar Axial Load

Fig. 83 shows that there was little variation in lumbar axial load with seat pitch. All the loads recorded were in tension. The peak value was 5154N. This is well below the estimated injury threshold of 12kN (29).

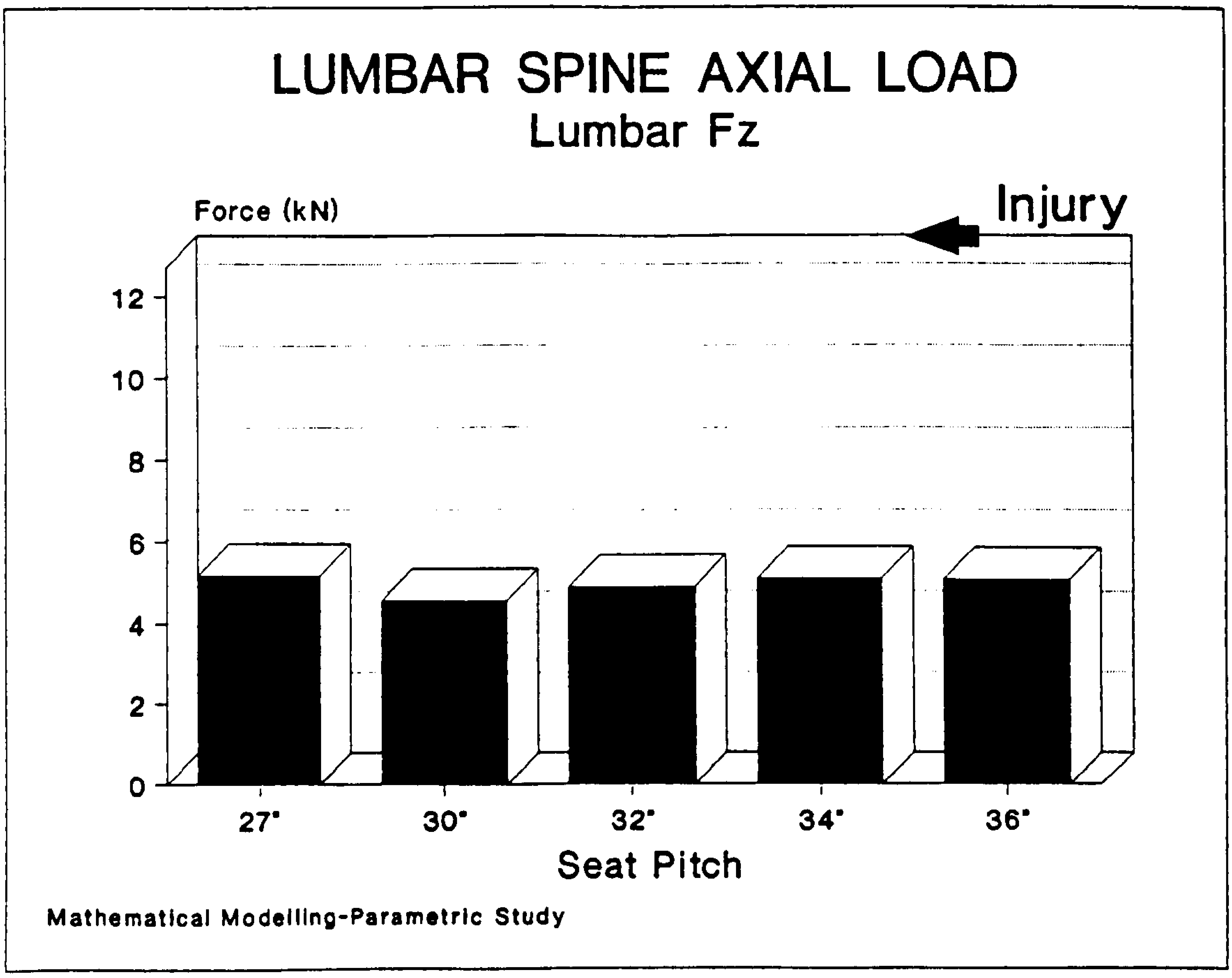

Fig. 83 Variation in Lumbar Axial Load with Seat Pitch

Femoral Axial Load

Fig. 84 shows the variation in femoral axial load with seat pitch.

At a 27" seat pitch knee contact occurred with the back of the forward seat. Accordingly compressive axial loads were recorded. The peak compressive load recorded was 2025N. This remains well below the injury threshold of 8.68kN (31).

At all the other seat pitches, the maximum axial loads recorded were in tension. All the loads were well below the estimated injury threshold of 7kN.

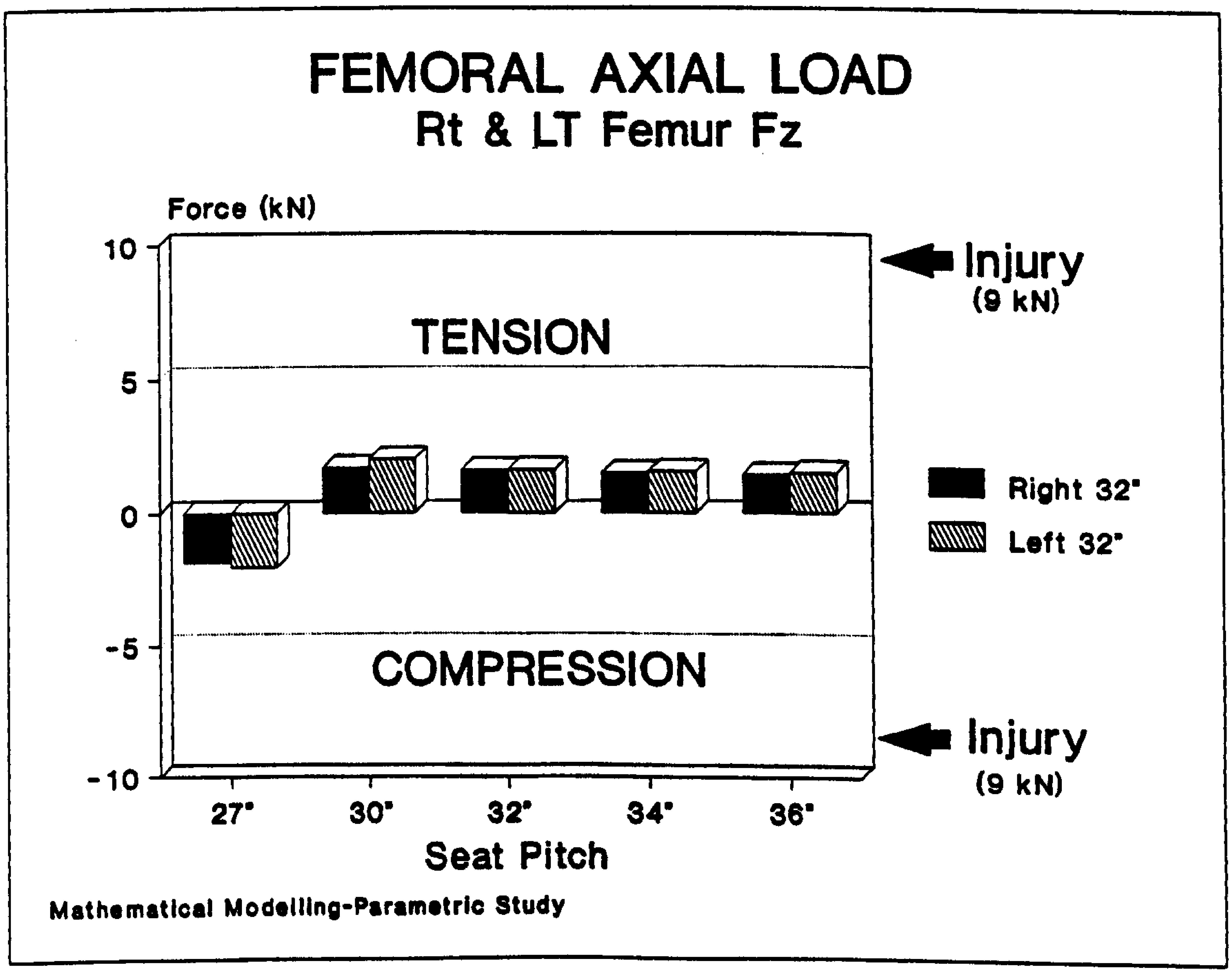

Fig. 84 Variation in Femoral Axial Load with Seat Pitch

Femoral Shear Load

Fig. 85 shows the variation in femoral shear loads for different seat pitches. There was a tendency for higher shear loads to be recorded at greater seat pitches. This presumably reflects the increased lateral movement permitted by the increased seat pitch.

The injury threshold for shear load applied to the human femur are difficult to predict as there is no equivalent data available for the human.

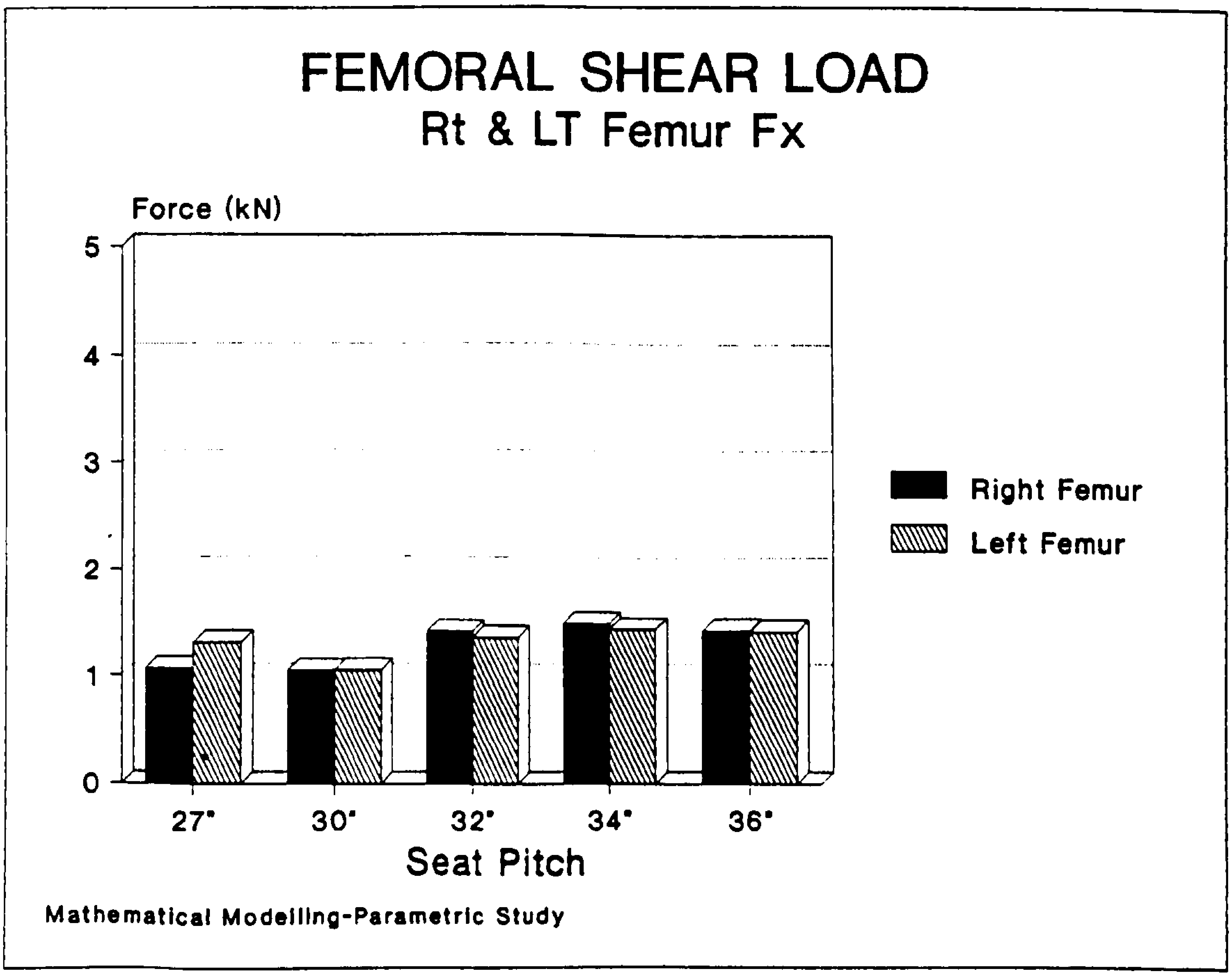

Fig. 85 Variation in Femoral Shear Load with Seat Pitch

Femoral Bending Moment

With the exception of a 30" seat pitch there is little variation in the femoral bending moments recorded for different seat pitches.

At a 30" seat pitch very high bending moments were recorded which were above the upper limit of the injury threshold range of 320Nm (36). The very high loads were related to foot entrapment. At this seat pitch the foot became trapped under the luggage retaining spa of the seat ahead. This resulted in knee hyperextension and very high femoral loading, (See Figs. 65 and 86) and was related to knee contact with the back of the seat ahead at this pitch, which caused an initial inward movement of the lower leg.

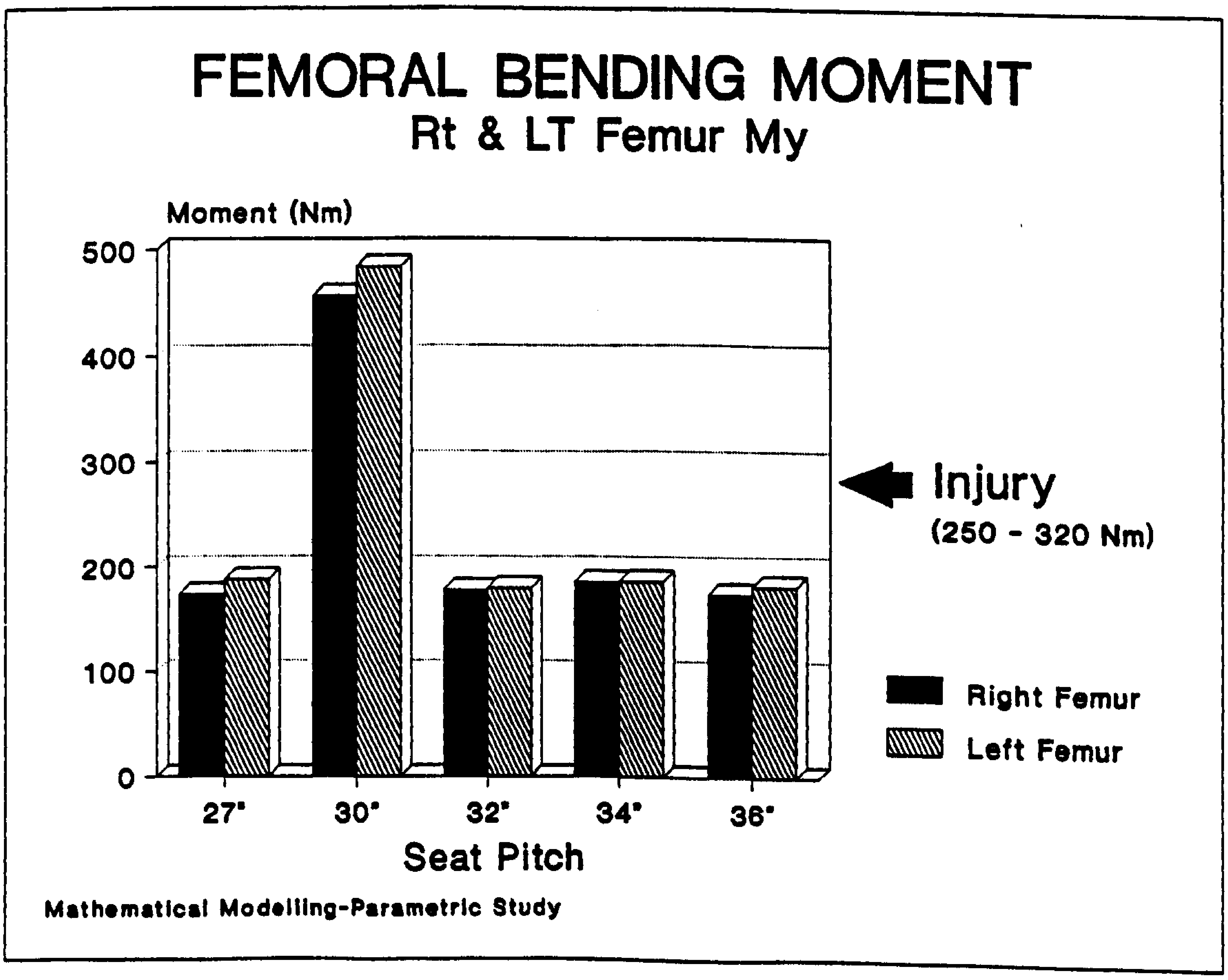

Fig. 86 Variation in Femoral Bending Moments with Seat Pitch

Tibia Shear Load

Figs. 87 and 88 show variations in tibia shear loads for different seat pitches.

All the loads recorded were relatively low with the exception of shear loads recorded in the x-axis at a 30" seat pitch. These loads were much higher than in all the other configurations and were related to foot entrapment occurring under the luggage retaining spar of the seat ahead (see Fig.65).

The significance of shear loads recorded in the tibia is difficult to predict as the equivalent data in the human is not available. However, the higher loads recorded at a 30" seat pitch may approach the injury threshold.

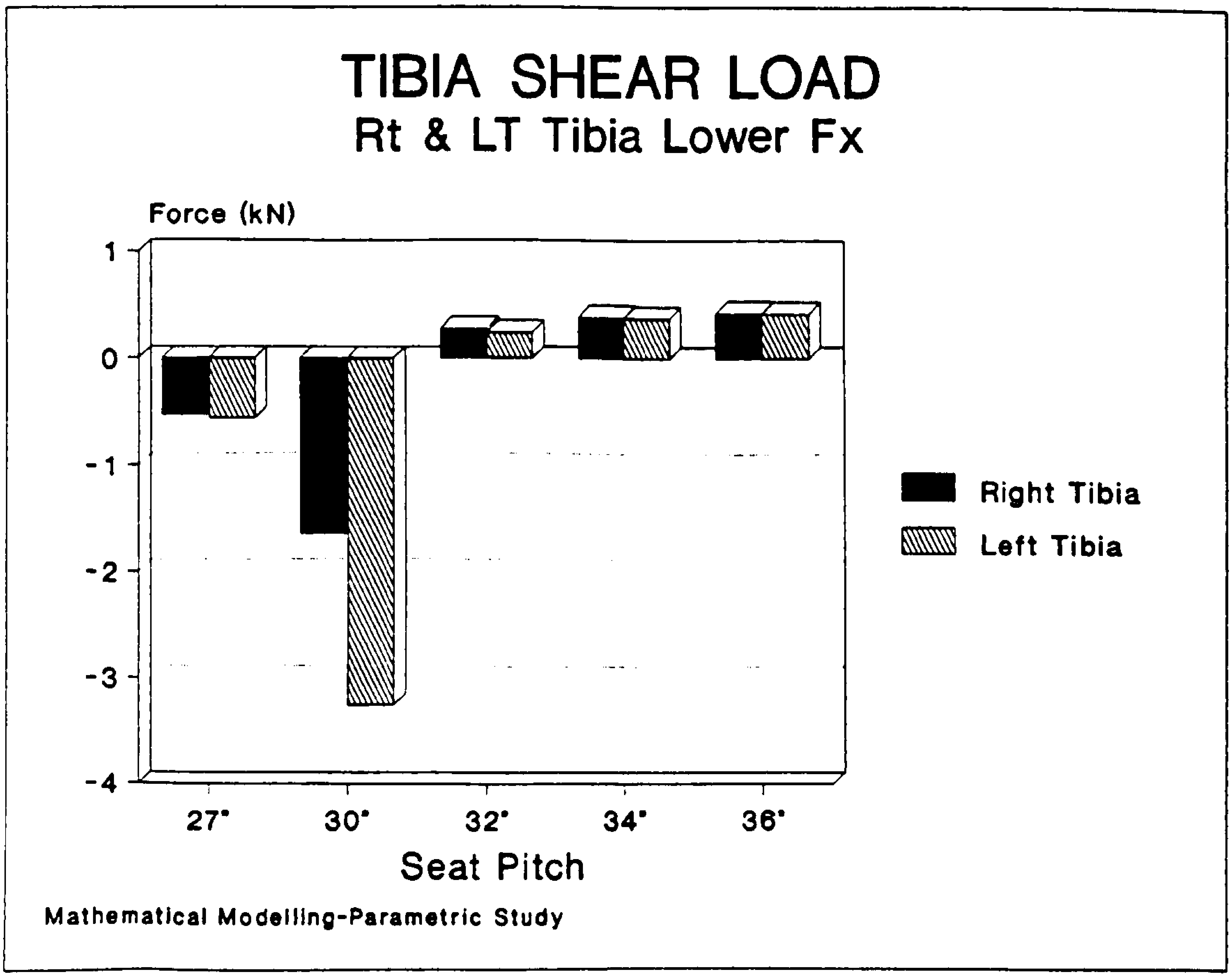

Fig. 87 Variation in Tibia Shear Load (Fx) with Seat Pitch

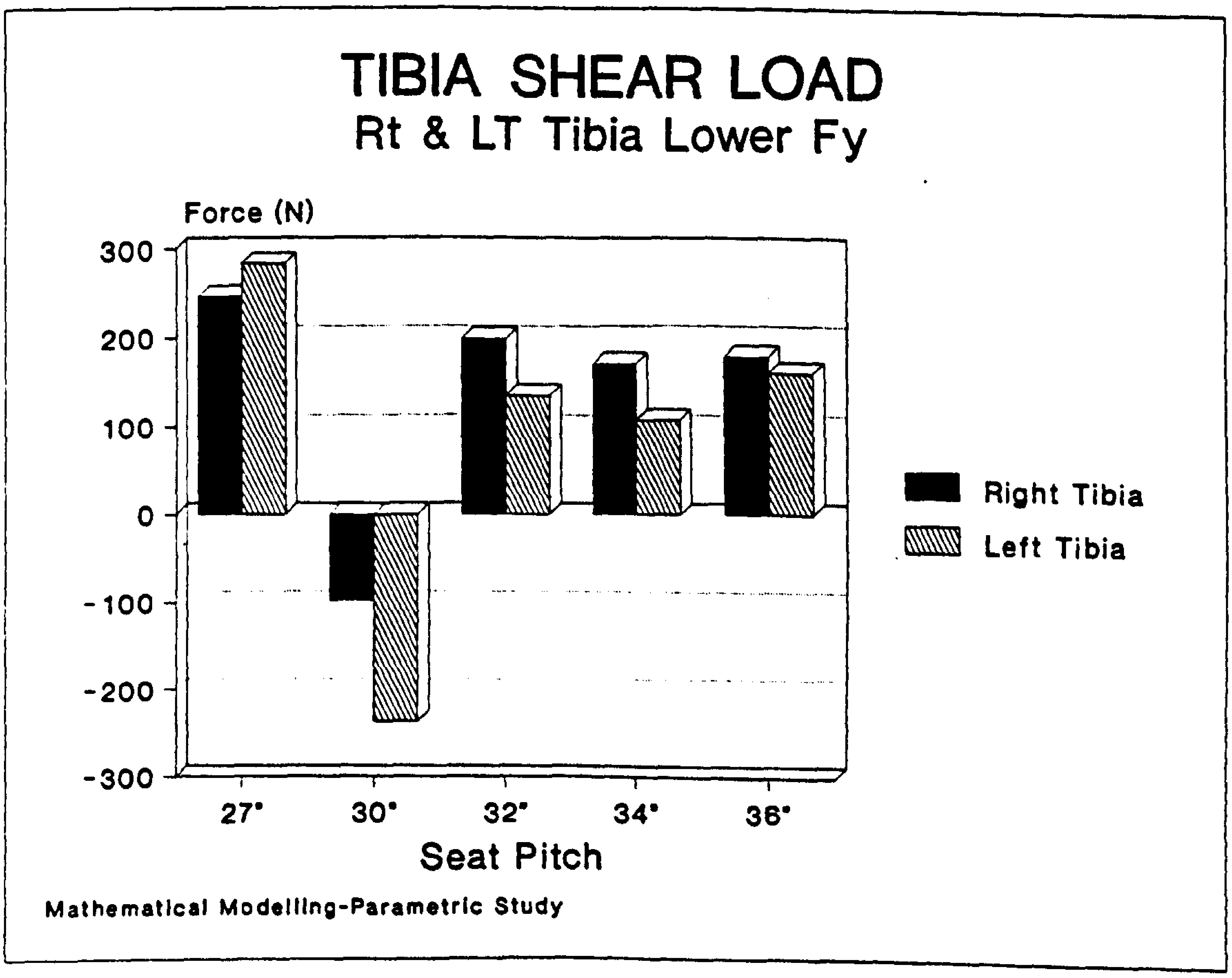

Fig. 88 Variation in Tibia Shear Load (Fy) with Seat Pitch

Tibia Axial Load

Fig. 89 shows the tibia axial loads recorded at different seat pitches. There was little variation in the axial loads recorded. All the loads recorded were well below the predicted injury threshold of 10.36kN in the male and 7.49kN in the female (28).

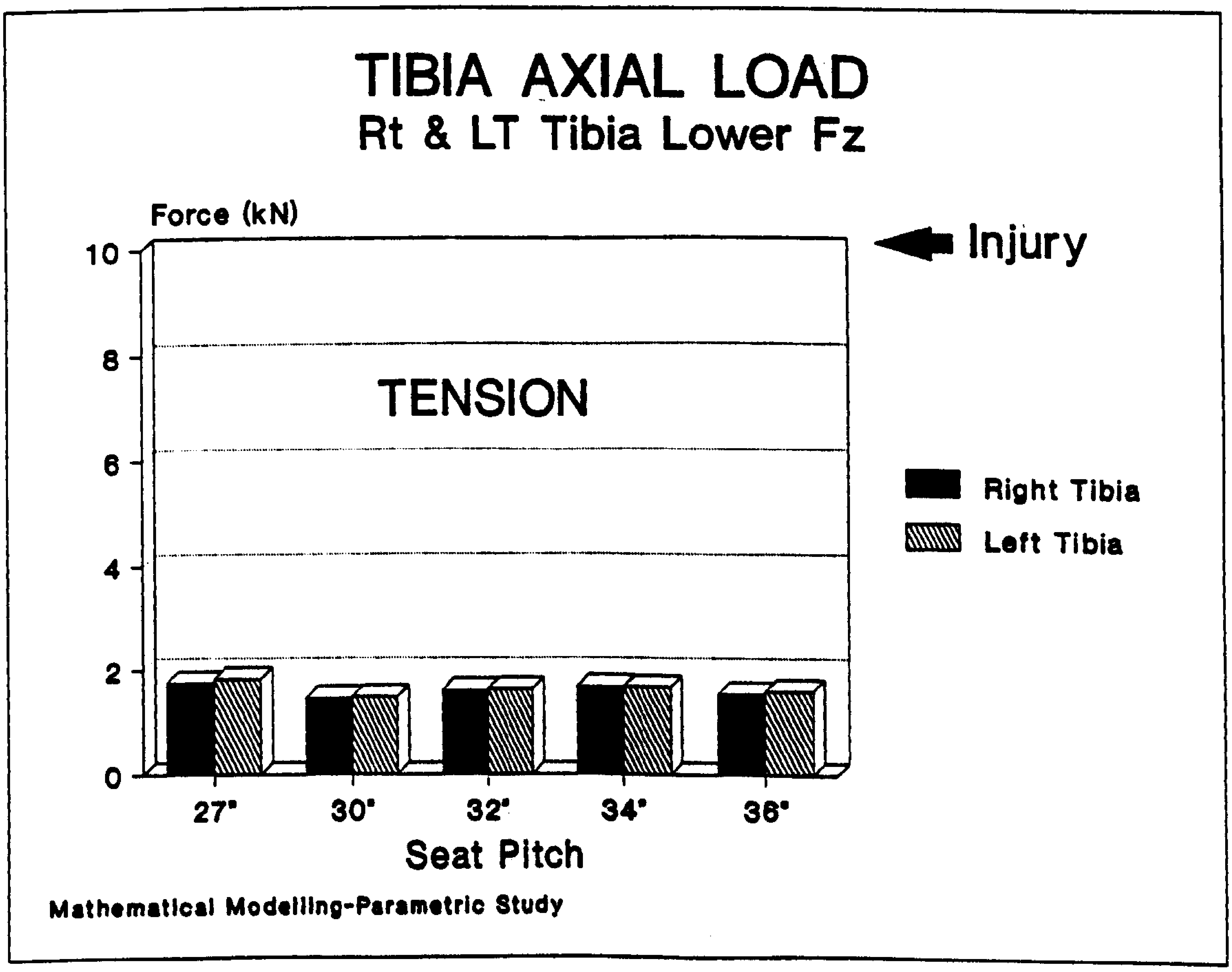

Fig. 89 Variation in Tibia Axial Load with Seat Pitch

2.5.3 Lower Leg Position

Head Injury Criterion

Fig. 90 illustrates the different HIC values recorded for different lower limb positions.

The HIC values increased as the legs move from a rearward position to a forward position. All the HIC values recorded were well below the injury threshold of 1,000.

A HIC value of 1,000 is defined as the injury threshold and represents the point at which 16% of individuals will suffer a significant brain injury (16).

This tendency for the HIC value to increase as the legs move forward is in contrast to those findings the impact tests described earlier where the HIC value tended to increase as the legs move rearward. The reason for this difference is uncertain.

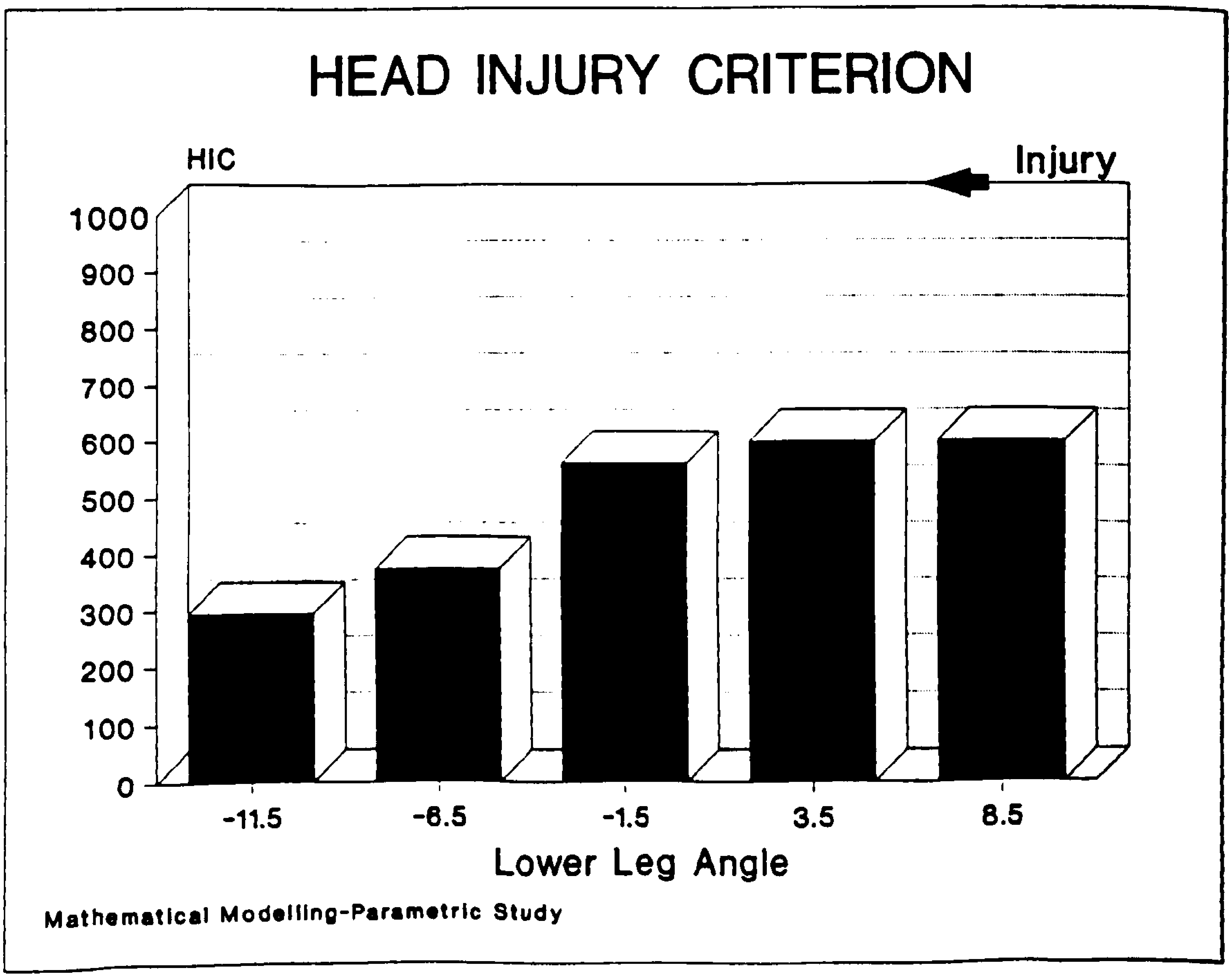

Fig. 90 Variation in Head Injury Criterion with Lower Leg Position

<u>Lap Belt</u>

Fig. 91 shows the lap belt loads recorded for different seat positions.

The lap belt loads are relatively uniform. There is a slight downward trend in the loads recorded as the tibia moves to a forward position. It is suggested that this is due to the lower torso sinking into the seat on impact causing load transference between the seat base and lap belt.

Human tolerance to lap belt forces in an impact are difficult to predict. The injury ranges between 9 and 19kN (23) (33). All the loads recorded are below the lower limit of this injury range.

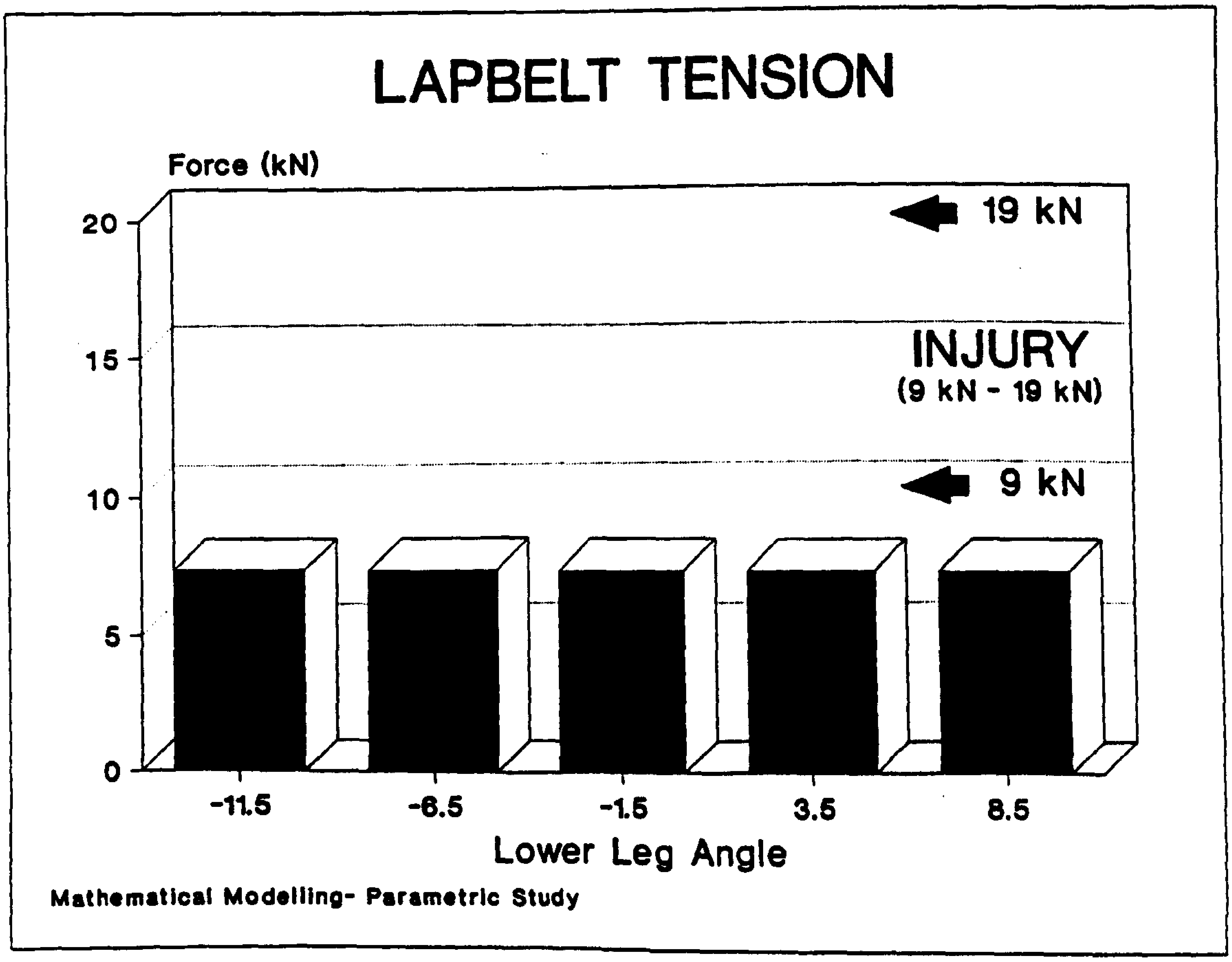

Fig. 91 Variation in Lap Belt Load with Lower Leg Position

Lumbar Axial Load

Fig. 92 illustrates the axial loads recorded in the lumbar spine for different lower limb positions. The loads remain relatively uniform irrespective of lower leg position. All the loads recorded were in tension.

The peak load recorded was 4944N and occurred with the legs 8.5° forward of the vertical.

All the loads recorded are well below the predicted injury threshold of 12kN (29).

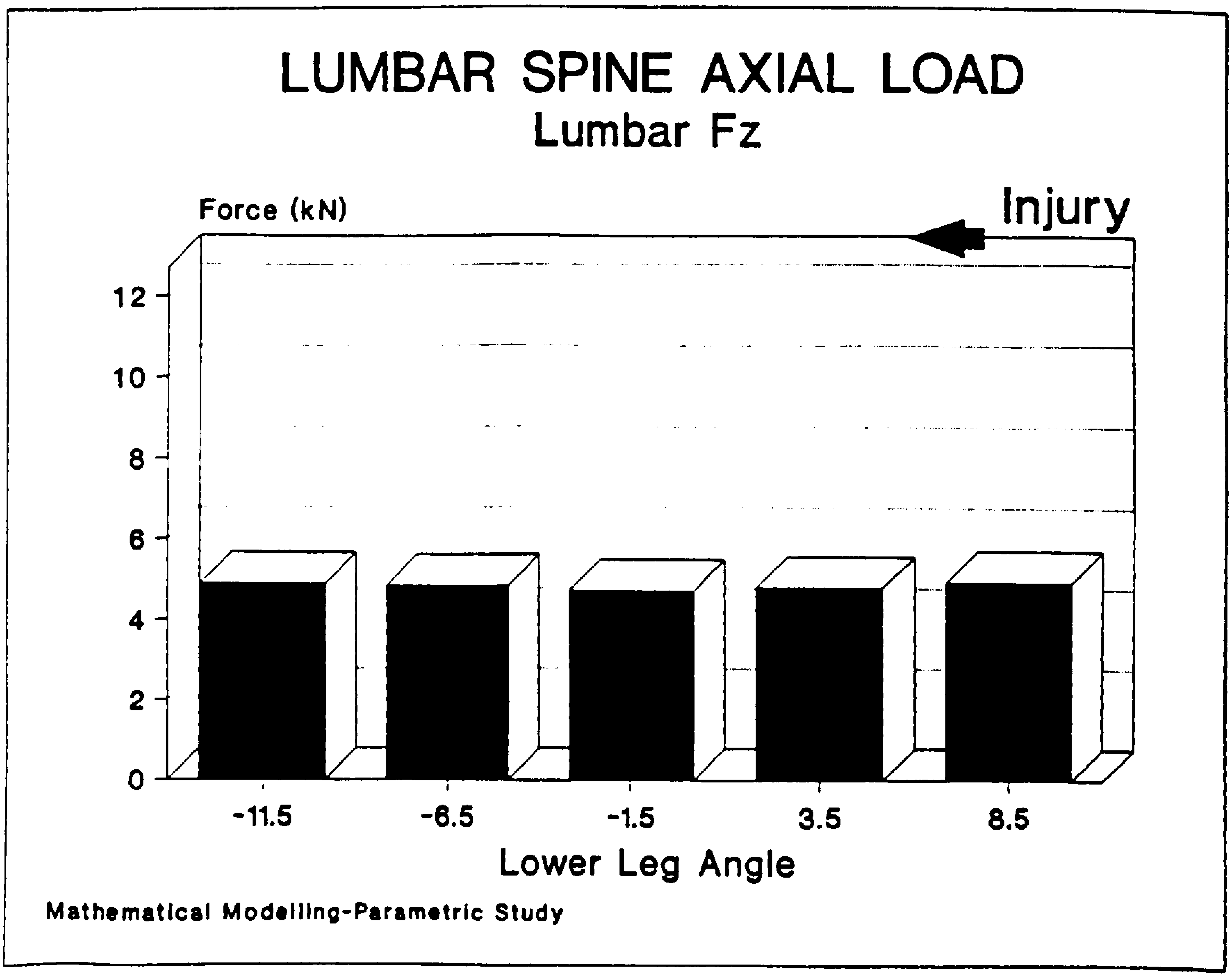

Fig. 92 Variation in Lumbar Axial Load with Lower Leg Position

Femoral Axial Load

Fig. 93 illustrates the axial loads recorded in the femur for different lower limb positions. The loads recorded are all in tension. The highest load was associated with the lower limbs in a forward position. The maximum load recorded was 1842N which is well below the injury threshold of 10kN (31).

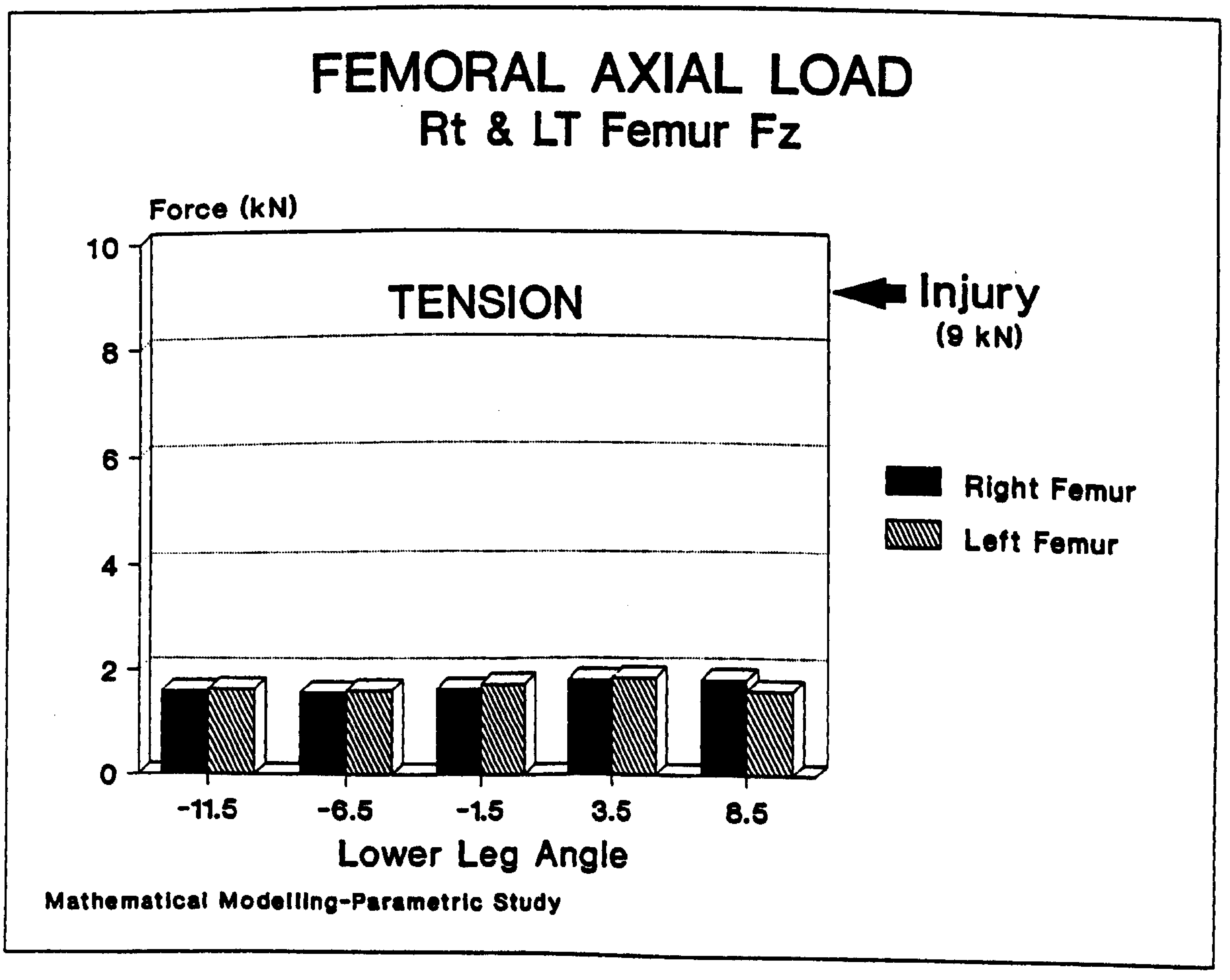

Fig. 93 Variation in Femoral Axial Load with Lower Leg Position

Femoral Shear Load

Fig. 94 illustrates the shear loads recorded in the femur for different lower limb positions.

It should be noted that the direction of the shear load was reversed when the legs were positioned 11.5° rearwards.

The significance of shear loads recorded in the femur are difficult to predict as the equivalent data in the human is not available for comparison.

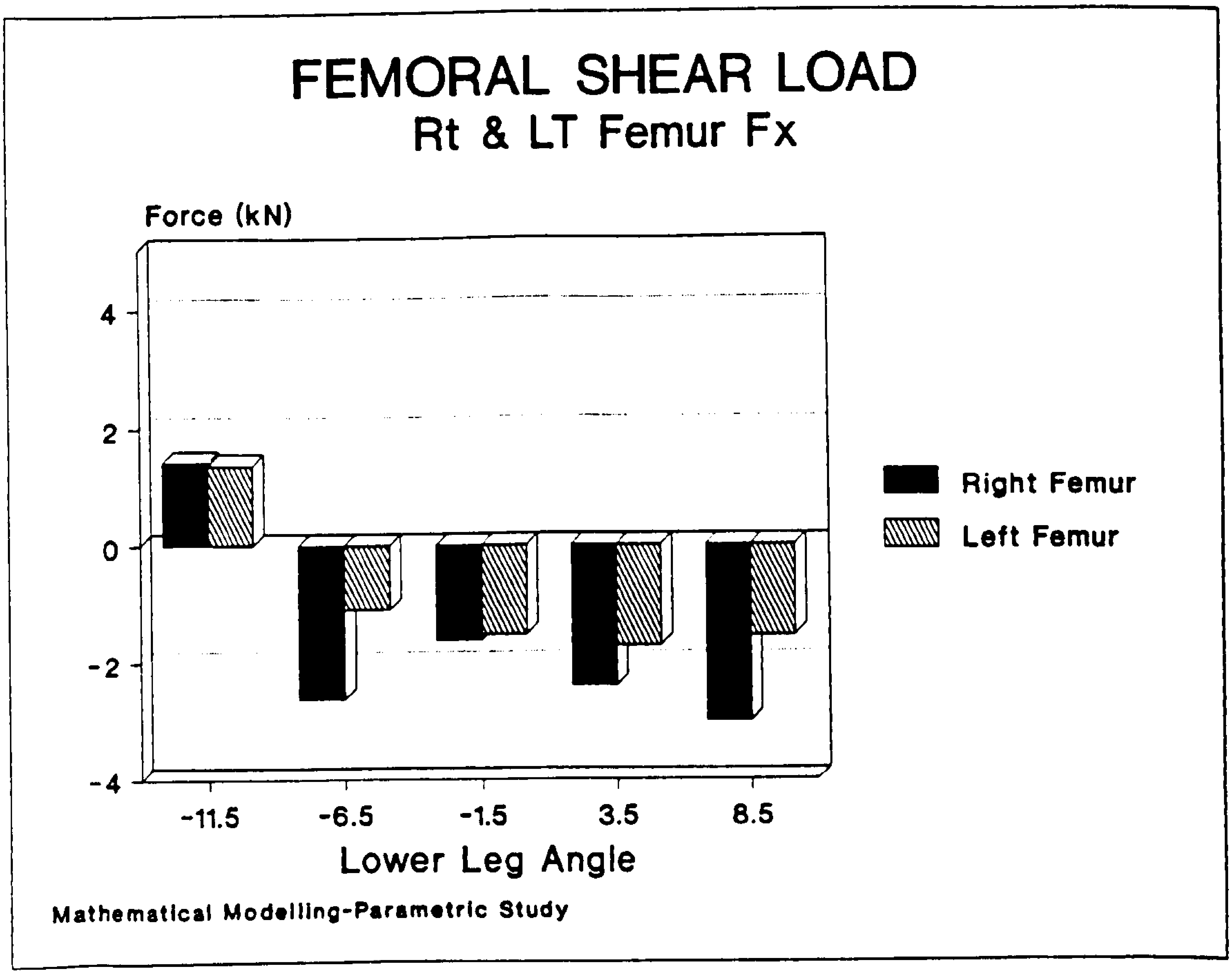

Fig. 94 Variation in Femoral Shear Load with Lower Leg Position

Femoral Bending Moment

Fig. 95 illustrates the femoral bending moments recorded for different lower limb positions.

When the lower limbs are positioned 11.5° rearwards, the loads recorded in the femurs are almost identical. With the limbs positioned 6.5° rearwards an increased load is recorded in the right femur. This increased loading was associated with foot entrapment under the luggage bar. For whilst flailing of the lower limbs did not occur, at the low coefficient of friction used, the foot was able to slide forwards and became trapped. At 1.5° rearwards much higher loads were recorded in the right femur and this was related to more marked foot entrapment under the luggage bar. The loads recorded approached the injury threshold of 250-320Nm (36).

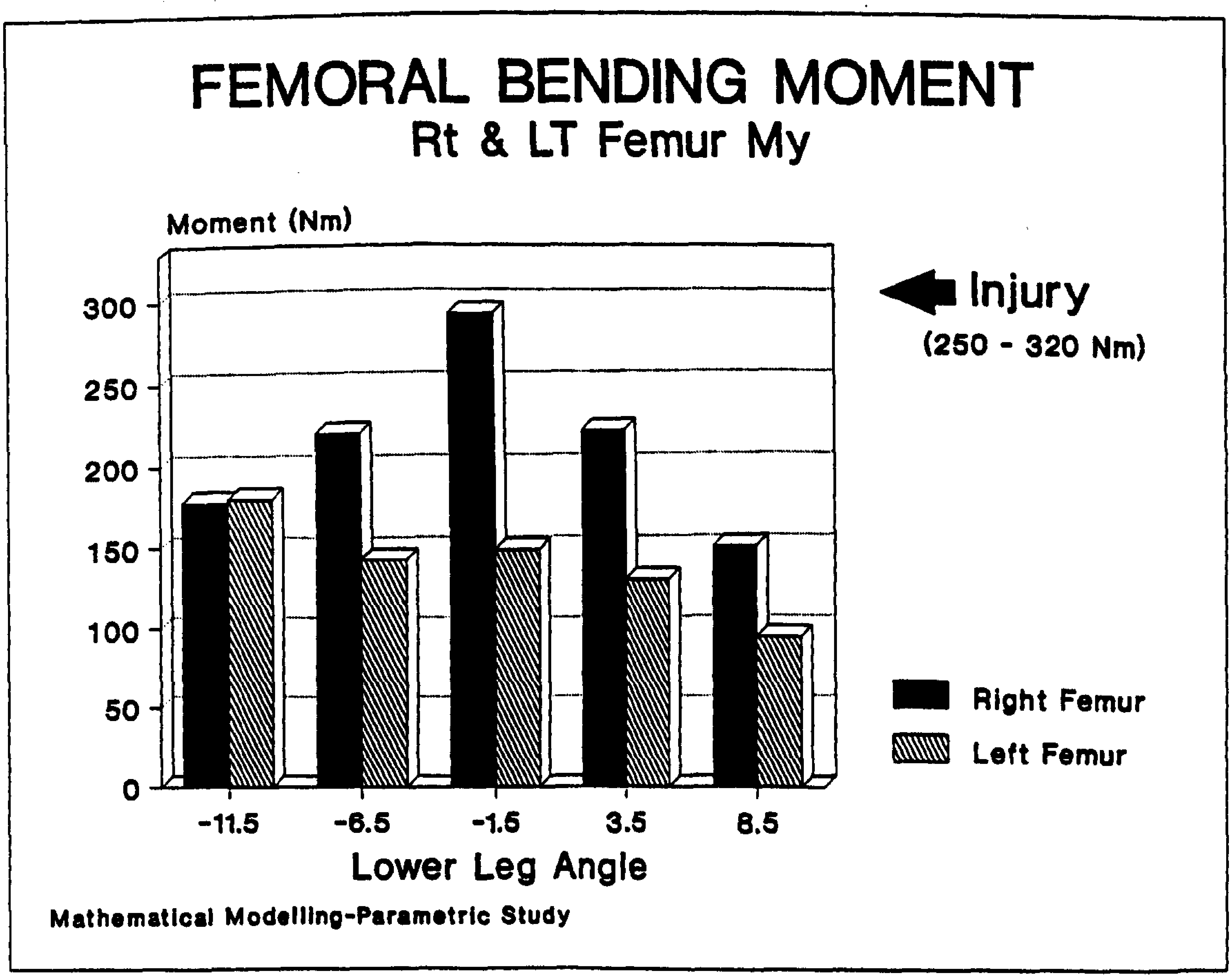

Fig. 95 Variation in Femoral Bending Moments with Lower Leg Position

Tibia Shear Load

Figs. 96 and 97 illustrate the shear loads recorded in both tibia for different lower limb positions. High shear loads were recorded with the lower limbs positioned forwards of the vertical. The increased loads were associated with foot entrapment below the front seat luggage bar.

The lateral loads recorded in the tibia parallel the forward loads.

The loads recorded are higher but the significance is difficult to predict as the equivalent data in the human is not available for comparison.

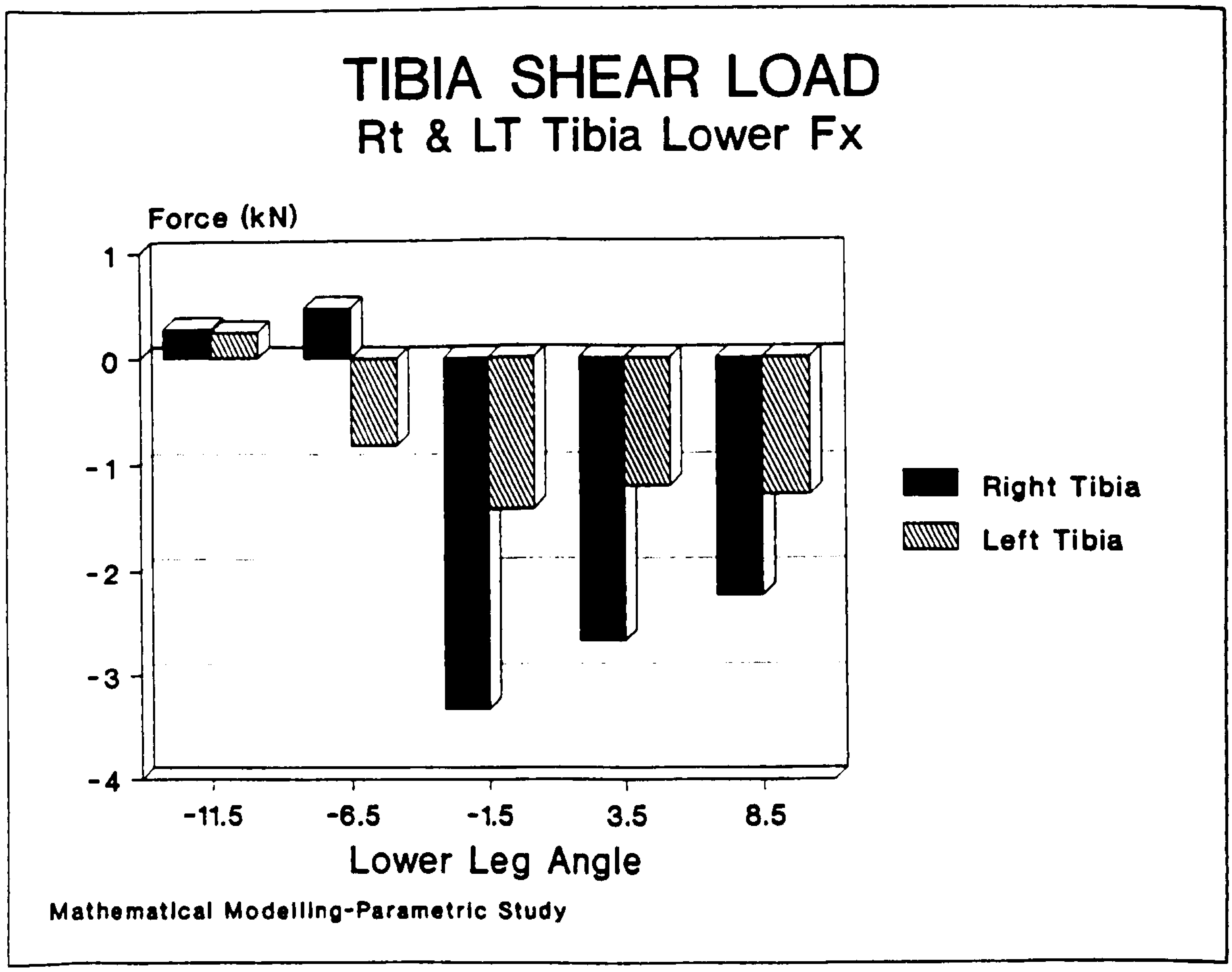

Fig. 96 Variation in Tibia Shear Load (Fx) with Lower Leg Position

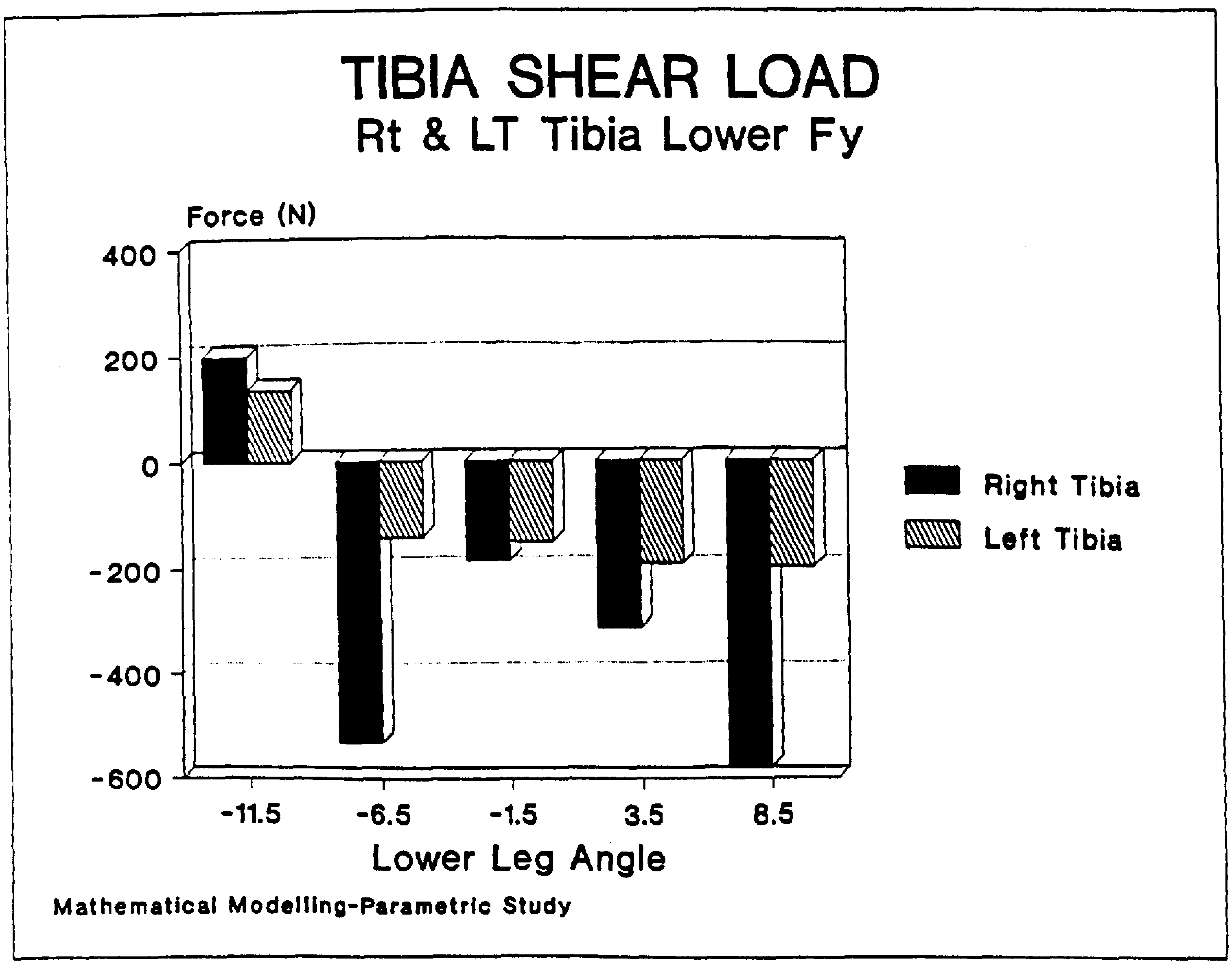

Fig. 97 Variation in Tibia Shear Load (Fy) with Lower Leg Position

Tibia Axial Load

Fig. 98 illustrates the axial loads recorded in the tibia for different lower limb positions. The loads recorded were all compressive loads and the highest values were associated with the lower limbs in a 1.5° forwards position.

All the loads recorded are below the predicted injury threshold of 10.36kN in the male and 7.49kN in the female (28).

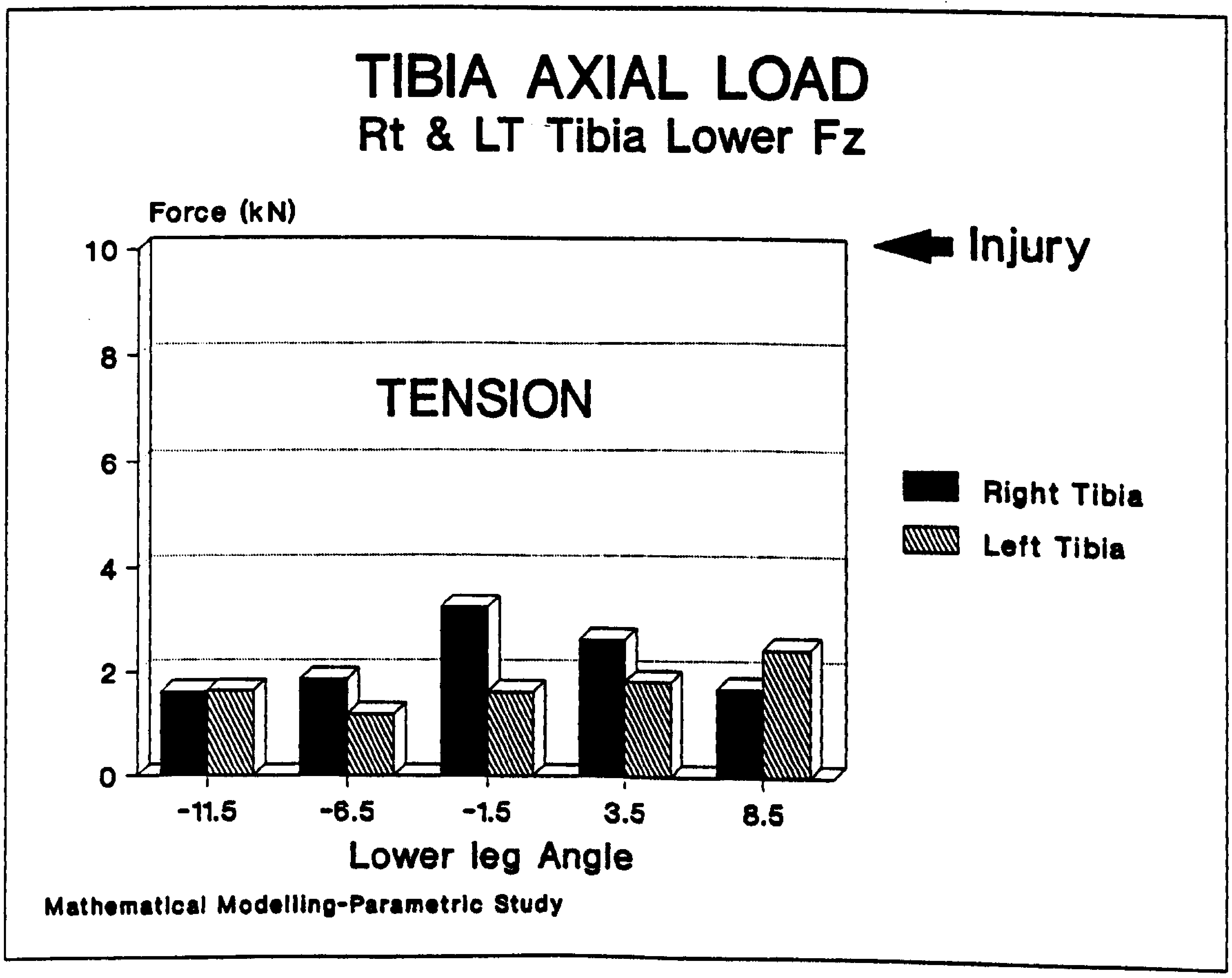

Fig. 98 Variation in Tibia Axial Load with Lower Leg Position

2.5.4 16G Pulse

Head Injury Criterion

The head injury criterion values were high at 16G impact pulse reflecting the high energy involved in the impact. It should be noted that the values remain below the injury threshold of 1,000 (16).

Lap Belt Load

The lap belt load recorded was higher than in the baseline impact reflecting the higher energy involved. It should be noted that the loads remained below the lower limit of the estimated injury range.

Lumbar Axial Load

The lumbar axial loads recorded at the 16G impact pulse were higher than in the baseline impact, reflecting the higher energy involved. The highest value recorded was 7843N. This is below the estimated injury threshold of 12kN (29).

Femoral Axial Load

The femoral axial load recorded was slightly higher than in the baseline model. This was a tension load and was below the injury threshold of 8.68kN (31).

Femoral Shear Load

The femoral shear load recorded was high at the 16G impact pulse reflecting the higher energy involved compared to the baseline impact.

Femoral Bending Moment

The femoral bending moments recorded were higher than in the simulation of the baseline impact. The maximum bending moment generated was 236Nm. This is below the estimated injury threshold of 250-320Nm (36).

Tibia Shear Load

The tibia shear loads recorded were marginally higher at the 16G impact pulse, reflecting the higher energy involved.

Tibia Axial Load

The tibia axial loads recorded were higher than in the baseline impact reflecting the higher energy involved.

2.6 SUMMARY

2.6.1 Foot to Floor Friction

The effect of increasing foot to floor friction was to reduce foot slide. There was no significant effect on Head Injury Criterion, lap belt load or lumbar axial load.

2.6.2 Seat Pitch

The effect of seat pitch on Head Injury Criterion vary according to which part of the seat ahead that the head struck.

A shortened seat pitch was associated with reduced loads in the lap belt due to the knee striking the back of the seat ahead. Consequently there was an increase seen in the compressive axial loads recorded in the femurs even at a shortened seat pitch these compressive axial femoral loads did not approach the injury threshold.

At a 32" seat pitch no knee contact occurred with the back of the forward seat.

High bending moments seen at a 30" seat pitch were associated with foot entrapment under the luggage retaining spar of the seat ahead. Such a phenomenon was associated with high bending moments in the femur which were of such a magnitude as to make injury likely. This effect was confirmed by analysis of the impact and comparing bending loads with foot entrapment on a time basis.

2.6.3 Lower Leg Position

HIC values increase as the legs were moved to a forwards position from a rearwards position. This effect is in contrast to the findings of the earlier impact tests and the reason for this difference is uncertain. All the HIC values recorded were below the injury threshold of 1,000.

Lap belt loads showed a slight decrease as the lower legs were angled rearwards of the vertical. However, the difference is not likely to be significant in terms of injury risk.

Lumbar axial loads showed little variation with changes in lower leg position.

The variation in forward bending moments is more difficult to interpret due to differences between the two legs. The effect of flailing was more difficult to establish as using the low coefficient of foot to floor friction (0.5), the foot was seen to slide forwards on the left side. This was not a flailing of the limb but a lower energy phenomenon.

2.6.4 16G Pulse

Assessment of the model in the baseline configuration in a simulated 16G impact pulse at the specified velocity of 13.41 m/s revealed an increase in the head injury criterion, the lap belt load, femoral shear load, femoral bending moment, tibia shear load and lumbar axial load. However, in none of these parameters were the increases meaningful in terms of increasing the risk of injury to the occupant.

2.7 CONCLUSIONS

1. The tendency for the lower limbs to flail upwards on impact is reduced by increasing the foot to floor friction and by positioning the lower legs rearward of the vertical.

   In the baseline model a foot to floor friction coefficient of 0.55 was used which represented a 'worst case scenario' when a smooth sole leather shoe was rested on a short pile carpet.

   Therefore it would seem advisable to wear a rubber sole shoe. Women wearing high heeled shoes represented a 'special case scenario'. It is suggested that the tendency for lower limbs to flail would be reduced by not wearing a shoe. This effect would be offset by the lack of protection which would result from not wearing shoes.

2. Axial loading of the femur does not appear to be a significant injury mechanism, even at a shortened 28" seat pitch.

3. Foot entrapment under the luggage retaining spar is associated with a significant increase in the loads measured in the femur and tibia such that injury is likely.

4. The loads recorded in the impact tests do not differ significantly from the loads estimated to occur at the slightly increased impact velocity specified in the FAA guidelines.

5. All the above conclusions must be viewed in the knowledge that the correlation of the mathematical model to impact test PB3673 was far from ideal.

CONCLUSIONS

1. IMPACT TESTING

1. The horizontal impact simulated in Experiment 1 appears to have a greater potential for inflicting injury upon the occupant.

2. The braced position would appear to have advantages over the unbraced position as it is associated with a reduced HIC value in a horizontal impact (Experiment 1) and reduced axial compressive loads in the lumbar spine in a vertical impact (Experiment 2).

3. High lap belt loads were recorded in the horizontal impacts (Experiment 1) in all of the dummy positions tested. The loads approached or exceeded the lower limit of the injury threshold range.

4. Axial loading of the femur due to knee contact with the back of the forward seat does not appear to be a significant injury mechanism even in a predominantly horizontal impact at a shortened 28" seat pitch.

5. Femoral bending appears to be a significant injury mechanism which might produce femoral shaft fractures in an impact aircraft accident.

6. A braced legs back position appears to reduce the risk of lower limb injury. In such a position, flailing is prevented and the lower limbs are not thrown forwards to impact with the sharp edges on the back of the forward seat. This is associated with a reduction in the tibial bending moments recorded. Moreover, hyperextension of the knee joint does not occur. Hyperextension of the knee joint would equate in the human with knee ligament injury.

7. If flailing of the lower limb is prevented increased axial loads are generated in the tibia but these do not approach the injury threshold.

8. High shear loads are recorded in the lumbar spine in all of the positions tested.

2. MATHEMATICAL MODELLING

1. The correlation between the mathematical model and the impact tests was far from ideal but represented the best achievable with the resources provided.

2. The tendency for the lower limbs to slide forward on impact is reduced by increasing foot to floor friction and positioning the lower limbs rearwards of the vertical. The tendency for the lower limbs to flail upwards is similarly reduced.

3. Compressive axial loading of the femur does not appear to be a significant injury mechanism even at a shortened seat pitch.

4. Femoral bending appears to be a significant injury mechanism which might produce femoral shaft fractures.

5. Foot entrapment under the luggage retaining spar of the seat ahead is associated with an increase in the loads recorded in the femur and tibia sufficient to cause injury.

6. Further research aimed at improving the correlation of the mathematical model to the impact test would be useful and would then allow the model to be used to investigate other parameters such as:

    1) seats adjacent to bulkheads,
    2) 95% + 5% occupant sizes, and
    3) different seat designs, etc.

RECOMMENDATIONS RELATING TO AIRCRAFT PASSENGER SAFETY

1. Passengers should adopt a braced position in order to minimise the risk of head injury.

   Passengers should adopt a legs back position in order to minimise the risk of lower limb injury.

   Such a modified position is shown in Fig. 99.

   This recommendation must be viewed with the knowledge that this research has looked at only one size of occupant and one type of seat design.

2. Bending loads applied to the femur appear to be a possible cause of injury. Methods to reduce such bending loads should be investigated.

3. A passenger seated in a forward facing seat even in the modified brace position is still exposed to considerable forces during an impact capable of producing injury to the lumbar spine, pelvis and femur. Accordingly, the possibility of passengers being seated in rearward facing seats should be investigated.

Fig. 99 Modified Crash Brace Position

REFERENCES

1. AAIB. Report on the Accident to Boeing 737-400 G-OBME near Kegworth, Leicestershire on January 1989. Air Accidents Investigation Branch, 1990:

2. Anton DJ. Minimising Impact Injuries To Occupants In A Fixed Wing Aircraft Accident. BMA Books, In Press:

3. Anton DJ. Protection/Injury Mitigation: Aircraft. In: Scientific Foundations of Trauma. Butterworth Heinemann, In Press:

4. Biss DJ, Pompa JA. A Kinematic and Dynamic Analysis of Occupant Responses To Lap Belt Only Restraint Forces. New Orleans, Louisiana: American Association of Automotive Medicine, 1987: 325-345.

5. Chandler RF. The Biomechanics of Restraint. In: Nahun AM, Melvin J ed. The Biomechanics Of Trauma. Appleton-Century-Crofts, 1985: 60-76.

6. Chandler RF. Brace For Impact Positions. Vth Annual International Aircraft Cabin Safety Symposium, Oakland, California: 1988: 279-290.

7. Chandler RF. Occupant Crash Protection In Military Air Transport. Paris: North Atlantic Treaty Organization Advisory Group For Aerospace Research And Development, 1990:

8. Chandler RF. 16 G Seat History - Now It Can Be Told. The International Symposium of the Rally of Endeavours to Improve Air Safety, Tokyo: 1992:

9. Culver CC. Lower Leg Axial Force Studies; exploratory tests using excised cadaver legs. Biomedical Sciences Department, General Motors Research Laboratories, 1984:

10. De Haven H. Relationship of Injuries to Structure in Survivable Aircraft Accidents. National Research Council, Report No. 440, 1945:

11. Dutton AD. A Versatile Linear Decelerator Track. Royal Air Force Institute of Aviation Medicine, IAM Technical Report No. 360, 1974:

12. Eiband AM. Human tolerance to Rapidly Applied Accelerations: A Summary of the Literature. National Aeronautics and Space Administration, 1959:

13. Engineers SOA. Performance Standard For Seats In Civil Rotorcraft And Transport Airplanes. Society Of Automotive Engineers, Aerospace Standard 8049, 1990:

14. FAA. Crash Injury Protection in Survivable Air Transport Accidents - US Civil Aircraft Experience from 1970-1978. Federal Aviation Authority, Report No. DOT/FAA/CT-82-118, 1983:

15. Garret JW, Braunstein PW. The Seat Belt Syndrome. J. Trauma 1962;2:220-237.

16. Goldsmith W, Ommaya AK. Head and Neck Injury Criteria and Tolerance Levels. In: Aldman B, Chapon A ed. The Biomechanics of Impact Trauma. Amsterdam: Elsevier Science Publishers B.V., 1984: 149-187.

17. Gumley G, Taylor TKF, Ryan MD. Distraction Fractures Of the Lumbar Spine. JBJS 1982;64-B:520-525.

18. King AI. The Spine - Its Anatomy, Kinematics, Injury Mechanisms and Tolerance To Impact. In: Aldman B, Chapon A ed. The Biomechanics Of Trauma. Elsevier Science Publishers, 1984: 191-227.

19. King AI, Chou CC. Mathematical modelling, simulation and experimental testing of biomechanical system crash response. J Biomechanics 1976;9:301-317.

20. Kleerekoper M, Feldkamp LA, Goldstein SA. The effect of aging on the skeleton - Implications for changes in tolerance. In: Biomechanics and medical aspects of lower limb injuries. Warrendale, PA: Society of Automotive Engineers, 1986: 91-96.

21. Learmount D. The Arrogant Decade. Flight International 1990;(January 1990):48-50.

22. Learmount D. The Complacent Year-Safety 1989. Flight International 1990;(January 1990):42-47.

23. Lewis ST, Stapp JP. Human Tolerance To Aircraft Seat Belt Restraint. Aviation Medicine 1958;(March 1958):187-196.

24. Lorenz A. Boeing and Airbus join up to build super jumbo jet. The Sunday Times, 20 December 1992.

25. Martens M, Van Audekercke R, deMeester P, Mulier JC. The mechanical characteristics of the long bones of the lower extremity in torsional loading. Journal of Biomechanics 1980;13(8):667-676.

26. Mason JK. Aviation Accident Pathology . London: Butterworths, 1962:

27. Mather BS. Observations on the effects of static and impact loading on the human femur. J. Biomechanics 1968;1:331-335.

28. Melvin JW, Evans FG. Extremities: Experimental aspects . In: Nahum AM, Melvin J ed. The Biomechanics Of Trauma. Norwalk, Connecticut: Appleton-Century-Crofts, 1985: 447-459.

29. Melvin JW, King AI, Alem NM. Advanced Anthropomorphic Test Device (AATD) Development Program . National Highway Traffic Safety Administration, 1985:

30. Mertz HJ. Anthropomorphic Models. In: Nahun AM, Melvin J ed. The Biomechanics Of Trauma. Norwalk, Connecticut: Appleton-Century-Crofts, 1985: 30-60.

31. Patrick LM, Mertz HJ, Kroell CK. Cadaver, knee, chest and head impact loads. New York: Society of Automotive Engineers, 1967: 106-117.

32. Pinkel II. A Proposed Criterion for the Selection of Forward and Rearward Facing Seats. The American Society of Mechanical Engineers, 1959:

33. Rowles JM. Impact Biomechanics of the Pelvis and Lower Limbs In Occupants Involved in an Impact Aircraft Accident. DM Thesis, Nottingham, 1993:

34. Smith WS, Kaufer H. A New Pattern of Spine Injury Associated with Lap-type Seat Belts: A Preliminary Report. University of Michigan Medical Centre Journal 1967;33(May/June):99-104.

35. Snyder RG, Crosby WM, Snow CC, Young JW, Hanson P. Seat Belt Injuries in Impact. Federal Aviation Authority, 1969:

36. St-Laurent A, Szabo T, Shewchenko N, Newman J. Design of a

Motorcyclist Anthropometric Test Device. 12th International Technical Conference on Experimental Safety Vehicles, Gothenberg, Sweden: 1989: 1-20.

37. Stapp JP, Lewis ST. Human Factors Of Crash Protection In Automobiles. Society Of Automotive Engineers, 1957:

38. Swearingen JJ. Evaluation of Head and Face Injury Potential of Current Airline Seats During Crash Decelerations. Report No. AM 66-18. Federal Aviation Administration, Office of Aviation Medicine, Civil Aeromedical Institute, Oklahoma City, Oklahoma, June 1966.

39. Viano DC, King AI, Melvin JW, Weber K. Injury biomechanics research: an essential element in the prevention of trauma. J. Biomechanics 1989;22(5):403-417.

40. Ward CC, Nagendra GK. Mathematical Models: Animal and Human Models. In: Nahum AM, Melvin J ed. The Biomechanics Of Trauma. Norwalk, Connecticut: Appleton-Century-Crofts, 1985: 77-100.

41. Widmayer JE, Brende OB. Commercial Jet Transport Crashworthiness Study. NASA Langley Research Centre, Report No. NASA CR 165849/FAA-CT-82-68, 1982:

42. Wilson R. Analyzing the Daily Risks of Life. Technology Review 1979;81(4):40-46.

43. Wismans J, Maltha J, van Wijk JJ, Janssen EG. MADYMO - A crash victim simulation computer program for biomechanmical research and optimization of designs for impact injury prevention. Advisory Group for Aerospace Research and Development, Report No. AGARD-CP-322: 24 1-11, 1982:

44. Yamada H. Strength of Biological Materials. Baltimore: Williams and Wilkins, 1970:

45. United States Army. Aircraft Crash Survival Design Guide. Report No. USARTL-TR-79-22, 1980.

46. FAA. Brace For Impact Positions. Federal Aviation Administration. Air Carrier Operations Bulletin No. 69-16, 1969.

47. FAA. Brace For Impact Positions. Federal Aviation Administration. Air Carrier Operations Bulletin No. 1-76-23, 1982.

48. Chapon A., Experimental Models in Biomechanics of Impact. In: Aldman B., Chapon A. ed. The Biomechanics of Impact Trauma. Amsterdam: Elsevier Science Publishers B.V. 1984: 85-89.

49. Chance G.Q., Note on a Type of Flexion Fracture of the Spine. British Journal of Radiology 1948: 21:452-3.

50. Nordin M., Frantel V.H., Basic Biomechanics of the Musculoskeletal System. Lea and Febiger, 1989.

51. Haidar R. Passenger Brace Position Study - Impact Testing. Report submitted to Civil Aviation Authority 1993.

52. Campbell B.J., Kihlberg J.K., Seat Belt Effectiveness In The Non Ejection Situation. Proceedings of the Seventh Stapp Car Crash Conference, 1963.

54. Nieboer J.J., Wismans J., Verschutt R. Occupant Simulation as an Aspect of Flight Safety Research. AGARD Conference Proceedings, 532, 1992.

55. Sadeghi M.M., Walton A.C. The Crash Reconstruction of the G-OBME Accident (8/1/1989) by Computer Simulation; The M1 Kegworth Air Accident Seminar, I.Mech.E., London, January 8, 1991.

56. KRASH Users' Seminar Proceedings; DLR Stuttgart, June 3-5, 1991.

57. Laananen D.H. Analysis of the Effects of Seat Parameters on Passenger Injury in Transport Aircraft Accidents. Computers in Engineering Conference. American Society of Mechanical Engineers, San Francisco, 1988.

58. Laananen D.H. Analysis of Aircraft Seats and Restraint Systems Using Programs SOMLA/SOMTA. KRASH Users Seminar Proceedings. Stuttgart, 1991.

59. Haidar R. The Use of Computer Simulation to Determine the Injury Mechanisms in the Kegworth Air Crash: The M1 Kegworth Air Accident Seminar, I.Mech.E., London. January 8,1991.

APPENDIX I

PUBLICATIONS PRODUCED BY MEMBERS OF THE NLDB STUDY GROUP (OR IN ASSOCIATION WITH THE STUDY GROUP)

Professor W A Wallace - Chairman of the NLDB Study Group

1. Wallace, W. A. (1989), Personal View - The M1 Plane Crash: The first twenty-four hours. **British Medical Journal** 298: 330-331

2. Kirsh, G., Learmonth, D. J. A., Martindale, J. P. & the NLDB Study Group (1989) The Nottingham, Leicester, Derby Aircraft Accident Study: A preliminary report three weeks after the accident. **British Medical Journal** 298: 503-505

3. Staff of the Accident and Emergency Departments of Derbyshire Royal Infirmary, Leicester Royal Infirmary and Queen's Medical Centre, Nottingham (1989). Coping with the early stages of the M1 disaster: At the scene and on arrival at hospital. **British Medical Journal** 298: 651-654.

4. Costley, J. A. (1989), **Aircraft Accident BD092 - M1 Motorway/East Midlands Airport - Sunday 8th January 1989.** The Report of the Trent Regional Health Authority Ref. Emergency Planning. JAC/C17/14.

5. Colton, C. L. (1989), The night of miracles. **Fragments** 8: 1-5.

6. Martindale, J. P. (1989), Response to the M1 aircrash. **BMA Newsletter** March 1989: 20.

7. Rowles, J. M. (1989), Three cities combine to analyze M1 crash injuries. **University of Nottingham Newsletter** March 1989: 1.

8. Harris, T. (1989), Kegworth: an ICU Experience. **Intensive Care Nursing** 5: 129-133.

9. Rowles, J. M. & the NLDB Study Group (1990), The Injury Severity Score as a predictor of hospital stay. **The Health Service Journal** June 7, 848-849.

10. Busuttil, A., Jones, J. S. P., (1990), **Deaths in Major Disasters - The Pathologist's Role**. A Report by the Royal College of Pathologists, London, July 1990.

11. Morgan, W. E., Salama, F. D., Beggs, F. D., Firmin, R. K., Rowles, J. M., & NLDB Study Group (1990), Thoracic injuries sustained by the survivors of the M1 (Kegworth) Aircraft Accident. **European Journal of Cardiothoracic Surgery** 4: 417-420.

12. Rowles, J. M., Robertson, C. S., Roberts, S. N. J. & the NLDB Study Group (1990) General surgical injuries in the survivors of the M1 Kegworth air crash. **Annals of the Royal College of Surgeons,** 72: 378-381.

13. The NLDB Study Group (1990), **NLDB Report on the M1 Aircraft Accident**, University of Nottingham, 15th October, 1990.

14. HW Structures & the NLDB Study Group (199)) **Occupant modelling in aircraft crash conditions.** Civil Aviation Authority - CAA Paper 90012.

15. McConachie, N. S., Wilson, F. M. A., Preston, B. J., Gregson, R. H. S., Jaspan, T., Rowles, J. M., Hellier, M. (1990). The impact of

the M1 aircrash on the radiological services at Queen's Medical Centre, Nottingham. **Clinical Radiology** 42: 317-320.

16. White, B. D., Rowles, J. M., Mumford, C., Firth, J. L. & the NLDB Study Group (1990). A clinical survey of head injuries sustained in the M1 Boeing 737 disaster: Recommendations to improve air crash survival. **British Journal of Neurosurgery,** 4: 503-510.

17. Wallace, W. A. (1991). The conception of the Nottingham, Leicester, Derby, Belfast (NLDB) study group. In: **The M1 Kegworth Air Accident - Engineering & Medical Aspects of Survivability**. The Institution of Mechanical Engineers, London: 1-5.

18. Allen, M. J. (1991). A description of the accident scene. In: **The M1 Kegworth Air Accident - Engineering & Medical Aspects of Survivability**. The Institution of Mechanical Engineers, London: 31-33.

19. Rowles, J. M., Learmonth, D. J. A., Martindale, J. P. (1991). The injuries sustained by the survivors. In: **The M1 Kegworth Air Accident - Engineering and Medical Aspects of Survivability**. The Institution of Mechanical Engineers, London: 35-46.

20. Bouch, C. (11191). Injuries sustained by the non-survivors. In: **The M1 Kegworth Air Accident - Engineering and Medical Aspects of Survivability**. The Institution of Mechanical Engineers, London: 49.

21. Kalyan, H. K., Colton, C. L., Webb, J. K. (1991). Biomechanics of external fixation. In: **The M1 Kegworth Air Accident - Engineering and Medical Aspects of Survivability**. The Institution of Mechanical Engineers, London: 51-61.

22. Kalyan, H. K., Webb, J. K., Colton, C. L. (1991). Biomechanics of

spinal fixation. In: **The M1 Kegworth Air Accident - Engineering and Medical Aspects of Survivability**. The Institution of Mechanical Engineers, London: 63-73.

23. Haidar, R. (1991). The use of computer simulation to determine the injury mechanisms of the Kegworth air crash. In: **The M1 Kegworth Air Accident - Engineering and Medical Aspects of Survivability**. The Institution of Mechanical Engineers, London: 75-82.

24. Anton, D. J. (1991). The role of crash simulation impact testing. In: **The M1 Kegworth Air Accident - Engineering and Medical Aspects of Survivability**. The Institution of Mechanical Engineers, London: 85-87.

25. White, B. D., Rowles, J. M, Mumford, C. J., Firth, J. L. (1991). Head injuries in the M1 Boeing 737 disaster - Suggestions to improve crash survival. In: **The M1 Kegworth Air accident - Engineering and Medical Aspects of Survivability**. The Institution of Mechanical Engineers, London: 89-94.

26. Hall, D. J., Rowles, J. M., Webb, J. K. (1991). Spinal injuries from the M1 air crash. In: **The M1 Kegworth Air Accident - Engineering and Medical Aspects of Survivability**. The Institution of Mechanical Engineers, London: 97-102.

27. Rock, N. I. C. (1991). Injury prevention through occupant analysis of the Kegworth air crash. In: **The M1 Kegworth Air Accident - Engineering and Medical Aspects of Survivability**. The Institution of Mechanical Engineers, London: 105-115.

28. NLDB Study Group (1991). The findings and recommendations of the BLDB Study Group. In: **The M1 Kegworth Air Accident - Engineering and Medical Aspects of Survivability**. The Institution

of Mechanical Engineers, London: 117-133.

29. Kayan H. K. (1991). The M1 Kegworth Air Accident: Engineering and Medical Aspects of Survivability. **Biomedical Engineering News,** April 1991: 1-2.

30. Wallace, W. A., Rowles, J. M., Haidar, R., and The NLDB Study Group (1991). Computer simulation of impact and correlation with bodily injuries. **Proceedings of the European Cabin Safety Conference 1990**, London, Civil Aviation Authority: 211-224.

31. Learmonth, D. J. A., Martindale, J. P., Rowles, J. M., Tait, G. R., Kirsh, G. and the Nottingham, Leicester, Derby and Belfast (NLDB) Study Group (1991). Initial management of open fractures sustained in the M1 aircraft disaster. **Injury**, 22: 207-211.

32. Fulford, P. (1991). Meeting Report - An aircraft accident: How to survive. Symposium at the Institution of Mechanical Engineers, London - January 8, 1991. **Journal of Bone and Joint Survey (Br.),** 73B: 695.

33. Rowles, J. M., Learmonth, D. J. A., Tait, G. R., Macey, A. C., and the NLDB Study Group (1991) Survivors of the M1 air crash: - Outcome of injuries after one year. **Injury**, 22: 362-364.

34. HW Structures (1991). **Report No. 5422A.** Aircraft crash victim simulation. Submitted to the Civil Aviation Authority - December 1991.

35. Tait, G. R., Rowles, J. M., Kirsh, G., Martindale, J. P., Learmonth, D. J. A. and the NLDB Study Group (1991). Delayed Diagnosis of injuries from the M1 aircraft accident. **Injury**, 22: 475-478.

36. Rowles, J. M., Kirsh, G. (1992). Chapter 9 - The management of major disasters. In: **Recent advances in Orthopaedics No. 6** - (Ed. A. Caterall): 133-143.

37. Rowles, J. M. (1993). Impact biomechanics of the pelvis and Lower limbs in occupants involved in an impact air crash. Doctor of Medicine Thesis, University of Nottingham.

38. White, B. D., Firth, J. L., Rowles, J. M. (1993). The effects of structural failure on injuries sustained in the M1 Boeing 737 disaster - January 1989. **Aviation, Space and Environmental Medicine**, 64: 95-102.

39. White, B. D., Firth, J. L., Rowles, J. M. and the NLDB Study Group (1993). The effect of brace position on injuries sustained in the M1 Boeing 737/400 disaster, January 1989. **Aviation, Space and Environmental Medicine**, 64: 103-109.

40. Rowles, J. M., Wallace, W. A., Anton, D. J. (1992). Can injury scoring techniques provide additional information for crash investigators? **Agard Conference Proceedings 532 - Aircraft Accidents: Trends in Aerospace Medical Investigation Techniques**: 12.1-12.10.

41. Rowles, J. M., Brownson, P., Wallace, W. A., Anton, D. J. (1992). Is axial loading a primary mechanism of injury to the lower limb in an impact aircraft accident? **Agard Conference Proceedings 532 - Aircraft Accidents: Trends in Aerospace Medical Investigation Techniques**: 13.1-13.8

42. Brownson, P. (1993). Report No. 1: Brace position study - impact testing.

43. HW Report 5483 (1993). Report No. 2: Brace position study - correlation study between impact testing and computer simulation.

44. Brownson, P. and HW Report (1993). Report No. 3: Brace position study - spine model development and analysis.

45. Brownson, P. (1993). The brace position for passenger aircraft - a biomechanical evaluation. Doctor of Medicine thesis submitted to University of Nottingham.